A Novel Investigation into the Role of Neurotrophic Factors in the Osteocyte and Bone

Catherine Jane Mary Stapledon

B. Hlth Sci (Hons)

Thesis by Publication and Convention submitted in fulfilment of the requirements for the degree of Doctor of Philosophy

May, 2020

Biomedical Orthopaedic Research Group

Discipline of Orthopaedics and Trauma

Adelaide Medical School

Faculty of Health and Medical Sciences

The University of Adelaide

South Australia,

Australia

THE UNIVERSITY of ADELAIDE

TABLE OF CONTENTS

Thesis Abstract

Degenerative diseases related to ageing are becoming some of the most prevalent health problems experienced by our population. Disorders of the brain and bone such as Alzheimer's disease (AD), Osteoporosis and Osteoarthritis (OA), respectively, occur in such a large proportion of the ageing population and it is believed that they may be mechanistically linked in their development.

This group of studies investigated the idea that proteins locally expressed in the Central Nervous System (CNS) may have roles in the bone and provide a mechanistic insight into the development of disease processes. A number of *in vitro* models were utilised in order to gain an understanding of the effects that known stimuli of bone resorption and formation (PTH, TNFα and 1,25D) had on APP, APLP-2 and NGF in the osteoblast to osteocyte differentiation process. *In vivo* studies were also performed to address the effects of *App* gene knock-out in the long bones of young mice and showed a development related defect in cortical bone remodelling. This study revealed a potential role for APP in the process of bone remodelling, which led onto the investigation of the effects of APP on osteocytes *in vitro.* There was no obvious effect of soluble APP695 (sAPP695) on osteocyte viability or expression of genes associated with bone resorption or formation.

As the ageing population is at high risk of hip fracture and dementia, a screening study of a population of neck of femur fracture (NOF) patients was conducted to determine relationships between the genes of interest and expression of a number of genes involved in the CNS, bone formation and bone resorption as well as skeletal structure. This study provided a novel insight into the NOF cohort as a whole, as well as differences between non-dementia and dementia patients by virtue of their gene expression and skeletal

structure of the femur. The overall findings from this chapter suggest a link between AD and osteoporosis through common molecular pathways, which we now believe APP and BACE1, previously referred to only in the context of the brain, to be a part of. These findings give rise to potential alternative treatment strategies for osteoporosis and fracture prevention through the targeting of the novel brain-related proteins.

As cleavage of APP leads to the formation of the neurotoxic amyloid beta (Aβ) peptide, a known contributor to the development of AD, it was important to investigate the effects of this peptide on skeletal development through the use of an *in vivo* model. Utilisation of the $App^{NL\text{-}G\text{-}F/NL\text{-}G\text{-}F}$ familial AD mouse model revealed an accelerated loss of cancellous bone in the 29-week-old male cohort when compares with wild-type littermate control animals, providing strong evidence for roles of Aβ and its precursor APP in the bone maintenance process observed throughout life. It was also shown that these Aβ peptides were present in the bone marrow of the femorae of these mice, which was coupled with an increased number of osteoclasts in these knock-in animals. To further elucidate what the presence of these peptides in the proximity of bone cells could do, human osteocytes were exposed to increasing concentrations of $A\beta_{1\text{-}42}$ peptides *in vitro*. This cell culture study revealed that osteocyte death could be initiated when exposed to the highest, 15 μM concentration of $A\beta_{1\text{-}42}$ peptides over a 96 hour time course. Furthermore, $A\beta_{1\text{-}42}$ peptides were also capable of upregulating the mRNA expression of markers characteristic of resorption: *RANKL*, *RANKL:OPG* and *MMP13*. This finding, together with the reduction in bone seen with ageing in the mouse model provides a new insight into the possible mechanistic link between Alzheimer's disease and osteoporosis by virtue of Aβ.

The final study conducted was focused around the efficacy of a new potential therapeutic agent for the treatment of pain associated with knee OA. NGF has previously been

characterised for its roles in the central nervous system, and in the bone in fracture healing, however its role in other bone pathology such as knee osteoarthritis has not been appreciated previously. Pentosan polysulphate sodium (PPS) was successful in dampening expression of nerve growth factor (NGF) and its pro-protein form (pro-NGF), CNS-related proteins involved in the pain response, in primary human osteocytes exposed to TNFα, a pro-inflammatory cytokine. This study was the first study to demonstrate that osteocytes could express NGF and pro-NGF and that PPS could block the proposed pain response initiated by upregulation of NGF in response to pro-inflammatory stimuli.

Overall, the studies conducted in this thesis were designed and implemented to ascertain a new understanding of the current literature about the links between the CNS and bone by virtue of APP, APLP2 and NGF as well as build upon the understanding of the relationship between Alzheimer's disease and bone loss.

Declaration

I, Catherine Stapledon certify that this work contains no material which has been accepted for the award of any other degree or diploma in my name in any university or other tertiary institution and, to the best of my knowledge and belief, contains no material previously published or written by another person, except where due reference has been made in the text.

In addition, I certify that no part of this work will, in the future, be used in a submission in my name for any other degree or diploma in any university or other tertiary institution without the prior approval of the University of Adelaide and where applicable, any partner institution responsible for the joint award of this degree.

The author acknowledges that copyright of published works contained within this thesis resides with the copyright holder(s) of those works. I give permission for the digital version of my thesis to be made available on the web, via the University's digital research repository, the Library Search and also through web search engines, unless permission has been granted by the University to restrict access for a period of time.

I acknowledge the support I have received for my research through the provision of an Australian Government Research Training Program Scholarship.

Signed: Date: 15/05/2020

Acknowledgements

I am extremely grateful for all of the encouragement and support that I have received over the past 4 years, which has led to the completion of my PhD. It has not been an easy path, but in the end, I am glad that I chose it. First and foremost, thank you to my family, especially my parents Rosemary and John, without whom I would not have been born, or supported wholeheartedly on this venture, you truly are the best parents and I appreciate all you've done for me. My siblings, Thomas, Bridget and Mary, you have been a great little support network & even when you didn't realise you were helping me, you were. The rest of my family members, especially Shirley and James thank you for always checking in and seeing how it was all going. My grandparents, who I lost throughout the course of my PhD, you would have been so excited to see this day and I wish you were here. To all of my close and beautiful friends - you have all been amazing throughout this whole process, listening to me, giving me support, dealing with me during my breakdowns. Emma, Zoe, Claire, Cloud, Alana, Nadia, Gabby, Caitlin and everyone else who has made an impact on my progress and life! To all of the holidays I went on to "keep me sane". My motto is "you always need something to look forward to" and I stood by that even when I probably should have been in the lab. You really did keep the dream alive and get me through some hard times.

I have had the opportunity to work in such a great group, full of amazing minds, who were always willing to answer my questions and help me in times where I thought my experiments would fail. Thank you to my work besties, Yolandi, Helen and Renee (Harvard) for always being there for me through the good and bad times. Your constant support and coffee really got me through this PhD. I will be forever grateful for our

“friendship”. I will miss our vending machine trips and kit kats, but I will never forget them ☺. A big thank you to everyone on level 7, you have all been so supportive and I’m so glad I got to know you all.

A special mention to Plinio Hurtado, who hardly knew me from a bar of soap 12 months ago, took me under his wing and supported me so much through the last year of my PhD. Having you as a mentor and friend made the end of my PhD journey such a bright and fun time. A special mention to all of the biomedical engineering guys who I’ve had the opportunity to get to know, you were all great and kept me sane! Thank you, Kieran, for all of the jokes, coffees and hang outs, you definitely made my time enjoyable.

Thank you to my co-supervisors Bogdan Solomon and Roberto Cappai, I wouldn’t have had such an interesting thesis if it wasn’t for you. Finally, thank you to my primary supervisor, Gerald Atkins. Thank you so much for all of your guidance and support throughout both my honours and PhD. I wouldn’t have been able to conduct such interesting research and learn so much without your mentorship. For that, I will be always grateful.

Peace out, C.

Arising Publications

Stapledon, CJM., Tsangari, H., Solomon, LB., Campbell, DG., Hurtado, P., Krishnan, R., Atkins, GJ. (2019) *Human osteocyte expression of Nerve Growth Factor: The effect of Pentosan Polysulphate Sodium (PPS) and implications for pain associated with knee osteoarthritis*. PLoS ONE 14(9) (Published)

Stapledon, CJM., Whyte, LS., Solomon, LB., Cappai, R., Sargeant, TJ., Atkins, GJ. *A direct link between Alzheimer's disease and osteoporosis: Amyloid Beta$_{1-42}$ Peptide overexpression causes age-related bone loss*. The Journal of Bone and Mineral Research. (In preparation for publication)

Stapledon, CJM., Stamenkov, R., Cappai, R., Solomon, LB., Atkins, GJ. *The Cancellous Bone Gene Expression of APP in a Cohort of Neck of Femur Fracture Patients*. Calcified Tissue International. (In preparation for publication)

Published Abstracts and Scientific Communications

Catherine JM Stapledon, Deepti K Sharma, Lucian B Solomon, Gerald J Atkins (2017) The *Roles of Amyloid Beta (A4) Precursor Protein and its Homologue Amyloid Precursor (A4) Like Protein 2 in Bone and its Connection with the Development of Dementia of the Alzheimer's disease Type*. The University of Adelaide, 2017 11th Annual Florey Postgraduate Conference; Faculty of Health and Medical Sciences (Poster)

Sharma, D., Robertson, T., Stamenkov, R., **Stapledon, C.,** Atkins, G., Clifton, P., Morris, H. (2017). Bone CYP27B1, CYP24A1 and Serum 25-Hydroxyvitamin D are Key Positive Factors for Trabecular Bone Architecture in Hip Fracture Patients. In *Journal of Bone and Mineral Research* Vol. 32 (pp. S101). Denver, CO: WILEY. (Poster)

Sharma, D., Stamenkov, R., Robertson, T., **Stapledon, C**., Atkins, G., Solomon, L., Morris, H. (2018). Serum 25-Hydroxyvitamin D and its Metabolism in Bone Tissue is Associated with Improved Bone Quality in Elderly Hip Patients. In *Osteoporosis International* Vol. 29 (pp. S271). Krakow, Poland: Springer London Ltd (Poster)

Sharma, D., Sawyer, R., Stamenkov, R., Robertson, T., **Stapledon, C.,** Atkins, G, Anderson, P. (2018). Serum 25-Hydroxyvitamin D and its Metabolism in Bone Tissue is Associated with Improved Bone Quality in Elderly Hip Fracture Patients. In *Journal of Bone and Mineral Research* Vol. 33 (pp. 205). Montreal, Canada: Wiley (Poster)

Stapledon CJM, Whyte LS, Starczak Y, Sargeant TJ, Cappai R, Solomon LB, Atkins GJ. *The effect of Alzheimer's disease on the bone: it's a lose lose situation.* The University of Adelaide, 2018 12th Annual Florey Postgraduate Conference; Faculty of Health and Medical Sciences (Poster)

Stapledon CJM, Whyte L S, Sargeant T J, Starczak Y, Cappai R, Solomon L B, Atkins G J. *Linking the Brain and the Bone: Skeletal Phenotyping of the App^{NL-G-F} 'Alzheimer's'*

Mouse. Australian Orthopaedic Association 2018 SA / NT Branch Scientific Meeting (Oral Presentation)

Catherine Stapledon, Renee Ormsby, Roberto Cappai, Lucian Bogdan Solomon and Gerald Atkins. (2019) *A Novel Investigation into the Effects of the Amyloid Precursor Protein on the Osteocyte* – The 25th Annual Australian and New Zealand Orthopaedic Research Society (ANZORS) Scientific Meeting – Canberra, Australia – 2019 (Podium Presentation)

Stapledon CJM, Whyte LS, Starczak Y, Sargeant TJ, Cappai R, Solomon LB, Atkins GJ. *The effect of Alzheimer's disease on the bone: it's a lose lose situation.* 29th Australian and New Zealand Bone Mineral Society Annual Scientific Meeting, Darwin, Australia – 2019 (Poster Presentation)

Stapledon, CJM, Whyte, LS, Solomon LB, Cappai R, Sargeant TJ, Atkins GJ. *A direct link between Alzheimer's disease and osteoporosis: Amyloid Beta$_{1-42}$ Peptide overexpression causes age-related bone loss.* The 11th Clare Valley Bone Group Meeting, Clare, Australia – 2020 (Oral Presentation in the Emerging Scientists Showcase Session)

Previous Publications by the Author

Yang D, Anderson PH, Wijenayaka AR, Barratt KR, Triliana R, **Stapledon CJM,** Zhou H, Findlay DM, Morris HA, Atkins GJ - *Both ligand and VDR expression levels critically determine the effect of 1α,25-dihydroxyvitamin-D3 on osteoblast differentiation.* (2017)

Prizes and Awards

2016: Accepted into the Doctor of Philosophy Program at the University of Adelaide

2016: Awarded Australian Post Graduate Award (APA) – Full time

2017: Florey Medical Research Foundation Prize for Poster presentation, presented at the University of Adelaide Faculty of Health and Medical Sciences 11th Florey Postgraduate Research Conference.

2017: Awarded Adelaide Medical School Prize at the 2017 11th Annual Florey Postgraduate Conference

2017: Chosen to participate in the "Industry Mentoring Network in STEM" pilot program

2018: Awarded a poster presentation for the 12th Annual Florey Postgraduate Conference

2019: Awarded a podium presentation for the Australian and New Zealand Orthopaedic Research Society Conference (ANZORS)

2019: Awarded ANZORS travel grant to attend the annual conference in Canberra, Australia

2020: Awarded oral presentation to present in the Emerging Scientists Showcase Session at the 11th Clare Valley Bone Group Meeting in the Clare Valley, Australia

Abbreviations

ANZBMS	Australian and New Zealand Bone Mineral Society
ANZORS	Australian and New Zealand Orthopaedic Research Society
AD	Alzheimer's disease
APP	amyloid beta (A4) precursor protein
APLP-1	amyloid beta (A4) precursor-like protein-1
APLP-2	amyloid beta (A4) precursor-like protein-2
BACE-1	beta secretase cleaving Enzyme-1
BAX	BCL-2-like protein 4
BCL-2	B-cell lymphoma 2
BMD	bone mineral density
CA12	carbonic anhydrase 12
cDNA	complementary deoxyribonucleic acid
CTSK	cathepsin K
DMP1	dentin matrix acidic phosphoprotein 1
EDTA	Ethylenediaminetetraacetic acid
FCS	foetal calf serum
FGF23	fibroblast growth factor 23
HEPES	4-(2-hydroxyethyl)-1-piperazineethanesulfonic acid
IL-6	interleukin-6
Lac.Ar	Osteocyte lacunar area
Lac.Ar/BAr (%)	Lacunar area per total bone area
M-CSF/CSF-1	macrophage-colony stimulating factor

MMPs	Matrix metallopeptidases
MMP13	matrix metalloproteinase-13
mRNA	messenger ribonucleic acid
NHBC	normal human bone cells
NHMRC	National Health and Medical Research Council of Australia
NOF	Neck of Femur
OPG	osteoprotegerin
N.Ot/BAr (%)	Osteocyte number per bone area
PBS	phosphate buffered saline
PHEX	phosphate-regulating neutral endopeptidase
PTH	Parathyroid hormone
RAH	Royal Adelaide Hospital
RANK	receptor activator of nuclear factor-kappa B
RANKL	receptor activator of nuclear factor-kappa B ligand
ROI	region of interest
RT-PCR	reverse transcription polymerase chain reaction
SEM	standard error of the mean
SOST	sclerostin
Top 20% Lac.Ar	Top 20% Osteocyte lacunar area
THR	Total Hip Replacement
TNFα	tumour necrosis factor alpha
TRAP/ ACP5	tartrate resistant acid phosphatase
Wnt	wingless integration

α-MEM	Minimum Essential Medium Eagle Alpha Modification
µ-CT	micro-computed tomography

Chapter 1

Literature Review

Conventional chapter

The aim of this review was to investigate the current literature surrounding links that have been found between the bone and the brain in the *in vitro* and *in vivo* contexts. This review focuses mainly on the amyloid beta (A4) precursor protein and its homologues amyloid beta (A4) precursor-like protein-2 and nerve growth factor in the bone and diseases of ageing such as Osteoporosis, Osteoarthritis and Alzheimer's disease.

Abstract

Diseases of ageing currently place a large burden on society physically, psychologically and economically. Two leading causes of death and disability in the ageing population are dementia and osteoporosis. Dementia is an umbrella term used to describe a group of disorders occurring as a result of cognitive decline. The most common form of dementia is Alzheimer's disease (AD), which through unknown pathological mechanisms results in progressive and detrimental hippocampal atrophy and subsequently, severe cognitive impairment. Osteoporosis is a degenerative skeletal disease in which homeostatic bone remodelling is significantly disrupted causing marked decreases in bone mineral density, frailty and increased risk of fracture. Both of these conditions, without appropriate and timely diagnosis impair daily life and ultimately result in death both primarily and from consequential health complications. While the current literature contains strong evidence supporting bone disease and dementia as two separate systems, similarities between brain and bone degenerative diseases have sparked research interest in favour of there being a mechanistic link, which may be by virtue of neurotrophins. There is, however, no concrete evidence to support the notion that bone disease can result in neurodegenerative disease, or *vice versa*. This review of the literature will focus on the studies which have investigated the links between bone and brain pathology, specifically cognitive decline and osteoporosis.

Musculoskeletal Background

Structure and Function of Bone Tissue

The bone is a dynamic and complex tissue comprised of numerous vital minerals and cell types. The organic matrix of bone is comprised primarily of organic type 1 collagen and inorganic hydroxyapatite-like mineral, which is a combination of calcium (Ca^{2+}) and phosphate ($PO4^{3-}$), impregnated with bone-derived proteins and their peptide derivatives (1). The main functions of the bone are classically regarded as providing mechanical support and protection of other organs, storage of vital minerals, such as Ca^{2+} (2, 3) and to support the formation of bone marrow, the major source of immune cells in the body. With the advent of intensive research into the function of bone cells, in particular the osteocyte (4-6) we now know that the essential roles of the skeleton and its constituent cells are far more wide-reaching.

There are two main types of bone found in the body: cortical and cancellous. Cortical bone is the major bone type, comprising 80% of all bone tissues with its main function to provide mechanical function, structural integrity and protection to internal organs (7). Cancellous bone constitutes the remaining 20% of bone; it is imperative for bone strength, houses the bone marrow and serves as the major metabolic component of bone (8). Although both types undergo bone remodelling, the coordinated process by which damaged bone is resorbed by the activity of osteoclasts and new bone laid down by the activity of osteoblasts, cancellous bone is constantly being repaired and restored due to it being a more metabolically active bone type, which is exposed to high levels mechanotransduction (9) .

The three main cells residing in the bone are the osteoclast, osteoblast and osteocyte. Each of these cell types work together to create a highly interconnected homeostatic skeletal system, exemplified by their interactions during bone remodelling (10, 11). This process occurs

throughout development and continues on throughout the entire lifetime of vertebrates to preserve bone integrity and stability.

Osteoclasts

Osteoclasts are terminally differentiated cells derived from haemopoietic cells of the monocyte-macrophage cell lineage (12, 13). The main function of the osteoclast is to resorb the bone mineral matrix during the catabolic phase of bone remodelling. Mature, osteoclasts are large, multinucleated cells, which can be found on the surface of calcified bone tissue and within the Howship's lacunae (14). Colony Stimulating Factor-1 (CSF-1) or Macrophage Colony Stimulating Factor (M-CSF) is an essential growth factor for myeloid lineage-derived cells, which have the potential to differentiate into a number of different cell types including macrophages, monocytes and osteoclasts (15, 16). M-CSF is a critical co-stimulatory cytokine for the formation and activation of osteoclasts (17), working in concert with receptor activator of nuclear factor kappa-B (NF-κB) ligand (RANKL). RANKL is a member of the tumour necrosis factor (TNF)-ligand superfamily designated TNFSF11 and is the primary differentiation factor for osteoclasts (18). RANKL can bind to two possible receptors, RANK (TNFRSF11A), or the decoy receptor osteoprotegerin (OPG; TNFRSF11B) (19, 20).

The coupling process of osteoblast mediated bone formation and osteoclast mediated bone resorption is controlled through the RANK/RANKL/OPG system (18-20). Osteoblast-lineage cells express RANKL and M-CSF, and together with osteoclasts and their precursors form the basic multicellular unit (BMU) characteristic of physiological bone remodelling. The RANKL/RANK interaction initiating resorption can be strongly or partially inhibited by OPG, which acts as a molecular chaperone, competing with RANKL to bind to RANK, and also preventing RANKL translocation to the plasma membrane (19, 21) . Osteoclastogenesis occurs when osteoclast precursor cells located in the bone marrow or peripheral blood come into

contact with and recognise osteoblast secreted RANKL and M-CSF (22) through their respective membrane-bound receptors – RANK and c-Fms (23) (Fig. 1). The M-CSF/c-Fms interaction is critical for triggering proliferation of myeloid progenitors into committed pre-osteoclasts (15). Following expansion of the precursor pool, RANKL-RANK signalling triggers fusion and differentiation events required to form a mature multi-nucleated osteoclast capable of bone resorption. Mature osteoclasts attach to the bone surface via cell surface expressed adhesion molecules including αvβ3 integrin, and the cytoskeleton rearranges to form an F-actin ring, resulting in the formation of a sealing zone on the basolateral surface of the cell. Through the ruffled border in this zone, the osteoclast pumps hydrogen ions through the coordinated function of intracellular carbonic anhydrase-2 (CA2) and the integral plasma membrane multi-subunit vacuolar ATPase (V-ATPase) to dissolve the bone mineral, and collagenases, principally cathepsin-K but also matrix metallopeptidase (MMP)-13 and MMP-14 (24), which break down the organic matrix, forming resorption pits on the bone surface in cancellous bone, the endocortical surface of cortical bone, and the inner surfaces of Haversian canals in cortical bone (**Fig. 1**) (25).

A large number of locally produced and systemic factors influence the bone remodelling process, many through the regulation of the RANKL/RANK/OPG axis. These include the active hormone form of vitamin D, 1, 25(OH) $_2$-vitamin-D_3 and parathyroid hormone (PTH). Both of these are endocrine hormones, which promote osteoclast resorption through inducing membrane bound expression of RANKL by osteoblasts and osteocytes (26) In addition, the pro-hormone form of vitamin D, 25(OH)vitamin D (25D), has also been shown to negatively regulate osteoclastic resorptive activity through osteoclastic expression of the 1-alpha hydroxylase, CYP27B1 (27). Osteocalcin (OCN) an osteoblast-derived protein (28) and tumour necrosis factor - α (TNFα) (29, 30) both regulate osteoblast-lineage expression of RANKL. Sclerostin (SOST), an osteocyte-derived protein that inhibits the Wnt/β-Catenin

signalling pathway, also induces RANKL secretion (22, 25) and stimulates osteoclast activity (22)

An imbalance in the activity of osteoclasts over bone formation can result in the development of a number of bone diseases. The main primary pathologies associated with increased osteoclast activity and bone resorption are osteoporosis (31, 32), a disease of low bone mass and fragility and Paget's disease of the bone, where there is excessive bone resorption by abnormal osteoclasts (33). In contrast, a suppression in osteoclast activity results in the development of osteopetrosis, a disease characterised by a high bone mass but poor bone quality phenotype, which can also be detrimental to health (34).

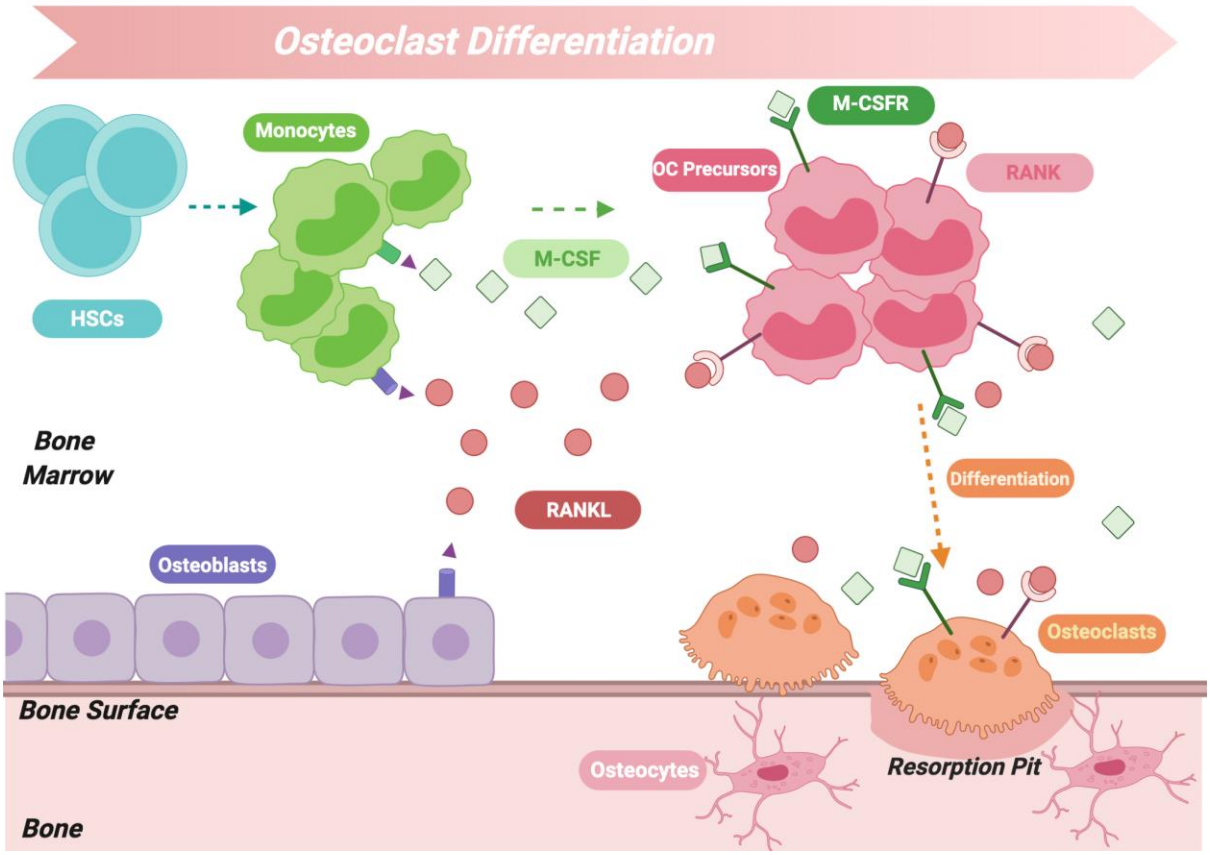

Figure 1: Schematic diagram illustrating the initiation and progression of osteoclastogenesis. Haematopoietic stem cells (HSCs) from the bone marrow differentiate into monocytic cells under the stimulation of M-CSF. RANKL expressed by osteoblasts and monocytes bind to RANK on the cell surface, promoting the differentiation of pre-osteoclastic cells into active, resorbing osteoclasts on the bone surface. Binding and recognition of M-CSF and RANKL via their respective receptors MCSF-R and RANK on the surface of pre-osteoclastic cells initiates the differentiation from pre-osteoclasts into active, resorbing osteoclasts on the calcified bone surface.

Osteoblasts

Osteoblasts are anabolic bone cells derived from bone marrow mesenchymal stem cell (BMSC) lineage cells (35). The primary function of the osteoblast is to synthesise and secrete new bone matrix either during development (modelling) or in response to osteoclastic resorption during bone remodelling. As previously mentioned, osteoblasts also regulate bone resorption and remodelling through expression of RANKL, M-CSF and OPG, and evidence suggests that it is the immature osteoblast that likely perform this function (36, 37). Differentiation of osteoblast progenitors is stimulated by the expression of runt-related transcription factor-2 (Runx2) and downstream expression of osterix (Osx), and by Wnt/β-catenin signalling (38) (**Fig. 2**). Many pathways have been recognised for their roles in the differentiation and maturation of the osteoblast. The Hedgehog signalling pathway, the first initiator of osteoblast differentiation, is responsible for the generation of Runx2 and Osx, both of are critically required for the development of mature osteoblasts (39). The NOTCH signalling pathway is best characterised for its role in the inhibition of osteoblast differentiation by virtue of downstream activation of Hairy and Enhancer of Split (HES) and HES-related with YRPW motif (HEY) family transcription factors (40).

Osteoblasts have three possible cellular fates once they have surpassed the pre-osteoblastic phase of differentiation. Osteoblasts can produce osteoid and embed themselves into their bone mineral matrix, where they undergo further differentiation into pre-osteocytes and then into mature osteocytes (**Fig. 2**) (41). The second fate for the osteoblast is to remain on the bone surface in a quiescent state as a bone lining cell (42), a cell type that is the least well-characterised. Finally, the majority of bone matrix-producing osteoblasts (approximately 80%) undergo programmed cell death (apoptosis), in order to control osteocyte spacing and maintain homeostasis within the bone environment (43).

Osteocytes

The osteocyte is the most numerous cell type in the bone tissue, comprising 90-95% of all bone cells in humans. It is also, historically, the most difficult bone cell type to study due to its location deep within the bone mineral matrix (44). As previously mentioned, osteocytes are mature, differentiated osteoblasts that have become embedded into the bone matrix (**Fig. 2**). One of the early functions that osteocytes play in the bone is the mineralisation of the organic bone matrix, termed osteoid, during bone formation (6, 22, 45) In the transition phase from osteoblast to osteocyte, there is a reduction in cytoplasmic volume and the development of dendritic processes, which extend out of the osteocyte and form a highly interconnected syncytium of cells (46). The osteocyte dendritic processes communicate via gap junctions and hemichannels, which allow for the transport of small molecules, such as ions both intra- and extracellularly (47). Osteocytes communicate these events to the cells lining the bone, forming a type of detection system which results in the stimulation and activation of osteoclasts and osteoblasts on the bone surface to initiate the bone remodelling process (48-50).

Osteocytes have been well documented for their expression of M-CSF and RANKL, critical cytokines involved in the control of osteoclast-mediated bone loss (37, 51-53). In the osteocyte-specific deletion of RANKL in mice, modified mice developed an osteopetrotic phenotype, indicating that osteocyte-produced RANKL in adult bone is imperative for induction of osteoclastic formation and activation (25, 53, 54).

As the major mechanosensory cell type in bone, osteocytes sense and respond to a large number of stimuli. Mechanical loading of bone and joints on the osteocyte lacuna-canalicular network has bone anabolic effects through inhibition of osteocyte-specific protein, sclerostin via the canonical Wnt signalling pathway (55, 56). This pathway is currently under investigation for its potential linkage between osteoporosis and dementia, which will be discussed below.

Osteocytes are also known to have systemic roles, such as the control of phosphate homeostasis, by virtue of their expression of the protein hormone, fibroblast growth factor-23 (FGF23) (57). They also tightly regulate the release of calcium from within the skeleton for milk production during lactation during times of Ca^{2+} deficiency in pregnancy, by the process of osteocytic osteolysis (58). Osteocytes are regulated by a number of osteotrophic factors, such as the hormone and pro-hormone forms of vitamin D, 1α, 25-dihydroxyvitamin D3 (1,25D) and 25-hydroxyvitamin D (25D), respectively (59). Other factors that are known to regulate osteocyte activity include PTH and SOST, which are important regulators of serum calcium and bone remodelling (3, 4). It is important to note that we are likely still only at the beginning of our understanding of the roles of osteocytes in systemic processes, and indeed in osteocyte biology *per se*, in particular in humans.

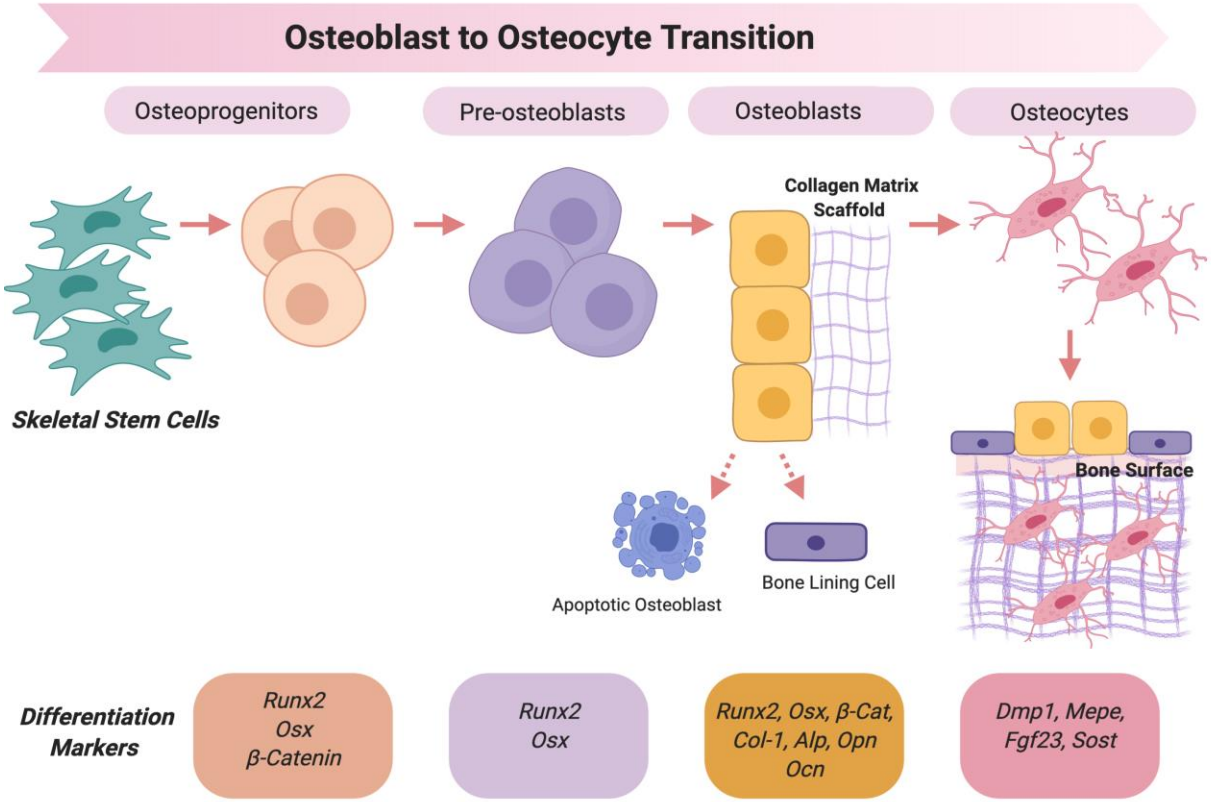

Figure 2: Differentiation of Osteoprogenitor cells into Osteocytes. Osteoprogenitor cells are derived from the mesenchymal stem cell (MSC) lineage. Under the promotion of Runx2, Osx and β-Catenin, MSCs preferentially differentiate into osteoprogenitor cells, which go on to form pre-osteoblast cells. Osteoblasts can then either go on to undergo programmed cell death (apoptosis), differentiate into inactive osteoblasts (bone lining cells) or form active bone-matrix secreting osteoblasts, which then become embedded into the matrix to form osteocytes. Differentiation markers produced at each point are indicative of the stage of differentiation and the cell type.

Runx2 *– Runt-related transcription factor 2;* ***Osx*** *– Osterix;* ***Col-1*** *– Type I Collagen;* ***Alp*** *– Alkaline Phosphatase;* ***Opn*** *– Osteopontin;* ***Ocn*** *– Osteocalcin;* ***Dmp1*** *– Dentin matrix acid phosphoprotein 1;* ***Mepe*** *– Matrix extracellular phosphoglycoprotein;* ***Fgf23*** *– Fibroblast growth factor 23;* ***Sost*** *– Sclerostin.*

Osteoporosis

Osteoporosis is a systemic degenerative disease of the bone, characterised by a significant reduction in bone mass and structural deterioration of the bone microarchitecture, resulting in weak and brittle bones. The dysregulation in bone remodelling that results in the reduction of bone density puts individuals with osteoporosis at high risk for low-energy fractures, which can be detrimental to the health of these individuals. The primary sites affected by osteoporosis are the distal radius, vertebra of the spine and the hip. There are a number of non-modifiable as well as modifiable risk factors predisposing an individual to the development of primary osteoporosis. Non-modifiable risk factors include gender (females > males), increasing age, family history/genetic profile and other comorbidities such as chronic kidney disease and RA and drugs used to manage symptoms such as glucocorticoids. Modifiable, lifestyle-related risk factors include smoking, alcohol consumption, Vitamin D and calcium deficiencies and inactivity/disuse.

Osteoporosis is defined by the World Health Organisation (WHO) as a bone mineral density (BMD) of at least 2.5 standard deviations (SD) below the average of a normal healthy woman for post-menopausal women and a BMD <2.5 SDs (T-score <-2.5) (60, 61) of a healthy man over 50 years of age. A diagnosis is made based on the BMD score attained from dual-energy X-ray absorptiometry (DEXA) measured at the hip and lumbar spine. There are currently over 4.7 million Australians living with osteoporosis or osteopenia, the prodromal stage before osteoporosis (T-score between -1 and -2.5). The most recent Australian Institute of Health and Welfare (AIHW) data reports that between 2016-17 there were 7382 hospitalisations for osteoporosis-related injuries alone (62). Large cohort studies such as the Dubbo Osteoporosis Study (63) and the Geelong Osteoporosis Study (64) have been imperative in the understanding of the effects of osteoporosis on morbidity and mortality within Australia, as well as forming new ideas for management of this disease.

Primary/idiopathic osteoporosis has the highest incidence rate and includes juvenile, postmenopausal and senile osteoporosis. Juvenile osteoporosis as the name suggests, occurs in children and adolescents and is usually linked to genetic mutations causing a low bone density and skeletal fragility (65). Post-menopausal osteoporosis occurs as the result of the sudden and sharp depletion in circulating oestrogen. This does not affect all post-menopausal women, however in those with a positive diagnosis, bone loss associated with ageing becomes accelerated leading to a substantial loss in cancellous bone and a loss of cortical bone to a lesser extent (66). Oestrogen is a known inhibitor of the RANK/RANKL signalling pathway, providing a protective effect against osteoclastic bone resorption. In post-menopausal women it has been established that RANKL expression by bone marrow mononuclear cells of post-menopausal women in comparison to pre-menopausal women (67). Menopause is also associated with increased secretion of the gonadotropins, luteinising hormone (LH) and follicle stimulating hormone (FSH). An elevated LH level in particular is a risk factor for AD in both women and men (68). LH and FSH are known to stimulate TNF-α production in post-menopausal women and TNFα is well known to cause increased bone resorption, through either RANKL or RANKL-independent mechanisms. TNF-α has also been shown to stimulate amyloid precursor protein (APP) promoter activity (69) and evidence exists that at least FSH is capable of direct stimulation of osteoclastic bone resorption (70).

Due to the reduction in bone strength and mass, osteoporosis leads to a significant increase in fracture risk, which is detrimental to human health and wellbeing. Hip fractures associated with frailty and osteoporosis usually occur at the femoral neck (56%), pertrochanteric region (38%) or subtrochanteric region (5.8%). When these fractures occur in the ageing population, they are usually a result of a fall or minimal trauma, associated with poor bone quality and strength. The AIHW reported in 2016 that ~95% of hospitalisations associated with hip fracture had >1 comorbidity (hypotension, anaemia, delirium or type II diabetes mellitus) (62). Hip fracture is

associated with premature death, when compared to the normal healthy population without a sustained hip fracture (71).

Osteoarthritis

Osteoarthritis (OA) is a chronic musculoskeletal disorder of unknown aetiology. The hallmark features of OA are articular cartilage degradation, synovial inflammation and abnormal bone remodelling (72-74). In Australia, 9.3 % of the population have a reported OA diagnosis, with the majority of those people being female. The risk for developing OA increases with a myriad of factors such as age (75) with risk increasing substantially after the age of 45 (76), obesity (77), genetic predisposition (78), biomechanical stress (79) and systemic inflammation (79). OA most commonly affects the joints of the hands, knees, hips, spine and feet. The pain associated with the onset and development of OA results in a reduction in the quality of life of individuals with an OA diagnosis. OA is diagnosed based on radiographic changes in at least one joint, indicated by the presence of osteophytes.

Like osteoporosis, OA is a leading cause of disability in the world. OA is the most commonly diagnosed form of arthritis in Australia, however OA of the knee holds the highest prevalence within Australia (74, 80). Knee OA (KOA) affects up to 50 % of people aged over 65 years (76). Without and in some cases, with pharmacological management of KOA, there is still a high degree of pain associated with the degeneration of the articular cartilage component. The most common explanation for KOA is “mechanical wear and tear” associated with ageing, substantial load bearing and disease; however, the chronic inflammatory response is being investigated as not only a result of OA, but also as a contributor to neurodegenerative disease, which will be explained. As OA is associated with inflammation, inflammatory mediators are the main drug targets. Treatment for OA is classified as either pharmacologic or non-pharmacologic. The main pharmacologic treatments to date are non-steroidal anti-

inflammatory drugs (NSAIDs) (81) and cyclooxygenase-2 (COX-2) inhibitors, which target inflammation and pain. Intraarticular cartilage injections are another mode of treatment, which attempt to reduce swelling associated with disease progression and pain (82). Unfortunately the reported analgesic effects are quite variable between patients and also very short-lived, therefore making this treatment option controversial (83). The main non-pharmacologic approach to treating OA is physical activity. Different exercise approaches such as land-based exercise and swimming have been shown to improve function and reduce pain in knee and hip OA (84, 85). Due to the large degree of heterogeneity between treatment outcomes in OA, a new approach to treating underlying cellular changes occurring throughout OA development should be investigated.

Central Nervous System Background

The Central Nervous System

The Central Nervous System (CNS) is considered the master regulator of the body. The two main components of the CNS are the brain and spinal cord. The brain and spinal cord work together to control the central regulation of the body. The CNS is composed of a number of cell types, the main type being the neuron. Neurons communicate with each other in a highly regulated network via axons and synapses, which extend out from the cell soma. These cells control bodily functions dependent on the brain region in which they are located. For example, neurons located in the hippocampal region control the formation and storage of memories, both semantic and episodic. In neurodegenerative diseases, specifically in AD, the hippocampal neurons are thought to be attacked by misfolded proteins existing as extracellular neurotoxic oligomers and intracellular neurofibrillary tangles, leading to the degeneration of neurons and a loss of function of the brain tissue in this region (86). Another example can be seen in Amyotrophic Lateral Sclerosis (ALS) where motor neurons located in the motor cortex of the brain and control skeletal muscle contractions are targeted and destroyed, leading to severe disability and ultimately death (87). Microglia and astrocytes are the other types of cells found in the CNS. Microglia account for 10-15% of CNS cells and play the role of the resident macrophage-like cell in the brain, responding to noxious stimuli and foreign molecules. Under homeostatic conditions, microglial cells recognise and take up foreign bodies, basically acting as antigen-presenting cells. Under pathological conditions, microglia become activated and stressed. When this occurs, it can be detrimental to the brain tissue, as it can result in inflammation and oxidative stress.

The Amyloid Beta (A4) Precursor Protein

The Amyloid Beta (A4) Precursor Protein (APP) is a 100 kDa type I transmembrane glycoprotein, which is encoded by the *APP* gene located on chromosome 21q (88). APP is composed of an extracellular domain, a transmembrane domain and a 50 amino acid (AA) long cytoplasmic tail domain (89). APP can be alternatively spliced at two exons to form isoforms. To date there are at least 10 known isoforms of APP, however the most common are the APP695, APP751 and APP770 amino acid forms (90). APP695 is predominantly expressed in the CNS whereas APP751 and APP770 can be found in peripheral tissues (91). APP is a member of the APP family, which in mammals includes the amyloid precursor-like proteins APLP1 and APLP2 and the amyloid precursor-like (APPL) in Drosophila (92). APP and APLP2 are both expressed ubiquitously while APLP1 expression is restricted to the brain (93).

APP has been widely researched for its physiological functions in the central nervous system (CNS) (94) as well as for its roles outside of the CNS. Izumi et. al established that the promoter region of *APP* was highly homologous between the human *APP* and mouse *App* genes whereas homology differed substantially in rats, indicating that murine models were closer to humans (95). In order to study the physiological functions of APP and its homologues, murine knock-out models have been developed. One of the first murine models developed was the single *App* knockout (APP KO) model by Zheng *et al.* in 1995 (96). APP KO mice were generated through the deletion of the 3.8 kB promoter encoding sequence and first exon to prevent *App* mRNA transcription. Results from this study revealed that at 14 weeks, the homozygous APP KO mice were fertile and viable but displayed reduced body weight, decreased locomotor activity, reduced forelimb grip and reactive gliosis (96). Further research into this model has identified a role for APP in vascular function in male APP KO mice (97). These results indicate functional roles for APP in development of the brain and vasculature as well as in neuroprotection. Full-length APP undergoes a series of proteolytic processing events, which result in the production

of a number of smaller protein fragments. These protein fragments are produced either through the non-pathogenic or pathogenic cleavage of APP by a family of secretases (α, β and γ) (98).

Proteolytic Processing of APP

There are two main proteolytic pathways known for full-length APP regulation, the non-amyloidogenic (α-secretase) and amyloidogenic (β-secretase) pathways. Cleavage of APP via the α-secretase pathway is non-pathogenic the initial cleavage event by α-secretase occurs within the amyloid beta (Aβ) domain, rendering production of the Aβ peptide impossible. The α-secretase enzyme first cleaves APP near the plasma membrane, which generates the production of the N-terminal fragment – soluble APP-alpha (sAPPα) and C-terminal fragment 83 (CTF-α/C83) (88). C83 is membrane-bound, whereas the sAPPα fragment is released into the extracellular space or into intracellular vesicles. Further processing of the membrane bound C83 terminal domain by γ-secretase, results in the release of the p3 peptide into the extracellular space and the APP intracellular domain (AICD), which is released into the cytoplasm (99). These cleavage events produce products thought to be involved in several neurodevelopmental events such as: neuroprotection, synaptic plasticity, cell adhesion as well as neuronal differentiation and proliferation (100). APP is initially cleaved at the N-terminus of the Aβ domain, located in the trans-Golgi network or in endosomes by the β-secretase cleaving enzyme-1 (BACE-1). This event generates the N-terminal C99 fragment and soluble APP-β fragment (sAPPβ), which like sAPPα, can be taken up by intracellular vesicles or released extracellularly. The membrane-bound C99 fragment is then cleaved by γ-secretase at the endoplasmic reticulum. Subsequently, the APP-CTFβ is cleaved by γ-secretase, resulting in the formation of the AICD and release of the Aβ peptide (usually between 1 and 43 amino acids in length) into the extracellular space (101) (**Fig. 3**).

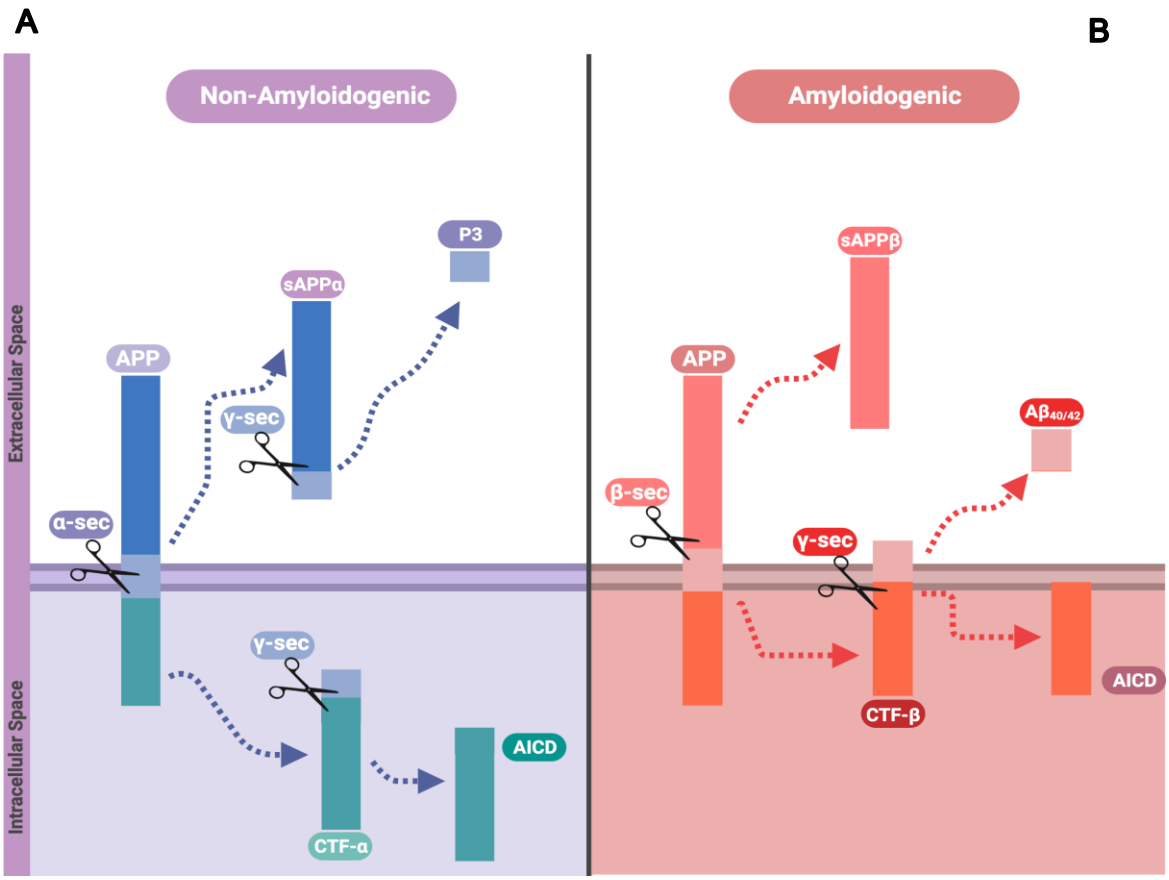

Figure 3: Proteolytic processing of Amyloid Beta (A4) Precursor Protein

(A) In contrast, APP can also be processed by α-secretase in a process known as ectodomain shedding. APP is cleaved by α-secretase resulting in the soluble APPα (sAPPα) product and an APP-CTF-α fragment. Processing by γ-secretase of the APP-CTF-α fragment results in the formation of the p3 peptide and the AICD. There is no production of Aβ via this proteolytic cleavage pathway, thus it is rendered non-amyloidogenic. **(B)** Cleavage of APP by β-secretase occurs in the N-terminus of the Aβ region, which forms a secreted APPβ (sAPPβ) fragment and a C-terminal fragment (APP-CTFβ). The CTFβ then undergoes cleavage by γ-secretase resulting in the formation of the APP Intracellular Domain (AICD)

Physiological Roles of APP

Functional roles for APP that have been identified within the CNS, include aiding in neuronal proliferation (102, 103), neurite outgrowth (104), synaptogenesis (105) and neurogenesis (106). The full extent of the physiological functions of APP are still not elucidated both within the CNS, as well as in the peripheral organs. In order to study the function of the *App* gene *in vivo,* a number of animal models have been created. Models of genetic deletion, conditionally expressed or overexpressed have been developed. These models have been established in a number of different species including *C. elegans* (roundworm) (107), *dropsophila* (fly) (108, 109), *Danio rerio* (zebrafish) (110), as well as numerous murine models. The expression of APP at the mRNA and protein level is now known not to be restricted to the brain. Different approaches to assess expression of *App* at the mRNA level have been used such as RNA sequencing (RNAseq), Microarray and Serial Analysis of Gene Expression (SAGE). Each of these techniques detect different levels of the candidate gene in different tissue types. *App* was detected in the bone marrow by Microarray and SAGE, but not by RNAseq for example. Detailed information for mRNA expression of *APP* is not available for bone. APP expression has been identified in a number of tissues at the protein level, including but not limited to, kidney, liver, heart, bone, lungs, cerebrospinal fluid (CSF), serum and pancreas (111). The levels of expression vary between tissue types with the highest levels of expression found in brain tissue and CSF and the lowest detected in the heart.

The Amyloid Beta (A4) Precursor like Protein-2

The other ubiquitously expressed member of the APP family, Amyloid Beta (A4) Precursor like Protein-2 (APLP2) has a similar expression pattern and shares a high degree of homology with APP. The main structural difference between APP and APLP2 is the lack of the Aβ domain in APLP2. Cleavage of the Aβ domain is responsible for the release of the peptide,

which can lead to the formation of pathological Aβ peptides, thus APLP2 expression does not exhibit pathological effects by virtue of Aβ. Due to the high degree of sequence homology shared between the APP and APLP2 proteins, it is possible that they may be functionally related. The individual physiological roles carried out by APLP2 are similar to that of APP and include cell growth, survival, metabolism and immune receptor expression (104). Like APP, APLP2 has been recognised for its potential role in tumour cell proliferation and migration. This can be seen in specifically Ewing's Sarcoma and Pancreatic cancer (112). It was shown to be abundantly expressed in these cancers and functioned by assisting cancer cells in the avoidance of death by T cells (113).

A combined *App* and *Aplp2* knocked out in C57Bl/6 mice ($App^{-/-}$ and $Aplp2^{-/-}$) resulted in post-natal death in 80% of the colony. It was proposed that *App* and *Aplp-2* genes held similar roles in postnatal development supporting a functional relationship between these genes (114, 115). Several studies went on to show that APP and APLP2 may possess roles in insulin and glucose homeostasis, growth (116) neuronal plasticity, synaptic morphology (92) and spatial learning (94). In contrast, the other member of the APP family, APLP1, located exclusively in the CNS and did not produce the same effects when alleles were knocked out. In the nervous system-specific APLP1 KO mouse, the main finding was a deficit in postnatal growth, but locomotor activity and grip strength remained unchanged when compared to wild-type control mice (115). If APLP2 function is dependent on or regulated by APP, it may be useful to also investigate the expression of APLP2 in the context of the bone, to elucidate possible related functionality.

The Amyloid Beta (Aβ) Peptide

The amyloid beta (Aβ) peptide is typically a 39 – 43 amino acid length protein produced by the proteolytic processing of APP. The two main variants of Aβ studied are the 40 and 42 residue proteolytic fragments. $A\beta_{1-40}$ is the predominant form produced in the brain, whereas $A\beta_{1-42}$ is the main variant found in Aβ plaques, a pathological hallmark of Alzheimer's disease (117). The insoluble $A\beta_{1-42}$ protein was first isolated from deposits in cerebrovascular amyloid angiopathy in human AD subjects upon post-mortem brain processing by Glenner and Wong in 1984 (118) and confirmed by Masters *et al.* in 1985 in the context of Down's Syndrome and AD (119). The discovery of $A\beta_{1-42}$ gave rise to the Amyloid Cascade Hypothesis (120), that senile plaques containing $A\beta_{1-42}$ could interfere with neuronal function and initiate the hyperphosphorylation of Tau protein, leading to the accumulation of fibrillar Tau tangles (121), and mediating neuronal cell death. In the context of Alzheimer's disease Aβ can be measured in the plasma and cerebrospinal fluid (CSF) as a possible biomarker of disease. The $A\beta_{1-42/1-40}$ ratio has been used as an indicator of disease severity for a number of years, however results have been controversial between studies with some reporting that a decreased $A\beta_{1-42/1-40}$ ratio correlated with disease onset and others have reported no clear relationship between disease onset, plasma or CSF $A\beta_{1-42/1-40}$ ratios. Results from the Australian Imaging, Biomarker & Lifestyle Flagship of Ageing (AIBL) study, a longitudinal study of participants over the age of 60, found that using plasma $A\beta_{1-42/1-40}$ provided a reliable biomarker for prediction of amyloid detection using Positron Emission Transmission (PET) scanning in these patients with a 77% sensitivity rate (122).

Despite APP being identified in peripheral tissues in a number of studies, there is not a large amount of evidence to support production of Aβ outside of the brain. To date, there have been a total of two studies to establish the production of Aβ in the bone (123, 124). Li *et al.* demonstrated increased mRNA expression of APP and $A\beta_{1-42}$ in osteoporotic bone biopsies

from humans and ovariectomised rats compared to control subjects. It was also established that $A\beta_{1-42}$ has the potential to stimulate osteoclast differentiation and activation, however the mechanism behind this observation was not alluded to (124). This is an area that requires further investigation at the molecular level.

Ageing, Dementia & Alzheimer's Disease

Ageing is a phenomenon commonly associated with death and disease. This process results in a number of changes, such as marked differences in body composition, energy production and energy utilisation. These changes can be detrimental to human health and well-being and result in the development of disease. During ageing, it is common for people to exist with chronic, low grade inflammation, referred to as "inflammaging" (125). Though low grade, the chronic nature of inflammaging is thought to create a damaging cellular environment (126). Studies have shown that inflammation and oxidative stress as a result of these inflammatory cascades can be a contributing factor in the development of neurodegenerative disease as well as bone disease. With increasing age, it is common for individuals to develop a number of comorbidities, of which neurodegenerative disease, bone disease and cancers are the most common (127). A clear common link between the development of AD and bone diseases, such as osteoporosis, is age.

"Dementia" is an umbrella term used to describe a group of neurodegenerative disorders, resulting from a dysregulation in the normal processes controlling brain functions and resulting in alterations in cognition. Dementia covers a number of different pathologies including Frontotemporal dementia, vascular dementias, Lewy Body dementia, dementias associated with Parkinson's disease, Huntington's disease, brain injury and alcohol consumption and finally Alzheimer's disease (AD) (**Fig. 4**). AD is the most prevalent dementia in the world, accounting for up to 70 % of all dementia diagnoses (128). In 2015 Alzheimer's disease

International (ADI) estimated a 5.2% global prevalence of dementia, equating to 46.8 million people living with dementia worldwide. The number of global dementia cases, based on no improvement in interventional therapies, is set to rise to 131 million by the year 2050 (128). Data now shows that there are at least 10 million cases of mild cognitive impairment (MCI) that progress to dementia every year (129). In 2017, dementia and AD were the second leading cause of death in Australians over the age of 75 behind coronary heart disease, and AD was the primary cause of death for females (11%) (130).

Development of AD can be due to gene mutations, which can be detected through gene sequencing, however the most common type of AD is sporadic in nature, with no associated gene mutations. Sporadic, late-onset AD (sLOAD) is the most prevalent form of AD, accounting for up to 95% of all AD cases. The pathological mechanism underlying its development is still in question, however the most widely accepted explanation for its pathogenesis is the Amyloid Cascade hypothesis (120, 131-133) (Fig. 5). Individuals at high risk for AD development are commonly over the age of 65 and female (134), however the highest risk factor for development is allelic variation in the Apolipoprotein E4 (*APOEε4*) gene (135). In AD, genetic inheritance of the *APOEε4* allele has been known to increase the risk of development in an age-dependent manner, which increases significantly in individuals after the age of 65. APOE is normally involved in mobilisation and redistribution of cholesterol and in the brain has been shown to aid in neuronal growth and repair (136) and the immune response (137). The APOEε4 isoform binds to Aβ at a rapid rate, which is thought to increase the density of the Aβ fibrils, making them more difficult clear from the brain (138).

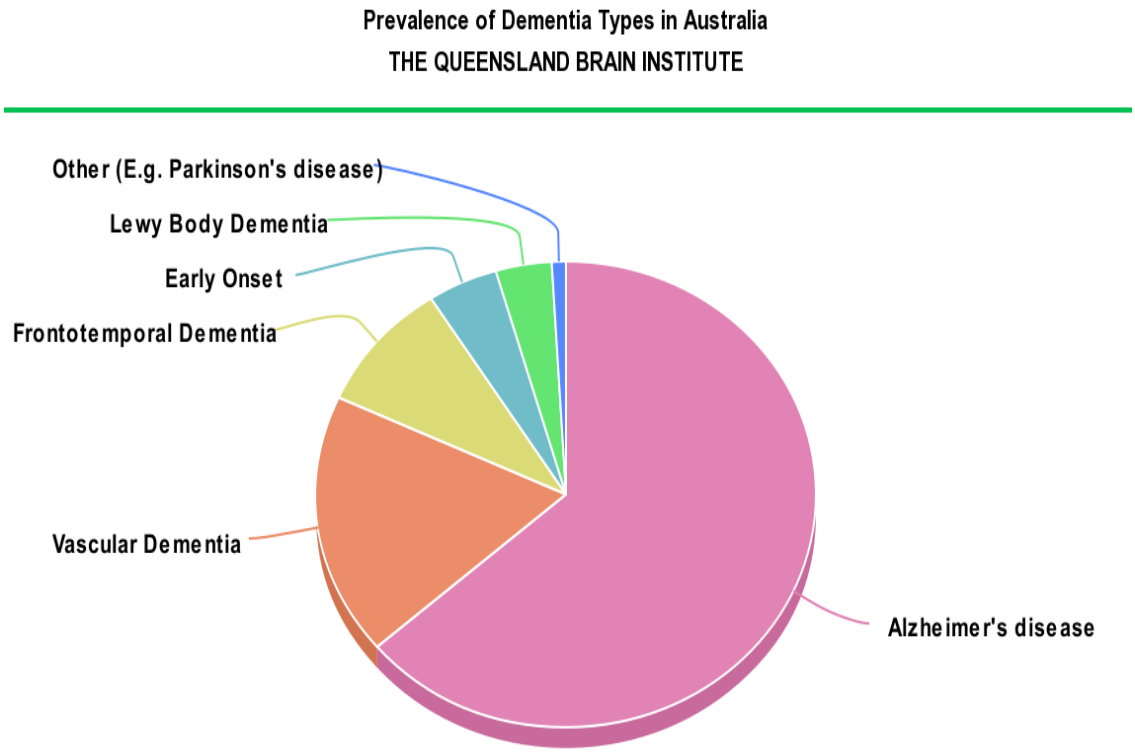

Figure 4: A visual representation of the prevalence of the most common dementia subtypes in Australia. Alzheimer's disease (60 – 70%); Vascular dementia (10 – 20%); Frontotemporal dementia (10%); Lewy Body dementia (4%); Early onset AD (1 – 5%); Other types seen in neurological diseases (< 1%). – *Data adapted from The Queensland Brain Institute – 8 Aug 2019*

Alzheimer's disease Development

The pathological hallmarks observed in AD are the formation of extracellular Aβ plaques and intracellular neurofibrillary tangles (NFTs) in the mediotemporal lobe (hippocampus, amygdala and entorhinal cortex) and its related neural networks in the brain (139). Initially, the development of Aβ plaques interfere with the normal functioning of the neurons through directly blocking synaptic transmission of neurotransmitters, which in turn initiates the hyperphosphorylation of Tau protein and formation of NFTs thus blocking transport of essential nutrients such as glucose within the neurons (**Fig. 5**). The brains response to these unwanted disruptions is to activate the resident macrophages of the brain, the microglia to take up and degrade Aβ plaques. This process induces chronic inflammation as the microglia are unable to successfully remove Aβ, which compromises brain integrity and neuronal viability (86, 140). As a result of these changes occurring in the brain, individuals developing AD exhibit symptoms such as a deterioration in episodic memory, behavioural disturbances, inability to recognise family members, an inability to carry out usual everyday tasks and eventually as the disease progresses to end stage an inability perform essential motor functions and eventual death (141).

Therapeutic Intervention

There is currently no proven prevention therapy or cure for AD. As is the case with most diseases of ageing, lifestyle modifications have been investigated for risk reduction and potential therapies, with a reported figure of one third of all AD cases could be prevented through lifestyle modifications (142, 143). Therapeutic treatments for AD have not been successful despite the in-depth understandings of the Aβ and Tau components of the disease. Targeting of neurotransmitters, which regulate normal brain activity has been the most successful therapy to date. The most commonly prescribed interventional drugs in clinical

practice are the Acetylcholinesterase Inhibitors (AChEI), marketed under the names Tacrine, Donepezil (144, 145), Rivastigmine (146) or Galantamine (147, 148). The use of AChEIs in AD was proposed based on the Cholinergic Hypothesis, which proposes that at the later stages of the disease there is a loss of cholinergic neurons, causing a marked reduction in circulating Acetylcholine (ACh) as a result of long-term oxidative stress from the generation of extracellular Aβ (149) and intracellular Neurofibrillary Tau tangles (150, 151). A dramatic loss of cholinergic neurons and activity in the forebrain, cerebral cortex and hippocampus (152) causative of a reduction in patient cognition and memory in cases of mild/moderate AD has also been observed (153). AChEIs target the AChE enzyme responsible for the degradation of Ach, one of the most important neurotransmitters in the brain, which controls muscle contraction, pain response activation and endocrine regulation (150). These drugs act centrally and provide vast improvements to memory and cognitive ability; however, these improvements are only short term, lasting from 1 – 3 years, as the pathological changes cannot be reversed by the AChEIs. Without the development of a deeper understanding of AD mechanisms and the contribution of other molecules to AD development, the burden of AD will continue to worsen.

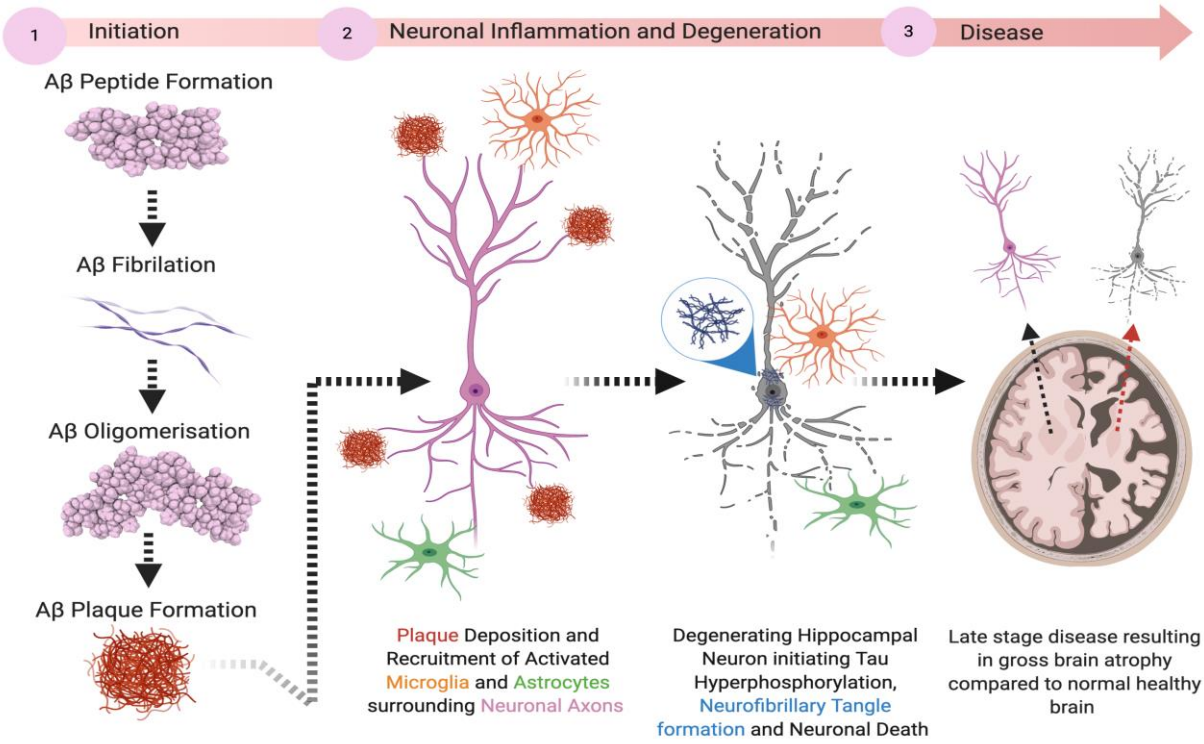

Figure 5: Schematic representation of the development of Alzheimer's disease based on the Amyloid Cascade Hypothesis. *1. Initiation* - Following the preferential cleavage of APP, Aβ peptides are released into the extracellular space where they oligomerise and accumulate into Aβ plaques. *2. Neuronal Inflammation and Degeneration* - Aβ plaques localise to neuronal axons and local inflammatory cells; microglia and astrocytes are activated in an attempt to clear the plaques. The inability to degrade Aβ plaques initiates neuronal inflammation and degeneration. The subsequent disruption in intracellular tau protein phosphorylation results in tau hyperphosphorylation and the formation of neurofibrillary tau tangles, which disrupt the metabolic processes within the neurons. *3. Disease* - These events lead to eventual neuronal cell death and brain tissue death, causing atrophy and the symptoms associated with Alzheimer's disease.

Early Onset Familial Alzheimer's disease

Early onset Familial Alzheimer's disease (eFAD) is a subtype of AD, accounting for up to 1-5% of all AD cases worldwide (Fig. 3). The large variation in cases has been estimated to incorporate undiagnosed individuals with eFAD. This subtype of AD affects individuals under the age of 65 and from as young as 30, with reports of development of pathological changes occurring up to 22 years before symptom presentation (154). Autosomal dominant mutations in the *APP* gene itself as well as missense mutations in the presenilin-1 (*PSEN1*) and presenilin-2 (*PSEN2*) genes (155) have been identified as known initiators of this genetic subtype of disease (98, 156). Mutations in the *APP* gene increase the rate of production of $A\beta_{1-42}$, reduce the clearance of $A\beta_{1-42}$ and increase the $A\beta_{1-42}$: $A\beta_{1-40}$ ratio. These mutations result in an increased Aβ production throughout life. PSEN1 and PSEN2 are subunits of the γ-secretase enzyme, responsible for the second stage cleavage of APP. There have been a number of murine models established with these mutations in order to understand the development of eFAD. Using *in vivo* and *in vitro* knock-in models containing mutated *PSEN1* and *PSEN2* have shown early formation and deposition of $A\beta_{1-42}$ as well as an increased production of $A\beta_{1-42}$ in a dose-dependent manner (157).

Current Links between Brain and Bone

Osteoporosis and Alzheimer's Disease/Dementia

Osteoporosis and Alzheimer's disease share a myriad of risk factors. These common risk factors shared between these debilitating diseases have formed the basis for the hypothesis that they are linked in their development. Risk factors shared between osteoporosis and AD include: Age (> 65), gender (with prevalence in females being greater than males in both diseases), chronic inflammation, *APOEε4* genotype, inactivity, Vitamin D deficiency, alcohol consumption and smoking. As well as sharing many common risk factors, it has been observed that osteoporosis and hip fracture occur at an increased rate in AD patients (158-160). Studies have focused on determining links between increased risks of dementia in osteoporosis patients (161), increased risk of osteoporosis specifically in AD patients (162) and low bone mineral density (BMD) and bone loss as risk factors for progression from mild cognitive impairment (MCI) to AD (163). However, there is still a large gap in our knowledge as to whether or not these pathologies are causal of each other by virtue of an underlying biological mechanism.

It is well established that bone mineral density (BMD) reduces throughout the ageing process (164-166). As reduction in BMD is one of the earliest indicators of the development of osteoporosis, it may also serve as a possible indicator of risk for the development of AD. Yaffe et.al conducted a prospective cohort study measuring calcaneal and hip BMD and cognition in an ageing cohort of post-menopausal women who were not undergoing oestrogen replacement therapy. Groups were stratified based on BMD T-scores: T-score <-2.5 – low BMD; T-score >-2.5 – regular BMD. An 8% reduction in cognitive scores of women in the low BMD group (T-score <2.5) when compared to women with a "normal" BMD was reported and women in the low BMD group had a 32-33 % greater odds ratio of cognitive deterioration (167). A recent meta-analysis conducted by Xiao-Ling et.al analysed over 30 papers in this research area and

concluded that there was an association between declining BMD, specifically in the femoral neck region, and AD, and AD patients were at a marked risk of developing osteoporosis and had a markedly reduced BMD when compared to all control groups (167). As vertebral and hip fractures in the elderly can be deleterious to quality of life, it is important to identify factors that put the elderly at increased risk of fracture. Positive associations between dementia, AD and fracture risk have been established in a number of studies (168-171). The Concord Health and Aging Project, a longitudinal study, which followed a cohort of 1705 community-dwelling men over a 6 year period found that the individuals who went on to develop dementia (n = 93), but not MCI (n = 120), had the highest risk of hip fracture (n = 43), but not vertebral fracture (n = 32) or other non-vertebral fracture (172). A retrospective cohort study of 10,052 patients investigated the difference in hip fracture development between newly diagnosed AD individuals and non-AD controls between 1988 and 2007 in the UK. Multivariate analysis established an overall increase in hip fracture among the AD cohort (173).

As previously mentioned, Aβ has been detected in osteoporotic human vertebral bone tissue (124) and has been shown to stimulate RANKL-induced osteoclastogenesis (174) in Tg2576 mice carrying the Swedish mutation of APP, which increases Aβ production. With the reduction in oestrogen occurring at the time of menopause, women may be at higher risk of development of osteoporosis and AD by virtue of increasing Aβ production. Further investigation into this relationship could provide evidence for detection of early pathological changes associated with AD development through routine testing of bone biopsies from post-menopausal fracture patients and oestrogen deficient male osteoporotic fracture patients. Aβ overproduction has also been linked to reduced activation of osteoblasts *in vivo* also using the Tg2576 mouse model of AD (175). In this model, the authors demonstrated a reduction in osteoblast formation, bone formation and enhanced osteoclast formation, suggesting a role for the *APPSwe* mutation in development of osteoporotic bone loss. These findings suggest that

overproduction of Aβ may contribute not only to the disruption in neuronal function seen AD brain but may also contribute to the development of osteoporosis through disrupted bone remodelling.

Inflammation, Osteoarthritis and Alzheimer's disease

Inflammation is a process by which the body's immune system responds to exposure to a foreign pathogen or pain stimulus. This response is mediated by a number of pro-inflammatory cell-types, cytokines and chemokines in an attempt to remove foreign molecules or signal pain. Inflammation is usually a beneficial process elicited to reduce the effects of infection and tissue damage, however if it occurs in a chronic and unregulated manner it can be detrimental to human health (176). There are two types of inflammatory response, type 1 and type 2. Type 1 is activated in response to rapidly replicating microorganisms such as bacteria and viruses and activates and adaptive immune response. Cell types involved in the innate immune response include T helper 1 (Th1) cell-associated cytokines interferon- γ (IFN-γ) and interleukin-12 (IL-12). Type 2 occurs in response to physical trauma resulting in damage to tissue and disruption to tissue integrity. A type 2 response elicits the activation of basophils, macrophages, mast cells, TH2 cells and eosinophils at the site of damage to begin the tissue healing process.

The involvement of chronic and acute inflammation has been recognised in a myriad of neurodegenerative disorders including AD (177) and ALS (178). It is also well characterised in the development of other peripheral diseases such as OA, rheumatoid arthritis (RA), Diabetes Mellitus, Obesity (179) and Myocardial Infarction (MI) (180). The inflammation induced in these diseases occurs in response to destruction of tissue due to extrinsic factors. Inflammation has been well characterised in AD mouse models (181) and in human AD patients (182-184), supported by the discovery of number of pro-inflammatory chemokines

and cytokines shown to be upregulated in AD (TNF-α (185), IL-1 (186), IL-6 , IL-12 and IL-23 (187)).

The brain is believed to be an immuno-privileged site; however, this is not necessarily the case in the context of disease. With increasing age, inflammation and disease status, the blood-brain barrier (BBB), which is usually tightly regulated and impermeable, becomes permeable or "leaky" (188). A leaky BBB can result in the admission of larger peripheral molecules into the brain. Peripheral inflammation is under investigation as a potential contributor to the development of neurodegenerative disease (189). Evidence for the peripheral production of Aβ from different tissues may contribute to the development of AD. One research group parabiotically joined Tg APPswe/PS1dE9 mice containing humanised AD mutations with wild type littermates to test whether circulating Aβ could be transferred via the bloodstream. A positive transfer of humanised Aβ between Tg APPswe/PS1dE9 after 12 months of parabiosis was detected in the circulation and brains of wild type mice, as were signs of cerebral amyloid angiopathy and Aβ plaques (190). These findings suggest that it is possible for Aβ to travel through the blood stream and across the blood brain barrier of otherwise normal animals and initiate disease, supporting the periphery as a source of Aβ production.

As one of the major underlying components of OA disease progression and severity is inflammation, it has been proposed that the inflammation occurring in distal joints may contribute to the development of AD (189, 191). Very little research has been conducted into the connections between OA and AD. In a paper by Kyrkanides et al., (191) findings supported the hypothesis that systemic inflammation typically seen in OA could potentially contribute to development and progression of AD in transgenic OA mice (191).

There is a high prevalence of pain-associated disorders in dementia patients. In one study of 28,047 participants, all with reported dementia subtypes (AD, vascular or other), 49.07 % of

the population suffered from at least one pain-associated disorder including OA, osteoporosis and headache. The most common of the three was OA, with 29.27 % of all individuals with an OA diagnosis (192). In humans, clinical research conducted on individuals undergoing knee or hip arthroplasty for OA showed a significant increase in mortality 5-years post-operation in patients with both OA and AD, in comparison to OA controls (193). Women over the age of 65-years lose cortical bone at an increased rate (194) and this is a feature of both osteoporosis and OA (195, 196).

Wnt/β-catenin Pathway Signalling and Dikkopf-related protein 1

The Wingless-related integration site (Wnt) signalling system is an evolutionarily conserved pathway crucial for embryonic development of all vertebrates and invertebrates (197). The Wnt proteins are a group of secreted glycoproteins, which ultimately regulate the proliferation of all cell types throughout growth and development. There are three different types of Wnt signalling pathways: The classical Wnt/β-catenin pathway, the planar cell polarity (PCP) pathway and the Wnt/Ca^{2+} pathway. The canonical Wnt/β-catenin (classical) pathway has been shown to play roles in the development and maintenance of bone as well as the CNS. In the context of bone, Wnt/β-catenin signalling is essential for osteoblast proliferation and differentiation (198). In the CNS Wnt signalling has been shown to be important in the processes of axon guidance, neuroblast migration, neural crest formation and neuronal proliferation and differentiation (199). Dysregulation of Wnt signalling is well characterised in the context of cancer. Without the proper regulation of the pathway, normal processes regulating cellular proliferation go unchecked resulting in uncontrolled cancer cell proliferation (200, 201).

In order for successful Wnt signalling to occur, Wnt molecules must bind to low-density lipoprotein related-receptor proteins 5 and 6 (LRPs) and Frizzled (Fzd) receptors to form a

receptor trimeric complex (202). The formation of this complex can be inhibited by a number of Wnt pathway inhibitors. The potent antagonist of Wnt signalling, Dikkopf-related protein 1 (Dkk1) is involved in regulation of the bone and brain microenvironments. Dkk1 blocks Wnt activity through binding to the Wnt co-receptors LRP5 and 6. Through this competitive binding of LRP5/6, Dkk1 prevents Wnt from forming a signalling complex with its cognate membrane receptor, Frizzled (Fz) as well as its co-receptors LRP5/6.

When Dkk1 is expressed at homeostatic levels in the body, it plays crucial roles in limb development (203), neural tube development and neurodevelopment (204). In the bone, secreted Dkk1 inhibits osteogenesis and osteoblast activity and mediates bone loss. With ageing, it has been shown that dysregulation leading to over expression of Dkk1 can be causative of inflammatory events, bone erosion, low BMD giving rise to the potential to develop osteoporosis (205). To support this, it has been demonstrated Dkk1 depleted mice display an increase in bone mass and mineralisation (206). Overexpression of Dkk1 can inhibit neuronal proliferation and differentiation, which can ultimately result in neuronal degradation and death (207). As Dkk1 can negatively regulate bone remodelling and CNS functions, it has brought to the attention of researchers that it may be a missing link between the bone and the brain.

Recent literature has proposed a possible role for this canonical Wnt signalling pathway antagonist in AD (207). As previously mentioned, Wnt proteins have been identified for their crucial roles in CNS and bone development and the regulation of bone remodelling, therefore it is plausible that Wnt proteins may provide a connection between neuronal and skeletal dysfunction (208). Activation of the canonical Wnt-signalling pathway by overexpression of the agonist Wnt3a or β-catenin or by inhibition of glycogen kinase synthase-3 in N2a cells was shown to reduce expression levels and activity of β-APP cleaving enzyme (BACE1), which in turn led to the reduction of Aβ peptides (207). Other studies focused on the dysregulation of

the canonical Wnt pathway and its negative effects on the brain and bone (208, 209). Dysregulation of this signalling in the brain also has been linked with microglial activation and recruitment of inflammatory cells. The recruitment process then creates an inflammatory response and as a result, oxidative stress, which is known to be damaging to cells can occur. This process is thought to contribute to the AD pathogenesis and progression as it can damage neurons and other cells of the neurovascular unit. Furthermore, oestrogen is thought to be both neuroprotective as well as protective against Dkk1 (208), thus overexpression of Dkk1 by virtue of disruption to the Wnt signalling pathway may be more likely in the aging population and in particular post-menopausal women with decreased oestrogen levels.

Nerve Growth Factor

Nerve growth factor (NGF) is well characterised in the literature as a neurotrophic factor with its main roles being carried out in the CNS, with other functions recognised in the endocrine and immune systems (210). NGF has been characterised in peripheral tissue containing sensory and nerve inputs such as within the bone and cartilage in fracture and normal states (211). Its reported physiological properties include promoting neurite growth, survival and differentiation in both peripheral sensory and sympathetic neurons (210). NGF and its precursor pro-NGF elicit their responses through binding to receptors or tyrosine kinase receptor (TrkA) or pan-neurotrophin receptor (p75NTR) respectively (212). TrkA and p75NTR were once thought to be exclusively expressed in the CNS, however it has also been demonstrated that they are also expressed in cancer tissues such as breast (213-215) and prostate (216, 217), where they are implicated in both carcinogenesis and survival, depending on expression levels. Deep somatic structures such as muscle, joints and bone are innervated with type C-fibres and activation of free nerve endings is usually associated with dull pain sensations (218). NGF and its precursor form (pro-NGF) have been implicated in pain associated with inflammation in OA, where osteoarthritic chondrocytes show high levels of

NGF mRNA expression (219). Despite its involvement in pain nociception, NGF has been correlated with improved outcomes of fracture (220) as well as reduce fracture healing time in TBI patients (221). Due to its expression being highly reported in both the brain and the bone, NGF may provide evidence of a potential linking molecule between AD and bone diseases by virtue of its involvement in pain and inflammatory pathways.

Insights from Down's syndrome

Down's syndrome (Down syndrome, Trisomy 21; DS) is a neurological chromosomal condition and has an incidence rate of 1 in every 800 live births. Individuals with DS display a number of behavioural and cognitive symptoms such as attention problems and obsessive/compulsive behaviours. A small proportion of individuals are also affected by autism spectrum disorders, which negatively influence communication skills as well as their intelligence quotient (IQ). As chromosome 21 is triplicated in DS, there is also a triplication of the *APP* gene, which as previously mentioned resides on chromosome 21. With recent reports of increases in lifespan to 50 years of age noted in the literature, the development of osteoporosis and AD in DS individuals is of high significance (222, 223). It has been reported that approximately 50% of all DS individuals will go on to develop Early Onset AD. The EOAD seen in DS individuals has been linked to mutations in the *APP* gene, like that seen in genetic-linked AD in non-DS individuals. Post-mortem brain analysis has shown the presence of both senile Aβ plaques and neurofibrillary tangles in the brain tissue of DS individuals with an AD diagnosis (224). The same study also revealed that prevalence of EOAD is not only higher in DS individuals, but is also more aggressive in nature, progressing quite rapidly leading to an early deterioration (224). Development of AD is usually detected in the third decade of life and reduces life expectancy significantly in people suffering from both DS and AD.

DS individuals are smaller in stature and have an overall lower bone mass and BMD compared to age and gender-matched controls (225). In 2013, McKelvey et.al, conducted a study into the effects of DS on bone turnover and bone density in a cohort of 30 DS subjects using DXA imaging and blood derived bone turnover markers. DXA imaging revealed 53.3% of the study group had a low BMD (Z-score < -2) at one of multiple sites (lumbar spine, distal radius, femoral neck and proximal femur). Serum P1NP was significantly reduced in the low BMD group, but there was no change in serum CTX between groups, suggestive of a reduction in bone formation (226).

Transgenic mouse models of DS have provided a great insight into the phenotypes associated with ageing in DS. Fowler et.al investigated the transgenic DS mouse model (Tg Ts65Dn) to determine effects of DS on bone structure and function. Marked changes were observed in the cortical and trabecular bone of the femorae and tibiae, with an overall decrease in the number of osteoclasts and osteoblasts per bone surface, as well as reduced serum levels of markers such as TRAP5b and procollagen type 1 N propeptide (P1NP), indicative of a decrease in bone resorption and formation respectively (227).

With recent reports of increases in lifespan to 50 years of age noted in the literature, the development of osteoporosis and AD in DS individuals is of high significance (222, 223). These studies provide a strong link between the development of AD and osteoporosis in the context of DS. Further investigation into EOAD and osteoporosis in DS may provide insights into the underlying mechanisms linking these diseases at a molecular level.

Conclusions

With the number of diagnoses of Alzheimer's disease, osteoporosis and osteoarthritis set to increase substantially over the next 30 years, it is imperative that the common mechanisms linking these deliberating diseases be further elucidated. The amount of research being conducted into ageing and degenerative diseases is constantly increasing, however there is still no effective therapy to combat an underlying mechanistic pathway consistent with the development and progression of these diseases. In order to further elucidate the links between age-related diseases of the skeletal and nervous systems, it is imperative that possible molecular targets be further studied and established. APP, APLP2, Aβ and NGF expression in the bone have been investigated to a certain point, however further investigation is still required to understand physiological as well as pathological roles in the bone.

Hypothesis and Aims

Hypothesis

Neurotrophic factors (APP, APLP2, BACE1 and NGF) are expressed in the bone microenvironment and perform physiological and pathological roles in bone remodelling.

Aims

1. To perform a number of different study types, which allow for a thorough investigation of the potential physiological roles and effects of APP, APLP2 and NGF in the bone.
2. To determine expression at the mRNA and protein levels of these neurotrophic factors in the bone and relate them to structure and function in normal and diseased states.
3. To understand the effects of different regulators of skeletal development and homeostasis on APP, APLP2 and NGF.
4. To uncover a mechanism, which links osteoporosis and Alzheimer's disease together at the cellular level.

Chapter 2

Characterisation of the expression of APP and its homologue APLP2 in the context of the osteocyte and bone

Conventional chapter

Having identified gaps in the knowledge surrounding the physiological roles of *APP* and *APLP2* in Chapter 1, the aim of this Chapter was to establish expression of these proteins in the context of bone. In this Chapter a number of cell culture models of osteoblast to osteocyte differentiation (SaOS2, NHBC, and NOF) were investigated for *APP* and *APLP2* mRNA expression across the differentiation process. The effects of osteotropic hormones PTH and 1,25D were also investigated for their effect on *APP* and *APLP2* mRNA expression. APP protein expression was established under normal conditions as well as under the stimulation of the pro-inflammatory cytokine, TNF-α in primary human osteocytes isolated from bone specimens. The effects of treating primary human osteocytes with soluble APP695 (sAPP695) were also explored to determine whether APP could elicit changes in osteocyte viability or gene expression. Finally, this chapter culminated in the analysis of the skeletal phenotype of the global *App* knock-out mouse model.

Preface

The aim of this Chapter was to explore the expression of APP and its homologue APLP2 in bone and in particular, the osteocyte. APP was examined at the mRNA level in the human osteosarcoma-derived cell line (SaOS2), normal human bone-derived primary osteoblasts (NHBCs), these cells differentiated into an osteocyte-like stage and in primary human osteocytes isolated directly from bone. Following on from these expression studies, the effects of the osteotropic factors $1\alpha,25(OH)_2$-vitamin D_3 (1,25D), being the active hormonal form of vitamin D, and Parathyroid Hormone (PTH) on *APP* expression over the differentiation from osteoblast to osteocyte were examined. The effect of tumour necrosis factor-α, a known pro-inflammatory cytokine on APP expression was also investigated in osteocytes, showing a concentration-dependent increase in expression. The *App* gene knockout murine model was also investigated for a skeletal phenotype. These experiments culminated in a final study whereby the effects of the secreted 695 amino acid splice variant of APP, sAPP695, on differentiated human osteocytes *in vitro* were studied. The combination of these experiments provides insight into the expression and regulation of APP by human and murine bone-derived cells. This research also provides the first insight into the effects of sAPP695 on osteocytes. Together, the findings presented here provide new information as to the expression and local effects of APP in osteocytes and bone.

Introduction

Production of *APP* by osteoclasts (124, 174) and osteoblasts (175, 228) as well as detection of Aβ (124) in bone tissue has been previously reported, however expression during the differentiation process from osteoblast to osteocyte has not yet been investigated. It is now well documented that osteocytes are key regulators of bone effector cell activity (6) and are capable of regulating osteoclast (22, 37, 53, 59) and osteoblast (3, 47) behaviour indirectly through expression of remodelling regulatory genes, such as Receptor Activator of Nuclear Factor kappa-B ligand (*RANKL*) and Osteoprotegerin (*OPG*) (229), as well as sclerostin (*SOST*) (3, 22). They do so in response to a number of external stimuli such as lactation during pregnancy and mechanical loading or unloading (6, 230). In some cases, these situations trigger osteocyte apoptosis, which is known to upregulate expression of known apoptotic regulatory genes *BAX* and *BCL2* (231, 232). Although apoptosis is thought to be a response to noxious stimuli, it can occur in osteocytes in order to maintain bone homeostasis and integrity (233), such as that seen in the context of micro-crack propagation (55).

Studies have investigated a potential relationship between cognition and Vitamin D status using population-based study approaches (234, 235). Based on the associations found between Vitamin D status and cognitive decline in these studies, a number of mouse models of AD have been investigated in the context of Vitamin D status and the effects of Vitamin D on cognition at a mechanistic level (236). Since vitamin D is well characterised as an osteotropic factor, such models may also reveal potential links between skeletal APP expression and cognition. The effects of the global knock-out of the *App* gene in the mouse genome has been investigated by one group previously. There were significant effects on the skeleton, with a reduction in both the cortical and cancellous bone thickness of long bones resultant from impaired bone development, providing a basis for a physiological role of *App* in skeletal development [175].

In this thesis chapter, expression and regulation of APP in osteoblast lineage cells was investigated in order to reveal the role(s) of this molecule in the bone and potentially systemically.

Hypotheses and Aims

Hypotheses

1. APP expression is related to bone remodelling and may be regulated by markers of bone cell activity such as PTH, 1,25D and TNF-α.
2. Bioactive sAPP695 will have intrinsic effects on osteocyte behaviour.
3. Global knock-out of *App* negatively affects skeletal development.

Specific Aims

1. Investigate the relative basal mRNA expression level of *APP* throughout the differentiation process of the human osteoblast-osteocyte transition model, SaOS2, and in human primary osteocytes derived from bone biopsies;
2. Determine effects of osteotropic factors 1,25D and PTH on *APP* mRNA expression throughout the differentiation process in both SaOS2 and NHB cells;
3. Determine whether APP is expressed at the protein level;
4. Examine the effects of sAPP695 on osteocyte survival and gene expression
5. Determine the effects of global *App* gene deletion in aged mice on the skeleton.

Materials and methods

Cell Culture

SaOS2 cells were obtained from the American Type Culture Collection (ATCC) and passaged in α-MEM (Gibco, NY, USA) supplemented with 10 % foetal calf serum (FCS), 10 mM HEPES buffer, 0.2 M L-Glutamine and penicillin/gentamycin in a humidified tissue culture incubator at 37 °C and 5 % CO_2. For experimentation, cells were plated at 2 x 10^4 cells/cm^2 and cultured until confluence was reached. Once confluence was achieved, medium was replaced with fresh medium containing 50 µg/ml ascorbate 2-phosphate (Sigma, St Louis, USA) and 1.8 mM potassium di-hydrogen phosphate (KH_2PO_4). Cells were cultured over a 35-day period and media were changed every 2-3 days. Cells were treated either with human recombinant 50 nM PTH_{1-34} (Sigma), or PBS vehicle control for 24 hr at each time point.

Normal Human Bone Cells (NHBC) were grown from femoral trabecular bone pieces taken from patients undergoing total hip replacement (THR) surgery for end-stage osteoarthritis and cultured as described previously (237). NHBC were grown in α-MEM containing 10% Foetal Calf Serum (FCS), 10 mM HEPES, 0.2 M L-Glutamine and penicillin/streptomycin at 37 °C until confluence was achieved. The same processes were undertaken with Neck of Femur (NOF) trabecular bone pieces. For experimentation, the cells were cultured under mineralising conditions in 5 % FCS, 10 mM HEPES, 0.2 M L-Glutamine, Pen/Strep, 1 % ascorbate 2-phosphate and 1.8 mM KH_2PO_4. Briefly, NHBC were plated at a density of 2 x 10^4 cells/cm^2 and cultured under differentiating conditions over differing periods of time.

Isolation of Primary Human Osteocytes

Human primary osteocytes were also isolated by sequential digestion from cancellous bone biopsies taken from the trochanteric region of the femur, collected from patients undergoing total hip replacement surgery for neck of femur fracture. Samples were processed in a sterile Class II biohazard hood. Samples were cut into 1 x 1 x 1 cm cubes and washed between 1 and 3 times with PBS to remove blood and fat cells. Osteocytes were then isolated from the bone chips using the previously established method (238). Following the first 4 isolation steps and washes, the 5^{th} and 6^{th} bone fractions were pooled together and plated onto collagen coated 8-well chamber slides in primary osteocyte media (α-MEM supplemented with 10 mM HEPES, 0.2 M L-Glutamine, Pen/Strep**,** 2.5 % FCS, 1 % KH_2PO_4) (238). After allowing cells to attach for 72 h, medium was replaced with osteogenic media. In some cases, cells were treated with 0.5 ng/ml recombinant human (rh)-TNF-α for 24 h.

RNA Extraction and Analysis

Cell layers were scraped into 750 µl Trizol reagent (Life Technologies, NY, USA), and total RNA extracted according to the manufacturer's instructions. The quantity and quality of RNA were measured using a NanoDrop spectrophotometer (Thermo Scientific, Adelaide, Australia), with a 260/280 value of >1.8 considered acceptable. 1 µg of RNA was reverse transcribed into cDNA using the iScript RT kit (BioRad, CA, USA). RT- PCR was performed on a CFX Connect Real Time PCR System (BioRad) using SYBR Green Fluor qPCR Mastermix (Qiagen, Limburg, The Netherlands) according to the manufacturer's instructions. Relative gene expression was calculated using the Delta CT method and normalised to expression of *18S* or Beta Actin (*ACTB*) levels.

Table 1: Forward (F) and reverse (R) primer sequences for real-time RT-PCR analysis

Gene of Interest	Direction	Oligonucleotide Sequence (5' – 3')
18S	F	GGAATTCCCGAGTAAGTGCG
	R	GCCTCACTAAACCATCCAA
APP	F	ATCCTGCAGTATTGCCAAGAAG
	R	CACAAAGTGGGGATGGGTC
APLP2	F	GCCCAGATGAAATCCCAGGT
	R	ATATCTGCACGCTGCTCCTG
BACE1	F	GCAGGGCTACTACGTGGAGA
	R	GTATCCACCAGGATGTTGAGC
BAX	F	TCCCCCCGAGAGGTCTTTT
	R	CGGCCCCAGTTGAAGTTG
BCL2	F	TGGGATGCCTTTGTGGAACTGTACG
	R	TAGATAGGCACCCAGGGTGATGCAAG
MCSF	F	CAGTTGTCAAGGACAGCAC
	R	GCTGGAGGATCCCTCGGACTG
MMP13	F	GGATCCAGTCTCTCTATGGT
	R	GGCATCAAGGGATAAGGAAG
OPG	F	GCTCACAAGAACAGACTTTCCAG
	R	CTGTTTTCACAGAGGTCAATATCTT
RANKL	F	CCACCCCCGATCATGGT
	R	TCAGCCTTTTGCTCATCTCACTAT

Oligonucleotide Primer Design for RT-PCR

Primers for the mRNA-specific amplification of human and mouse *App* and *Aplp2* genes were designed from published gene sequences to flank intron/exon boundaries using Amplify 3x design software (Madison, Wisconsin, USA). Primers predicted target specificity for the genes of interest and were tested using BLAST analysis (NCBI). Primers were purchased from Geneworks (Thebarton, SA, Australia). All primers were validated for mRNA specificity using a non-reverse transcribed template control.

Immunostaining of Isolated Osteocytes with α-APP 22C11 Monoclonal Antibody

Cells were washed twice with 1 x PBS and fixed with Histochoice clearing agent (Merck KGaA; Damrstadt, Germany) for 30 min. Fixative was removed and cells were washed thoroughly with ddH_2O a total of three times. Blocking buffer (1 x PBS, 5 % normal rabbit serum) was added to each well and incubated at RT in a humid chamber for 30 min. Cells were incubated with either 22C11 primary antibody or 1B5 negative control IgG antibody for 45 min at 4°C. Wells were washed and Alexa Fluor 647 secondary antibody (1:2000 D.F) added to each well and incubated at RT for 1 h. Following washes, cells were immersed in fluorescence stabilising FluoroBrite™ D-MEM (Gibco) and imaged by confocal microscopy at 60 x magnification.

Treatment of NHBC with sAPP695

Cell Culture

NHBC were plated at a density of 5 x 10^4 cells/ml in 12-well plates, 9 x 10^3 cells/400 µl in chamber slides and 5 x 10^3 cells/200 µl in 96-well plates. After 24 h in proliferation media to

allow attachment to surfaces, media was changed to low serum mineralisation media (α-MEM, 0.5 % FCS, 1 % ascorbate, 1 % KH_2PO_4 and 1 % dexamethasone). Media changes were performed 2-3 times per week and cells were differentiated up to day 28 when they reached a mature osteocyte-like phenotype (237, 239, 240).

sAPP695 Preparation

Aliquots of sAPP695 (9 mg/ml stock solution) were supplied by Professor Roberto Cappai, The University of Melbourne (recombinantly expressed and purified in-house). A 0.5 µM working stock was made up in differentiation media and 1.0 nM and 10 nM treatments were made in differentiation media containing 2 % B27 cell growth supplement (Gibco, Dun Laoghaire, Ireland) in place of FCS due to a requirement for serum-free reaction conditions (241). Day 28 differentiated NHBC were treated with either 1 or 10 nM concentrations of sAPP695, with control wells containing normal media supplemented with 2% B27. Cells were cultured for either 24, 72 or 96 hours in normal culture conditions as mentioned previously.

Cell Viability Staining and Confocal Imaging

NHBC were cultured for 28 days in 8-well cell-imaging chamber slides (Eppendorf. NSW, AUS) and treated with respective concentrations of sAPP695 at time points previously mentioned (238, 242). These were stained with Calcein AM (R&D Systems, Inc, MN, USA) and Ethidium Homodimer-3 (Biotium, CA, USA) (1:2000) into serum-free media and added to each well of 8-well chamber slides. Following the addition of the dyes to each well, chamber slides were incubated at 37°C for 30 min. Following incubation confocal imaging was conducted using an Olympus Fluoview FV3000 Confocal Laser Scanning Microscope. An average of 5 images were taken for each well (2 wells per treatment per time point) at 10 X

magnification. All cell counts were conducted using ZEN Black software (Zeiss, Oberkochen, Germany). Background was removed using the remove all structures feature and cells were counted manually based on size and the original image. Live osteocytes in chamber slides were stained with SiR-actin (Cytoskeleton Inc., Denver, CO, USA) (1:10000), Calcein AM (1:2000) (Biotium) and NucSpot Live 488 Nuclear Stain (1:5000) (Biotium, CA, USA). This was used as a qualitative, observational technique to determine changes in cell morphology.

App Knock-out Mouse Model

Tissues from 60-day-old male and female APPKO mice, containing a germline deletion of the *App* gene on a C57Bl6/J background were obtained with approval from the University of Adelaide Animal Ethics Research Committee from Professor Roberto Cappai (The University of Melbourne) using a scavenger license. Because this mouse strain is bred using an APPKO x APPKO strategy, wild-type (WT) C57Bl6/J control mice, matched for age and gender, were obtained from the University of South Australia Animal Facility and humanely killed. Femora and L1 vertebrae of all mice were dissected, fixed in 10% buffered formalin for 1 week and stored in 70 % Ethanol (EtOH) until imaging took place.

Micro-Computed Tomography

Femora and L1 spinal vertebra were scanned using the *Skyscan 1174 compact micro-CT* scanner (Bruker microCT, Kontich, Belgium). All scans were performed at a fixed 6.4 µm threshold, with 0.8 degree of movement and a frame average of 2. Oversized scans were conducted on each femur and L1 vertebra; images were reconstructed using the N-Recon software (Bruker). Reconstructed images were realigned either sagittal for femora analysis or

coronal for vertebral analysis using Data Viewer. Analysis was conducted on trabecular bone 1mm below the growth plate of the femur, and cortical bone in the mid-shaft where no trabecular bone was present. The region of interest (ROI) for cortical bone was defined as 0.5 mm above the geometric mid-point calculated by subtracting the measurement at the distal end of the femur from that at the proximal end and dividing by 2. Vertebral analysis of was conducted on the full length of the vertebra.

Statistical Analyses

All statistical analysis was performed using GraphPad Prism (v7.02). To determine differences between treatment groups, non-parametric, two-tailed Student's t-tests were applied to the datasets. Analysis of the investigated μCT parameters was performed using two-tailed, parametric, Welch's t-tests, as the data were normally distributed.

Results

APP mRNA expression in SaOS2 cells differentiated for 35 days in vitro

In order to test if human osteoblast lineage cells express *APP* and its homologue *APLP2*, we first utilised the SaOS2 model (human osteosarcoma cell line) of human osteoblast to osteocyte transition (243). SaOS2 cells were cultured for a total of 35 days, over which time they differentiate to a mature osteocyte-like stage (243), and RNA was extracted at days 0, 7, 14, 21, 28 and 35. In order to determine the effects of PTH, a regulator of bone formation, cells were also treated with 50 ng/ml recombinant PTH at each time-point for 24 h. Real-time RT-PCR analysis for mRNA expression of *APP* revealed a differentiation-dependent increase in basal levels of *APP* (**Fig. 1a**). Treatment with PTH did not alter *APP* expression until D35, where *APP* was significantly suppressed (**Fig. 1a**). Analysis of *APLP2* mRNA expression showed up-regulatory effects of PTH at days 7 and 28 (**Fig. 1b**).

The effects of 1,25D on these cells were also investigated. Treatment of SaOS2 cells with 1 and 10 nM 1,25D over 4 weeks showed a bimodal distribution of expression of *APP* (**Fig. 2a**) with increases in expression observed at weeks 0 and 2 and reductions observed at weeks 1 and 4. There was also a dose-dependent increase in *APP* mRNA expression over the first 3-weeks of differentiation, suggesting that *APP* expression may be 1,25D responsive. Interestingly, at week 4, 1,25D did not alter *APP* expression, suggesting that 1,25D may not affect *APP* expression in the mature osteocyte (**Fig. 2a**). *APLP2* expression followed a similar pattern as *APP* (**Fig. 2b**), with a significant upregulation in expression stimulated by 1 & 10 nM 1,25D at wk 3 but this was not observed at any other time-points.

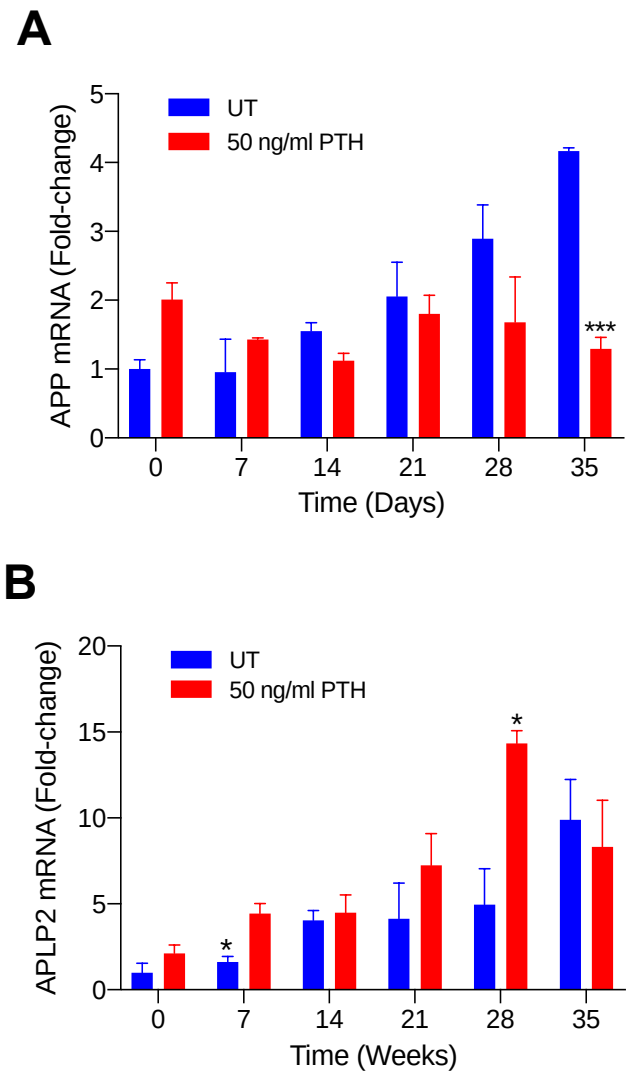

Figure 1: *APP* and *APLP2* mRNA expression in response to 50 ng/ml PTH over a 35-day treatment period. (A) *APP* mRNA expression was unaffected by PTH treatment at the early stages of differentiation but appeared to be suppressed at D35, when cells reached a mature osteocyte-like phenotype (***p = 0.0003); **(B)** PTH was shown to upregulate *APLP2* mRNA expression at D7 (* p = 0.0140) and D28 (* p = 0.0134) but there were no effects observed at other time points during differentiation.

One-way ANOVA with multiple comparisons; Mean ± SEM; n = 3

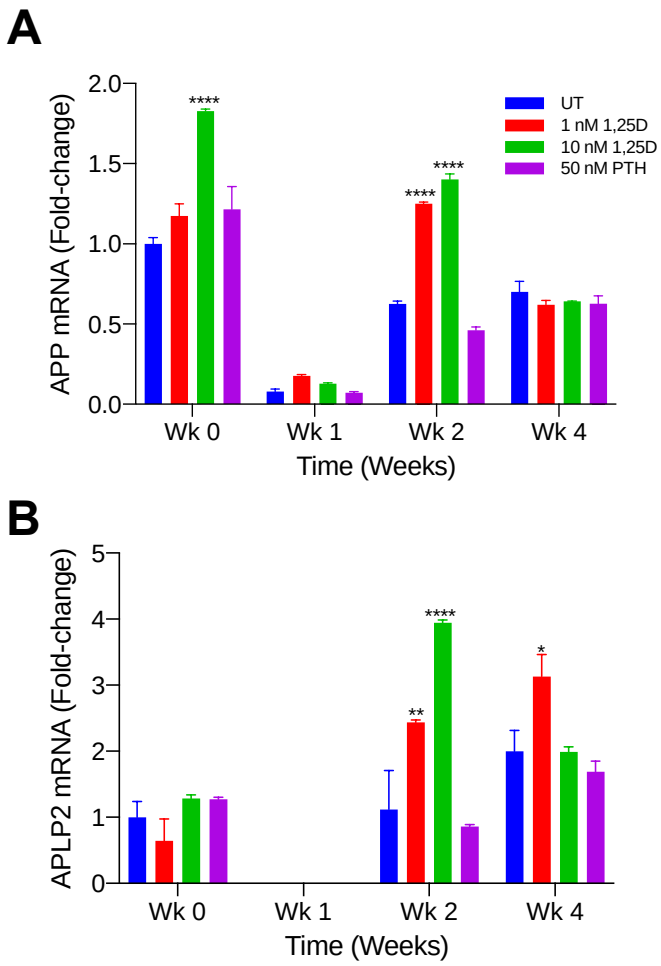

Figure 2: *APP* and *APLP2* mRNA expression in differentiating SaOS2 cells over a 4-week treatment period with 1 nM or 10 nM 1,25D or 50 nM PTH. A. *APP* mRNA expression was significantly upregulated compared to untreated (UT) with 10 nM 1,25D at week 0 and 2 (****p <0.0001 respectively). *APP* was also upregulated by 1 nM 1,25D at week 2 (****p < 0.0001); there was no observable change with PTH treatment; **B.** A similar pattern of expression is observed with *APLP2* being significantly upregulated compared to UT by 1 & 10 nM 1,25D at week 2 (**p = 0.0031 & ****p < 0.0001 respectively) but this was not seen at any other time point. At week 4 there was only a significant upregulation of *APLP2* by 1 nM 1,25D (*p = 0.0107). There were no changes observed by 50 nM PTH at any time point when compared to UT.

One-way ANOVA with multiple comparisons; Mean ± SEM; n = 3

APP mRNA is expressed by Normal Human Bone Cells differentiated in vitro for 4 weeks and responds to treatment with 1,25D and PTH

In order to test if *APP* expression was also a feature of human primary osteoblastic cells, we assayed NHBC cultures derived from the proximal femur of patients undergoing total hip replacement surgery for primary hip osteoarthritis. These cells were differentiated to a mature osteocyte-like stage over 4 weeks (3, 242, 244-247). *APP* was expressed at the mRNA level at each time point over the 4-week period, albeit with a bimodal distribution of expression with a peak in expression being observed at weeks 1 and 2 (**Fig. 3a**). *APP* was again 1,25D responsive but unlike the findings with SaOS2, a dose response of induction was observed at each time point tested. PTH treatment at 50 nM significantly upregulated *APP* mRNA expression at weeks 0 and 4 (**Fig. 3a**).

The effects of these treatments on *APLP2* mRNA expression were not as pronounced, with a significant reduction in expression seen at week 2 induced by PTH and a significant increase in expression observed at week 4 (**Fig. 3b**) by all treatments. For reasons unclear, at time 0 it was not possible to detect expression of *APLP2* in the 10 nM 1,25D and 50 nM PTH samples (**Fig. 3b**).

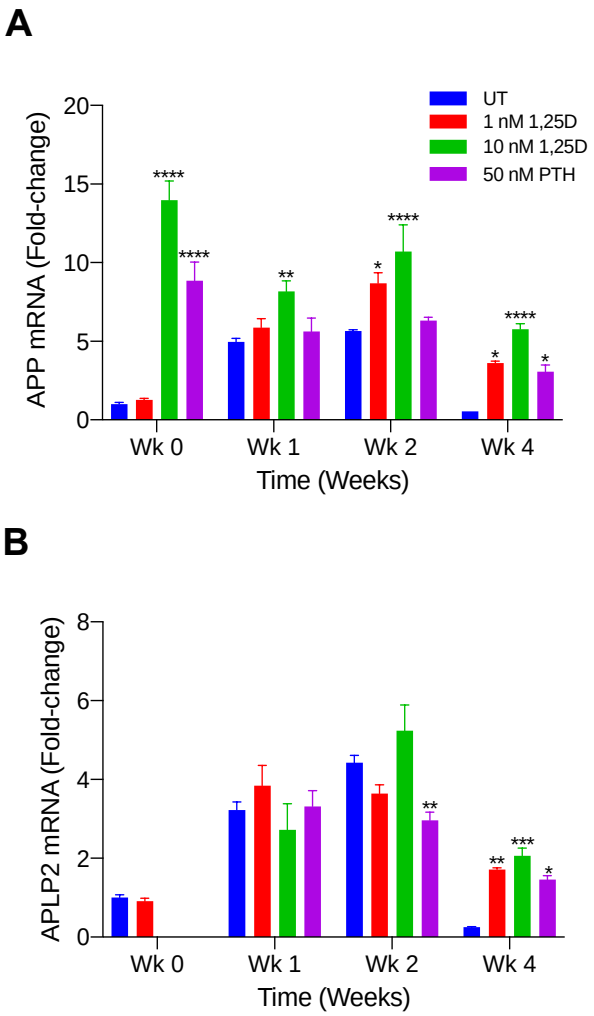

Figure 3: *APP* and *APLP2* mRNA expression in differentiating NHB cells treated with 1 or 10 nM 1,25D or 50 nM PTH. A. *APP* mRNA expression was increased by 1 nM 1,25D at weeks 2 & 4 (*p = 0.0143 & *p = 0.0125 respectively). The 10 nM 1,25D treatment upregulated *APP* expression at each time point when compared to UT (****p <0.0001 weeks 0, 2 & 4 and **p = 0.0088 week 1). 50 nM PTH significantly increased *APP* gene expression at weeks 0 ($p < 0.0001$) and 4 ($p = 0.0207$) when compared with UT. **B.** *APLP2* mRNA expression was significantly reduced by 50 nM PTH at the week 2 time point (**p = 0.0059) and was significantly increased by 1 nM 1,25D (**p = 0.057), 10 nM 1,25D (***p = 0.0007) and 50 nM PTH (*p = 0.0252).

APP and *APLP2* are expressed at appreciable levels in NOF cancellous bone biopsies differentiated for 42 days

The gene expression patterns of *APP* and *APLP2* were also examined in human proximal femoral bone obtained from patients undergoing total hip replacement for fragility neck of femur fracture (NOF), as a result of osteoporosis. Primary human osteoblasts derived from NOF cancellous bone were analysed over 42 days to determine patterns of expression with differentiation and mineralization (OD450). As mineralisation is a key readout associated with osteoblast to osteocyte transition (45), it was important to determine whether *APP* and *APLP2* could be considered markers of immature or mature osteoblasts or osteocytes (**Fig. 4**). Mineralisation is also a dynamic process and can be positively or negatively controlled by the differentiating or mature osteocyte (5). In general, *APP* mRNA expression peaked between 7 and 14 days, over the early phase of mineralisation, and decreased thereafter as mineralisation and cell maturation increased (**Fig. 4a & c**). *APLP2* expression was similar but appeared to be less time dependent (**Fig. 4b & d**). Overall, however, *APP* and *APLP2* expression correlated positively with each other, and both correlated negatively with mineralisation (**Fig. 4g & h)**. This could mean that while these genes are expressed in mature cells, they are associated with an anti-anabolic/pro-catabolic role (5).

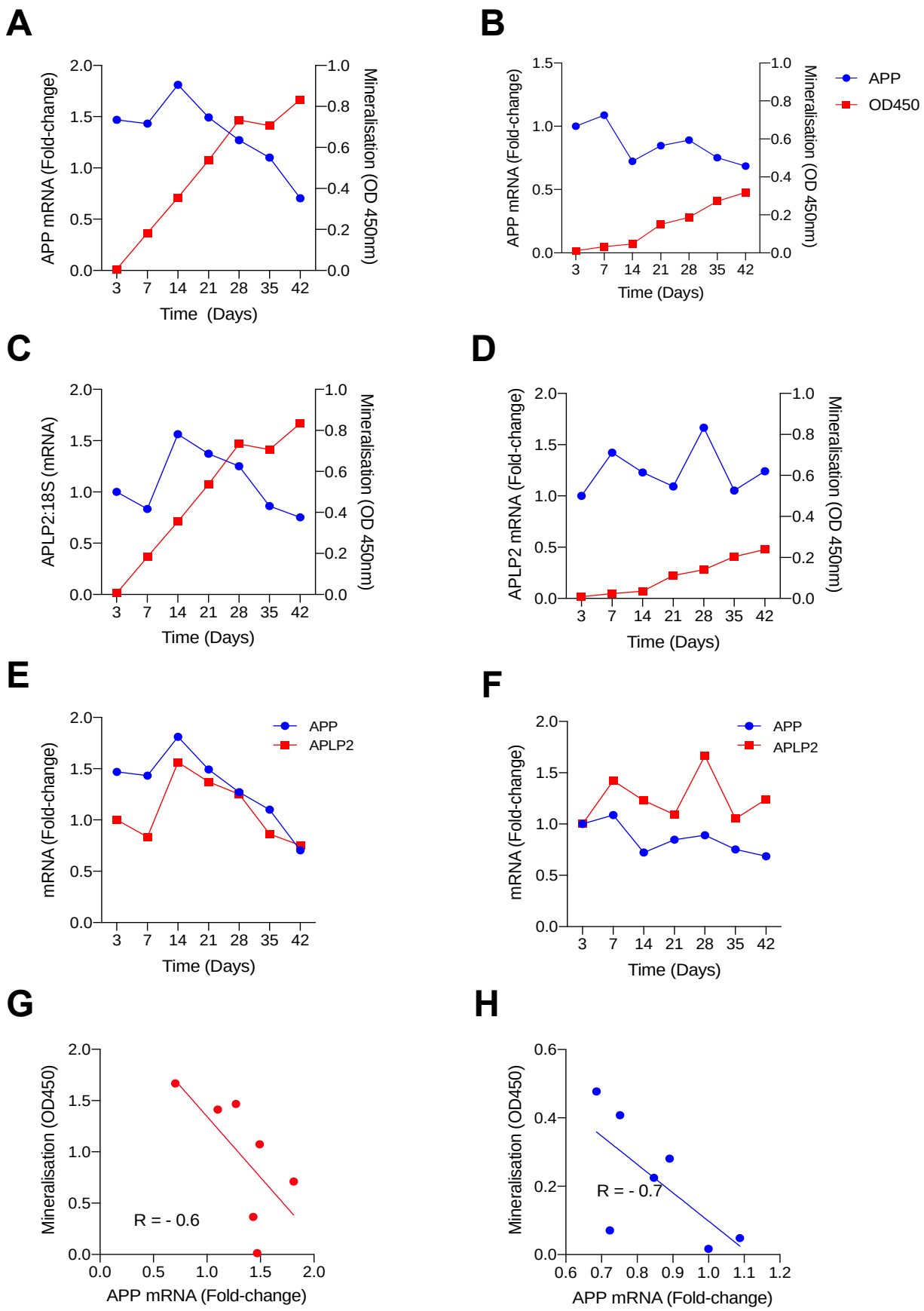
A
APP mRNA (Fold-change)
Mineralisation (OD 450nm)
Time (Days)
B
APP
OD450
C
APLP2:18S (mRNA)
D
APLP2 mRNA (Fold-change)
E
mRNA (Fold-change)
APLP2
F
G
Mineralisation (OD450)
R = - 0.6
H
R = - 0.7

Figure 4: *APP* and *APLP2* mRNA expression over 42-day differentiation of cancellous bone derived osteoblasts from two donors. **A.** Donor 1 - *APP* mRNA expression vs mineralisation. **B.** Donor 2 - *APP* mRNA expression vs mineralization. **C.** Donor 1 – *APLP2* mRNA expression vs mineralization. **D.** Donor 2 – *APLP2* mRNA expression vs mineralization. **E.** Donor 1 – *APP* and *APLP2* are expressed at similar mRNA levels over the 42-day differentiation period. **F.** Donor 2 – Expression patterns of *APP* and *APLP2* differ slightly at day 21 and day 42. **G.** Donor 1 – A moderate, negative relationship was observed between *APP* mRNA expression and mineralisation. **H.** Donor 2 – A strong, negative relationship was observed between *APP* mRNA and mineralisation.

Recombinant TNF-α upregulates *APP* and *IL-6* in a dose-dependent manner in human NHBCs

As TNF-α is a known pro-inflammatory cytokine and is involved in the bone remodelling pathway as a negative regulator of osteoblast/osteocyte anabolic activity (246), the effects of recombinant human TNF-α on *APP* expression were investigated in human bone cells. TNF-α has also been shown to induce *APP* expression in adipocytes (248). IL-6 is known to be stimulated by TNF-α in a concentration-dependent manner so was tested as a control response gene and displayed a positive upregulation in mRNA expression at 0.1, 0.5 and 1 ng doses (**Fig. 5a**). *APP* mRNA expression followed the same trend as *IL6* in response to TNF-α and was significantly increased at each concentration when compared to UT (**Fig. 5b**).

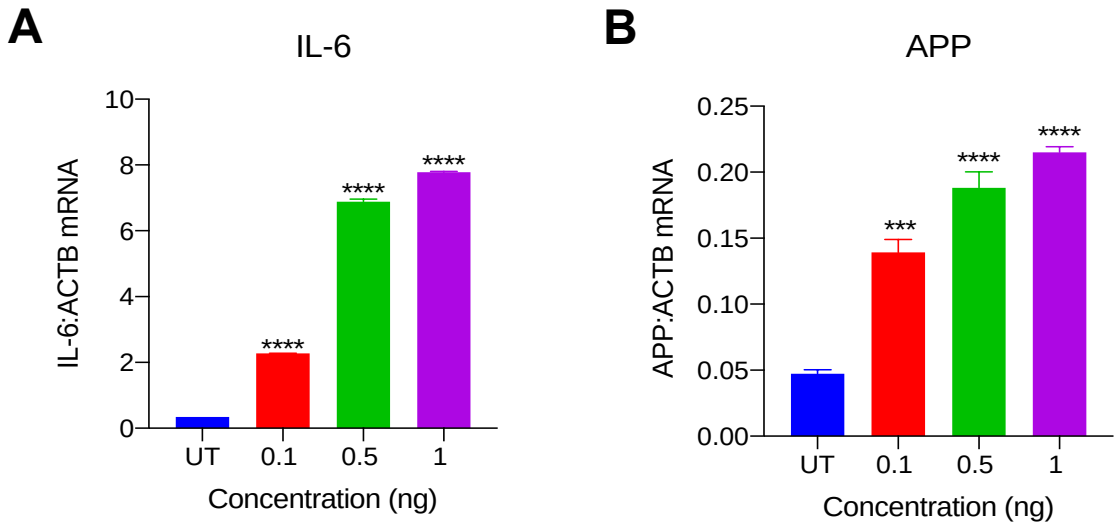

Figure 5: *APP* mRNA expression in primary human osteocytes is stimulated by increasing TNF-α levels in a similar pattern to known inflammatory cytokine involved in bone resorption *IL-6*. A. *IL-6* mRNA expression is significantly upregulated with increasing concentrations of TNF-α (**** - p <0.0001). **B.** *APP* mRNA expression is also significantly upregulated under the stimulation of increasing concentrations of TNF-α (*** p = 0.0002; **** p <0.0001).

n = 3/treatment; one-way ANOVA, p < 0.05*

The APP protein is detectable in freshly isolated human osteocytes and upregulated with TNF-α treatment

In order to test if APP expression is a feature of human osteocytes *in vivo*, we isolated osteocytes from patient-derived bone biopsies using a sequential enzymatic/EDTA digestion technique (238, 242). The late fractions of the digest shown to constitute osteocytes, were cultured untreated for 72 h to allow attachment and then immunostained using the anti-human APP MAb 22C11, and these stained positive (**Fig. 6**). When osteocytes were treated with the pro-inflammatory cytokine rh-TNF-α (0.5 ng/ml), the intensity of the staining was increased (**Fig. 6**). The 22C11 staining was confirmed to be specific by substituting an isotype-matched negative control IgG for the primary MAb step (**Fig. 6**). Despite repeated attempts, it was not possible to isolate sufficient cell numbers to allow for RT-PCR analysis for *APP* mRNA expression levels.

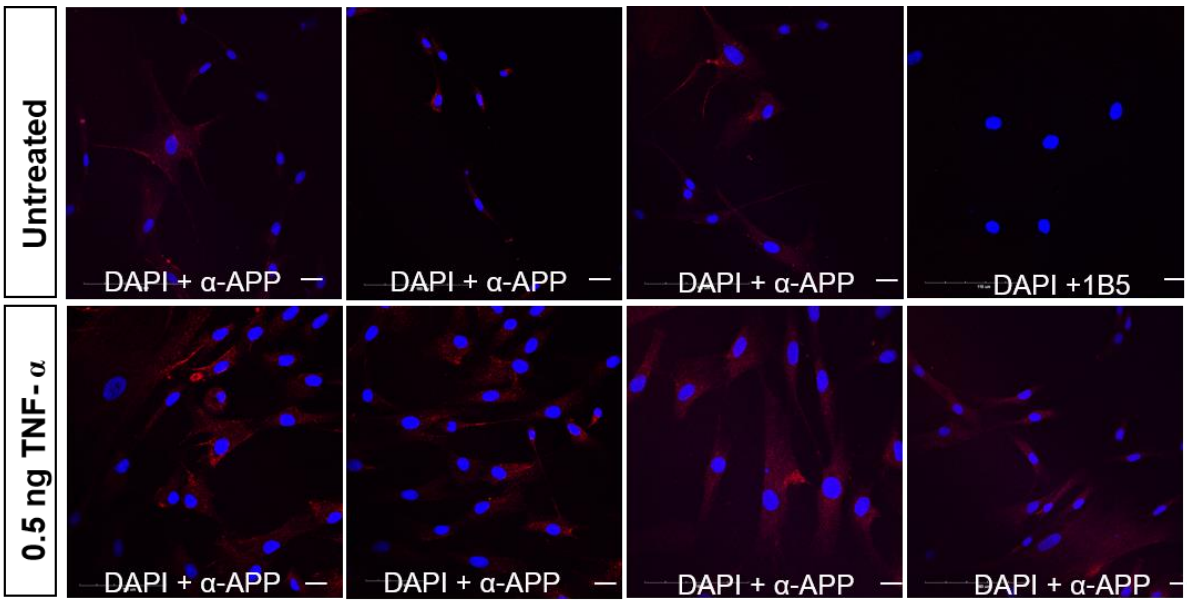

Figure 6: The regulation of APP expression in response to rh-TNF-α in freshly isolated osteocytes. Full-length APP 22C11 MAb tested against isolated human osteocytes either untreated or treated with 0.5 ng rh-TNF-α and NOF bone sections. Row 1. Untreated isolated osteocytes stained with DAPI live cell stain and 22C11 MAb **(1 - 3).** Negative staining for IgG control 1B5 **(4)**; **Row 2.** 0.5 ng rh-TNF-α treated isolated osteocytes stained with DAPI and 22C11 MAb shows intense levels of stain compared to untreated **(1 – 4).**

Effect of sAPP695 on human osteocyte viability

Having established that human osteocytes expressed both *APP* mRNA and APP protein, we next investigated the potential functional consequences of expression. To do this, we tested the effects of the sAPP695: the physiologically produced, α-secretase cleaved, soluble species of APP, (249), over a 96 hour time course. We first sought to examine the effect of sAPP695 on osteocyte viability. Known apoptosis-related genes *BAX* (pro-apoptotic) and *BCL2* (anti-apoptotic) mRNA levels were measured at each time point. Expression of *BAX* was not affected by exposure to 1 or 10 nM sAPP695 at any time point when compared to UT but was significantly increased by 10 nM when compared with 1 nM sAPP (**Fig. 7a**). *BCL2* mRNA expression was unchanged over the time-course and with treatments (**Fig. 7b**). Finally, the *BAX: BCL2* mRNA ratio was not significantly altered at any time point between UT and treatments, however it was significantly upregulated by 10 nM at 72 h when compared to 1 nM sAPP (**Fig. 7c**), consistent with a pro-apoptotic effect.

As the sAPPα cleavage product is produced through the non-amyloidogenic pathway, it was hypothesized that it would have no effect on osteocytes. However, at 24 h there was a significant increase in the number of dead cells observed when comparing the highest concentration, 10 nM sAPP695 to the untreated cells (**Fig. 7d**). This observation may be due to sAPP695 having toxic effects at 10 nM. There was no significant change in the number of dead osteocytes when treated with 1 nM sAPP695. At 72 h there was no significant difference observed with either the 1 or 10 nM sAPP (**Fig. 7e**). Finally, when analysing the number of dead osteocytes at the 96 h time point, we did not observe any changes between the control and treatment wells (**Fig. 7f**). These findings suggest that $sAPP_{695}$ at a 1 nM concentration does not affect osteocyte viability in a time-dependent manner, however initial exposure of osteocytes to a 10 nM dosage has the ability to initiate osteocyte death, likely through induction of apoptosis. Initial exposure of osteocytes to the highest concentration of sAPP695 resulted in a

significant death response at 24 h, and those dead cells would likely have detached from the well and not been present for assay at later time points. The surviving cells likely proliferated over the time course together resulting in an apparent plateau in the total cell number.

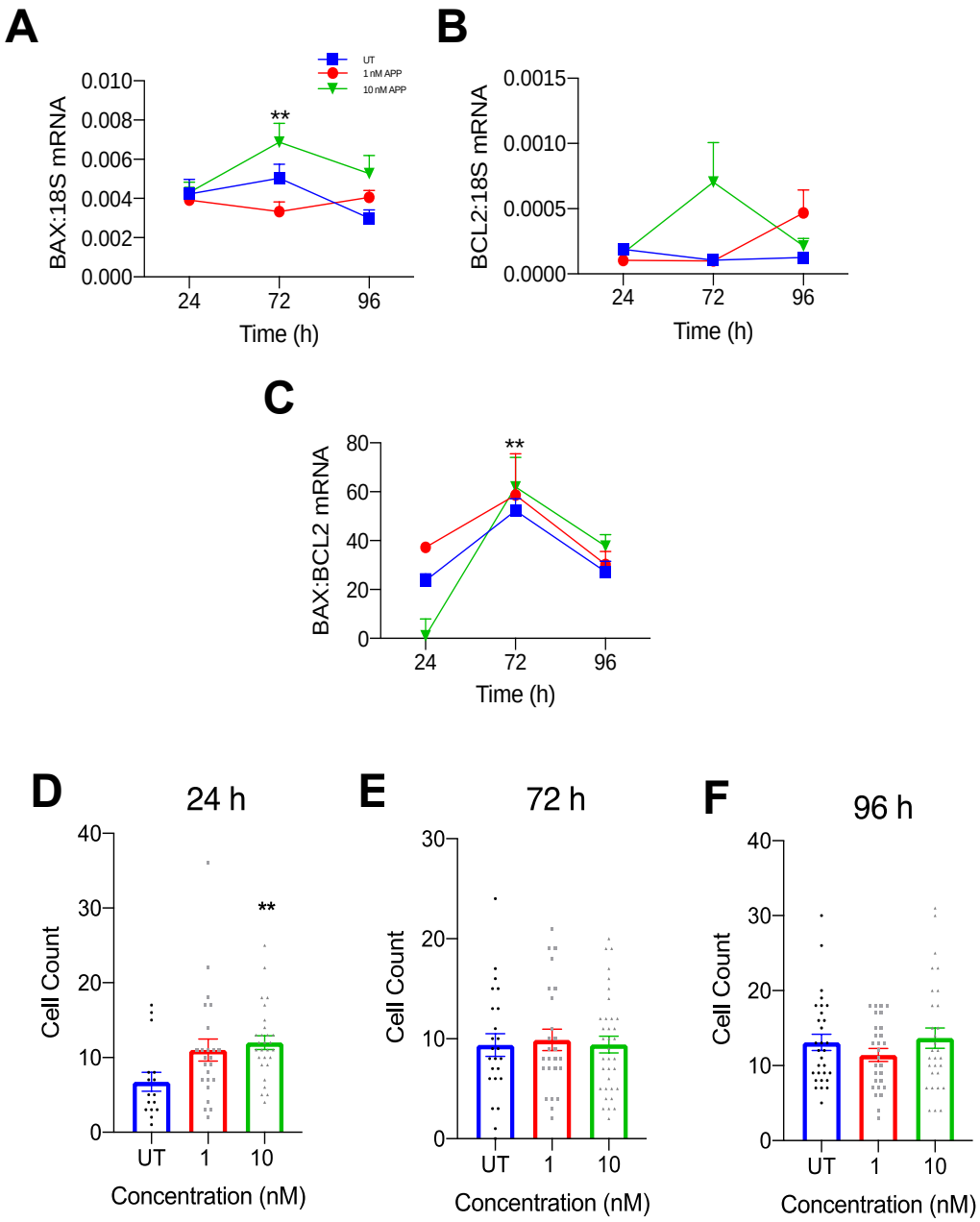
A
B
C
D
E
F
UT
1 nM APP
10 nM APP
BAX:18S mRNA
BCL2:18S mRNA
BAX:BCL2 mRNA
Time (h)
24
72
96
**
24 h
72 h
96 h
Cell Count
Concentration (nM)
UT
1
10

Figure 7: The addition of sAPP695 to differentiating osteocytes *in vitro* over 96 hours has effects on *BAX* mRNA and cell viability. Effects of 1 and 10 nM sAPP695 on osteocyte viability. A. *BAX* mRNA expression was unchanged when compared with UT at each time point, however there was a significant increase at 72 h between 1 & 10 nM treatments (** p = 0.0012). **B.** *BCL2* was not significantly regulated in response to 1 or 10 nM sAPP695 when compared to UT at any time point. **C.** the *BAX: BCL2* ratio is significantly increased at 72 h by 10 nM sAPP695 compared with the 1 nM treatment (**p = 0.0052) but there was no difference compared with UT. **D.** The number of dead cells was significantly increased at 24 h by 10 nM sAPP695 (**p = 0.0024) compared to UT but was not affected by 1 nM sAPP695 (p = 0.0982). **E.** There was no concentration-dependent change in the number of dead cells observed at 72 h when compared to UT (p > 0.9999 respectively). **F.** There was no observable change between UT and treatments at 96 h (p > 0.9999 respectively).

*Experimental triplicates; One-way ANOVA (Kruskal-Wallis); * p < 0.05*

Effect of sAPP695 on human osteocyte function-related gene expression

Next, the effect of sAPP695 treatment on markers of bone remodelling was investigated. There was no significant change in expression of the bone resorption initiator *RANKL* when compared to the control at any time point (**Fig. 8a**). The same was seen for the RANKL inhibitor gene, *OPG* (**Fig. 8b**). Thus, there was no effect of sAPP695 on the *RANKL*:*OPG* mRNA ratio (**Fig. 8c**). Expression of another important osteoclastogenesis factor, *MCSF* was also analysed, and was found to be significantly down-regulated, only at 24 h by the low dose (1 nM) treatment of sAPP695 (**Fig. 8e**). Overall, $sAPP_{695}$ had little effect on the mRNA levels of expression of bone remodelling genes.

In order to examine possible effects of sAPP695 on osteocytic osteolysis related genes, we examined the expression of two related proteases, *CTSK* and *MMP13* (48, 240); as shown (**Fig. 8d & f**), there were no effects of sAPP695 on the expression of these markers.

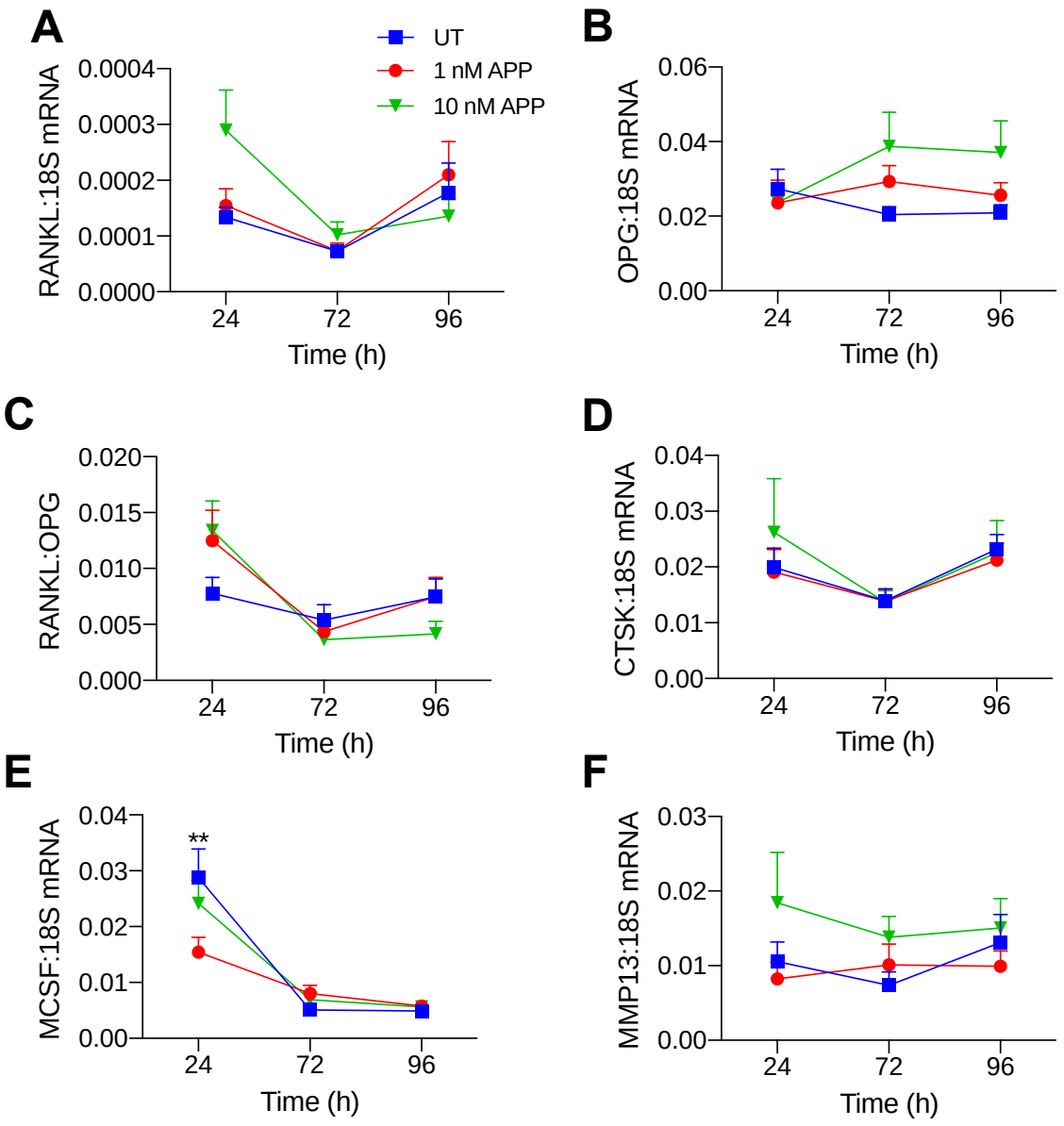
A
UT
1 nM APP
10 nM APP
RANKL:18S mRNA
0.0004
0.0003
0.0002
0.0001
0.0000
24
72
96
Time (h)
B
OPG:18S mRNA
0.06
0.04
0.02
0.00
24
72
96
Time (h)
C
RANKL:OPG
0.020
0.015
0.010
0.005
0.000
24
72
96
Time (h)
D
CTSK:18S mRNA
0.04
0.03
0.02
0.01
0.00
24
72
96
Time (h)
E
MCSF:18S mRNA
**
0.04
0.03
0.02
0.01
0.00
24
72
96
Time (h)
F
MMP13:18S mRNA
0.03
0.02
0.01
0.00
24
72
96
Time (h)

Figure 8: Response of bone resorption related markers to 1 and 10 nM sAPP695 over 96 h time-course. A. *RANKL* is not altered in response to 1 or 10 nM sAPP695 at any time point ($p > 0.990$); **B.** *OPG* mRNA expression is not significantly up or downregulated by 1 or 10 nM sAPP695 at any time point (24 h: $p > 0.990$ respectively; 72 h: $p = 0.9253$ & $p = 0.3227$; 96 h: $p > 0.9990$ & $p = 0.4826$); **C.** The *RANKL:OPG* ratio is not affected by 1 or 10 nM sAPP695 ($p > 0.9990$); **D.** There are no time or concentration-dependent effects on mRNA expression of *CTSK* ($p > 0.9990$); **E.** *MCSF* is significantly upregulated at 24 h by 1 nM but not 10 nM sAPP695 (**$p = 0.0016$ & $p = 0.7946$ respectively) when compared to UT but not at any other time point ($p > 0.9000$).

*Experimental triplicates; One-way ANOVA with multiple comparisons; * p > 0.05*

Effect of sAPP695 on endogenous APP processing

We also sought to determine if expression levels of *APP* itself or the protease known for cleaving APP via the amyloidogenic pathway, *BACE1* were altered through exposure to sAPP695. Both *APP* and *BACE1* mRNA was significantly reduced compared to control at 24 h (**Fig. 9a & b**). Similarly, *APP* expression was dampened by the 10 nM concentration of sAPP695 at 24 h ($p = 0.0255$), however there was no effect on *BACE1* at this time point. Finally, we saw that at 96 h there was a significant reduction in *APP* mRNA expression at the 10 nM dose of sAPP695 (**Fig. 9a**), an effect that was not observed in the 1 nM sAPP695 treated osteocytes at this time point.

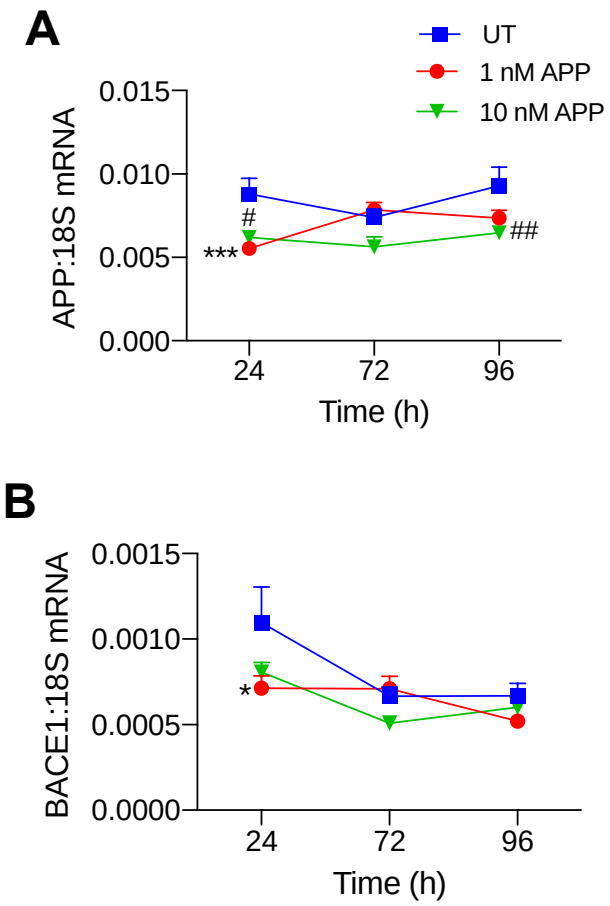

Figure 9: Effects of sAPP695 on *APP* and *BACE1* mRNA expression over a 96 h time course. A. *APP* mRNA expression is significantly reduced at 24 h by both 1 & 10 nM sAPP 695 when compared to UT (***p = 0.0009 & #p = 0.0255 respectively). At 72 h there was no change in mRNA expression however at 96 h there was a significant reduction at the 10 nM concentration (##p = 0.0088). **B.** At 24 h in *BACE1* mRNA expression was dampened by 1 nM sAPP (*p = 0.0120) treatment but not with 10 nM sAPP. There were not observable effects of sAPP695 on *BACE1* expression at any other time points.

*Experimental triplicates; one-way ANOVA; * $p < 0.05$*

Effects of *App* Knockout (APPKO) on skeletal phenotype

To examine whether the expression of *APP* in bone could have functional consequences in an *in vivo* context femoral trabecular and cortical bone of WT C57Bl/6J mice and age- and sex-matched APP KO mice were analysed for a skeletal phenotype. Cortical width, endosteal and periosteal bone perimeters were analysed by micro-CT and reconstructed (**Fig. 10**).

Initial analysis of the cortical bone thickness in a 1 mm ROI at the midpoint revealed no difference between genotypes in the male cohort (**Fig. 10a**), however a significant increase in this parameter was observed in the female group (**Fig. 10b**). In both male and female APP KO mice (n = 4/gender) there was a significant decrease in both endosteal perimeter (**Fig. 10c & d**) and periosteal perimeter (**Fig. 10e & f**) when compared to their age and gender-matched controls, suggesting a defect in periosteal bone formation and/or endosteal bone resorption/remodelling in APP KO animals.

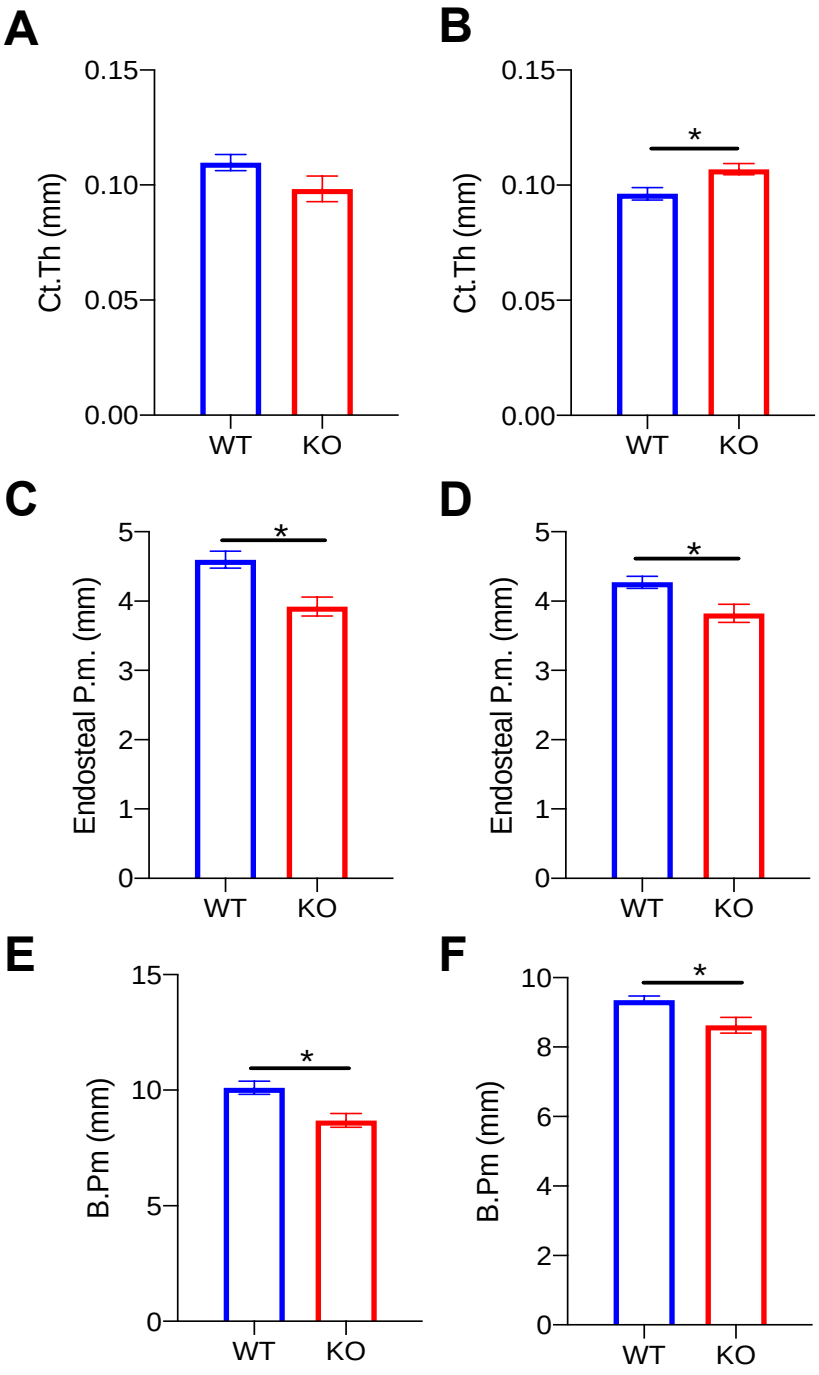
A
0.15
0.10
0.05
0.00
Ct.Th (mm)
WT
KO
B
0.15
0.10
0.05
0.00
Ct.Th (mm)
*
WT
KO
C
5
4
3
2
1
0
Endosteal P.m. (mm)
*
WT
KO
D
5
4
3
2
1
0
Endosteal P.m. (mm)
*
WT
KO
E
15
10
5
0
B.Pm (mm)
*
WT
KO
F
10
8
6
4
2
0
B.Pm (mm)
*
WT
KO

Figure 10: There is a cortical bone phenotype in both male and female APPKO mice when compared to WT controls. Cortical bone microCT analysis conducted at the femoral midshaft in a 1 mm ROI. A. Cortical thickness (Ct.Th) was not significantly changed between male APP KO and WT mice; **B.** Cortical thickness was significantly increased in female APPKO when compared to WT (* p = 0.02); **C.** APPKO males endosteal perimeter was significantly reduced (*p = 0.018) when compared to WT; **D.** APPKO females endosteal perimeter was significantly reduced (*p = 0.034) when compared to WT; **E.** Periosteal perimeter (B.Pm) was significantly reduced in male APPKO mice (*p = 0.04); **F.** B.pm was also significantly reduced in female APPKO mice (*p = 0.021).

*n = 4/genotype/gender; Student's Two-tailed T-Test; * p < 0.05; mean + SEM*

Cancellous bone analysis of the Vertebra and Femora

As changes in vertebral bone volume occur with age and disease such as osteoporosis, it was important to determine whether the knock-out of *App* had an effect on the vertebrae. These bones consist mainly of cancellous bone contained in a thin cortical shell. Consistent with the long bone cancellous bone analyses, trabecular bone parameters in the lumbar vertebrae (L1) were not different between WT and APP KO mice in either gender (**Fig. 11a & b**).

Analysis of the cancellous bone compartment in a 2 mm ROI below the growth plate showed no significant differences in either gender between WT and KO (**Fig. 11c & d)**. This result indicates that skeletal phenotype was restricted to the cortical bone.

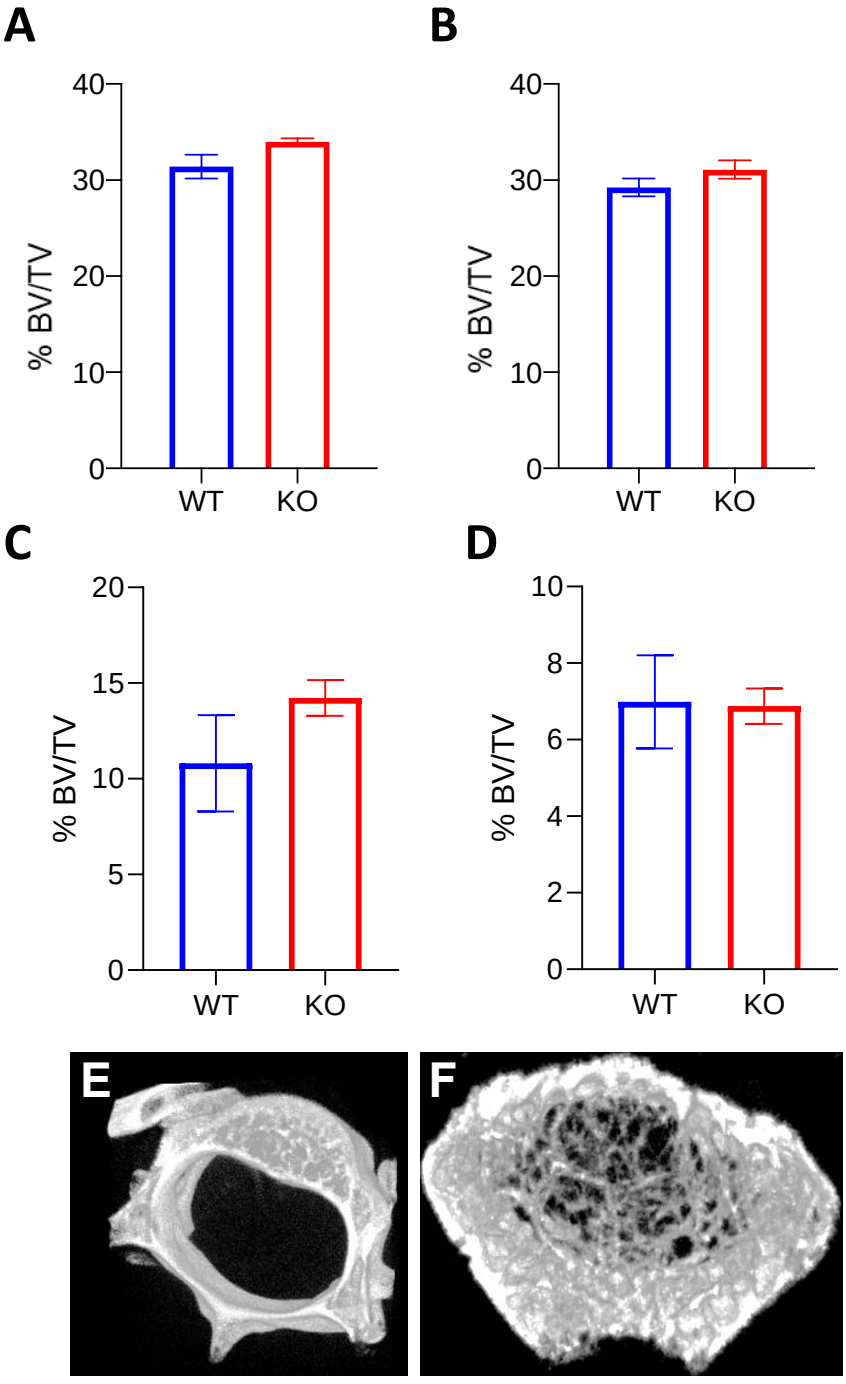
A
40
30
20
10
0
% BV/TV
WT
KO
B
40
30
20
10
0
% BV/TV
WT
KO
C
20
15
10
5
0
% BV/TV
WT
KO
D
10
8
6
4
2
0
% BV/TV
WT
KO
E
F

Figure 11: Analysis of the cancellous bone volume fraction (% BV/TV) in both the vertebra and femora did not reveal any changes between genotypes in both genders. **A.** Vertebral % BV/TV was unchanged between male WT & APPKO mice ($p = 0.2639$). **B.** There is no significant effect on vertebral % BV/TV in female APPKO mice ($p = 0.1047$). **C.** There is no significant change in femoral % BV/TV between WT and KO males ($p = 0.307$). **D.** There is no significant change in femoral % BV/TV in female APPKO mice when compared to WT control animals ($p = 0.935$). **E.** Three-dimensional reconstruction of vertebra. **F.** 3D reconstruction of femur.

*n = 4/genotype/gender; Student's Two-tailed T-Test; * $p < 0.05$; mean + SEM*

Discussion

This study provides a number of unique insights into *APP* and *APLP2* mRNA expression by human osteoblasts and osteocytes *in vitro.* Not only has it been shown that *APP* and *APLP2* are responsive to 1,25D and PTH, known regulators of osteoclastic resorption (250), osteoblast activity (251) as well as osteocyte functions (59), but they are also co-regulated in models of osteoblast to osteocyte transition. As the bone is such a diverse microenvironment, containing a number of different regulatory pathways, it is important that the effect of known osteotropic modulatory molecules is characterised.

Regulation of *APP* expression in response to TNF-α has not been investigated in human primary osteocytes until now. In the bone, increased levels of TNF-α stimulate the upregulation of IL-6, another pro-inflammatory cytokine. Overexpression of IL-6 in transgenic mice results in increased bone turnover, reduced osteoblast number, increased osteoclast number and a subsequent development of osteopenia (252). Stimulation of IL-6 expression by TNF-α has been shown to have direct effects on osteoclastogenesis, independent of inflammation (253). The parallel increase in *APP* mRNA expression with increasing concentrations of rh-TNF-α highlights the potential role for *APP* in the initiation of osteoclastogenesis. Alternatively, the increase in *APP* may indicate a compensatory negative feedback loop, whereby *APP* is increased to block IL-6 for example and prevent osteoclastogenesis, however the APPKO phenotype suggests that a lack of *App* may also prevent osteoclast activity as seen with the increase in cortical thickness in the female mice.

Overall, gene expression analysis of NHBs treated with 1 nM sAPP695 revealed no significant changes in mRNA expression of the genes examined when compared with the untreated control. It appeared that the 10 nM concentration of sAPP695 had a protective effect on osteocytes. At each time point there was a reduction in the expression levels of bone resorption

markers such as *RANKL* and *MMP13*. These findings indicate that high levels of APP in the bone may not be indicative of disease and may have physiological roles in bone remodelling, which is supported by the results indicated by the mouse model. In order to further elucidate the function of APP in the bone, it would be beneficial to determine expression of the secretases responsible for the processing of APP (α, β and γ-secretases).

The results observed from the 60-day-old APPKO mouse model revealed a cortical bone specific phenotype. The female-specific increase in cortical thickness observed may pertain to aberrant cortical bone formation or a decrease in cortical bone resorption. The endosteal surface has a high rate of osteoclast-mediated bone resorption, therefore the significant reduction in endosteal perimeter observed in both genders is indicative of a defect in this process. This parameter is a major contributor to femoral bone strength as narrower structures are inherently weaker than wider tube-like structures of a given wall thickness. There has been one other study to investigate the effects of the knock-out of *App* on the skeleton (228). In that study, a reduction in both trabecular and cortical bone parameters were observed, which authors believed to be due to a decrease in osteoblast-mediated bone formation. It is difficult to define the mechanism behind this observation without performing histological analysis of the femora of these mice; for example, performing tartrate resistant acid phosphatase (TRAP) staining could elucidate whether there was an increase in TRAP-positive osteocytes in the cortical bone. However, taken together this study suggests a pro-catabolic role for APP in the skeleton, at least in a site-specific manner, both in terms of osteoblast/osteocyte mediated bone mineralisation, and promoting endocortical remodelling.

Study Limitations

In order to optimise studies for the future, it is important to address limitations. One of the first points to address in this study is the number of biological replicates used for the cell culture

experiments. The number of biological replicates was 1, with experimental triplicates and technical triplicates for the PCR analysis. It is important that in the future with this work, based on availability of samples that this be replicated with at least 2 – 3 more donors to confirm the pattern of *APP* and *APLP2* expression in differentiating osteoblasts is consistent over the time points investigated. In order to further improve upon this study and increase the power of the results, collecting protein lysates and conducting Western Blot assays would make for a much stronger experiment. The ability to demonstrate expression at the mRNA and protein level is important for establishing its functionality in a tissue and can contribute to the establishment of other involved pathways. The treatment of mature human osteocytes with 1 and 10 nM sAPP695 revealed 24 h as the main time point where changes in gene expression were observed. There is a possibility that this APP species produces effects in an acute manner, therefore a long-term time 96 h treatment window may be too long to observe sAPP695 activity in vitro. To improve on this study, it would be beneficial to perform a short-term time course, investigating the effects of sAPP695 at 3, 6, 12 and 24 h post exposure.

Another limitation to this study was the use of global knock-out animals. Although the APPKO model has been studied widely and is a good model for establishing vital functions of *App*, it cannot be confirmed if the effects seen on the skeleton are due to pre or post-natal developmental defects that persist throughout life or develop as a result of ageing. The design and implementation of a conditional APPKO mouse model to study the effects of a loss of *APP* in osteocytes using an osteocalcin-CRE recombinase knockdown model would be a better model for determining effects localised within the skeletal network.

Chapter 3

Relationships between the Bone Expression of Alzheimer's Disease-Related Genes, Bone Remodelling Genes and Cortical Bone Structure in Neck of Femur Fracture

Manuscript submitted to *Calcified Tissue*

The links between osteoporosis, fracture and Alzheimer's disease have been established in a number of studies previously mentioned. As APP and APLP2 had been characterised in the previous chapter, we next wanted to establish expression levels in a cohort of fracture patients and relate expression with expression of other genes associated with bone loss, gain and remodelling, Vitamin D and creatinine levels and finally structural bone parameters of the contralateral femur.

Statement of Authorship

Title of Paper	The Cancellous Bone Gene Expression of *APP* in a Cohort of Neck of Femur Fracture Patients
Publication Status	☐ Published ☐ Accepted for Publication ☐ Submitted for Publication ☒ Unpublished and Unsubmitted work written in manuscript style
Publication Details	This unpublished manuscript draft will be submitted to Osteoporosis International

Principal Author

Name of Principal Author (Candidate)	Catherine JM Stapledon		
Contribution to the Paper	First author on the paper, generated data, performed all experimental work and analyses and interpreted all data obtained. Made the decision to publish and created manuscript draft.		
Overall percentage (%)	80 %		
Certification:	This paper reports on original research I conducted during the period of my Higher Degree by Research candidature and is not subject to any obligations or contractual agreements with a third party that would constrain its inclusion in this thesis. I am the primary author of this paper.		
Signature		Date	07/05/2020

Co-Author Contributions

By signing the Statement of Authorship, each author certifies that:

i. the candidate's stated contribution to the publication is accurate (as detailed above);

ii. permission is granted for the candidate in include the publication in the thesis; and

iii. the sum of all co-author contributions is equal to 100% less the candidate's stated contribution.

Name of Co-Author	Roberto Cappai		
Contribution to the Paper	Contributed to study design, made the decision to publish and assisted with manuscript draft preparation.		
Signature		Date	7 May 2020

Name of Co-Author	Roumen Stamenkov		
Contribution to the Paper	Assisted with sample collection, performed parts of data analysis and interpretation, made the decision to publish.		
Signature		Date	7 May 2020

Name of Co-Author	L. Bogdan Solomon
Contribution to the Paper	Provided samples for analysis, contributed to study design, made the decision to publish, assisted in manuscript draft preparation.
Signature	Date 7. May 20

Name of Co-Author	Gerald J Atkins
Contribution to the Paper	Senior author, assisted with design and implementation of study and supervised study. Contributed to interpretation of data and made the decision to publish.
Signature	Date 13-5-20

Relationships between the Bone Expression of Alzheimer's Disease-Related Genes, Bone Remodelling Genes and Cortical Bone Structure in Neck of Femur Fracture

Catherine J.M. Stapledon[1], Roumen Stamenkov[2], Roberto Cappai[3], Jillian M. Clark[1,4], L. Bogdan Solomon[1, 2], Gerald J. Atkins[1,2]✉

[1]Centre for Orthopaedic and Trauma Research, Adelaide Medical School, The University of Adelaide, Adelaide, SA, Australia

[2]Department of Orthopaedics & Trauma, Royal Adelaide Hospital, Adelaide, SA, Australia

[3]Department of Pharmacology and Therapeutics, The University of Melbourne, Melbourne, VIC, Australia

[4]South Australian Spinal Cord Injury Research Centre, Hampstead Rehabilitation Centre, Lightsview, SA, Australia

✉Corresponding author: gerald.atkins@adelaide.edu.au

ORCID Identifiers:

CJS 0000-0002-2827-2396

RC 0000-0002-9505-8496

JMC 0000-0002-9076-6573

LBS 0000-0001-6254-2372

GJA 0000-0002-3123-9861

Mini-abstract

We examined possible relationships between osteoporosis and dementia by analysing bone gene expression in patients treated for osteoporotic hip fracture. We found relationships between genes implicated in Alzheimer's disease and bone remodelling, and relationships between Alzheimer's disease gene expression and bone structure, supporting a common link between osteoporosis and dementia.

Abstract

Purpose: Neck of femur (NOF) fracture is a prevalent fracture type amongst the ageing and osteoporotic populations, commonly requiring total hip replacement (THR) surgery. Increased fracture risk has also been associated with Alzheimer's disease (AD) in the aged. Here, we sought to identify possible relationships between the pathologies of osteoporosis and dementia by analysing bone expression of neurotrophic or dementia-related genes in patients undergoing THR surgery for NOF fracture.

Methods: Femoral bone samples from 66 NOF patients were examined for expression of the neurotrophic genes amyloid precursor protein (*APP*), APP-like protein-2 (*APLP2*), Beta Secretase Cleaving Enzyme-1 (*BACE1*) and nerve growth factor (NGF). Relationships were examined between the expression of these and of bone regulatory genes, systemic factors and bone structural parameters ascertained from plain radiographs.

Results: We found strong relative levels of expression and positive correlations between *APP, APLP2, BACE1* and *NGF* levels in NOF bone. Significant correlations were found between *APP, APLP2, BACE1* mRNA levels and bone remodelling genes *TRAP, RANKL*, and the *RANKL:OPG* mRNA ratio, indicative of potential functional relationships at the time of

fracture. Analysis of the whole cohort, as well as non-dementia and dementia sub-groups, revealed structural relationships between *APP* and *APLP2* mRNA expression and lateral femoral cortical thickness.

Conclusion: These findings suggest that osteoporosis and AD may share common molecular pathways of disease progression, perhaps explaining the common risk factors associated with these diseases. The observation of a potential pathologic role for AD-related genes in bone may also provide alternative treatment strategies for osteoporosis and fracture prevention.

Key words: Osteoporosis, neck of femur, fracture, APP, dementia, Alzheimer's disease.

Introduction

In Australia, the proportion of individuals aged 65 and over has increased from 12.3% to 15.9% in a twenty year period (130). This has resulted in a parallel rise in the rate of development of age-related pathologies. Neck of femur (NOF) fracture is a painful and debilitating fragility-related fracture, that negatively impacts the lives of over 19,000 Australians every year (62). The risk of developing fragility fractures, such as NOF, increases substantially with increasing age (254). Other risk factors associated with the development of a NOF fracture include gender, with females being at greater risk than males, low bone mineral density (BMD) attributable to osteopenia or osteoporosis (255, 256) and prior fracture (257). Osteoporosis is one of the most common musculoskeletal diseases associated with increased fracture risk. The epidemiology of dementia mirrors that of osteoporosis. Dementia is the second leading cause of death and disability in Australia (258, 259) and shares many of the same risk factors as fracture and osteoporosis. The most commonly occurring form of dementia in Australia is Alzheimer's disease (AD), which accounts for up to 70% of all dementia diagnoses. There are currently no effective therapeutics for the prevention or treatment of AD.

Previous studies have sought to determine links between increased fracture risk and the development of AD and other forms of dementia (158, 172, 260-264). A number of risk factors have been identified through observational cohort studies linking these pathologies, including age, gender, vitamin D status, bone mineral density (BMD) and comorbidities, such as chronic kidney disease (265). Data from the Australian New Zealand Hip Fracture Registry indicate that while 59% of hip fracture patients reported no problem with cognition prior to hospital admission, 41% of such patients had either not been assessed for cognition prior or were suffering from a cognition-related illness (266). Recent studies have reported that patients with a low BMD have a higher incidence of AD and subsequent risk of fracture, however underlying mechanisms linking these major health issues are yet to be determined (162, 267-270).

Hip fractures associated with frailty and OP usually occur at the femoral neck (56%), pertrochanteric region (38%) or subtrochanteric region (5.8%). They are often a result of a fall or minimal trauma, associated with poor bone quality and strength. The cellular mechanisms underlying fragility fracture are associated in part with dysregulated bone remodelling leading to net bone loss. The RANKL/RANK/OPG signalling pathway plays a prominent role in this process, controlling the formation and activity of the key bone resorbing effector cell in the bone remodelling process, the osteoclast (271). However, low bone formation rates and poor bone quality at key skeletal sites, as well as muscle quality and mass are other important determinants of bone strength and resistance to low trauma fracture. Osteocytes have emerged as an important controlling cell type in various aspects of bone remodelling, as well as in a number of systemic roles (6, 272). The presence of an intact osteocytic network is also important in the maintenance of bone integrity and this degrades with ageing and the onset of osteoporosis (273-275). Osteocyte-derived factors, such as RANKL and sclerostin, encoded by the *SOST* gene, have emerged as important therapeutic targets in the treatment of osteoporosis (6). Osteocyte control of RANKL-dependent osteoclastogenesis has been shown in response to mechanical (276, 277), as well as metabolic and dietary signals (278, 279). In adult human bone, osteocytes are a prominent source of RANKL (280). We have shown that pathological stimuli, such as orthopaedic implant derived wear particles also likely exert an effect through this pathway (237). Human osteocytes have also been reported to express neurotrophic factors, including nerve growth factor (NGF) (242) and the amyloid precursor protein (APP) (281). The study by Li and colleagues (281) also reported osteocyte expression of the neurotoxic peptide $A\beta_{1\text{-}42,}$ derived from post-translational processing of APP by the beta-secretase BACE1, and which is a known contributor to AD pathogenesis.

In this study, we sought to uncover links connecting the pathologies of osteoporosis and dementia by investigating the bone expression of AD-related and neurotrophic genes in bone

taken from patients undergoing surgery for NOF fracture, and relating this to bone turnover-related gene expression, as well as bone structure. We present evidence for novel relationships between neuropathic gene expression, bone remodelling and bone structure, potentially contributing to fragility fracture and reflecting cognition in this cohort of patients.

Materials and Methods

Sample Collection

Intertrochanteric trabecular bone biopsies, plasma and pre-surgical radiographs were collected from patients undergoing hip arthroplasty for a fracture NOF at the Royal Adelaide Hospital (RAH) Adelaide, South Australia, between July 2018 and July 2019. During preoperative preparation, patients or next of kin, depending on cognitive state, were asked to participate in this study, and informed written consent was obtained. Date of surgery, patient age, comorbidities, creatinine levels, vitamin D status and medication history were collected from patient case notes. The study was approved by the Human Research Ethics Committee of the RAH (Protocol no 130114; HREC/13/RAH/33).

Cohort Demographics and Comorbidities

Participants were screened upon hospital admission prior to surgery and daily thereafter using the Confusion Assessment Method (CAM) in association with the Abbreviated Mental Test Score (AMTS) (282). Perioperatively, participants were assessed for cognitive impairment using the Mini-Mental State Examination (MMSE) (283). In some cases, participants had a diagnosis of AD or dementia prior to hospital admission. Participants were excluded if their bone samples yielded poor RNA quality or amount (260:280nm absorbance ratio < 1.7; yield

< 100 ng/µl). Thus, of the 93 consented participants who provided bone biopsies and plasma samples, 66 were included for further analysis, including 53 females (80.3 %) and 13 males (19.7 %). Comorbidity data was obtained from the SA Health OACIS Medical Record Database from the RAH. Demographic and comorbidity data are shown in **Table 1**.

Processing of Bone Biopsies

During surgery tube saw cancellous bone biopsies were taken from the intertrochanteric region before the femoral canal was prepared for receiving the femoral stem. Samples were submerged in saline in a sterile container and collected from theatre within 48 hours of surgery. All samples were processed in a sterile biosafety cabinet. Each sample was cut into approximately 2 cm^3 cubes and washed 3-4 times with sterile 1 x phosphate buffered saline (PBS) to remove loosely adherent cells and debris. Samples were then stored at -80°C for up to two weeks before processing for RNA. Samples for histology were stored in Osteosoft® solution (Merck KGaA; Darmstadt, Germany), for one week and processed for histological analysis.

RNA Extraction

Bone biopsies stored at -80°C between 1 and 7 days were placed into liquid nitrogen contained in a ceramic mortar sprayed with RNaseZap® (ThermoFisher Scientfic, MA, USA). Samples were pulverised using an RNaseZap-treated pestle. Bone remnants were transferred into a 1.5 ml RNAse-free reaction tube (Eppendorf AG, Hamburg) containing 1 ml of TRIZOL reagent (Life Technologies, NY, USA). RNA extraction was conducted as per the manufacturer's instructions (284). Complementary DNA (cDNA) synthesis was performed using iScript™ RT kit (Bio-Rad, Hercules, CA, USA), as per the manufacturer's instructions.

Real-Time RT-PCR

Real-time RT PCR was conducted for amyloid precursor protein (*APP*), amyloid precursor-like protein-2 (*APLP2*), beta-secretase cleaving enzyme-1 (*BACE1*), 25-hydroxyvitamin D 1∝-hydroxylase (*CYP27B1),* dentin matrix acid phosphoprotein-1 (*DMP1*), nerve growth factor (*NGF)*, osteocalcin (*OCN*), osteoprotegerin (*OPG)*, receptor activator of nuclear factor kappa-B ligand (*RANKL*), sclerostin (*SOST*) and tartrate resistant acid phosphatase (*TRAP*). Oligonucleotide primers were designed to be human mRNA-specific. Primer sequences are shown in **Supplementary Table 1**. Cycle threshold (CT) values were normalised to those of the *18S* housekeeping gene using the delta-CT method (2^-(CT1-CT2)) (285).

Radiographic Analysis

Calibrated Anterior-Posterior (AP) plain radiographs of the contralateral femur were used in PACS software to measure medial (M) and lateral (L) cortical thicknesses, and M-L medullary width and femoral width using CARESTREAM software version 5.7 **(**Windsor, CO, USA).

Statistical Analyses

All statistical testing was conducted using the GraphPad Prism Analysis Program v.7.02 (GraphPad Prism, La Jolla, CA, USA). Gene expression levels were analysed using a non-parametric, One-way Analysis of Variance (ANOVA) test, correcting for multiple comparisons. Relationships between the expression of various genes were tested using Spearman's correlation analysis. A p value < 0.05 was considered significant for all analyses.

Results

Characteristics of participants

The mean age of the 66 patients investigated was 81.9 ± 9.15 years (range 58 – 96). Serum 25(OH)vitamin D (Vitamin D) levels ranged from 11 – 154 nM. Serum creatinine levels were widely variable, ranging from 40 – 303 pM. The most common pre-fracture comorbidities within the study population were hypertension (65.15 %), hypercholesterolemia (30.30 %), osteoarthritis (25.76 %), type II Diabetes Mellitus (25.76 %), atrial fibrillation (24.24 %), gout (24.24 %), and osteoporosis (18.18 %) (**Supplementary Table 2**). Including those identified in-hospital, 13 (19.69 %) participants had a diagnosis of dementia. In this study, there were a total of 5 in-hospital deaths (7.6%), 2 males (15.4% of the male group) and 3 females (5.7% of the female group).

Gene expression analysis of the NOF cohort

In order to investigate potential functional relationships between genes with known roles in neuronal function or neurodegenerative disease and those with known roles in bone remodelling, real-time RT PCR analysis was performed. Initial analysis revealed high mRNA expression levels of *APP, APLP2* and of the marker of osteoclast activity, *TRAP* (**Fig. 1a**). In comparison to *APP* and *APLP2, BACE1* levels were lower although present in all bone samples. A strong correlation between *APP* and *APLP2* expression was observed (r = 0.88; **Fig. 1b**). *APP* mRNA expression also correlated with those of *BACE1* ($p < 0.0001$), *DMP1* ($p = 0.0004$), *NGF* ($p = 0.014$), *OPG* ($p = 0.0005$), *RANKL* ($p < 0.0001$), the *RANKL:OPG* mRNA ratio ($p = 0.021$) and *TRAP* ($p < 0.0001$) (**Fig. 1b**). *APLP2* mRNA expression also correlated with that of *BACE1* ($p = 0.003$), however the relationship was not as strong as *APP* and *BACE1*. *APLP2* correlated with the same genes as *APP* (*DMP1* $p = 0.033$; *NGF* $p = 0.0203$; *OPG* $p =$

0.027; RANKL $p < 0.0001$; *RANKL:OPG* ratio $p = 0.0009$ and *TRAP* $p < 0.0001$). There were observable correlations between *BACE1* and *DMP1* ($p = 0.0003$), *NGF* ($p = 0.017$), *OPG* ($p < 0.0001$), *RANKL* ($p = 0.0003$) and *TRAP* ($p < 0.0001$). *APLP2* was positively correlated with the same set of genes. *BACE1* was the only gene to reveal a positive correlation with age, however it did not correlate with the *RANKL:OPG* mRNA ratio, an indicator of active bone resorption (**Fig. 1b**). There was a strong negative correlation between the *RANKL:OPG* mRNA ratio and *SOST* mRNA expression ($r = -0.659$, $p < 0.0001$).

Relationships between bone gene expression and systemic markers

Correlation analysis was performed in order to determine whether relationships existed between routinely assessed serum vitamin D and serum creatinine levels and bone cell gene expression. Whole cohort analysis did not reveal statistically significant relationships between any of the genes analysed and serum vitamin D (**Supplementary Table 3**). Serum creatinine levels, an indicator of normal kidney function (286, 287), were also tested. Interestingly, a significant positive correlation was observed between serum creatinine levels and *OPG* mRNA expression ($r = 0.346$; $p = 0.006$) (**Supplementary Table 3**). However, no other relationships between serum vitamin D or creatinine with bone gene expression were found.

Whole cohort relationships between gene expression and bone structure

As most NOF patients did not have bone densitometry performed prior to their fracture, BMD values were not available. However, physical measurements of the proximal femur from plain radiograph images were analysed for: 1 – lateral cortical thickness, 2 – medial cortical thickness, 3 – medullary width and 4 – femoral width (**Fig. 2a - e**).

Spearman's *r* values were calculated between expression of genes of interest and femoral structural measures. Analysis of markers of bone remodeling revealed significant correlations between lateral cortical thickness of the femur and *RANKL, TRAP, DMP1* and *OPG* (**Table 1**). The strongest negative correlation was observed between femoral cortical thickness and *RANKL*, followed by *TRAP*, *OPG* and *DMP1* (**Table 1**, **Fig. 3**). These findings served to validate the approach taken and imply that femoral cortical thickness is causally related to the expression of these genes. There were no correlations between any of the structural parameters and *BACE1* (**Table 1**). Interestingly, negative correlations were observed between *APP* and *APLP2* mRNA expression and lateral cortical thickness (**Table 1**, **Fig. 3**). This suggests that expression of these genes is associated with loss of cortical bone thickness through influences on bone remodelling.

Individual gene expression relationships between dementia and non-dementia

Next, subgroup analysis was performed based on dementia status within the NOF cohort. Subjects were dichotomised as either non-dementia or dementia, the latter based on any diagnosed form. Initial analysis demonstrated a similar pattern within each group as the entire NOF cohort, in terms relative expression of each gene. There were no significant differences between the non-dementia and dementia groups for any of the genes analysed (**Supplementary Fig. 1**).

Gene expression and femoral structural parameter relationships between dementia and non-dementia subgroups

To determine whether relationships between neurotrophic genes of interest and remodelling genes differed between non-dementia and dementia subgroups, non-parametric Spearman's

correlation analyses were performed. In the non-dementia group, there were significant correlations observed between *APP* and *APLP2* ($p < 0.0001$), *BACE1* ($p < 0.0001$), *DMP1* ($p = 0.0009$), *OPG* ($p < 0.0001$), *RANKL* ($p < 0.0001$) and *TRAP* ($p < 0.0001$). Similar correlations were observed between *APLP2* and these genes and there was also a significant correlation with *RANKL:OPG* ratio ($p = 0.007$), which was not observed with *APP*. *BACE1* was shown to be significantly correlated with *DMP1* (R = 0.42; $p = 0.002$), *NGF* (R = 0.54; $p = 0.007$), *OPG* (R = 0.38; $p = 0.0078$), *RANKL* (R = 0.465; $p < 0.0001$) and *TRAP* (R = 0.5; $p = 0.0004$) (**Fig. 4a**).

In the dementia group, there were notably fewer correlations between genes of interest (**Fig. 4b**). Like in the non-dementia group, *APP* significantly correlated with *APLP2* ($p < 0.0001$), however there was no correlation with *BACE1* expression. There were weak correlations of trending significance between *APP* and *NGF* ($r = 0.667$, $p = 0.083$) and *APP* and the *RANKL:OPG* mRNA ratio ($r = 0.573$; $p = 0.056$). A strong positive correlation was, however, apparent between *APP* and *TRAP* mRNA (r = 0.857; p = 0.0004). Analysis of *APLP2* revealed a similar pattern, with a strong correlation observed with *NGF* (r = 0.83; p = 0.015) and *TRAP* (r = 0.69; p = 0.017). *BACE1* mRNA expression was significantly correlated with *OCN* (R = 0.70; $p = 0.01$) and *OPG* ($r = 0.86$; $p < 0.0001$) and the correlation between *BACE1* and *RANKL* was trending ($r = 0.52$; $p = 0.084$). Interestingly, correlations between *BACE1* and *OCN* expression were not observed in the non-dementia group. In addition, *OCN* and *OPG* were only significantly correlated in the dementia group. Finally, there was a strong negative relationship observed between *RANKL* mRNA expression and that of *SOST* in the dementia group ($r = -0.86$) (**Fig. 4b).**

To determine whether gene expression correlated with structural femoral parameters in non-dementia and dementia groups, Spearman's correlation testing was performed. Analysis of the non-dementia group only did not reveal any significant relationships between either *APP,*

APLP2 or BACE1 and structural femoral parameters (**Table 2**). There were however negative correlations observed between lateral cortical thickness and *OPG* (r = -0.41)*, RANKL* (r = -0.45) and *TRAP* (r = -0.35). There were also correlations observed between the structural parameters lateral cortical thickness, medial cortical thickness (r = 0.354; p = 0.021) and femoral width (r = 0.378; p = 0.014). In addition, *RANKL, RANKL:OPG* and *TRAP* mRNA expression were negatively correlated with femoral width in the non-dementia group.

Analysis of the dementia group revealed a trending negative correlation between *APP* and lateral cortical thickness (r = -0.591; p = 0.061). Analysis of the femoral regions revealed strong correlations between lateral cortical thickness and medial cortical thickness (r = 0.597; p = 0.057) and a negative correlation with medullary width (r = -0.782; p = 0.006) (**Table 2**).

Relationships between genes of interest and serum Vitamin D or creatinine

Analyses of all genes against serum Vitamin D and creatinine levels were performed to determine if there were differences between dementia and non-dementia groups. There were no significant correlations between *APP, APLP2 or BACE1* and Vitamin D or creatinine. In both the non-dementia and dementia groups however, there were correlations between *OPG* mRNA expression and serum creatinine levels (**Supplementary Fig. 2**).

Discussion

Osteoporosis leading to fragility fracture of the hip and dementia are known to afflict a similar demographic. These diseases not only contribute to high rates of morbidity and mortality in the aged but also place a huge economic burden on the health care system. Patients undergoing arthroplasty for the management of their fracture are a diverse cohort of a wide age range, who suffer from a myriad of comorbidities, which makes them a difficult group to assess at the molecular level. In keeping with this being a 'silent disease' (256), only 18% of patients in this study had a pre-existing diagnosis of osteoporosis. This is one of the first cohort studies combining bone genetics, bone structure, systemic measures and co-morbidity information in the NOF population in Australia in an attempt to uncover links between these pathologies.

Whole cohort analysis revealed for the first time strong coordinated expression of the CNS related genes *APP, APLP2* and *BACE1* in adult human bone tissue. Intriguingly, the expression of these genes was closely related to known markers of bone turnover, *RANKL* and *TRAP,* and osteoblast activity, *OPG* and *DMP1.* The strongest correlations were observed between *APP, APLP2, BACE1* and *RANKL* and *TRAP* not only in the whole cohort analysis, but also within the dementia subgroup. These strong associations are suggestive of a linked functionality between genes involved in CNS homeostasis and pathology in bone remodelling. In the context of NOF fracture, the relationships were still existent in the non-dementia group as well as the dementia group, indicating that there may be an acceleration of bone loss in this subgroup, however this warrants further analysis of a larger cohort powered to determine differences between various classifications of cognitive impairment. Despite many of the relationships seen in both the non-dementia and dementia groups being consistent, there were unexpected relationships between *BACE1, OCN* and *OPG* observed solely in the dementia group. These correlations unique to dementia bone specimens may indicate possible alternate mechanisms of bone loss occurring. These observations may indicate a role for genes involved in the

homeostasis of the CNS in processes such as bone resorption through either direct or indirect mechanisms. However, as these are associations, it is not possible to determine the driver of each relationship observed.

The strong relationship evident between serum creatinine and *OPG* mRNA expression in the whole NOF cohort was an unexpected finding. Previous relationships between serum OPG and creatinine have been noted in the context of severe artery calcification (288), where increased serum OPG was found to be a potential marker for all-cause mortality in patients with chronic kidney disease. This relationship requires further elucidation in the context of fracture as it may be an indicator of other comorbidities.

Analysis of the femoral cortical bone parameters is a useful tool to assess relationships between bone structure and gene expression. The cortical thickness index has been tested as a surrogate for BMD in hip fracture patients (289-291). In this study, the structural parameter most closely related to the largest number of functional genes was lateral cortical thickness. A similar pattern was observed within the whole cohort with inverse relationships between the expression of all of *RANKL, TRAP, OPG* and *DMP1* and lateral cortical thickness, suggesting that all of these genes known to be related to bone remodelling are linked to increased bone loss or reduced bone formation at this particular site. In particular, *TRAP* expression was strongly correlated with a number of different genes and parameters, and can be a marker of not only osteoclastic resorption but also osteocytic osteolysis (6). This highlights the need to investigate further the role of osteocytes in age-related bone loss and potential accelerated bone loss in dementia. Interestingly, the expression of *APP* and *APLP2* were also correlated with this structural parameter, implicating these neurotrophic genes in the control of bone structure. In the subgroup analysis, despite the small number of participants in the dementia group, these trends were still observed. The inverse relationships between *APP* and *APLP2* and cortical thickness suggests positive roles for these genes in net bone loss. Future studies are warranted to

determine if these genes contribute to cortical thinning or cortical porosity, characteristic of osteoporosis and fracture risk (292).

As this was a study solely of a population undergoing emergency total hip replacement surgery for NOF, we cannot determine whether the relationships observed are specific to NOF or are generalizable to the population as a whole. However, in a time where average life expectancies and the ageing population are increasing, it is imperative to understand the genetic changes that are occurring in the bone in these later stages of life. In particular, links between cognitive decline and systemic manifestations of ageing and frailty, such as osteoporosis, need to be better understood.

Acknowledgements

The authors thank the nursing and surgical staff of the Orthopaedic and Trauma Service of the Royal Adelaide Hospital for help in obtaining patient samples. GJA was supported by a National Health and Medical Research Council of Australia (NHMRC) Senior Research Fellowship. CJMS was supported by an Australian Postgraduate Award scholarship.

Disclosures

The authors have no disclosures.

References

1. Health AIo, Welfare (2019) Deaths in Australia. AIHW, Canberra

2. Health AIo, Welfare (2018) Hip fracture incidence and hospitalisations in Australia 2015–16. AIHW, Canberra

3. Cummings SR, Melton LJ (2002) Epidemiology and outcomes of osteoporotic fractures. Lancet 359:1761-1767

4. Zupan J, Mencej-Bedrac S, Jurkovic-Mlakar S, Prezelj J, Marc J (2010) Gene-gene interactions in RANK/RANKL/OPG system influence bone mineral density in postmenopausal women. J Steroid Biochem Mol Biol 118:102-106

5. Watts JJ, Abimanyi-Ochom J, Sanders KM (2013) Osteoporosis costing all Australians: a new burden of disease analysis - 2012 to 2022.

6. Kanis JA, Johnell O, De Laet C, et al. (2004) A meta-analysis of previous fracture and subsequent fracture risk. Bone 35:375-382

7. AIHW (2012) Dementia in Australia.

8. Alzheimer's A (2015) 2015 Alzheimer's disease facts and figures. Alzheimers Dement 11:332-384

9. Downey CL, Young A, Burton EF, Graham SM, Macfarlane RJ, Tsapakis EM, Tsiridis E (2017) Dementia and osteoporosis in a geriatric population: Is there a common link? World J Orthop 8:412-423

10. Friedman SM, Menzies IB, Bukata SV, Mendelson DA, Kates SL (2010) Dementia and hip fractures: development of a pathogenic framework for understanding and studying risk. Geriatr Orthop Surg Rehabil 1:52-62

11. Guo P, Wang S, Zhu Y, Shen X, Jin X, Qian M, Tang H (2012) Prevalence of osteopenia and osteoporosis and factors associated with decreased bone mineral density in

elderly inpatients with psychiatric disorders in Huzhou, China. Shanghai Arch Psychiatry 24:262-270

12. Hsu B, Bleicher K, Waite LM, Naganathan V, Blyth FM, Handelsman DJ, Le Couteur DG, Seibel MJ, Cumming RG (2018) Community-dwelling older men with dementia are at high risk of hip fracture, but not any other fracture: The Concord Health and Aging in Men Project. Geriatr Gerontol Int 18:1479-1484

13. Wang HK, Hung CM, Lin SH, et al. (2014) Increased risk of hip fractures in patients with dementia: a nationwide population-based study. BMC Neurol 14:175

14. Tysiewicz-Dudek M, Pietraszkiewicz F, Drozdzowska B (2008) Alzheimer's disease and osteoporosis: common risk factors or one condition predisposing to the other? Ortopedia, traumatologia, rehabilitacja 10:315-323

15. Liu Y, Wang Z, Xiao W (2018) Risk factors for mortality in elderly patients with hip fractures: a meta-analysis of 18 studies. Aging Clin Exp Res 30:323-330

16. Maravic M, Ostertag A, Urena P, Cohen-Solal M (2016) Dementia is a major risk factor for hip fractures in patients with chronic kidney disease. Osteoporos Int 27:1665-1669

17. ANZHFR (2018) ANZHFR Bi-National Annual Report of Hip Fracture Care 2018. Australian and New Zealand Hip Fracture Registry

18. Amouzougan A, Lafaie L, Marotte H, Dėnariė D, Collet P, Pallot-Prades B, Thomas T (2017) High prevalence of dementia in women with osteoporosis. Joint bone spine 84:611-614

19. Frame G, Bretland KA, Dengler-Crish CM (2020) Mechanistic complexities of bone loss in Alzheimer's disease: a review. Connective tissue research 61:4-18

20. Kang HG, Park HY, Ryu HU, Suk SH (2018) Bone mineral loss and cognitive impairment: The PRESENT project. Medicine 97:e12755

21. Liu D, Zhou H, Tao Y, Tan J, Chen L, Huang H, Chen Y, Li Y, Zhou R (2016) Alzheimer's Disease is Associated with Increased Risk of Osteoporosis: The Chongqing Aging Study. Current Alzheimer research 13:1165-1172

22. Zhou R, Deng J, Zhang M, Zhou HD, Wang YJ (2011) Association between bone mineral density and the risk of Alzheimer's disease. Journal of Alzheimer's disease : JAD 24:101-108

23. Walsh MC, Choi Y (2014) Biology of the RANKL-RANK-OPG System in Immunity, Bone, and Beyond. Frontiers in immunology 5:511

24. Prideaux M, Findlay DM, Atkins GJ (2016) Osteocytes: The master cells in bone remodelling. Curr Opin Pharmacol 28:24-30

25. Dallas SL, Prideaux M, Bonewald LF (2013) The osteocyte: an endocrine cell ... and more. Endocrine reviews 34:658-690

26. Zarrinkalam MR, Mulaibrahimovic A, Atkins GJ, Moore RJ (2012) Changes in osteocyte density correspond with changes in osteoblast and osteoclast activity in an osteoporotic sheep model. Osteoporosis international : a journal established as result of cooperation between the European Foundation for Osteoporosis and the National Osteoporosis Foundation of the USA 23:1329-1336

27. Milovanovic P, Zimmermann EA, Riedel C, et al. (2015) Multi-level characterization of human femoral cortices and their underlying osteocyte network reveal trends in quality of young, aged, osteoporotic and antiresorptive-treated bone. Biomaterials 45:46-55

28. Tiede-Lewis LM, Dallas SL (2019) Changes in the osteocyte lacunocanalicular network with aging. Bone 122:101-113

29. Hemmatian H, Bakker AD, Klein-Nulend J, van Lenthe GH (2017) Aging, Osteocytes, and Mechanotransduction. Current Osteoporosis Reports 15:401-411

30. Qin L, Liu W, Cao H, Xiao G (2020) Molecular mechanosensors in osteocytes. Bone research 8:23

31. Ben-awadh AN, Delgado-Calle J, Tu X, Kuhlenschmidt K, Allen MR, Plotkin LI, Bellido T (2014) Parathyroid hormone receptor signaling induces bone resorption in the adult skeleton by directly regulating the RANKL gene in osteocytes. Endocrinology 155:2797-2809

32. Xiong J, Piemontese M, Thostenson JD, Weinstein RS, Manolagas SC, O'Brien CA (2014) Osteocyte-derived RANKL is a critical mediator of the increased bone resorption caused by dietary calcium deficiency. Bone 66:146-154

33. Mueller RJ, Richards RG (2004) Immunohistological identification of receptor activator of NF-kappaB ligand (RANKL) in human, ovine and bovine bone tissues. J Mater Sci Mater Med 15:367-372

34. Ormsby RT, Solomon LB, Yang D, Crotti TN, Haynes DR, Findlay DM, Atkins GJ (2019) Osteocytes respond to particles of clinically-relevant conventional and cross-linked polyethylene and metal alloys by up-regulation of resorptive and inflammatory pathways. Acta Biomater 87:296-306

35. Stapledon CJM, Tsangari H, Solomon LB, Campbell DG, Hurtado P, Krishnan R, Atkins GJ (2019) Human osteocyte expression of Nerve Growth Factor: The effect of Pentosan Polysulphate Sodium (PPS) and implications for pain associated with knee osteoarthritis. PloS one 14:e0222602

36. Li S, Liu B, Zhang L, Rong L (2014) Amyloid beta peptide is elevated in osteoporotic bone tissues and enhances osteoclast function. Bone 61:164-175

37. Hodkinson HM (1972) Evaluation of a mental test score for assessment of mental impairment in the elderly. Age and ageing 1:233-238

38. Creavin ST, Wisniewski S, Noel-Storr AH, et al. (2016) Mini-Mental State Examination (MMSE) for the detection of dementia in clinically unevaluated people aged 65

and over in community and primary care populations. The Cochrane database of systematic reviews Cd011145

39. Hummon AB, Lim SR, Difilippantonio MJ, Ried T (2007) Isolation and solubilization of proteins after TRIzol extraction of RNA and DNA from patient material following prolonged storage. Biotechniques 42:467-470, 472

40. Livak KJ, Schmittgen TD (2001) Analysis of relative gene expression data using real-time quantitative PCR and the 2(-Delta Delta C(T)) Method. Methods 25:402-408

41. Myers GL, Miller WG, Coresh J, et al. (2006) Recommendations for improving serum creatinine measurement: a report from the Laboratory Working Group of the National Kidney Disease Education Program. Clin Chem 52:5-18

42. Ceriotti F, Boyd JC, Klein G, Henny J, Queralto J, Kairisto V, Panteghini M, Intervals ICoR, Decision L (2008) Reference intervals for serum creatinine concentrations: assessment of available data for global application. Clin Chem 54:559-566

43. Krzanowski M, Krzanowska K, Dumnicka P, Gajda M, Woziwodzka K, Fedak D, Grodzicki T, Litwin JA, Sulowicz W (2018) Elevated Circulating Osteoprotegerin Levels in the Plasma of Hemodialyzed Patients With Severe Artery Calcification. Ther Apher Dial 22:519-529

44. Baumgartner R, Heeren N, Quast D, Babst R, Brunner A (2015) Is the cortical thickness index a valid parameter to assess bone mineral density in geriatric patients with hip fractures? Arch Orthop Trauma Surg 135:805-810

45. Dorr LD, Faugere MC, Mackel AM, Gruen TA, Bognar B, Malluche HH (1993) Structural and cellular assessment of bone quality of proximal femur. Bone 14:231-242

46. Sah AP, Thornhill TS, LeBoff MS, Glowacki J (2007) Correlation of plain radiographic indices of the hip with quantitative bone mineral density. Osteoporos Int 18:1119-1126

47. Buenzli PR, Thomas CD, Clement JG, Pivonka P (2013) Endocortical bone loss in osteoporosis: the role of bone surface availability. Int J Numer Method Biomed Eng 29:1307-1322

Figure Legends

Figure 1: Gene expression and correlation analysis for the whole NOF cohort. A. Gene expression of each gene of interest normalised to the 18S housekeeping gene. B. A heat map representation of the relationships between each gene of interest using the Spearman's correlation co-efficient. *r* values are reported. Relationship direction and strength are indicated by the legend: 0 – 1.0 indicates positive relationship between genes and - 1.0 – 0 indicates a negative relationship between genes. The significance of *r* values is indicated by $*p < 0.05$, $**p < 0.01$ and $***p < 0.001$.

Figure 2: Examples of AP plain radiographic images of the hip joint with manual linear measurements applied conducted using the CARESTREAM program. (A) Measurement of the lateral cortex. (B) Measurement of the medial cortex. (C) Measurement of the femoral canal *measured from the most distal point of the lesser trochanter perpendicular to femoral midline. (D) Femoral midline measurement. (E) Measurements of the femoral neck used for analysis: 1 – Lateral cortical thickness (μm); 2 – Medial cortical thickness (μm); 3 – Medullary width (mm); 4 – Femoral width (mm).

Figure 3: Relationships between gene expression and bone structure. Individual NOF patient radiographs were assessed for the structural parameter lateral cortical thickness, measures of which were compared with relative gene expression from the same patient, as described in Materials and Methods. Significant correlations were observed between lateral cortical thickness and A) *APP*, B) *APLP2*, C) *RANKL,* D) *TRAP,* E) *DMP1,* F) *OPG* mRNA expression. *r* values and associated values for *p* are indicated. Number of pairs = 65/parameter.

Figure 4: Gene expression and correlation analysis of sub-groups dichotomized on any diagnosis of dementia. Gene expression of each gene of interest was normalised to the 18S housekeeping gene. Heat map representation of the relationships between each gene of interest using the Spearman's correlation co-efficient (*r*) for A) Non-dementia and B) Dementia sub-groups. Relationship direction and strength are indicated by the legend: 0 – 1.0 indicates positive relationship between genes and - 1.0 – 0 indicates a negative relationship between genes. The significance of *r* values is indicated by $*p < 0.05$, $**p < 0.01$ and $***p < 0.001$.

Supplementary Figure 1: Gene expression analysis for non-dementia and dementia groups. Real-time RT-PCR analysis of genes of interest normalised to the 18S housekeeping gene for non-dementia group ($n = 53$) versus the dementia group ($n = 13$). There were no statistical differences between groups for any gene (Student's t-test). Data are depicted as means only.

Supplementary Figure 2: Correlations between *OPG* mRNA expression and serum creatinine in non-dementia and dementia groups. A. *OPG* mRNA expression was moderately correlated with serum creatinine in the non-dementia group (n = 48). B. *OPG* and serum creatinine were positively correlated in the dementia group (n = 13).

Table 1: Whole Cohort Correlation Analysis of Gene Expression with Structural Parameters.

Relative gene expression was generated by Real-time RT-PCR normalised to 18S rRNA levels. Structural parameters measured from plain radiographs: Lateral cortex (LC); Medial cortex (MC); Femoral canal (FC); Proximal femur outer (PFO). Significant correlations and their respective *p* values are bolded.

Gene	LC (1)		MC (2)		FC (3)		PFO (4)	
	r	*p*	*r*	*p*	*r*	*p*	*r*	*p*
APP	**-0.329**	**0.007**	-0.068	0.585	-0.021	0.866	-0.152	0.224
APLP2	**-0.354**	**0.004**	-0.116	0.359	-0.007	0.958	-0.182	0.147
BACE1	-0.196	0.118	-0.090	0.478	-0.032	0.798	-0.137	0.276
CYP27B1	0.196	0.120	-0.007	0.955	0.140	0.270	0.175	0.166
DMP1	**-0.253**	**0.042**	0.053	0.674	-0.012	0.923	-0.103	0.415
NGF	-0.196	0.276	-0.157	0.384	0.045	0.804	-0.104	0.565
OCN	-0.032	0.802	0.011	0.930	0.014	0.910	0.020	0.872
OPG	**-0.313**	**0.014**	0.030	0.817	0.034	0.792	-0.070	0.590
RANKL	**-0.385**	**0.002**	-0.096	0.467	-0.078	0.553	**-0.294**	**0.023**
RANKL:OPG	-0.142	0.279	-0.114	0.386	-0.217	0.095	**-0.358**	**0.005**
SOST	0.120	0.544	0.140	0.477	0.243	0.213	0.317	0.100
TRAP	**-0.316**	**0.013**	-0.069	0.596	-0.127	0.329	-0.247	0.054

Table 2: Correlation Analysis of Gene Expression with Structural Parameters in Non-dementia and Dementia subgroups.

NON-DEMENTIA

	LC (1)		*MC (2)*		*FC (3)*		*PFO (4)*	
Gene	*r*	*p*	*r*	*p*	*r*	*p*	*r*	*p*
APP	-0.246	0.117	-0.252	0.108	-0.090	0.572	-0.247	0.114
APLP2	-0.262	0.094	-0.245	0.118	-0.095	0.551	-0.256	0.102
BACE1	-0.135	0.396	-0.147	0.353	-0.094	0.554	-0.215	0.172
CYP27B1	**0.356**	**0.022**	0.137	0.393	-0.042	0.792	0.074	0.647
DMP1	-0.175	0.267	0.150	0.343	-0.109	0.492	-0.118	0.458
NGF	-0.184	0.425	-0.271	0.234	0.013	0.955	-0.109	0.638
OCN	0.086	0.589	0.028	0.862	-0.054	0.734	-0.006	0.970
OPG	**-0.415**	**0.008**	-0.087	0.593	0.120	0.461	-0.108	0.506
RANKL	**-0.454**	**0.003**	-0.195	0.227	-0.052	0.750	**-0.312**	**0.050**
RANKL:OPG	-0.143	0.377	-0.240	0.136	-0.205	0.204	**-0.316**	**0.047**
SOST	0.192	0.445	0.158	0.531	0.238	0.341	0.269	0.280
TRAP	**-0.354**	**0.025**	-0.187	0.249	-0.129	0.428	**-0.325**	**0.041**

DEMENTIA

	LC (1)		*MC (2)*		*FC (3)*		*PFO (4)*	
Gene	*r*	*p*	*r*	*p*	*r*	*p*	*r*	*p*
APP	-0.624	0.060	-0.224	0.537	0.261	0.470	-0.212	0.560
APLP2	-0.479	0.166	-0.286	0.420	0.418	0.233	0.091	0.811
BACE1	-0.264	0.435	-0.087	0.802	0.045	0.903	-0.309	0.356
CYP27B1	-0.236	0.513	-0.297	0.407	0.200	0.584	0.200	0.584
DMP1	-0.418	0.233	-0.559	0.098	0.200	0.584	-0.552	0.105
NGF	-0.500	0.267	-0.107	0.840	0.214	0.662	0.179	0.713
OCN	-0.345	0.299	-0.114	0.739	0.064	0.860	-0.309	0.356
OPG	-0.073	0.838	0.091	0.790	-0.155	0.654	-0.327	0.327
RANKL	-0.273	0.448	-0.219	0.541	0.055	0.892	-0.503	0.144
RANKL:OPG	-0.176	0.632	0.164	0.649	-0.018	0.973	-0.261	0.470
SOST	-0.286	0.556	-0.536	0.236	0.429	0.354	0.286	0.556
TRAP	-0.391	0.237	0.178	0.599	0.200	0.557	0.173	0.615

Figures

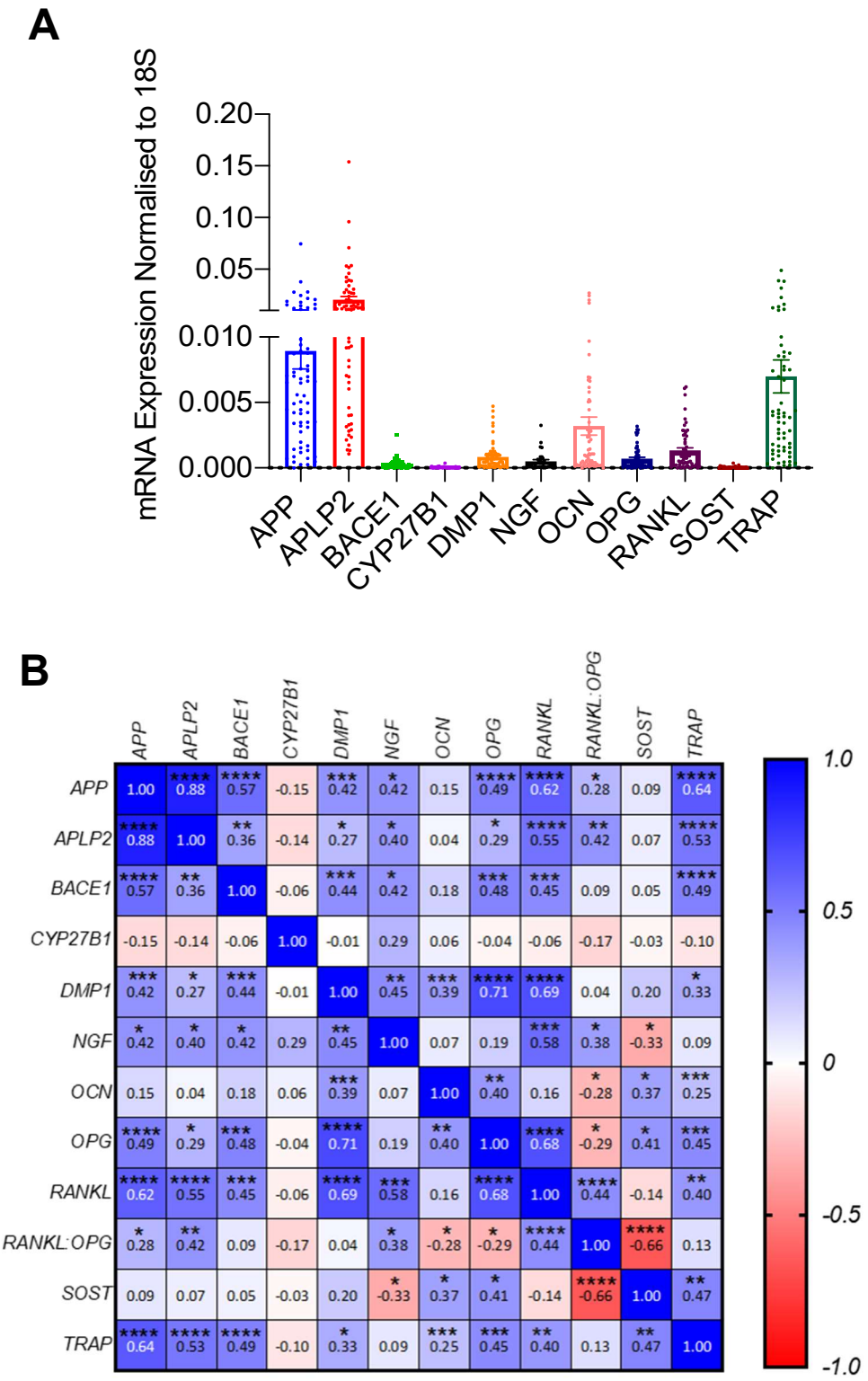

Figure 1.

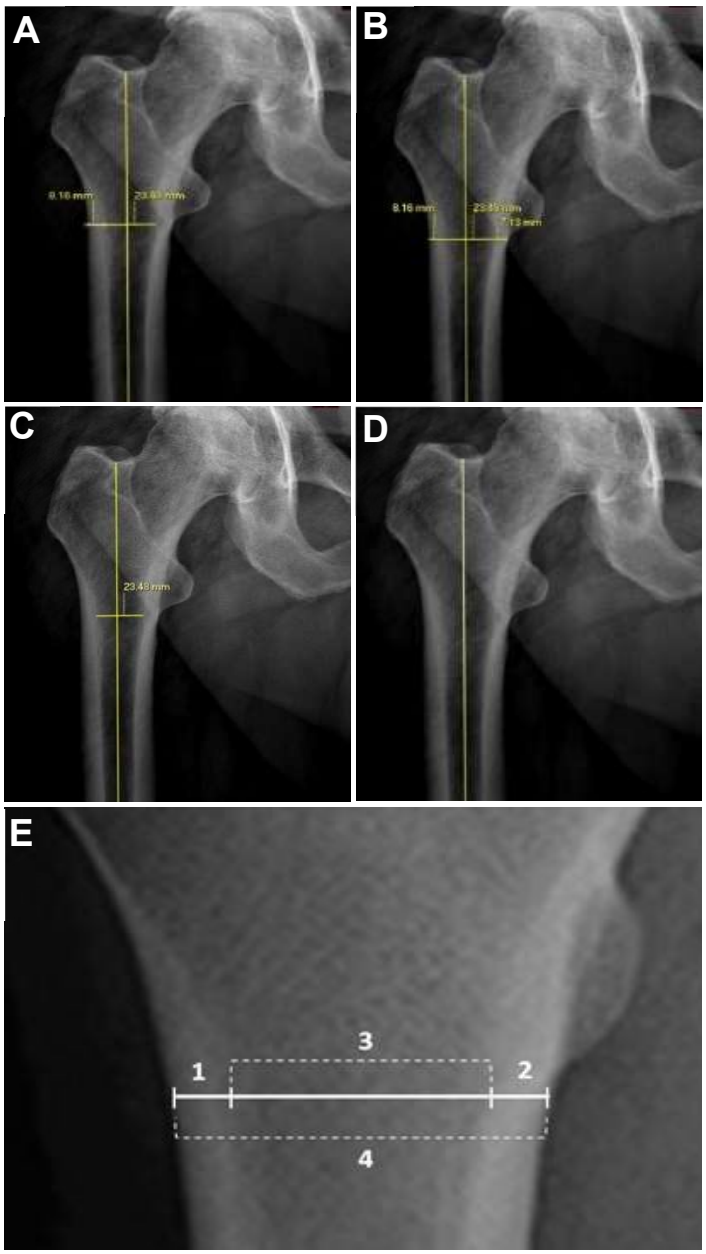

Figure 2.

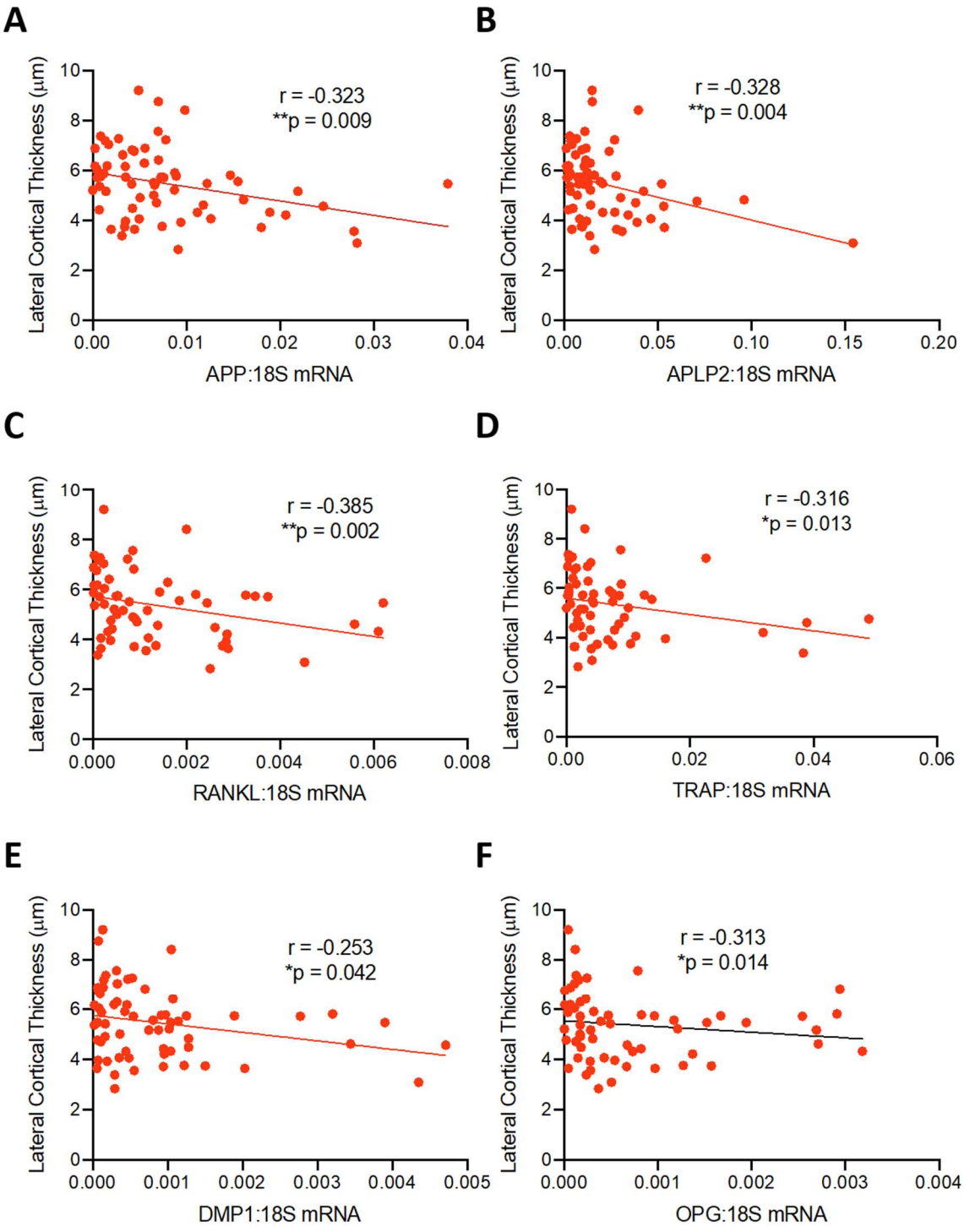
A
Lateral Cortical Thickness (µm)
r = -0.323
**p = 0.009
APP:18S mRNA
B
Lateral Cortical Thickness (µm)
r = -0.328
**p = 0.004
APLP2:18S mRNA
C
Lateral Cortical Thickness (µm)
r = -0.385
**p = 0.002
RANKL:18S mRNA
D
Lateral Cortical Thickness (µm)
r = -0.316
*p = 0.013
TRAP:18S mRNA
E
Lateral Cortical Thickness (µm)
r = -0.253
*p = 0.042
DMP1:18S mRNA
F
Lateral Cortical Thickness (µm)
r = -0.313
*p = 0.014
OPG:18S mRNA

Figure 3.

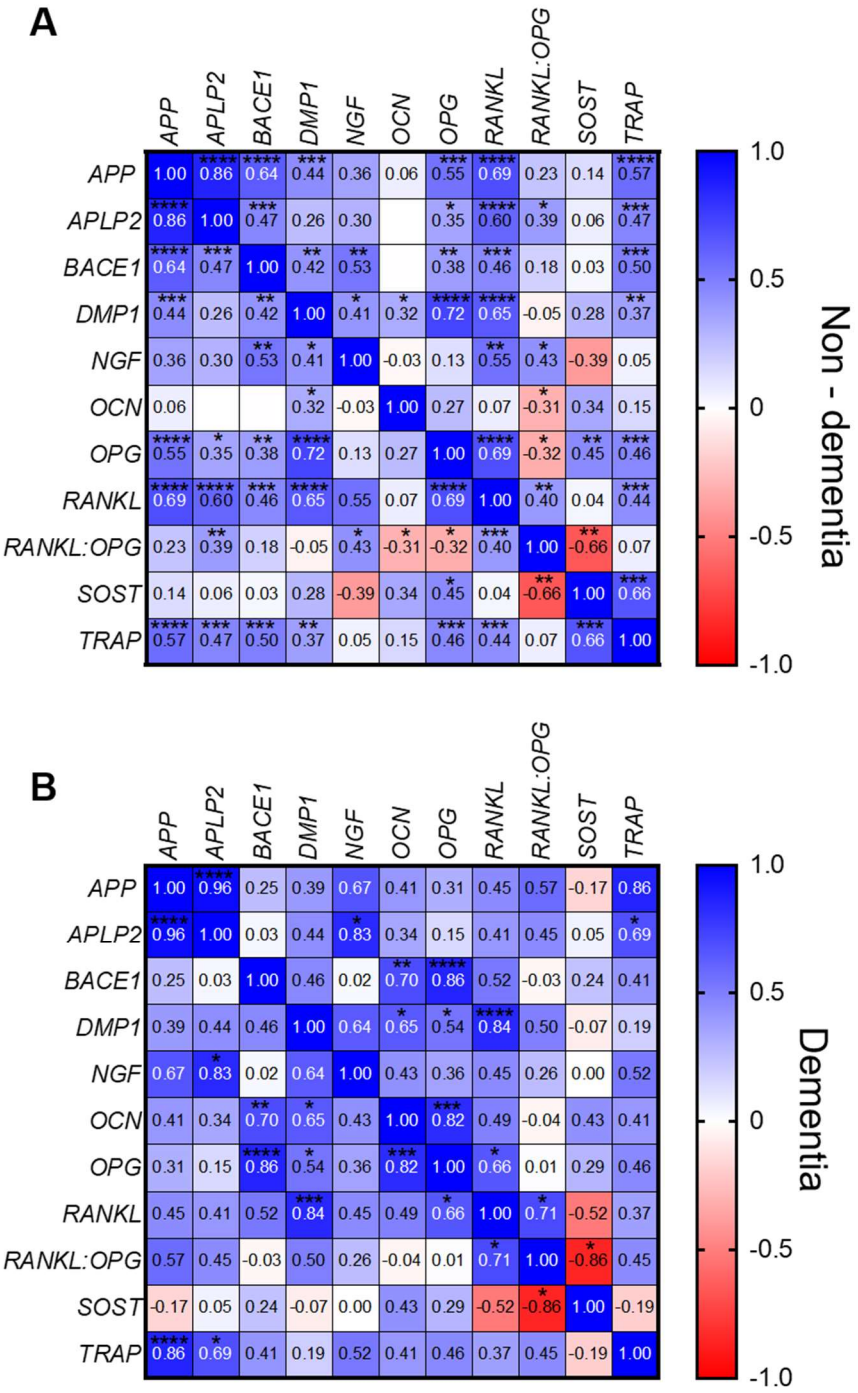
A
APP
APLP2
BACE1
DMP1
NGF
OCN
OPG
RANKL
RANKL:OPG
SOST
TRAP
1.0
0.5
0
-0.5
-1.0
Non - dementia
B
Dementia

Figure 4

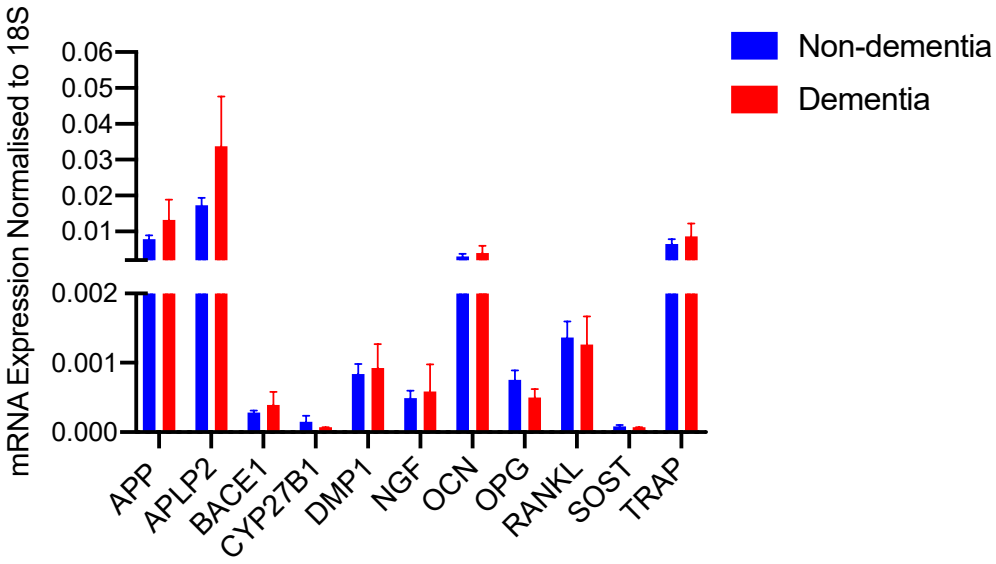

Supplementary Figure 1: Gene expression analysis for non-dementia and dementia groups. Real-time RT-PCR analysis of genes of interest normalised to the 18S housekeeping gene for non-dementia group (n = 53) versus the dementia group (n = 13). There were no statistical differences between groups for any gene (Student's t-test). Data are depicted as means only.

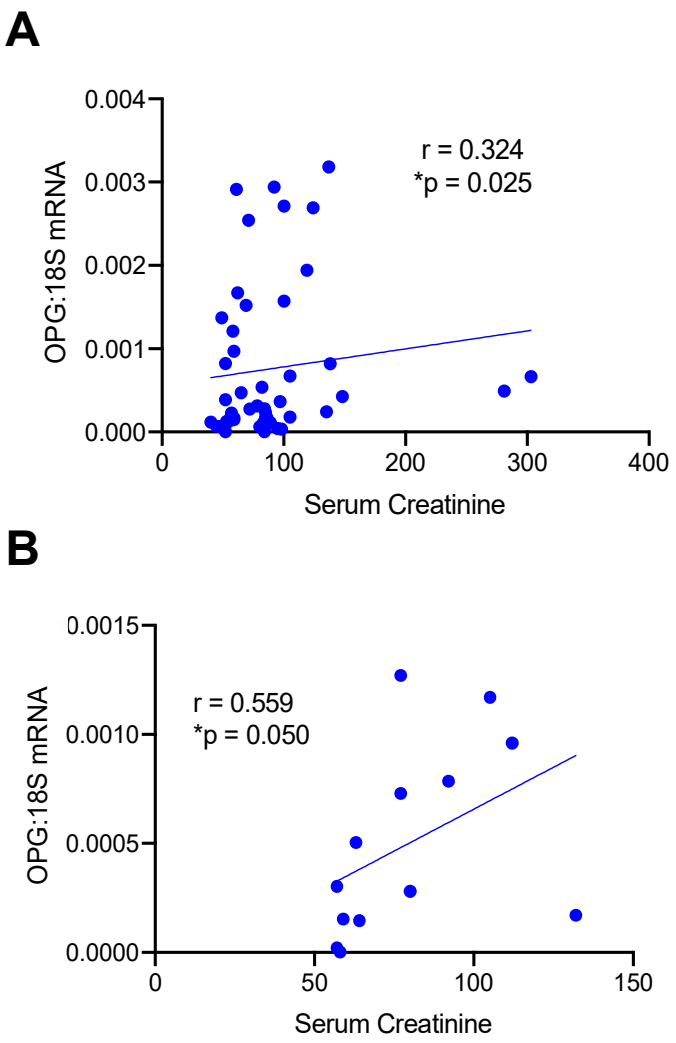

Supplementary Figure 2: Correlations between *OPG* mRNA expression and serum creatinine in non-dementia and dementia groups. A. *OPG* mRNA expression was moderately correlated with serum creatinine in the non-dementia group (n = 48). B. *OPG* and serum creatinine were positively correlated in the dementia group (n = 13).

Supplementary Table 1. Forward and reverse primer sequences for real-time RT-PCR

Gene	Direction	Primer Sequences (5′ – 3′)
18S	F	GGAATTCCCGAGTAAGTGCG
	R	GCCTCACTAAACCATCCAA
APP	F	ATCCTGCAGTATTGCCAAGAAG
	R	CACAAAGTGGGGATGGGTC
APLP2	F	GCCCAGATGAAATCCCAGGT
	R	ATATCTGCACGCTGCTCCTG
BACE1	F	GCAGGGCTACTACGTGGAGA
	R	GTATCCACCAGGATGTTGAGC
CYP27B1	F	TGGCCCAGATCCTAACACATTT
	R	GTCCGGGTCTTGGGTCTAACT
DMP1	F	GATCAGCATCCTGCTCATGTT
	R	AGCCAAATGACCCTTCCATTC
NGF	F	CACACTGAGGTGCATAGCGT
	R	TGATGACCGCTTGCTCCTGT
OCN	F	TGAGAGCCCTCACACTCCTC
	R	ACCTTTGCTGGACTCTGCAC
OPG	F	GCTCACAAGAACAGACTTTCCAG
	R	CTGTTTTCACAGAGGTCAATATCTT
RANKL	F	CCAAGATCTCCAACATGACT
	R	TACACCATTAGTTGAAGATACT
SOST	F	ACCGGAGCTGGAGAACAACA
	R	GCTGTACTCGGACACGTCTT
TRAP	F	GTGCAGACTTCATCCTGTCTCTA
	R	AATACGTCCTCAAAGGTCTCC

Supplementary Table 2: Cohort demographics and pre-fracture comorbidities.

Cohort Demographics	*n*	*Prevalence (%)*	*Age (mean ± SD)*
Female	53	80.30	82.4 (9.15)
Male	13	19.70	80.2 (9.28)
Whole Cohort	66	100.0	81.9 (9.15)

Comorbidity	***n***	***Prevalence (%)***	***Comorbidity***	***n***	***Prevalence (%)***
Hypertension	43	65.15	*Anaemia*	4	6.06
Hypercholesterolemia	20	30.30	*Alcohol Abuse*	3	4.55
Osteoarthritis	17	25.76	*Aortic Stenosis*	3	4.55
Type 2 Diabetes Mellitus	17	25.76	*Asthma*	3	4.55
Atrial Fibrillation	16	24.24	*Cardiac Stent*	3	4.55
Gout	16	24.24	*Glaucoma*	3	4.55
Dementia	13	19.69	*Paroxysmal AF*	3	4.55
Osteoporosis	12	18.18	*Recurrent Falls*	3	4.55
GORD	11	16.67	*Smoker*	3	4.55
Depression	8	12.12	*Total Knee Replacement*	3	4.55
Hypothyroidism	8	12.12	*Peripheral Vascular Disease*	3	4.55
Chronic Obstructive Pulmonary Disease	7	10.61	*Angina*	2	3.03
Recurrent UTI	7	10.61	*Aortic Valve Replacement*	2	3.03
Anxiety	5	7.58	*Breast Cancer*	2	3.03
Macular Degeneration	5	7.58	*Hemi arthroplasty*	2	3.03
Myocardial Infarction	5	7.58	*Hiatus Hernia*	2	3.03
Hearing Impairment	4	6.06	*Ovarian Cancer*	2	3.03
Cholecystectomy	4	6.06	*Parkinson's Disease*	2	3.03
Chronic Kidney Disease	4	6.06	*Pulmonary Embolism*	2	3.03
Stroke	4	6.06	*Thyroid Cancer*	2	3.03
Diverticulosis	4	6.06	*Urinary Incontinence*	2	3.03
Hysterectomy	4	6.06			

Supplementary Table 3: Correlation analysis between serum Vitamin D and serum creatinine and genes of interest in the whole NOF cohort.

Gene	Vitamin D (*R*)	Creatinine (*R*)
APP	-0.031	0.025
APLP2	0.017	-0.043
BACE1	0.133	0.170
CYP27B1	0.109	-0.038
DMP1	0.096	0.064
NGF	-0.102	0.179
OCN	0.234	-0.001
OPG	0.039	0.346**
RANKL	0.009	0.150
RANKL:OPG	-0.025	-0.154
SOST	0.260	-0.231
TRAP	0.113	0.014

Significance is indicated by **$p < 0.01$

Chapter 4

A direct link between Alzheimer's disease and osteoporosis: Amyloid Beta$_{1-42}$ Peptide overexpression causes age-related bone loss

Manuscript for submission to the *Journal of Bone and Mineral Research*

The current literature surrounding the relationship between Alzheimer's disease and osteoporosis is limited. There are a number of studies that report correlations between the development of these diseases, however there is little known regarding the underlying pathological mechanisms, which may be the missing link. It is still yet to be determined whether Alzheimer's disease predisposes to osteoporosis or vice versa, therefore in order to further elucidate a cellular mechanism responsible for the development of these concomitant diseases, the effects of Aβ overexpression were explored using cell culture models as well as the App$^{NL\text{-}G\text{-}F/NL\text{-}G\text{-}F}$ murine model of familial Alzheimer's disease.

Statement of Authorship

Title of Paper	A direct link between Alzheimer's disease and osteoporosis: Amyloid Beta$_{1-42}$ Peptide overexpression causes age-related bone loss
Publication Status	☐ Published ☐ Accepted for Publication ☐ Submitted for Publication ☒ Unpublished and Unsubmitted work written in manuscript style
Publication Details	This unpublished manuscript draft will be submitted to the Journal of Bone and Mineral Research (JBMR).

Principal Author

Name of Principal Author (Candidate)	Catherine JM Stapledon		
Contribution to the Paper	First author on the paper, generated data, performed majority of experimental work and interpreted all data obtained. Made the decision to publish and created manuscript draft.		
Overall percentage (%)	80 %		
Certification:	This paper reports on original research I conducted during the period of my Higher Degree by Research candidature and is not subject to any obligations or contractual agreements with a third party that would constrain its inclusion in this thesis. I am the primary author of this paper.		
Signature		Date	29/04/2020

Co-Author Contributions

By signing the Statement of Authorship, each author certifies that:

i. the candidate's stated contribution to the publication is accurate (as detailed above);

ii. permission is granted for the candidate in include the publication in the thesis; and

iii. the sum of all co-author contributions is equal to 100% less the candidate's stated contribution.

Name of Co-Author	L. Bogdan Solomon		
Contribution to the Paper	Provided samples for analysis, made the decision to publish, assisted in manuscript draft preparation.		
Signature		Date	7 May 2020

Name of Co-Author	Roberto Cappai		
Contribution to the Paper	Supplied reagents for experimentation, assisted with design of study, contributed to interpretation of data, made the decision to publish and assisted with manuscript draft preparation.		
Signature		Date	7 May 2020

Name of Co-Author	Gerald J Atkins		
Contribution to the Paper	Senior author, assisted with design and implementation of study and supervised study. Contributed to interpretation of data and made the decision to publish.		
Signature		Date	19-5-20

A direct link between Alzheimer's disease and osteoporosis: Amyloid Beta$_{1-42}$ Peptide overexpression causes age-related bone loss

Stapledon, CJM[1], Solomon LB[1, 2], Cappai R[3], Atkins GJ[1, 2*]

[1]Centre for Orthopaedic and Trauma Research, Adelaide Medical School, The University of Adelaide, Adelaide, SA, Australia

[2]Department of Orthopaedics & Trauma, Royal Adelaide Hospital, Adelaide, SA, Australia

[3]Department of Pharmacology and Therapeutics, The University of Melbourne, Melbourne, VIC, Australia

*Corresponding author: gerald.atkins@adelaide.edu.au

Running Title: A link between Alzheimer's disease and osteoporosis

Key words: Osteoporosis, Alzheimer's disease

Abstract

Alzheimer's disease is associated with aberrant proteolytic processing of the Amyloid Precursor Protein (APP) and production of the amyloid beta (Aβ) peptides. Recent studies have suggested that there may be a causal link between the development of Alzheimer's disease and concomitant degenerative disorders of the bone, such as osteoporosis. To examine for direct links between increased circulating levels of Aβ on the skeleton, the $App^{NL\text{-}G\text{-}F/NL\text{-}G\text{-}F}$ knock-in mouse Alzheimer's disease model was investigated for a skeletal phenotype. Long bones of skeletally mature adult 12-week old and middle-aged 29-week old, $App^{NL\text{-}G\text{-}F/NL\text{-}G\text{-}F}$ and age-matched wild-type controls were analysed for differences in bone micro-architectural parameters and bone cell morphology and number using micro-computed tomography and histological techniques, respectively. Twelve-week-old $App^{NL\text{-}G\text{-}F/NL\text{-}G\text{-}F}$ trabecular bone parameters were indistinguishable from wild-type controls indicating normal skeletal development in the Aβ knock-in animals. However, 29-week old $App^{NL\text{-}G\text{-}F/NL\text{-}G\text{-}F}$ mice had developed a severe bone loss phenotype with decreased trabecular bone volume fraction BV/TV% by 31% ($p = 0.0079$), trabecular number (Tb.N) and trabecular thickness (Tb.Th), and increased trabecular spacing (Tb.Sp), trabecular pattern factor (Tb.Pf) and structural model index (SMI). Histological analysis revealed strongly elevated osteoclast measures in the $App^{NL\text{-}G\text{-}F/NL\text{-}G\text{-}F}$ mice compared to wild-type. To test whether bone loss could be due to a direct effect on osteoclastogenesis, we generated osteoclasts from normal human donor peripheral blood mononuclear cells (PBMC) in culture with recombinant RANKL/M-CSF but found no effect of added $A\beta_{1\text{-}42}$ peptide. To test for an effect on osteocyte-driven osteoclastogenesis, primary human osteocytes were differentiated from human bone biopsy explant cultures. Osteocytes were treated with either 0, 1.5, 5 or 15μM of $A\beta_{1\text{-}42}$ peptide. Live/dead analysis revealed that $A\beta_{1\text{-}42}$ peptide at 15μM caused osteocyte cell

death at 24, 72 and 96 h. Gene expression analysis of these cultures revealed a strong up-regulation of *RANKL* mRNA expression relative to OPG mRNA. Together, these findings suggest that increased $A\beta_{1\text{-}42}$ peptide levels causative of Alzheimer's disease, could also play a role in age-related osteoporosis by increasing osteocyte-driven osteoclastogenesis. Our findings provide the first direct mechanistic link between Aβ-driven Alzheimer's disease and osteoporosis.

Introduction

Dementia is an umbrella term used to describe a group of neurodegenerative disorders, arising from different pathologies, with the most commonly occurring form being Alzheimer's disease (AD). AD is currently the second leading cause of death in the Australian population [(1)], within which, AD including both sporadic and familial subtypes combined, accounts for up to 70% of all cases of dementia [(2,3)]. The pathogenesis of AD is most commonly explained by the Amyloid Cascade Hypothesis, which was formed following the isolation of Amyloid Beta (Aβ) Plaques and Neurofibrillary Tangles from the brains of AD patients and the identification of familial AD associated mutations in the Amyloid Precursor Protein gene, *APP* [(4-6)].

Aβ peptides are formed from the proteolytic processing of APP, which is ubiquitously expressed in the human body. APP is processed by the beta secretase cleaving enzyme (BACE-1) [(7)], which results in the release of the soluble APPβ (sAPPβ) domain and the membrane-bound C99 fragment. Further cleavage of the C99 fragment by gamma secretase (γ-secretase) [(8)], leads to the release of the APP intracellular domain (AICD) and the production of $A\beta_{1-42}$ [(9,10)]. Under pathological conditions in the brain, such as inflammation and stress, $A\beta_{1-42}$ peptides aggregate and form Aβ plaques [(5,11)]. These so-called senile plaques impair neuronal function, resulting in subsequent hyperphosphorylation of the Tau protein and production of pathological neurofibrillary tangles [(12,13)].

A recent mouse model of AD is the $APP^{NL\text{-}G\text{-}F/NL\text{-}G\text{-}F}$ mouse, developed at the RIKEN Institute, Japan [(14)]. This model was designed to express three human *APP* mutations responsible for development of familial AD (FAD), knocked into the mouse *App* gene. This results in APP protein expression at physiological levels, thus avoiding potential

effects of global over-expression [15], with increased levels of $A\beta_{1-42}$. These mice have characteristic behavioural and histological brain changes consistent with AD [14,16-18], however the extra-neuronal phenotype is unknown.

One of the strongest co-morbidity associations of dementia are neck of femur (NOF) fractures. Individuals with dementia were shown to be up to 3 times more likely than a cognitively intact older adult to sustain a hip fracture [19], most of which are caused by osteoporosis [20]. The hypothesis proposing a link between the development of AD and fracture risk as a result of skeletal degradation has been investigated in a number of observational studies [21-25]. More recently there have been studies investigating this in regards to the mechanisms that may be causative of this link between the two degenerative diseases [26-29]. The involvement of the osteoblast and osteoclast have been researched in separate capacities, involvement of the osteocyte, the regulator of bone mass and the cell that orchestrates responses to mechanical stress. We showed recently that in patients who had suffered a NOF fracture, bone *APP* expression was high and correlated with the expression of *BACE1*, as well as the bone remodelling genes, *TRAP*, *RANKL*, *OPG*, and the *RANKL*:*OPG* mRNA ratio [30], being a key indicator of bone resorption in these patients [31]. In addition, APP expression correlated negatively with cortical bone thickness in these patients, together implying a role for APP, and potentially its post-translational products, in bone loss and in the underlying pathology of hip fracture [30].

A number of studies have addressed potential effects of Aβ on the osteoblast [29] and osteoclast [26-28], however there remains a gap in knowledge regarding the potential effects of Aβ on the bone's most abundant cell type, the osteocyte. The osteocyte plays numerous physiologic regulatory roles, including control of bone remodelling and mechanosensation [32]. Osteocytes have been shown to express *APP* and Aβ in osteoporotic tissue by immunofluorescence [27]. Indeed, we found that in addition to being

correlated with *RANKL*, expression of which is associated with osteoblasts and osteocytes, *APP* mRNA expression in NOF bone was strongly correlated to that of the mature osteocyte marker *DMP1* [30], implying their co-expression.

In this study we investigated whether the skeleton is affected by increased levels of $A\beta_{1-42}$ by assessing the skeletal phenotype of the $App^{NL\text{-}G\text{-}F/NL\text{-}G\text{-}F}$ transgenic mouse model and the effects of $A\beta_{1-42}$ on human osteoclasts and osteocytes.

Materials and Methods

App$^{NL-G-F/NL-G-F}$ Knock-In (KI) mice

All animal experimentation was approved by the South Australian Health and Medical Research Institute (SAHMRI) Animal Ethics Committee (Approval No. SAM129) and the University of Adelaide Animal Ethics Committee (Approval No. M-2015-082). *App*$^{NL-G-F/NL-G-F}$ founder mice [14] were obtained from the RIKEN Institute and re-derived. Male *App*$^{NL-G-F/NL-G-F}$ and wild-type controls on the same C57BL/6J background were aged until six-months. Mice were humanely euthanised at either 12 or 29 weeks of age and perfusion-fixed with 4% (w/v) paraformaldehyde (PFA) in PBS. Brains were post-fixed in 4% (w/v) PFA in PBS for 7 days and embedded in paraffin wax.

Micro-Computed Tomography Analysis

Following perfusion fixation of mice, left hand side femora were dissected and placed in 70% ethanol (EtOH) until time of scanning. Femora were imaged *ex vivo* using a Skyscan *in Vivo* 1076 Microtomograph (µCT) (Bruker, Kontich, Belgium). Femora were removed from EtOH, wrapped in gauze and placed in a plastic straw containing 70% EtOH to prevent drying of the sample and movement during the scanning.

All scans were performed at an isotropic image pixel size of 9 µm with a 0.5 mm aluminium filter, at 0.6° rotation step, frame averaging of 2.0 and HU of 9872. Scans were reconstructed using the NRecon Reconstruction Program version 1.6.10.4 (Micro Photonics Inc, PA, USA). Reconstructed scans were realigned trans-axially using the DataViewer version 1.5.2.4 software (Bruker, MA, USA). The final dataset was then

analysed using the CT Analysis (CTan) version 1.15 Analysis Program (Bruker, MA, USA). All bone quantification from reconstructed and realigned datasets was performed using CTAN software (v.1.7, Bruker, MA, USA). A 2 mm metaphyseal region of interest (ROI) was isolated from the distal femur and trabecular bone within the ROI was manually traced. Parameters analysed included, bone volume fraction (BV/TV, %), trabecular thickness (Tb.Th, mm), trabecular number (Tb.N, #/mm), trabecular separation (Tb.Sp, mm), trabecular pattern factor (Tb.Pf) and structural model index (SMI). The ROI analysed for cortical bone was defined as a 1mm ROI, 0.5 mm above and 0.5 mm below the geometric mid-point calculated by subtracting the measurement at the distal end of the femur from that at the proximal end and dividing by 2. Bone parameters measured for the cortical bone ROI included: Total volume (TV μ^3), bone volume (BV μ^3), Cortical Thickness (Tb.Th (Pl)), Tissue perimeter (T.Pm, mm), Bone perimeter (B.Pm, mm) and endosteal perimeter (B.Pm – T.Pm, mm).

Histological Analysis

Right hand side femurs and tibias were dissected and decalcified using Osteosoft® solution (Merck KGaA; Darmstadt, Germany), for 4-5 weeks, with regular solution changes. All samples were embedded in paraffin wax and 5-micron (μm) sections were cut for histological analysis using a microtome. Sections were stained with Toluidine Blue for osteocyte number and lacunar area measurements and stained with Tartrate-Resistant Acid Phosphatase (TRAP) for osteoclast counts and osteoclast surface per bone surface (Oc.S/B.S) [33]. All slides were imaged using the Nanozoomer slide scanner (Hamamatsu Photonics K.K, Shizuoka, Japan) at 40 x magnification. All osteocyte and osteoclast analyses were conducted using Nanozoomer NDP View 2.7.25 software

(Hamamatsu Photonics). Osteocytes, trabeculae and TRAP-positive osteoclasts were traced using a Bamboo Pen and Touch (Wacom, Kazo, Saitama, Japan).

Amyloid Beta$_{1-42}$ Peptide Preparation

Aβ_{1-42} peptide was obtained from the ERI Amyloid Laboratory, LLC (Oxford, CT, USA). Aβ_{1-42} at a concentration of 0.5 mg was dissolved in 100 µl of 60 nM NaOH, vortexed, and sonicated for 15 min in an iced water bath. 350 µl of sterile Milli-Q water and 50 µl of 10x PBS pH 7.4 were added to the Eppendorf tube and centrifuged for 5 min at maximum speed (16,000 RCF) in a tabletop centrifuge. Following this, the concentration was measured using a Nano-drop 2000/2000 c spectrophotometer (ThermoFisher Scientific Inc, Middletown, VA, USA) using the settings: molecular weight = 4514 Da, extinction coefficient at 1.0 cm path length E = 13.18 µM, λ_{range} = 190-350 nm, $\lambda_{analysis}$ = 214 nm [13,34,35].

Human primary osteocyte-like cells

Trabecular bone samples were obtained from the proximal femur from patients undergoing total hip replacement for neck of femur (NOF) fracture, with informed patient consent and ethical approval by the RAH Human Research Ethics Committee (HREC/14/RAH/53). Osteoblast-like cells were cultured from dissected bone as previously described [36]. Primary human osteoblasts were differentiated for 28 days until cells reached a mature osteocyte-like stage [37-39]. Cells were plated at a density of $5x10^4$ cells/ml in 12-well plates, $9x10^3$ cells/400 µl in chamber slides and $5x10^3$ cells/200 µl in 96-well plates. After 24 h in proliferation media to allow attachment to surfaces, media was changed to low serum mineralisation media (α-MEM, 0.5% FCS, 1% ascorbate, 1%

KH_2PO_4 and 1% dexamethasone). Media changes were performed 2-3 times per week and cells were differentiated up to day 28 when they reached a mature osteocyte-like phenotype.

Following preparation of $A\beta_{1-42}$ peptide, as described above, 1.5 µM, 5 µM and 15 µM Aβ stock solutions were prepared in differentiation media containing 2 % B27 cell culture supplement [40] (Gibco, Dun Laoghaire, Ireland) and added to respective wells of day 28 osteocyte-like cultures for treatment. At the time of treatment, media was changed from 0.5 % FCS to 2 % B-27 cell culture supplement (Gibco).

Culture of Osteoclasts from Human Peripheral Blood Mononuclear Cells (PBMC)

Peripheral blood (~16 ml) was collected from three healthy volunteers into heparinised vacuettes. Blood was cooled to ambient temperature and then processed using Lymphoprep™ (STEMCELL Technologies, VIC, Australia), as per the manufacturer's instructions. The PBMC layer was extracted and transferred into a 50 ml sterile tube containing 10 ml of α-MEM + 10 % FCS. The mixture was then topped up to 50 ml with PBS and centrifuged for 10 min with an alternating speed from 100 to 1200 RCF. Supernatant was then removed and washed with PBS and centrifuged for 10 min. Following removal of supernatant, remaining cells were resuspended, and cell counts performed. Cells were cultured in 96 well plates at a density of 2 x 10^5 cells per well. After 24 h of culture in α-MEM containing 10% FCS, media were replaced with either osteoclastogenic media, comprising α-MEM/10% FCS/recombinant human (rh-) RANKL (100 ng/ml) and rh-macrophage colony stimulating factor (rh-M-CSF; 25 ng/ml), or control media without added rh-RANKL. Media were changed every 2 days

and at day 9 refreshed with either osteoclastogenic or control media as appropriate, or osteoclastogenic media also containing recombinant Aβ peptide at 5 μM or 15 μM. Replicate plates were fixed after 24 or 48 h with 4% w/v glutaraldehyde in PBS for 20 min. Plates were then washed with dH_2O and 100 μl of trisaminomethane (TRIS; pH 9.4) was added to each well and incubated for 30 min at 37°C. Plates were rinsed and acid phosphatase (AcP) stain, containing 0.1g sodium nitrite, 100 μl basic fuchsin, 0.035 g tartaric acid, 35 ml sodium acetate, 0.04 g napthol and 2 ml dimethylformamide was added to each well. Plates were incubated for 15 min at 37°C then rinsed in dH_2O and the cells imaged using an inverted light microscope (Nikon) at 20X magnification.

Immunohistochemistry

DAB (3, 3'-diaminobenzidine) immunohistochemical staining was conducted on paraffin sections using the 82E1 mouse anti-human $A\beta_{1-42}$ monoclonal antibody (IBL, MN, USA) for detection of soluble and fibril $A\beta_{1-42}$, as advised by LS Whyte - SAHMRI. Sections were heated at 60°C for 15 min and taken through the rehydration steps (100% xylene, 100% EtOH, 90% EtOH, 70% EtOH, 50% EtOH and water). Antigen retrieval was performed by immersing sections in formic acid (10% v/v) for 10 min. Sections were blocked with normal horse serum (NHS, 10% v/v in PBS) for 30 min. Slides were then either left unstained (primary antibody omission), stained with 82E1 antibody at a 1:200 dilution, or with the IgG1 negative control antibody (IB5) at the same concentration. Sections were incubated at 4°C overnight. On day 2 sections were incubated with 0.3% hydrogen peroxide to block endogenous peroxidase activity for 30 min, rinsed and incubated with rabbit anti-mouse secondary antibody at a 1:2000 dilution for 90 min. Sections were then incubated with the Vectastain Elite ABC HRP kit (Cat. PK-6100)

(Vector Laboratories, Peterborough, UK) for 1 h at room temperature. Slides were then immersed in DAB substrate for 7 min, rinsed, counterstained with hematoxylin and cover slipped. Slides were scanned at 40 x magnification using the Nanozoomer and analysed using Nanozoomer software.

Cell Viability and Morphology imaging using Immunofluorescence Staining and Confocal Microscopy

Normal human osteocytes were cultured for 28 days in 8-well cell-imaging chamber slides and treated with respective concentrations of $A\beta_{1-42}$ peptides at time points previously mentioned [41,42]. These were stained with Calcein AM (R&D Systems, Inc, MN, USA) and Ethidium Homodimer-3 (Biotium, CA, USA) (1:2000) into serum-free media and added to each well of 8-well chamber slides. Following the addition of the dyes to each well, chamber slides were incubated at 37°C for 30 min. Following incubation confocal imaging was conducted using an Olympus Fluoview FV3000 Confocal Laser Scanning Microscope. An average of 5 images were taken for each well (2 wells per treatment per time point) at 10 X magnification. All cell counts were conducted using ZEN Black software (Zeiss, Oberkochen, Germany). Background was removed using the remove all structures feature and cells were counted manually based on size and the original image. Live osteocytes in chamber slides were stained with SiR-actin (Cytoskeleton Inc., Denver, CO, USA) (1:10000), Calcein AM (1:2000) and NucSpot Live 488 Nuclear Stain (1:5000) (Biotium, CA, USA).

Gene Expression Analysis

Total RNA was extracted from duplicate wells for each time point and treatment using the TRIZOL method (Life Technologies, New York, USA). All samples were reconstituted into 20 µl of diethyl-pyrocarbonate (DEPC) treated water. Final RNA concentrations were measured using a Nano-drop spectrophotometer (Thermofisher Scientific, city, state/country). Complementary DNA (cDNA) was synthesized from 1 µg total RNA using the iScript cDNA synthesis kit (Bio-Rad, Hercules, California, USA), as per manufacturer's instructions. Real-time RT-PCR was performed using SYBR Green master mix reagent (Qiagen, Limburg, The Netherlands) on a Bio-Rad CFX Connect thermocycler (Bio-Rad, Hercules, California, USA). Melt curves and CT products were analysed on the CFX manager version 3.1 (Bio-Rad, Hercules, California, USA). Messenger RNA (mRNA) expression was analysed for *APP*, Beta Secretase Cleaving Enzyme-1 (*BACE1*), BCL2 Associated X Protein (*BAX*), B-cell Lymphoma-2 (*BCL2*), Matrix Metallopeptidase 13 (*MMP13*), Osteoprotegerin (*OPG*) and Receptor activator of nuclear factor kappa-B ligand (*RANKL*) and normalised to levels of *18S* rRNA (Supplemental Table 1).

Statistical Analysis

All statistical analysis was performed using GraphPad Prism (v7.02). To determine differences between treatment groups, non-parametric, two-tailed Student's t-tests were applied to the datasets. Analysis on µCT parameters was performed using two-tailed, parametric, Welch's t-tests, as the data were normally distributed.

Results

Skeletal structural properties of *App*$^{NL\text{-}G\text{-}F/NL\text{-}G\text{-}F}$ mice

The 12-week old male *App*$^{NL\text{-}G\text{-}F/NL\text{-}G\text{-}F}$ knock-in (KI) mice femora were analysed by μCT scanning for changes in both cancellous and cortical bone parameters. There were no micro-architectural changes between WT and KI mice in terms of either cancellous bone volume fraction (%BV/TV), Trabecular Number (Tb.N), Trabecular Thickness (Tb.Th), Trabecular Separation (Tb.Sp), Trabecular Pattern Factor (Tb.Pf) or Structural Model Index (SMI) (Fig. 1).

Femora of 29-week old KI mice, however, showed a significant 33% reduction in %BV/TV when compared to age-matched controls (Fig. 2a; $p = 0.0079$). Tb.N was reduced by 31% in the KI femora (Fig. 2b; $p = 0.0079$). Tb.Th was unaffected between groups (Fig. 2c; $p = 0.4051$), Tb.Sp increased by 17% in KI mice (Fig. 2d; $p = 0.0323$); Tb.Pf also increased with a 25% change between WT and KI (Fig. 2e; $p = 0.0322$). Finally, there was a 14% increase in the SMI, a measure of erosion of trabeculae from plate-like to rod-like structures (Fig. 2f; 0.0406).

Cortical bone structure was also examined by μCT analysis. 12-week old male mice revealed no significant differences between genotypes for any cortical bone parameter analysed (Fig. S1). Investigation of the 29-week old mice also did not show significant changes in cortical thickness (Ct.Th) (Fig. S1b). Neither the periosteal perimeter (B.Pm) nor cortical perimeter (T.Pm) were changed between WT and KI groups (T.Pm: $p = 0.0635$; B.Pm: $p = 0.1905$). The endosteal perimeter, determined by subtracting the B.Pm from the T.Pm was also not affected in the KI group ($n = 4 – 5$/group; $p = 0.5556$). These observations suggest that $A\beta_{1\text{-}42}$ primarily exerts an effect on the cancellous bone compartment.

App$^{NL\text{-}G\text{-}F/NL\text{-}G\text{-}F}$ mouse bone exhibits increased osteoclastic bone resorption

To determine if the cancellous bone phenotype was associated with altered osteoclastic parameters, bone sections were histochemically stained for TRAP, a marker for osteoclasts. The total osteoclast count revealed a significant increase in the KI compared to the WT animals (Fig. 3a). Analysis of the osteoclast surface per bone surface (Oc.S/BS) revealed that KI cancellous bone had an increased surface area occupied by bone resorbing osteoclasts (Fig. 3b).

Effect of $A\beta_{1\text{-}42}$ peptide on osteoclastogenesis

To investigate the basis for the increased number of osteoclasts in KI bone, we exposed osteoclasts generated from human PBMC in response to recombinant RANKL/M-CSF to a high concentration of $A\beta_{1\text{-}42}$ (15 μM), shown previously to be toxic to neurons [13]. The addition of $A\beta_{1\text{-}42}$ had no discernible effect on osteoclastogenesis, as determined by counting the number of TRAP-positive multinucleated cells (Fig. 4). This suggests that effects of $A\beta_{1\text{-}42}$ overexpression on osteoclast formation occur by an indirect mechanism.

Presence of Amyloid Beta deposits in the long bones of 29-week-old male *App*$^{NL\text{-}G\text{-}F/NL\text{-}G\text{-}F}$ mice

Immunohistochemical staining with the 82E1 MAb revealed apparent Aβ accumulations in the bone marrow of the KI but not the WT mice (Fig. 5a). Brain sections served as a positive control for the presence of Aβ, and *APP*$^{NL\text{-}G\text{-}F/NL\text{-}G\text{-}F}$ brain showed a similar

staining pattern of 82E1 staining to the corresponding bone, whereas the control brain was negative (Fig. 5b).

Effects of Aβ overexpression on osteocyte bone histology and function

Osteocytes are an important cell type in the regulation of adult bone osteoclastogenesis [43]. Histological analysis of $APP^{NL\text{-}G\text{-}F/NL\text{-}G\text{-}F}$ bone revealed similar osteocyte lacunar numbers and lacunae size compared with age and gender matched controls (Fig. 6), suggesting that no gross changes in the physiology of osteocytes in the mutant animals.

To further investigate effects on osteocytes, we exposed cultures of human primary osteocyte-like cells to synthetic peptides of human $A\beta_{1\text{-}42}$. The three concentrations used in this study have been previously validated in the context of toxicity to neurons [13]. Untreated cells for the duration of the experimental period maintained a defined actin cytoskeleton with rounded nuclei and abundant Calcein AM staining (Fig. 7a) indicative of healthy, metabolically active cells. $A\beta_{1\text{-}42}$ dose-dependently disrupted this morphology, with $A\beta_{1\text{-}42}$ at 15 μM exerting the most dramatic effect. Viable cell counting revealed that low levels of $A\beta_{1\text{-}42}$ (1.5 μM) had no effect on osteocyte viability when compared to untreated cultures over a 96 h time course. Analysis of osteocytes treated with 5.0 μM $A\beta_{1\text{-}42}$ showed a significant increase in cell death at 24 h and 72 h time points when compared to the control wells. Cultures exposed to $A\beta_{1\text{-}42}$ 15 μM exhibited early and sustained increased levels of cell death compared to the untreated controls (Fig. 7b).

Effects of exogenous $A\beta_{1-42}$ peptide on human osteocyte-like cell gene expression

Basal mRNA expression levels of *BACE1* and its substrate *APP* were measured in the human bone-derived differentiated osteocytes (Fig. 8a). Gene markers of bone remodelling were also examined. As shown in Figure 8, the mRNA levels of bone resorption marker *RANKL* (Fig. 8b) and the ratio of *RANKL* to its inhibitor *OPG* were progressively increased from 72 h by the 15μM $A\beta_{1-42}$ concentration when compared to the control treatment (Fig. 8d). A stimulatory effect of $A\beta_{1-42}$ was also evident for the osteocytic osteolysis marker *MMP13* (Fig. 8e) suggesting osteocyte-osteoclast cooperation in degrading bone in response to elevated $A\beta_{1-42}$.

Discussion

Previous studies have determined effects of mouse *App* mutations on bone, osteoblasts and osteoclasts [26,44-46], however this is the first study to determine a skeletal phenotype in the $App^{NL\text{-}G\text{-}F/NL\text{-}G\text{-}F}$ knock-in model, the first model to successfully introduce three well characterised humanised *APP* mutations into the mouse *App* gene, representing a physiologically relevant APP-FAD model [14]. This model avoids potential confounding effects of APP overexpression, where other mutant models have between a 2-3-fold increase in basal APP levels [15,26]. As there is an absence of Tau protein neurofibrillary tangles in this model, it also provides the opportunity to determine whether increased production of $A\beta_{1\text{-}42}$, an increased $A\beta_{42/40}$ ratio and increases in Aβ aggregation events affect bone independently of other AD causes. The global *App* knock-out model $(App^{-/-})$ showed effects on the skeleton, with a reduction in cortical and trabecular thickness of the long bones [47], resulting from impaired skeletal development and providing a basis for a physiological role of APP in this process. Analysis of 12-week-old $App^{NL\text{-}G\text{-}F/NL\text{-}G\text{-}F}$ mice showed no significant differences to wild-type controls in either cancellous or cortical bone measures, indicating no developmental skeletal defects in this model. Whyte et al., demonstrated the formation of $A\beta_{1\text{-}42}$ plaques in the hippocampal region of the brains of 29-week old $App^{NL\text{-}G\text{-}F/NL\text{-}G\text{-}F}$ male mice but not in wild-type controls [16]. This is consistent with our finding of Aβ accumulations in both the bone marrow of these animals as well as brain tissue. The observed reduction in BV/TV%, driven by a decrease in Tb.N with increased Tb.Sp, at 29 weeks demonstrates an adult onset bone loss phenotype. Histological analysis revealed an increase in osteoclast surface per bone surface, confirming that the bone loss was due to increased osteoclastic bone resorption. The observation that recombinant $A\beta_{1\text{-}42}$ had no augmentation effect on RANKL/M-CSF induced osteoclastogenesis in a stromal-free assay using human PBMC as a source of

osteoclast precursors, suggested increased osteoclastogenesis was by an indirect mechanism. In mice, osteocyte-specific conditional deletion of *Rankl* (*Tnfsf11*) under control of either the *Dmp1* [48] or *Sost* [49] promoters resulted in significant reductions in osteoclastic bone resorption, demonstrating that in adult bone, osteocytes are a predominant source of control of osteoclastogenesis. Here, treatment of human osteocytes differentiated *in vitro* from bone explant culture-derived osteoblasts resulted in increased *RANKL* expression and of the *RANKL*:*OPG* mRNA ratio at the highest concentration used (15 μm), suggesting osteocyte support of osteoclastogenesis could be a potential mechanism for the observed bone loss. The expression of *MMP13* was also increased was also increased following exposure to $A\beta_{1-42}$, suggestive of osteocytic osteolysis in the human cells [50]. This phenomenon occurs physiologically during lactation, where osteocytes resorb bone to release calcium into the blood stream and meet the Ca^{2+} demand [51,52], as well as under pathological conditions, such as contact with foreign wear particles in prosthetic implant failure [53] and in response to prolonged glucocorticoid exposure [54]. While osteocyte lacunae measures were unchanged in the animals examined, the upregulation of MMP13 in osteocytes could reflect osteocyte coordination of osteoclastogenesis [32].

In order to determine whether $A\beta_{1-42}$ could exert its potent effects peripherally and in a more localised manner, immunostaining using the amino-terminal Aβ-specific 82E1 MAb was conducted on mouse long bones, using age and gender matched brain tissue as a positive control. Diffuse immunostaining occurred throughout the bone marrow of both tibiae and femora. Staining revealed no evidence of $A\beta_{1-42}$ in the bone marrow of control mice. The presence of $A\beta_{1-42}$ in the bone marrow of aged KI mice suggests that this toxic peptide may possess the ability to travel via blood vessels into the bone marrow and exert its effects on bone mass peripherally. Alternatively, cells which make up the bone, such

as osteoclasts, osteoblasts or osteocytes, which we now know express APP and BACE1, may be a source for the production of $A\beta_{1-42}$ in these transgenic mice.

The induction of cell death in human osteocytes exposed to 5 and 15 μM $A\beta_{1-42}$ suggests at least one pathway for the increased osteoclastogenesis observed *in vivo*. While we did not observe loss of osteocyte numbers per unit of bone in the $App^{NL\text{-}G\text{-}F/NL\text{-}G\text{-}F}$ mice, it is possible that osteocyte apoptosis *in vivo* is followed quickly by resorption of the affected region. The mechanism(s) of cell death induction in osteocytes has not been explored here but could be similar to those seen in the context of neurons [55]. Notably, osteocyte and neuronal morphologies and their respective networks share many features in common [56] and the dendritic network of osteocytes is pivotal for their survival as they are the communication source between cells [57]. For example, this network allows osteocytes to share energy sources in response to stress signals, rescuing affected cells from apoptosis [58]. $A\beta_{1-42}$ may have the ability to interfere with the delivery of biological signals between osteocytes, similar to the process that we see occurring in the context of neuronal axons in the CNS.

The low 1.5 μM concentration of $A\beta_{1-42}$ did not cause cell death when compared to the control. It is commonly noted that individuals without a diagnosis of Alzheimer's disease still have detectable levels of Aβ in their cerebrospinal fluid [59] and plasma [60,61], without having any cognitive or motor deficits. Further studies should be undertaken to examine the effects of low levels of circulating Aβ on peripheral tissues.

This is the first study to investigate the skeletal effects of the 3 x humanised FAD mutations knocked into the $APP^{NL\text{-}G\text{-}F/NL\text{-}G\text{-}F}$ mouse model of AD. The results from the mouse model coupled with the *in vitro* data suggest that $A\beta_{1-42}$ peptides cause excessive adult-onset bone loss, due in part to the upregulation of osteoclastic markers *RANKL* and

RANKL:OPG by osteocytes and perhaps linked to an apoptotic effect on osteocytes. This study therefore provides evidence for a pathological role of $A\beta_{1-42}$ in the skeleton and a mechanistic link between AD and osteoporosis. Further research is warranted to determine if treatments targeting bone loss in osteoporosis also protect against AD, or whether new treatment strategies are required that are able to target both the brain and the periphery in the fight against the neurotoxic and osteolytic oligomeric $A\beta_{1-42}$ peptide.

Acknowledgements

The authors thank Dr Joe Ciccososto and Dr Marsha Tan from the Department of Pharmacology and Therapeutics at the University of Melbourne for their help with the production and supply of the $A\beta_{1-42}$ peptides used in this study. We thank Drs Takashi Saito and Takaomi Saido from the RIKEN Center for Brain Science Laboratory for Proteolytic Neuroscience for provision of the App^{NL-G-F} mice.

Disclosures

The authors all state that they have no conflicts of interest.

References

1. Launer LJ. Statistics on the burden of dementia: need for stronger data. Lancet Neurol. Jan 2019;18(1):25-7.
2. Prince M, Bryce R, Albanese E, Wimo A, Ribeiro W, Ferri CP. The global prevalence of dementia: a systematic review and metaanalysis. Alzheimers Dement. Jan 2013;9(1):63-75 e2.
3. Canberra Uo. Dementia Australia Dementia Prevalence Data 2018-2058. Commissioned research undertaken by NATSEM, University of Canberra. 2018.
4. Hardy J, Allsop D. Amyloid deposition as the central event in the aetiology of Alzheimer's disease. Trends Pharmacol Sci. Oct 1991;12(10):383-8. Epub 1991/10/01.
5. Hardy JA, Higgins GA. Alzheimer's disease: the amyloid cascade hypothesis. Science. Apr 10 1992;256(5054):184-5. Epub 1992/04/10.
6. Selkoe DJ. The molecular pathology of Alzheimer's disease. Neuron. Apr 1991;6(4):487-98. Epub 1991/04/01.
7. Sun J, Roy S. The physical approximation of APP and BACE-1: A key event in alzheimer's disease pathogenesis. Dev Neurobiol. Mar 2018;78(3):340-7.
8. Wolfe MS. Gamma-secretase: structure, function, and modulation for Alzheimer's disease. Curr Top Med Chem. 2008;8(1):2-8.
9. Storey E, Cappai R. The amyloid precursor protein of Alzheimer's disease and the Abeta peptide. Neuropathol Appl Neurobiol. Apr 1999;25(2):81-97.
10. Patterson D, Gardiner K, Kao FT, Tanzi R, Watkins P, Gusella JF. Mapping of the gene encoding the beta-amyloid precursor protein and its relationship to the Down syndrome region of chromosome 21. Proc Natl Acad Sci U S A. Nov 1988;85(21):8266-70.

11. Hardy J. Alzheimer's disease: the amyloid cascade hypothesis: an update and reappraisal. J Alzheimers Dis. 2006;9(3 Suppl):151-3.

12. Martin L, Latypova X, Wilson CM, Magnaudeix A, Perrin ML, Yardin C, et al. Tau protein kinases: involvement in Alzheimer's disease. Ageing Res Rev. Jan 2013;12(1):289-309.

13. Jana MK, Cappai R, Pham CL, Ciccotosto GD. Membrane-bound tetramer and trimer Abeta oligomeric species correlate with toxicity towards cultured neurons. J Neurochem. Feb 2016;136(3):594-608.

14. Saito T, Matsuba Y, Mihira N, Takano J, Nilsson P, Itohara S, et al. Single App knock-in mouse models of Alzheimer's disease. Nature neuroscience. May 2014;17(5):661-3. Epub 2014/04/15.

15. Sasaguri H, Nilsson P, Hashimoto S, Nagata K, Saito T, De Strooper B, et al. APP mouse models for Alzheimer's disease preclinical studies. The EMBO journal. Sep 1 2017;36(17):2473-87. Epub 2017/08/05.

16. Whyte LS, Hemsley KM, Lau AA, Hassiotis S, Saito T, Saido TC, et al. Reduction in open field activity in the absence of memory deficits in the App(NL-G-F) knock-in mouse model of Alzheimer's disease. Behav Brain Res. Jan 15 2018;336:177-81.

17. Mehla J, Lacoursiere SG, Lapointe V, McNaughton BL, Sutherland RJ, McDonald RJ, et al. Age-dependent behavioral and biochemical characterization of single APP knock-in mouse (APP(NL-G-F/NL-G-F)) model of Alzheimer's disease. Neurobiol Aging. Mar 2019;75:25-37.

18. Hamaguchi T, Tsutsui-Kimura I, Mimura M, Saito T, Saido TC, Tanaka KF. App(NL-G-F/NL-G-F) mice overall do not show impaired motivation, but cored

amyloid plaques in the striatum are inversely correlated with motivation. Neurochem Int. May 16 2019;129:104470.

19. Friedman SM, Menzies IB, Bukata SV, Mendelson DA, Kates SL. Dementia and hip fractures: development of a pathogenic framework for understanding and studying risk. Geriatr Orthop Surg Rehabil. Nov 2010;1(2):52-62. Epub 2010/11/01.

20. Metcalfe D. The pathophysiology of osteoporotic hip fracture. Mcgill J Med. Jan 2008;11(1):51-7. Epub 2008/06/05.

21. Chen YH, Lo RY. Alzheimer's disease and osteoporosis. Ci Ji Yi Xue Za Zhi. Jul-Sep 2017;29(3):138-42.

22. Luckhaus C, Mahabadi B, Grass-Kapanke B, Jänner M, Willenberg H, Jäger M, et al. Blood biomarkers of osteoporosis in mild cognitive impairment and Alzheimer's disease. Journal of neural transmission (Vienna, Austria : 1996). Jul 2009;116(7):905-11. Epub 2009/05/27.

23. Zhou R, Zhou H, Rui L, Xu J. Bone loss and osteoporosis are associated with conversion from mild cognitive impairment to Alzheimer's disease. Current Alzheimer research. 2014;11(7):706-13. Epub 2014/08/15.

24. Tysiewicz-Dudek M, Pietraszkiewicz F, Drozdzowska B. Alzheimer's disease and osteoporosis: common risk factors or one condition predisposing to the other? Ortopedia, traumatologia, rehabilitacja. Jul-Aug 2008;10(4):315-23. Epub 2008/09/10.

25. Liu D, Zhou H, Tao Y, Tan J, Chen L, Huang H, et al. Alzheimer's Disease is Associated with Increased Risk of Osteoporosis: The Chongqing Aging Study. Current Alzheimer research. 2016;13(10):1165-72. Epub 2013/08/08.

26. Cui S, Xiong F, Hong Y, Jung JU, Li XS, Liu JZ, et al. APPswe/Abeta regulation of osteoclast activation and RAGE expression in an age-dependent manner. J Bone Miner Res. May 2011;26(5):1084-98. Epub 2011/05/05.

27. Li S, Liu B, Zhang L, Rong L. Amyloid beta peptide is elevated in osteoporotic bone tissues and enhances osteoclast function. Bone. Apr 2014;61:164-75.

28. Li S, Yang B, Teguh D, Zhou L, Xu J, Rong L. Amyloid beta Peptide Enhances RANKL-Induced Osteoclast Activation through NF-kappaB, ERK, and Calcium Oscillation Signaling. Int J Mol Sci. Oct 10 2016;17(10).

29. Xia WF, Jung JU, Shun C, Xiong S, Xiong L, Shi XM, et al. Swedish mutant APP suppresses osteoblast differentiation and causes osteoporotic deficit, which are ameliorated by N-acetyl-L-cysteine. J Bone Miner Res. Oct 2013;28(10):2122-35.

30. Stapledon CJM, Stamenkov R, Cappai R, Clark JM, Solomon LB, Atkins GJ. Relationships between the Bone Expression of Bone Remodelling and Alzheimer's Disease-Related Genes and Cortical Bone Structure in Neck of Femur Fracture Submitted for Publication.

31. Fazzalari NL, Kuliwaba JS, Atkins GJ, Forwood MR, Findlay DM. The ratio of messenger RNA levels of receptor activator of nuclear factor kappaB ligand to osteoprotegerin correlates with bone remodeling indices in normal human cancellous bone but not in osteoarthritis. Journal of bone and mineral research : the official journal of the American Society for Bone and Mineral Research. Jun 2001;16(6):1015-27. Epub 2001/06/08.

32. Prideaux M, Findlay DM, Atkins GJ. Osteocytes: The master cells in bone remodelling. Curr Opin Pharmacol. Jun 2016;28:24-30.

33. Ryan JW, Starczak Y, Tsangari H, Sawyer RK, Davey RA, Atkins GJ, et al. Sex-related differences in the skeletal phenotype of aged vitamin D receptor global knockout mice. J Steroid Biochem Mol Biol. Nov 2016;164:361-8. Epub 2015/12/23.

34. Hung LW, Ciccotosto GD, Giannakis E, Tew DJ, Perez K, Masters CL, et al. Amyloid-beta peptide (Abeta) neurotoxicity is modulated by the rate of peptide aggregation: Abeta dimers and trimers correlate with neurotoxicity. J Neurosci. Nov 12 2008;28(46):11950-8. Epub 2008/11/14.

35. Smith DP, Smith DG, Curtain CC, Boas JF, Pilbrow JR, Ciccotosto GD, et al. Copper-mediated amyloid-beta toxicity is associated with an intermolecular histidine bridge. J Biol Chem. Jun 2 2006;281(22):15145-54. Epub 2006/04/06.

36. Ormsby RT, Cantley M, Kogawa M, Solomon LB, Haynes DR, Findlay DM, et al. Evidence that osteocyte perilacunar remodelling contributes to polyethylene wear particle induced osteolysis. Acta Biomater. Mar 2016;33:242-51. Epub 2016/01/23.

37. Ormsby RT, Solomon LB, Yang D, Crotti TN, Haynes DR, Findlay DM, et al. Osteocytes respond to particles of clinically-relevant conventional and cross-linked polyethylene and metal alloys by up-regulation of resorptive and inflammatory pathways. Acta Biomater. Mar 15 2019;87:296-306. Epub 2019/01/29.

38. Yang D, Wijenayaka AR, Solomon LB, Pederson SM, Findlay DM, Kidd SP, et al. Novel Insights into Staphylococcus aureus Deep Bone Infections: the Involvement of Osteocytes. MBio. Apr 24 2018;9(2). Epub 2018/04/25.

39. Kogawa M, Wijenayaka AR, Ormsby RT, Thomas GP, Anderson PH, Bonewald LF, et al. Sclerostin regulates release of bone mineral by osteocytes by induction

of carbonic anhydrase 2. J Bone Miner Res. Dec 2013;28(12):2436-48. Epub 2013/06/06.

40. Ciccotosto GD, Tew D, Curtain CC, Smith D, Carrington D, Masters CL, et al. Enhanced toxicity and cellular binding of a modified amyloid beta peptide with a methionine to valine substitution. J Biol Chem. Oct 8 2004;279(41):42528-34. Epub 2004/08/05.

41. Stapledon CJM, Tsangari H, Solomon LB, Campbell DG, Hurtado P, Krishnan R, et al. Human osteocyte expression of Nerve Growth Factor: The effect of Pentosan Polysulphate Sodium (PPS) and implications for pain associated with knee osteoarthritis. PloS one. 2019;14(9):e0222602. Epub 2019/09/27.

42. Prideaux M, Schutz C, Wijenayaka AR, Findlay DM, Campbell DG, Solomon LB, et al. Isolation of osteocytes from human trabecular bone. Bone. Jul 2016;88:64-72. Epub 2016/04/26.

43. O'Brien CA, Nakashima T, Takayanagi H. Osteocyte control of osteoclastogenesis. Bone. Jun 2013;54(2):258-63. Epub 2012/09/04.

44. Wang TH, Jiang Y, Xiao LP. [Expression of amyloid beta-protein in bone tissue of APP/PS1 transgenic mouse]. Zhonghua Yi Xue Za Zhi. Jan 1 2013;93(1):65-8.

45. Yang MW, Wang TH, Yan PP, Chu LW, Yu J, Gao ZD, et al. Curcumin improves bone microarchitecture and enhances mineral density in APP/PS1 transgenic mice. Phytomedicine : international journal of phytotherapy and phytopharmacology. Jan 15 2011;18(2-3):205-13. Epub 2010/07/20.

46. Zhao L, Liu S, Wang Y, Zhang Q, Zhao W, Wang Z, et al. Effects of Curculigoside on Memory Impairment and Bone Loss via Anti-Oxidative Character in APP/PS1 Mutated Transgenic Mice. PLoS One. 2015;10(7):e0133289.

47. Pan JX, Tang F, Xiong F, Xiong L, Zeng P, Wang B, et al. APP promotes osteoblast survival and bone formation by regulating mitochondrial function and preventing oxidative stress. Cell Death Dis. Oct 22 2018;9(11):1077.

48. Xiong J, O'Brien CA. Osteocyte RANKL: new insights into the control of bone remodeling. Journal of bone and mineral research : the official journal of the American Society for Bone and Mineral Research. Mar 2012;27(3):499-505. Epub 2012/02/23.

49. Xiong J, Piemontese M, Onal M, Campbell J, Goellner JJ, Dusevich V, et al. Osteocytes, not Osteoblasts or Lining Cells, are the Main Source of the RANKL Required for Osteoclast Formation in Remodeling Bone. PloS one. 2015;10(9):e0138189. Epub 2015/09/24.

50. Tang SY, Herber RP, Ho SP, Alliston T. Matrix metalloproteinase-13 is required for osteocytic perilacunar remodeling and maintains bone fracture resistance. J Bone Miner Res. Sep 2012;27(9):1936-50. Epub 2012/05/03.

51. Mercer RR, Crenshaw MA. The role of osteocytes in bone resorption during lactation: morphometric observations. Bone. 1985;6(4):269-74. Epub 1985/01/01.

52. Lotinun S, Ishihara Y, Nagano K, Kiviranta R, Carpentier VT, Neff L, et al. Cathepsin K-deficient osteocytes prevent lactation-induced bone loss and parathyroid hormone suppression. J Clin Invest. May 21 2019;129:3058-71.

53. Tsourdi E, Jähn K, Rauner M, Busse B, Bonewald LF. Physiological and pathological osteocytic osteolysis. Journal of musculoskeletal & neuronal interactions. Sep 1 2018;18(3):292-303. Epub 2018/09/05.

54. Verborgt O, Tatton NA, Majeska RJ, Schaffler MB. Spatial distribution of Bax and Bcl-2 in osteocytes after bone fatigue: complementary roles in bone

remodeling regulation? J Bone Miner Res. May 2002;17(5):907-14. Epub 2002/05/15.

55. Leong YQ, Ng KY, Chye SM, Ling APK, Koh RY. Mechanisms of action of amyloid-beta and its precursor protein in neuronal cell death. Metabolic brain disease. Jan 2020;35(1):11-30. Epub 2019/12/08.

56. Buenzli PR, Sims NA. Quantifying the osteocyte network in the human skeleton. Bone. Jun 2015;75:144-50. Epub 2015/02/25.

57. Civitelli R. Cell-cell communication in the osteoblast/osteocyte lineage. Arch Biochem Biophys. May 15 2008;473(2):188-92. Epub 2008/04/22.

58. Gao J, Qin A, Liu D, Ruan R, Wang Q, Yuan J, et al. Endoplasmic reticulum mediates mitochondrial transfer within the osteocyte dendritic network. Sci Adv. Nov 2019;5(11):eaaw7215. Epub 2019/12/05.

59. Vanderstichele H, Van Kerschaver E, Hesse C, Davidsson P, Buyse MA, Andreasen N, et al. Standardization of measurement of beta-amyloid(1-42) in cerebrospinal fluid and plasma. Amyloid. Dec 2000;7(4):245-58.

60. Xu W, Kawarabayashi T, Matsubara E, Deguchi K, Murakami T, Harigaya Y, et al. Plasma antibodies to Abeta40 and Abeta42 in patients with Alzheimer's disease and normal controls. Brain Res. Jul 11 2008;1219:169-79.

61. Wang MJ, Yi S, Han JY, Park SY, Jang JW, Chun IK, et al. Oligomeric forms of amyloid-beta protein in plasma as a potential blood-based biomarker for Alzheimer's disease. Alzheimers Res Ther. Dec 15 2017;9(1):98.

Figure Legends

Figure 1: Micro-CT analysis of cancellous bone in 12 week old age-matched male wild-type (WT) and *App*$^{NL\text{-}G\text{-}F/NL\text{-}G\text{-}F}$ (KI) mice femora. (A) % BV/TV is unchanged between genotypes (p = 0.9785); (B) Tb.N is unchanged between genotypes (p = 0.6283); (C) Tb.Th (p = 0.1064); (D) Tb.Sp (p = 0.8918); (E) Tb.Pf (p = 0.9522); (F) SMI (p = 0.7688). Data shown are means ± standard errors of the mean (SEM) (n = 5/group).

Figure 2: Micro CT analysis of the trabecular bone in 29 week old age-matched male wild-type (WT) and *App*$^{NL\text{-}G\text{-}F/NL\text{-}G\text{-}F}$ (KI) mice (n = 5/group). (A) Bone volume: tissue volume ratio (**p = 0.0040) (B) Trabecular number (**p = 0.0063); (C) Trabecular thickness (*p = 0.0107) (D) Trabecular separation (*p = 0.0456) (E) Trabecular bone pattern factor (*p = 0.0357) (F) Structure model index (*p = 0.0460); (G) 3D-reconstructed image of wild-type and knock-in trabecular bone from 2mm ROI. Data shown are means ± SEM (n = 5/group).

Figure 3: Histological assessment of osteoclast measures. Tartrate Resistant Acid Phosphatase (TRAP) staining was performed of 29 wk-old male mouse femora with a hematoxylin counterstain. (A) Osteoclast surface per bone surface measurements are increased in *App*$^{NL\text{-}G\text{-}F/NL\text{-}G\text{-}F}$ (KI) mice when compared with wild-type (WT) control mice (n = 4; p = 0.0003); (B) Total osteoclast number wild-type compared to knock-in animals (n = 4/group; p < 0.0001); (C) Representative image of the 2 mm ROI below the growth plate analysed for osteoclast counts.

Figure 4: Direct effects of $A\beta_{1-42}$ on osteoclastogenesis. Human PBMC were cultured under osteoclastogenic conditions, as described in Materials and Methods in the presence or absence of $A\beta_{1-42}$ peptides. (A) Cell counts of multinucleated TRAP positive cells in culture ($p > 0.05$ for all comparisons). (B) Representative of TRAP-positive multinucleated cells.

Figure 5: Detection of $A\beta_{1-42}$ accumulations in 29 week-old male mice in both brain and bone tissue. (A) Positive 82E1 staining of bone marrow of $App^{NL-G-F/NL-G-F}$ mouse femur. (B) Positive control brain tissue from the same animal with Aβ plaque deposition. Arrows are indicative of areas of plaque deposition.

Figure 6: Osteocyte lacunae measures in $App^{NL-G-F/NL-G-F}$ mice. Osteocyte lacunae were visualised by Toluidine Blue staining in the long bones of 29 week-old male mice, as described in Materials and Methods. Sections were analysed for (A) osteocyte lacunar area (Lac.Ar) and (B) osteocyte number per bone area (Ot.N/B.Ar). Measurements were made from at least two 5 µm thick sections/bone sample, each comprising between 30 – 60 osteocyte lacunae. Data shown are means ± SD, n = 5 mice/group.

Figure 7: Effect of $A\beta_{1-42}$ peptides on osteocyte viability. (A) Representative confocal microscopy images of primary human osteocytes stained with immunofluorescent stains Calcein AM (blue), NucSpot (green) and Sir-Actin (purple); (B) Osteocyte viability measurements at 24, 48 and 96 h post-exposure to 0, 1.5, 5 or 15 µM $A\beta_{1-42}$.

Figure 8: Effect of $A\beta_{1-42}$ peptides on osteocyte gene expression. Human primary osteocytes were cultured and treated with recombinant $A\beta_{1-42}$ peptides at either 0 (untreated control), 1.5, 5 or 15 μM, as described in Materials and Methods. Relative mRNA levels of osteoclastic and osteocytic osteolysis markers over a 96-hour treatment period were measured using real-time RT-PCR. (A) Basal mRNA levels of *APP* and *BACE1* mRNA; (B) *RANKL*; (C) *OPG*; (D) *RANKL*: *OPG* mRNA ratio; (E) *MMP13* mRNA expression levels. Data shown are means ± SD of biological triplicate treatments. Significant difference to corresponding untreated control is indicated by # $p < 0.05$.

Table 1: Forward (F) and reverse (R) primer sequences for real-time RT-PCR gene expression analysis.

Gene Name	*Direction*	*Oligonucleotide Sequence (5′ – 3′)*
18S	F	GGAATTCCCGAGTAAGTGCG
	R	GCCTCACTAAACCATCCAA
APP	F	ATCCTGCAGTATTGCCAAGAAG
	R	CACAAAGTGGGGATGGGTC
BACE1	F	GCAGGGCTACTACGTGGAGA
	R	GTATCCACCAGGATGTTGAGC
MMP13	F	GGATCCAGTCTCTCTATGGT
	R	GGCATCAAGGGATAAGGAAG
OPG	F	GCTCACAAGAACAGACTTTCCAG
	R	CTGTTTTCACAGAGGTCAATATCTT
RANKL	F	CCACCCCCGATCATGGT
	R	TCAGCCTTTTGCTCATCTCACTAT

Figures

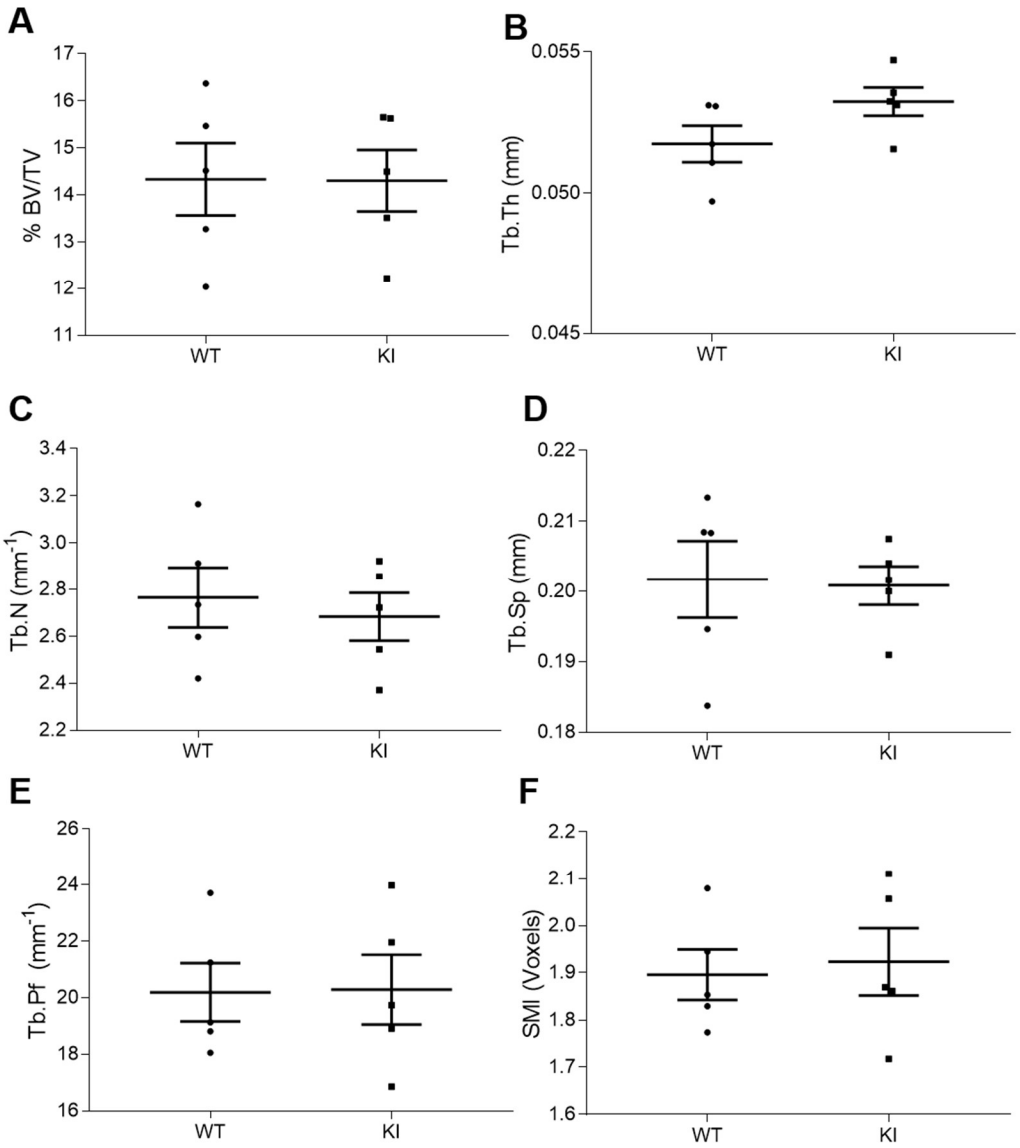

Figure 1

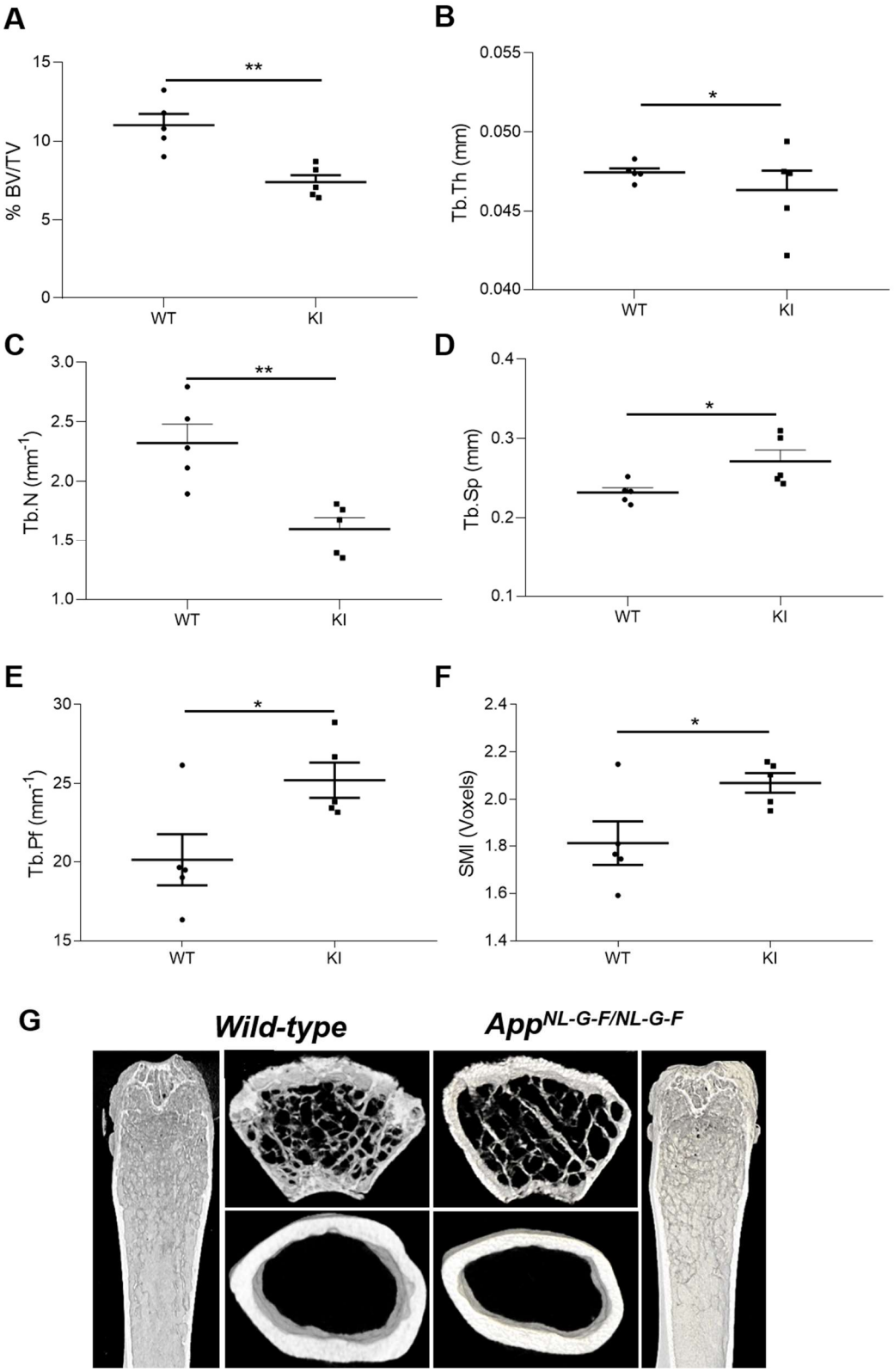
A
% BV/TV
15
10
5
0
**
WT
KI
B
Tb.Th (mm)
0.055
0.050
0.045
0.040
*
WT
KI
C
Tb.N (mm-1)
3.0
2.5
2.0
1.5
1.0
**
WT
KI
D
Tb.Sp (mm)
0.4
0.3
0.2
0.1
*
WT
KI
E
Tb.Pf (mm-1)
30
25
20
15
*
WT
KI
F
SMI (Voxels)
2.4
2.2
2.0
1.8
1.6
1.4
*
WT
KI
G
Wild-type
App NL-G-F/NL-G-F

Figure 2

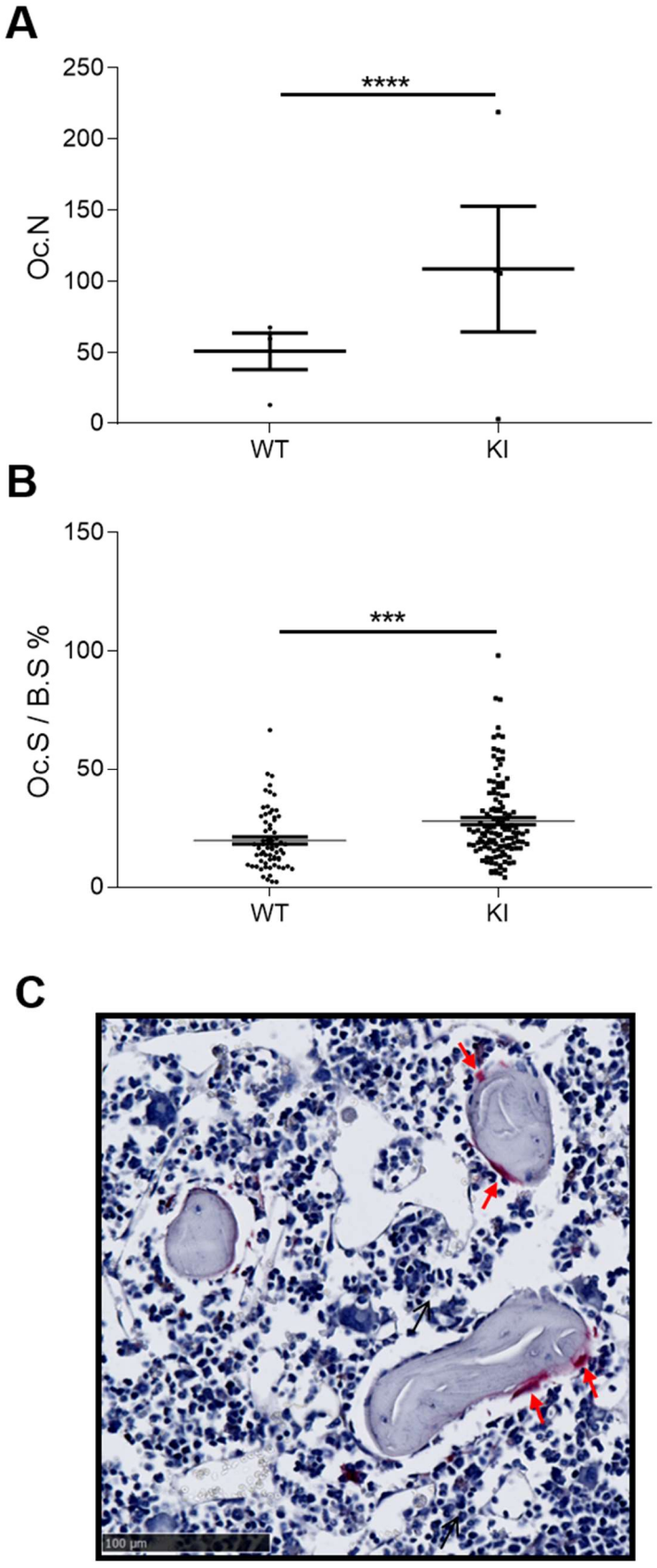

Figure 3

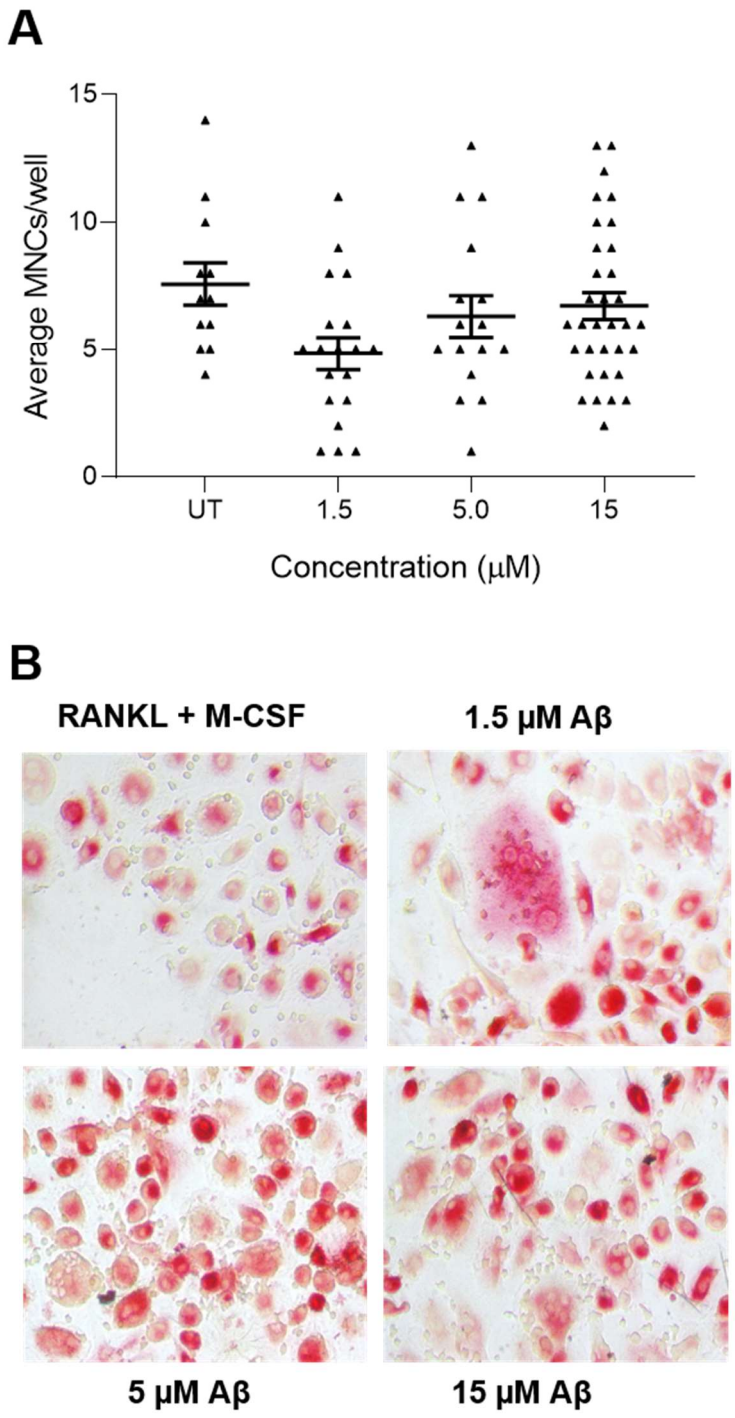
A
15
10
5
0
Average MNCs/well
UT
1.5
5.0
15
Concentration (μM)
B
RANKL + M-CSF
1.5 μM Aβ
5 μM Aβ
15 μM Aβ

Figure 4

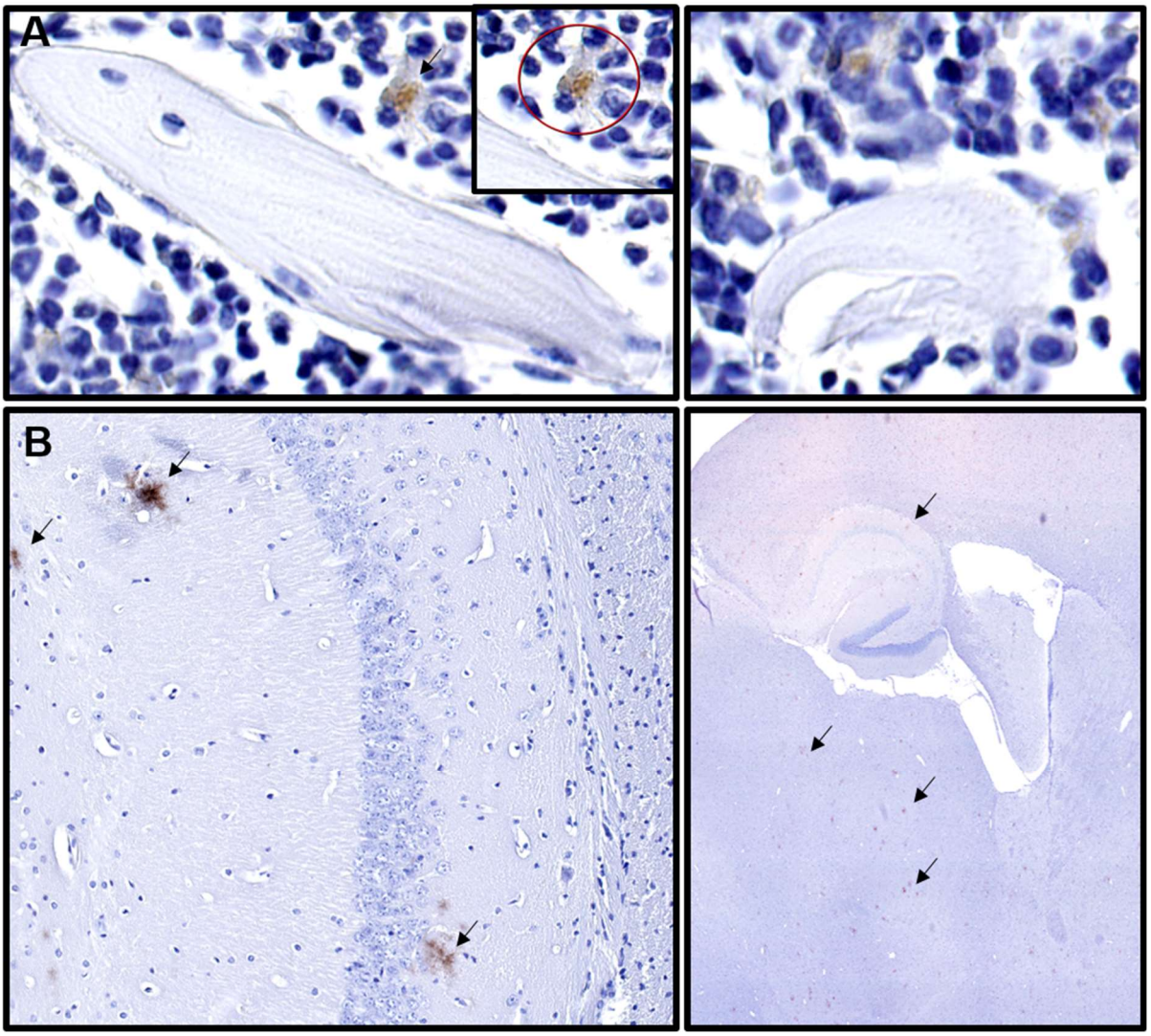

Figure 5

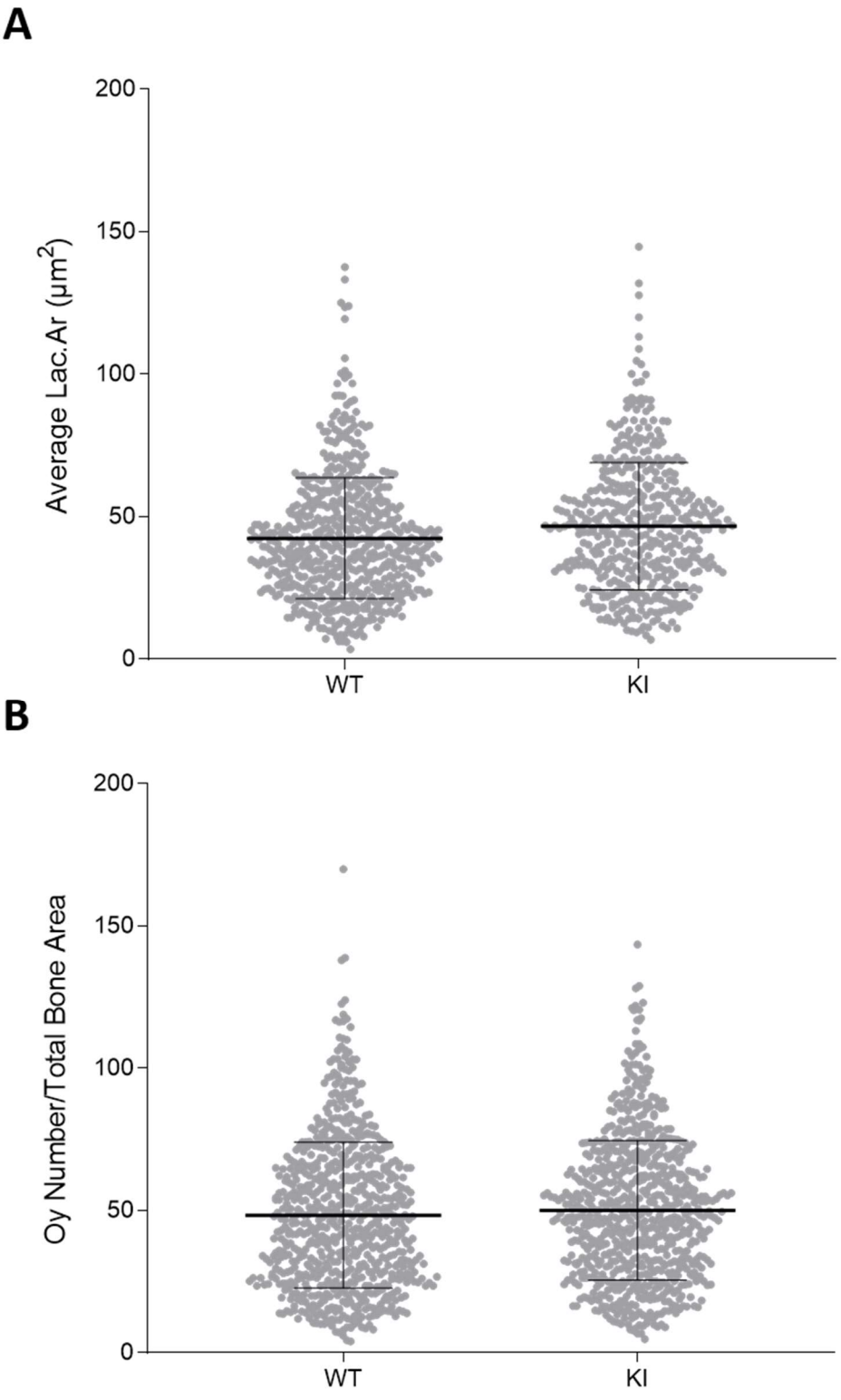
A
200
150
100
50
0
Average Lac.Ar (µm2)
WT
KI
B
200
150
100
50
0
Oy Number/Total Bone Area
WT
KI

Figure 6

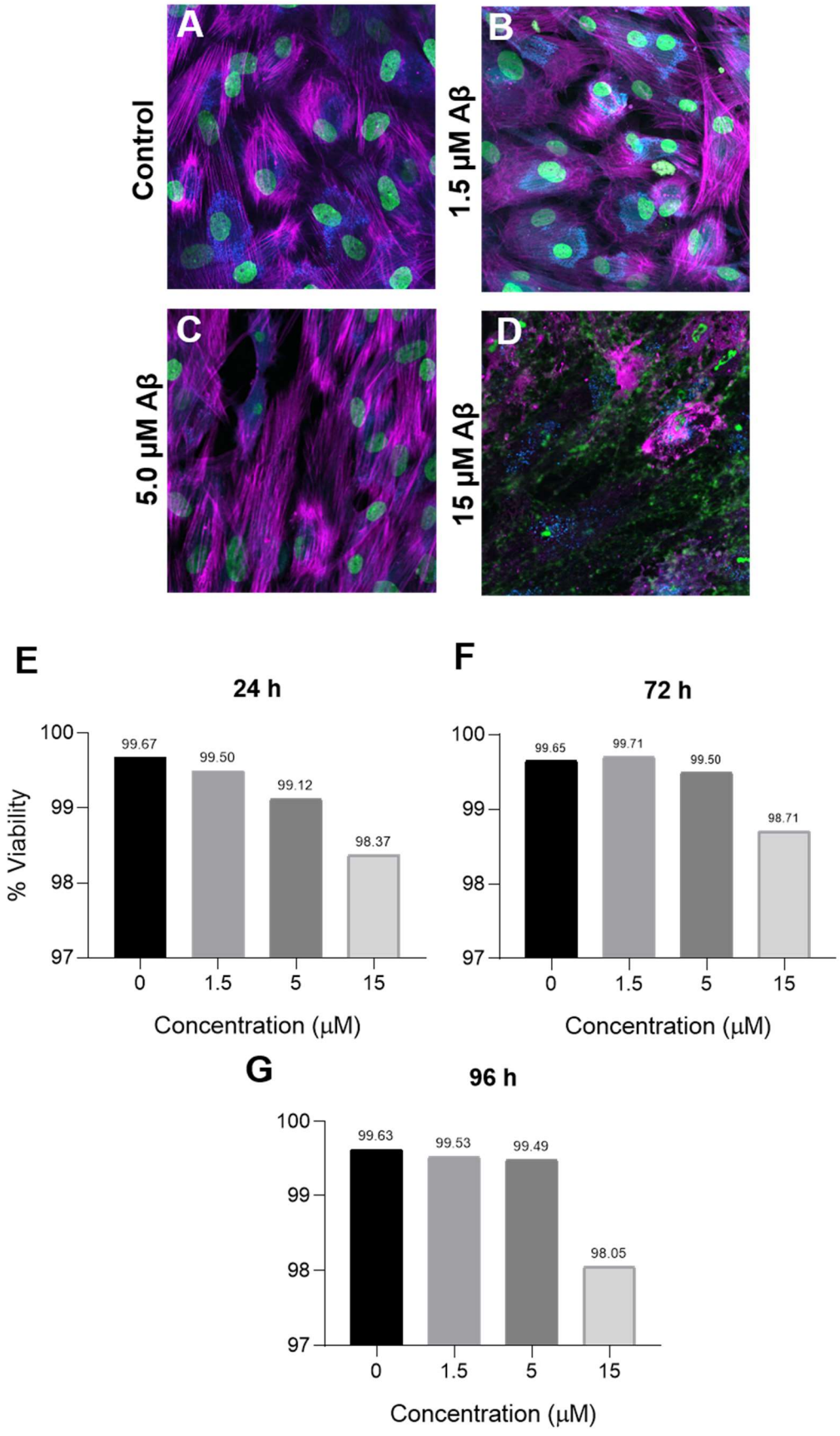
A
Control
B
1.5 µM Aβ
C
5.0 µM Aβ
D
15 µM Aβ
E
24 h
% Viability
100
99
98
97
99.67
99.50
99.12
98.37
0
1.5
5
15
Concentration (µM)
F
72 h
99.65
99.71
99.50
98.71
Concentration (µM)
G
96 h
99.63
99.53
99.49
98.05
Concentration (µM)

Figure 7

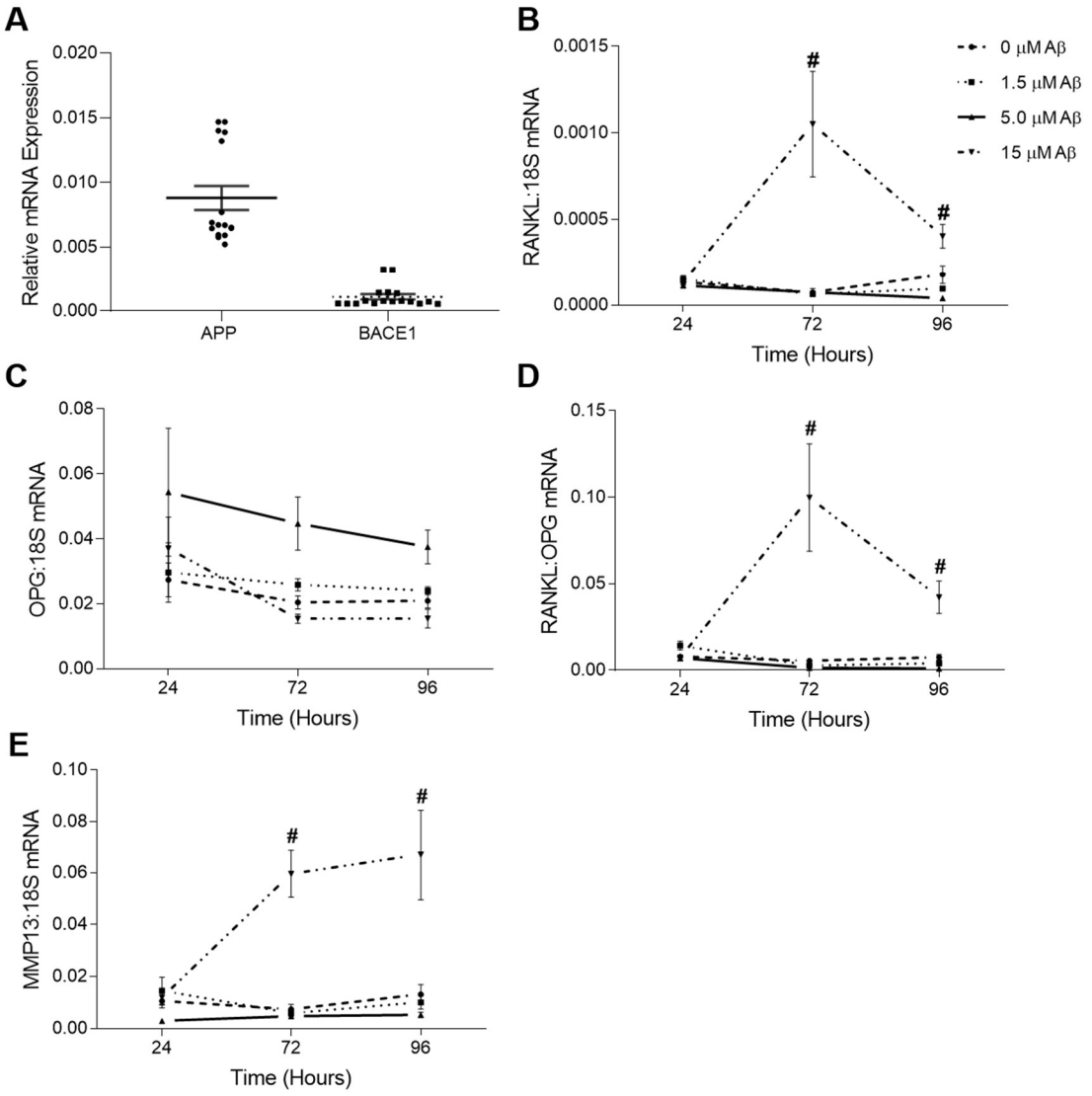
A
Relative mRNA Expression
0.020
0.015
0.010
0.005
0.000
APP
BACE1
B
RANKL:18S mRNA
0.0015
0.0010
0.0005
0.0000
#
#
24
72
96
Time (Hours)
0 μM Aβ
1.5 μM Aβ
5.0 μM Aβ
15 μM Aβ
C
OPG:18S mRNA
0.08
0.06
0.04
0.02
0.00
24
72
96
Time (Hours)
D
RANKL:OPG mRNA
0.15
0.10
0.05
0.00
#
#
24
72
96
Time (Hours)
E
MMP13:18S mRNA
0.10
0.08
0.06
0.04
0.02
0.00
#
#
24
72
96
Time (Hours)

Figure 8

Chapter 5

Human osteocyte expression of Nerve Growth Factor: The effect of Pentosan Polysulphate Sodium (PPS) and implications for pain associated with knee osteoarthritis

Accepted for publication in *PLOS ONE* September 3, 2019

This final study was performed on the basis that locally produced NGF in the bone could elicit pain in the context of knee osteoarthritis. In Chapter 3, it was established that NGF was expressed by bone cells derived from cancellous bone biopsies in patients undergoing fracture repair surgery, which validated the concept of a role for NGF in bone loss and pain. In this Chapter, the authors determined that NGF and its pro-form were expressed in human bone derived from patients with knee osteoarthritis. It was also shown that NGF and pro-NGF could be stimulated by the pro-inflammatory cytokine, TNF-α and that the increase in expression at the mRNA and protein level could be suppressed by a new pain-mediator, pentosan polysulphate sodium (PPS). This study provides a new potential therapy for the treatment of pain associated with knee OA mediated by NGF and pro-NGF.

Statement of Authorship

Title of Paper	**Human osteocyte expression of Nerve Growth Factor: the effect of Pentosan Polysulphate Sodium (PPS) and implications for pain associated with knee osteoarthritis**
Publication Status	☑ Published ☐ Accepted for Publication ☐ Submitted for Publication ☐ Unpublished and Unsubmitted w ork w ritten in manuscript style
Publication Details	Published in PLoS One Open Access Journal on the 26th of September, 2019

Principal Author

Name of Principal Author (Candidate)	Catherine Stapledon
Contribution to the Paper	First author on the paper, generated data, performed majority of experimental work and interpreted all data obtained. Made the decision to publish, participated in the preparation of the manuscript and approved the final version for submission.
Overall percentage (%)	80%
Certification:	This paper reports on original research I conducted during the period of my Higher Degree by Research candidature and is not subject to any obligations or contractual agreements with a third party that would constrain its inclusion in this thesis. I am the primary author of this paper.
Signature	Date 16/10/2019

Co-Author Contributions

By signing the Statement of Authorship, each author certifies that:

i. the candidate's stated contribution to the publication is accurate (as detailed above);

ii. permission is granted for the candidate in include the publication in the thesis; and

iii. the sum of all co-author contributions is equal to 100% less the candidate's stated contribution.

Name of Co-Author	Helen Tsangari
Contribution to the Paper	Assisted with data generation, performed analyses and interpreted data obtained.
Signature	Date 16/10/2019

Name of Co-Author	L. Bogdan Solomon
Contribution to the Paper	Provided samples for analysis, made the decision to publish, participated in preparation of manuscript and approved final version for submission.
Signature	Date 16/10/2019

Name of Co-Author	David G Campbell
Contribution to the Paper	Provided samples for analysis, made the decision to publish, participated in preparation of manuscript and approved final version for submission.
Signature	Date 16/10/2019

Name of Co-Author	Plinio Hurtado
Contribution to the Paper	Assisted with materials acquisition, contributed intellectually and assay design.
Signature	Date 16/10/2019

Name of Co-Author	Ravi Krishnan
Contribution to the Paper	Co-senior author, conceived the study, contributed to experimental design, supplied materials, participated in the preparation of the manuscript, made decision to publish and approved the final version for submission.
Signature	Date 16/10/2019

Esigned by:
Ravi Krishnan
2020.04.21 22:53:27 +0930
I approve this document Chief Scientific Officer, Paradigm Biopharmaceuticals Ltd

Name of Co-Author	Gerald J Atkins
Contribution to the Paper	Co-senior and communicating author, conceived the study, designed and supervised the study, participated in the preparation of the manuscript, made decision to publish and approved the final version for submission.
Signature	Date 16/10/2019

PLOS ONE

RESEARCH ARTICLE

Human osteocyte expression of Nerve Growth Factor: The effect of Pentosan Polysulphate Sodium (PPS) and implications for pain associated with knee osteoarthritis

Catherine J. M. Stapledon[1], Helen Tsangari[1], Lucian B. Solomon[1,2], David G. Campbell[1,3], Plinio Hurtado[4], Ravi Krishnan[5☯]*, Gerald J. Atkins[1☯]*

1 Centre for Orthopaedic & Trauma Research, The University of Adelaide, Adelaide, South Australia, Australia, **2** Orthopaedic and Trauma Service, Royal Adelaide Hospital, Adelaide, South Australia, Australia, **3** Wakefield Orthopaedic Clinic, Calvary Wakefield Hospital, Adelaide, South Australia, Australia, **4** Renal Unit, Royal Adelaide Hospital, Adelaide, South Australia, Australia, **5** Paradigm Biopharmaceuticals Ltd., Melbourne, Victoria, Australia

☯ These authors contributed equally to this work.
* rkrishnan@paradigmbiopharma.com (RK); Gerald.atkins@adelaide.edu.au (GA)

OPEN ACCESS

Citation: Stapledon CJM, Tsangari H, Solomon LB, Campbell DG, Hurtado P, Krishnan R, et al. (2019) Human osteocyte expression of Nerve Growth Factor: The effect of Pentosan Polysulphate Sodium (PPS) and implications for pain associated with knee osteoarthritis. PLoS ONE 14(9): e0222602. https://doi.org/10.1371/journal.pone.0222602

Editor: Dominique Heymann, Universite de Nantes, FRANCE

Received: February 14, 2019

Accepted: September 3, 2019

Published: September 26, 2019

Data Availability Statement: All relevant data are within the manuscript and its Supporting Information files.

Funding: This study was funded by a research grant from Paradigm Biopharmaceuticals Ltd (https://paradigmbiopharma.com/) and from a Project Grant awarded to GJA from the National Health and Medical Research Council of Australia (NHMRC) (Project ID1106029). CJMS was

Abstract

Pentosan polysulphate sodium (PPS) is a promising therapeutic agent for blocking knee pain in individuals with knee osteoarthritis (KOA). The mode of action of PPS in this context is unknown. We hypothesised that the osteocyte, being the principal cell type in the subchondral bone, was capable of expressing the pain mediator Nerve Growth Factor (NGF), and that this may be altered in the presence of PPS. We tested the expression of NGF and the response to PPS in the presence or absence of the proinflammatory cytokine tumour necrosis factor-alpha (TNFα), in human osteocytes. For this we differentiated human primary osteoblasts grown from subchondral bone obtained at primary knee arthroplasty for KOA to an osteocyte-like stage over 28d. We also tested NGF expression in fresh osteocytes obtained by sequential digestion from KOA bone and by immunofluorescence in KOA bone sections. We demonstrate for the first time the production and secretion of NGF/proNGF by this cell type derived from patients with KOA, implicating osteocytes in the pain response in this pathological condition and possibly others. PPS inhibited TNFα-induced levels of proNGF secretion and TNFα induced *NGF* mRNA expression. Together, this provides evidence that PPS may act to suppress the release of NGF in the subchondral bone to ameliorate pain associated with knee osteoarthritis.

Introduction

Osteoarthritis of the knee (KOA) is a common and painful condition, for which the first line of management is the prescription of analgesics to control pain. The aetiology of KOA is incompletely understood but is known to be associated with the increased expression of proinflammatory mediators, including tumour necrosis factor alpha (TNFα) and interleukin 1-beta

supported by an Australian Postgraduate Award scholarship. GJA is an NHMRC Senior Research Fellow. Paradigm Biopharmaceuticals Ltd provided additional funding in the form of salary to RK. The specific roles of these authors are articulated in the 'author contributions' section. The funders did not have any role in the study design, data collection and analysis, decision to publish, or preparation of the manuscript beyond those specified.

Competing interests: RK is a full-time employee of Paradigm Biopharmaceuticals Ltd. (https://paradigmbiopharma.com/). As a staff member of Paradigm Biopharmaceuticals Ltd, RK is entitled to long term and short-term incentives. Australian Provisional Patent Application 2018903820 and Australian Provisional Patent Application 2019900326 which are both entitled "Treatment of pain with polysulfated polysaccharides" have been filed by Paradigm Biopharmaceuticals Ltd who is the proprietor of the intellectual property. This does not alter the authors' adherence to PLOS ONE policies on sharing data and materials. All other authors declare that no competing interests exist.

(IL-1β) [1]. These are thought to stimulate the localised production of cartilage-degrading enzymes, such as matrix metallopeptidase (MMP) family member-13 (MMP-13). After exhaustion of nonoperative management options, KOA is ultimately treated by performing a total knee arthroplasty (TKA), in which the diseased joint is replaced by a prosthesis. Patient reported pain is the major indicator for TKA [2].

Bone is a well innervated tissue, with bone sensory neurons deriving solely from the dorsal root ganglia of the spinal cord [3]. The secreted neurotropic protein beta-Nerve Growth Factor (NGF) is a major contributor to pain in a number of chronic conditions, including KOA [4–6]. Furthermore, NGF mRNA expression is known to be induced by both TNFα and IL-1β in an experimental mouse model of osteoarthritis [7]. NGF binds to at least two receptors expressed by neurons, tropomyosin receptor kinase A (TrkA) and the pan-neurotropin receptor p75/NTR, where it can have diverse biological effects, either promoting neuronal growth or causing neuron apoptosis, depending on whether the neuron also expresses the co-receptor, sortilin [8]. A neutralising antibody treatment that sequesters NGF, tanezumab®, has yielded promising results in the treatment of pain associated with KOA [1, 4–6], consistent with NGF being both a key readout and a mediator of pain for this condition. NGF is first translated as a pro-protein form (proNGF), which is post-translationally processed (proteolytically cleaved) to the mature form by the action of furin or furin-like pro-protein convertases [8]. Currently, the accurate detection of soluble NGF levels using commercially available enzyme linked immunosorbent assays (ELISAs) is problematic due to the influence on readouts of proNGF; if present, proNGF interferes with the readouts of a number of commercially available ELISA kits in an unpredictable fashion, in terms of both the magnitude and the direction (increase or decrease) of the effect [9]. It is therefore necessary to defer quantitative assessment to the levels of proNGF [9].

Pentosan Polysulphate Sodium (PPS) is an FDA-approved drug for the treatment of interstitial cystitis and bladder pain syndrome, with an excellent safety profile [10]. It is currently being tested for its efficacy as a treatment for KOA with promising results [11, 12]. The mode of action of PPS appears to be multi-factorial, and includes replenishment of the glycosaminoglycan (GAG) layer in the case of its effect in interstitial cystitis, as well as effects on intracellular signalling, in particular the nuclear factor kappa-B (NFκB) [13] and the IL-1β-iNOS [14] pathways in chondrocytes. Importantly, KOA is a disease of the entire joint, with changes to the sub-chondral bone, as well as to the synovium and cartilage [1]. The contribution of each tissue to disease progression and to the associated pain is incompletely understood. In advanced KOA, there is nearly complete degradation of the cartilage with a paucity of healthy chondrocytes remaining. This suggests that mediators of pain may derive to a significant extent from the underlying sub-chondral bone. The most numerous cell type in hard bone tissue is the osteocyte, and these cells are increasingly recognised as the key controlling cell type in many local and systemic physiological processes [15, 16]. In conditions associated with osteoarthritis, the osteocyte is involved in the inflammatory, osteolytic response to implant-derived wear particles [17] and also elicits impressive pro-inflammatory responses to bacteria in the condition of periprosthetic joint infection [18].

We hypothesised that osteocytes are capable of producing NGF in the inflammatory milieu of the subchondral bone in KOA and that PPS may act by inhibiting this production. To test this hypothesis, we examined the expression of NGF in freshly isolated human primary osteocytes. We then tested the effects of PPS on the responses of human primary osteocyte-like cultures, differentiated from the proximal tibiae of patients suffering from advanced KOA and undergoing TKA. Treatment with recombinant TNFα was used as the proinflammatory stimulus, and the effects on the relative expression of *NGF* mRNA was examined. ProNGF protein levels were also determined. We show for the first time that human osteocytes are capable of

producing NGF, suggesting that they potentially contribute to localised pain responses. We also show that PPS suppresses *NGF* mRNA transcription and proNGF secretion by osteocytes and reverses the stimulatory effects of TNFα on these processes. Together, our findings suggest a hitherto unknown role for osteocytes in the pain response and a mechanism for the pain benefit in KOA patients taking PPS.

Materials and methods

Ethical statement

All studies with human patient derived material were covered by pre-existing ethics committee approval by the Human Research Ethics Committees of the Royal Adelaide Hospital (Approval No. 130114) and Calvary Health Care Limited (Approval No. 13-CHREC-E006). All donor material was obtained with written informed patient consent.

Donors and osteocyte-like cells

In order to represent the clinical relevance of the findings from this study, the effects of PPS were to be tested on osteocyte-like cultures [17, 19–23] derived by differentiation *in vitro* for a period of 28 days from cells isolated from the subchondral bone of the proximal tibia of three patients with advanced knee OA who underwent total knee arthroplasty (TKA) surgery (KOA). To examine potential differences with non-OA bone, cells were also isolated from the proximal femur of three patients who underwent total hip arthroplasty (THA) for neck of femur fracture (NOF). The gender of all donors was female, and groups were age-matched, with the mean age of KOA being 77.0 ± 8.5 years and that of the NOF group being 77.7 ± 5.5 years ($p = 0.91$).

Cryopreserved cells from each donor (all at passage 0 or 1) were thawed and cultured for 10 days in T75 cm^2 tissue culture flasks. Once confluent, cells were removed by collagenase/dispase digestion, washed by centrifugation, counted and adjusted to 5 x 10^5 cells/ml. Cells were then seeded into either 12-well tissue culture trays or into 8-well chamber slides, at 1 x 10^5 and 2 x 10^4 cells/well, respectively. After 24h, media were replaced with osteogenic differentiation medium, consisting of αMEM, 5% v/v foetal calf serum (FCS), 1.8 mM potassium dihydrogen phosphate (KH_2PO_4), 100 μM Ascorbate-2-phosphate (As2P), 10 mM HEPES, 1 x 10^{-8} M Dexamethasone and 0.2 mM L-Glutamine. During the differentiation process, samples were collected at days 3, 14 and 28 in Trizol reagent for total RNA preparation and gene expression analysis (see below). Cultures seeded into chamber slides were examined for *in vitro* mineralisation using the Alizarin Red staining technique, as previously described [22].

PPS and TNFα treatments

PPS (bene pharmaChem GmbH & Co. KG, Geretstried, Germany) was dissolved in sterile PBS as a stock solution at 1.0 mg/ml. Differentiated cells were either untreated or pre-treated with final concentrations of PPS at 1, 5 or 50 μg/ml in culture medium for 72h. The tested doses of PPS were based on the effective and maximally active levels published in a previous study [24]. Media were then replaced with the same concentrations of PPS with or without the addition of recombinant human (rh) TNFα (1 ng/ml) and then cultured for a further 48h. Culture supernatants were collected and total RNA and cDNA prepared, as described below.

Isolation of human osteocytes

Osteocytes were isolated directly from human KOA bone samples ($n = 4$), according to our published protocol [25]. Briefly, bone obtained from TKA was rinsed vigorously in sterile PBS

and then subjected to six serial digestions of collagenase/dispase/EDTA, with intervening recovery of released cells by centrifugation and washing in PBS. The cells obtained from digests 4–6, corresponding to an osteocyte-enriched fraction [25] were pooled, washed twice further by centrifugation and resuspension in PBS and then seeded into 8-well glass bottomed chamber slides. After allowing cells to recover for 72h, they were either immunostained or pre-treated with PPS and then treated with combinations of PPS and rhTNFα, as indicated.

Gene expression analysis

Total RNA was prepared from Trizol lysates, according to the manufacturer's instructions, with the exception that due to evidence for PPS interference in the generation of assayable cDNA, RNA precipitates were washed 3 times in 75% ethanol instead of the usual single wash step, in an attempt to remove residual PPS. RNA preparations were tested for yield and purity using a Nanodrop microvolume spectrophotometer (Thermo Fisher). One microgram of RNA from each sample was reverse transcribed using a Superscript™ II kit (Thermo Fisher), as per manufacturer's instructions. Real-time RT-PCR was performed for genes including Nerve Growth Factor (*NGF*), its receptors *NTRK1* (*TRKA*) and *NGFR* (*P75NTR*), *MMP13*, *RANKL*, *OPG*, *OCN*, *DMP1* and *SOST*, relative to housekeeping gene (*ACTB*) expression. Oligonucleotide primer sequences for each of these are shown in **Table 1**.

ELISA analysis

Culture supernatants were stored frozen (-80˚C) until use, whereupon they were thawed at 4˚C, and assayed by ELISA for human NGF (Cat. No: EHNGF; Thermo Fisher Scientific) or proNGF (Cat. No: BEK-2226-2P; Biosensis) protein levels, as per the manufacturers' instructions.

Immunostaining

Cells seeded in 8-well chamber slides and differentiated for 28 days or freshly digested from bone were either untreated or treated with rhTNFα (1 ng/ml), PPS (50μg/ml; 'PPS50') or PPS50 + rhTNFα, as indicated. For immunostaining, media were removed and wells rinsed three times with PBS (pH 7.4). Cells were then fixed with 100μl of Histochoice (Sigma-Aldrich) tissue fixative for 1 hour at room temperature. After fixation, wells were rinsed twice with distilled H_2O and stored at 4˚C until staining. Cells were blocked with 50μl of blocking buffer

Table 1. Human mRNA-specific oligonucleotide primer sequences.

Gene	Forward Primer Sequence	Reverse Primer Sequence
ACTB [17][a]	5′-cgcgagaagatgacccagatc-3′	5′-tcaccggagtccatcacg-3′
DMP1 [17]	5′-gatcagcatcctgctcatgtt-3′	5′-agccaaatgacccttccattc-3′
MMP13 [17]	5′-ggatccagtctctctatggt-3′	5′-ggcatcaagggataaggaag-3′
NGF [26]	5′-cacactgaggtgcatagcgt-3′	5′-tgatgaccgcttgctcctgt-3′
NGFR/TRKA [27]	5′-cctggacagcgtgacgttc-3′	5′-cccagtcgtctcatcctggt-3′
P75NTR [27]	5′-cctggacagcgtgacgttc-3′	5′-cccagtcgtctcatcctggt-3′
OCN [17]	5′-atgagagccctcacactcctcg-3′	5′-gtcagccaactcgtcacagtcc-3′
OPG [17]	5′-gctcacaagaacagactttccag-3′	5′-ctgttttcacagaggtcaatatctt-3′
RANKL [17]	5′-ccaagatctccaacatgact-3′	5′-tacaccattagttgaagatact-3′
SOST [17]	5′-accggagctggagaacaaca-3′	5′-gctgtactcggacacgtctt-3′

[a]Published references to primer pairs are indicated next to gene names; all primer pairs were designed and/or validated in-house.

https://doi.org/10.1371/journal.pone.0222602.t001

(5% v/v normal rabbit serum in 1 x PBS) for 20 minutes at room temperature in a humid chamber. Cells were then rinsed with wash buffer (0.1% v/v normal rabbit serum in PBS) three times. Cells were stained with either mouse monoclonal antibody (MAb) *anti*-human NGF (25623; Thermo Fisher Scientific), *anti*-human NGFR (2F1C2; Thermo Fisher Scientific), *anti*-human TrkA (6B2; Thermo Fisher Scientific), or *anti*-human SOST (MAb 220902.11; R&D Systems, Minneapolis, MN, USA) primary antibodies and their respective isotype controls (IgG_1; MAb 1B5), diluted as indicated. Cells were incubated with primary antibody for 40 minutes at 4˚C. For unconjugated MAbs, chamber slides were then rinsed 3 x with wash buffer and 50μl of rabbit α-mouse Alexa-fluor secondary antibody (1:2000 dilution), also containing nuclear DAPI stain (1:2000 dilution; diamidino-2-phenylindole; Thermo Fisher) was added for 1h at room temperature. Wells were then washed three times with wash buffer.

Finally, FluoroBrite DMEM (Life Technologies) was added to each well to image using confocal microscopy (FV3000 Confocal Microscope, Olympus Lifescience).

For double-labelling purposes, anti-NGF was directly conjugated to fluorescein isothiocyanate (FITC; Sigma Chemical Co., St. Louis, MO, USA). For this MAb 25623 was first dialysed against carbonate/bicarbonate buffer (1l; pH 9.6) at 4˚C overnight. FITC was dissolved to 1mg/ml in anhydrous DMSO. 15μl FITC solution was added to 100μg anti-NGF and the tube mixed on a rotator for 2 h at room temperature. Unbound FITC was removed using size-exclusion chromatography on a Sephadex G-25 column (Pharmacia Biotech, Piscataway, NJ, USA). The absorbance of 0.5 ml fractions at 280nm and 492nm was determined using a NanoDrop One spectrophotometer (Thermo Fisher Scientific) and the concentration of FITC-conjugated antibody determined by the formula: concentration (mg/ml) = A_{280} –(A_{492} x 0.35)/1.4. To remove aggregates, the antibody solution was centrifuged at 16,400 RCF for 15 minutes prior to use. As a positive control for immunostaining, we identified the small cell lung carcinoma cell line NCI-H266 (ATCC, Masassas, VA, USA) to be NGF-expressing using the Harmonizome database [28]. For these assays, FITC-conjugated X-63 MAb (Biosensis, Thebarton, SA, Australia) was used as a negative control; direct conjugates were incubated for 40 min, aspirated and the wells washed three times, as above.

Bone isolated from KOA patients was fixed, decalcified, embedded and sectioned, as described [18]. Bone sections (5 μm) were first heated at 60˚C for 15 min to melt excess paraffin and then dewaxed. For antigen retrieval, slides were then incubated in 10% formic acid in distilled water for 10 min, rinsed in PBS and then immunostained, as above.

Data and statistical analysis

Data were analysed by two-way analysis of variance (ANOVA) with Holm-Sidak's multiple comparison post-hoc tests using GraphPad Prism software (GraphPad Prism, La Jolla, CA, USA). Values for $p < 0.05$ were considered statistically significant.

Results and discussion

NGF expression by cultured osteocytes

Human primary osteoblasts isolated from the subchondral bone of patients undergoing TKA for osteoarthritis of the knee (KOA) or THA for neck of femur fracture (NOF) were cultured under differentiating conditions for a period of 28d [16–21, 29]. Overall the NOF cultures mineralised to a significantly greater extent than KOA donors, as assayed by Alizarin Red staining (**S1 Fig**). The reason for this could relate either to the site harvested (proximal femur for NOF and subchondral proximal tibia for KOA), or more likely, to the dysregulated mineralisation evident in differentiating osteoblasts from patients with osteoarthritis, as we have previously reported for cells isolated from the proximal femur [22]. All KOA donors' cells

displayed strong characteristics of pre-osteocytes/osteocytes by day 3, expressing appreciable mRNA for *DMP1*, *SOST* and *OCN* (Fig 1A–1C). *DMP1* and *SOST* mRNAs were expressed to a similar level overall based on delta-cycle threshold (ΔCT) values, while *OCN* mRNA was more abundantly expressed. The expression of *DMP1* and *OCN* increased by D14 and then declined by D28, consistent with the acquisition of a mature osteocyte-like phenotype associated with loss of organelles and a decrease in the overall metabolic level [16, 30]. The

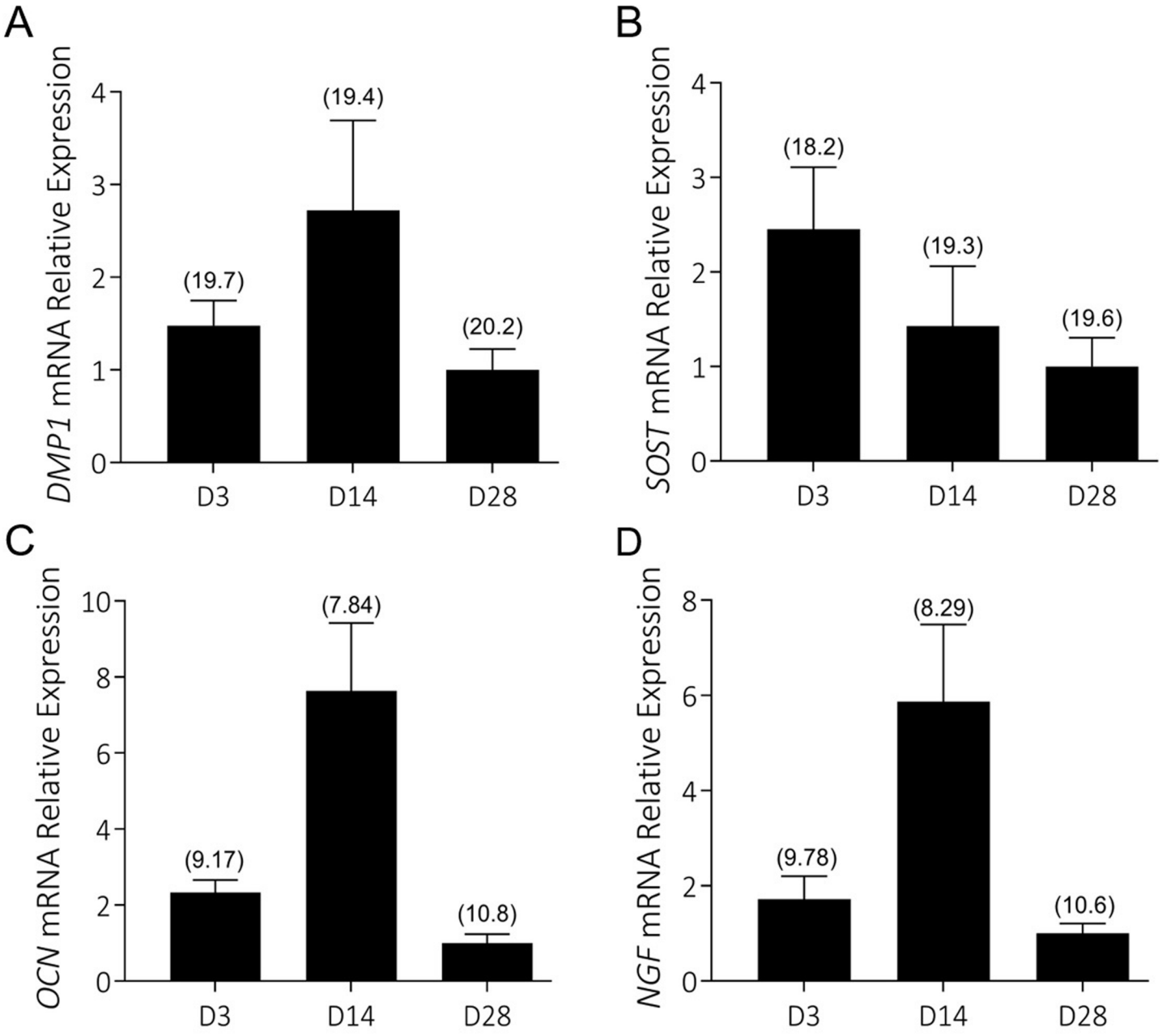

Fig 1. Human differentiating KOA osteoblast/osteocyte cultures express NGF: Cells from 3 KOA patients were cultured under pro-osteogenic conditions for up to 28d, as described in Materials and Methods. Gene expression was measured by real-time RT-PCR at various timepoints for: A) *DMP1*; B) *SOST*; C) *OCN*; D) *NGF*. Data (means + standard error of the mean (SEM)) were normalised to the expression of *18S* rRNA using the $2^{-(\Delta CT)}$ method and are shown relative to the expression of each gene at the end of the time course pooled from 3 donors' cells. The mean ΔCT for each timepoint is indicated in parentheses above each histogram.

https://doi.org/10.1371/journal.pone.0222602.g001

expression of *NGF* mRNA was relatively abundant in these cultures, similar to that of *OCN*, from all donors' cells tested and mirrored that of the differentiation markers above, peaking at day 14 and declining by day 28 (Fig 1D). Furthermore, all KOA donors' cells secreted appreciable full-length NGF protein detected in the supernatant (111.9 ± 48.8 pg/ml).

NGF expression by freshly isolated human osteocytes and in human bone

To examine NGF protein expression, we optimised staining of a directly conjugated anti-NGF antibody to NCI-H266 cells (Fig 2, *top row*). NGF expression was also tested in cells obtained by sequential digestion from human KOA bone. We have published previously that fractions IV-VI obtained using this method are enriched for mature osteocytes [25]. As shown in Fig 2. (*middle row*), numerous cells in the osteocyte-enriched fractions stained brightly for NGF

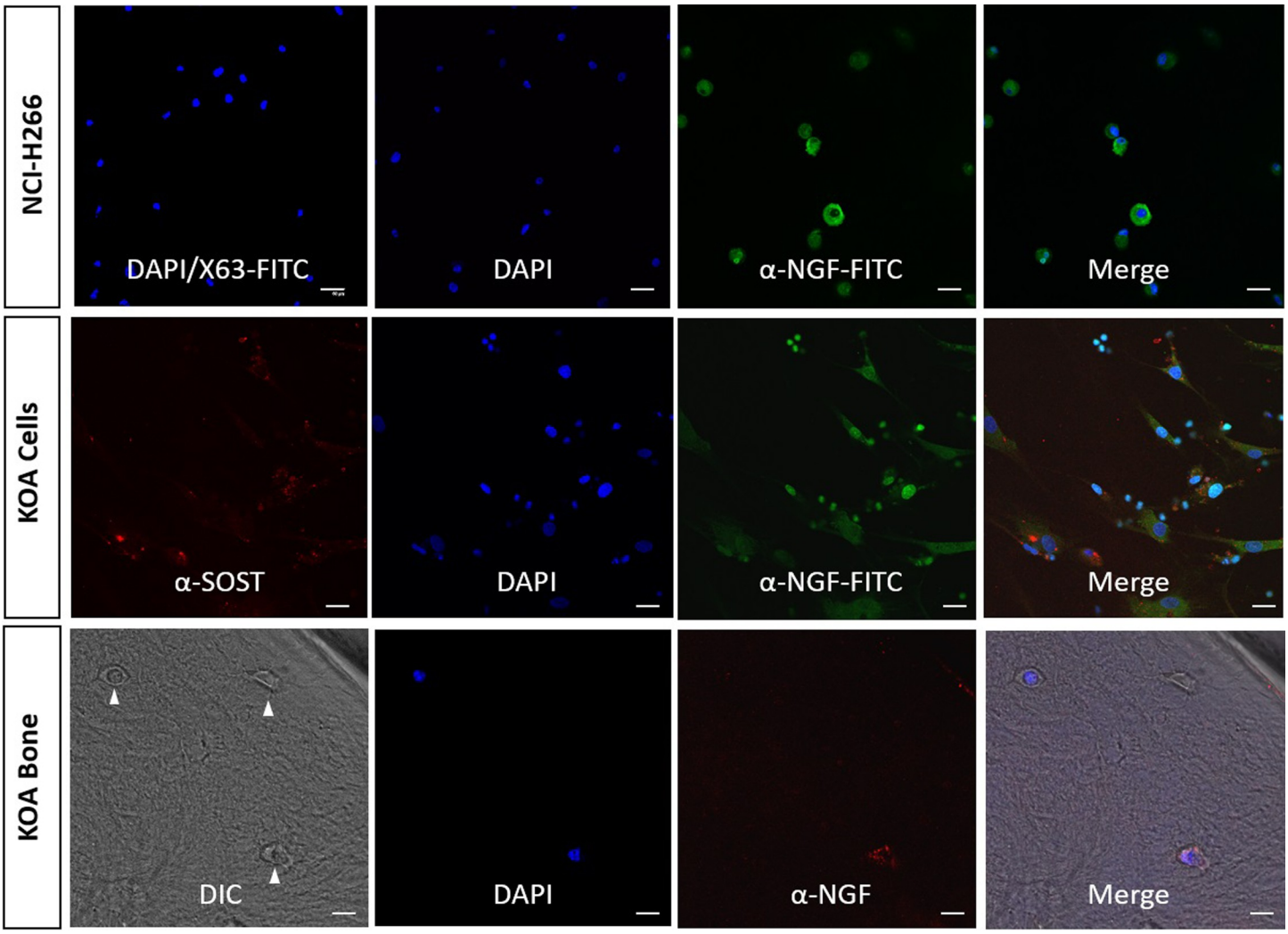

Fig 2. NGF expression in isolated human osteocytes and in KOA bone. Directly conjugated α-NGF MAb was tested against NCI-H266 cells and compared against a directly conjugated negative control antibody, X-63 (*upper row*). Fractions IV-VI of a KOA bone digest were similarly stained for NGF, and staining compared against the expression of the osteocyte marker SOST/sclerostin (*middle row*). Dual staining revealed intracellular but not co-localised staining for both NGF and SOST in these cells. Specificity of staining was confirmed using negative control IgG_1 MAb. Finally, NGF positivity was evident in osteocytes (white arrows) *in situ* in decalcified KOA bone (*bottom row*), here using unconjugated α-NGF MAb, as described in Materials and methods. Bone morphology is revealed by digitial interference contrast (DIC). In all cases nuclei were visualised by DAPI stain (blue). Scale bars represent 50 μm.

https://doi.org/10.1371/journal.pone.0222602.g002

expression and co-stained for the osteocyte marker SOST/sclerostin. Furthermore, osteocyte expression of NGF was evident in stained sections of human KOA subchondral bone (Fig 2, *bottom row*). Together with the observations in differentiated cultures above, this is the first report to our knowledge of NGF expression by human osteocytes. A previous study using a fluorescence reporter system to identify NGF expression in mouse bone, reported osteoblast but not osteocyte expression of NGF in response to mechanical loading of the ulna [3]. It is possible that the reporter system used lacked the sensitivity to detect low levels of NGF, or that the difference observed is due to interspecies, relative age, skeletal site, stimulus (mechanical rather than pro-inflammatory), as well as the influence of osteoarthritis on osteocyte expression.

In an attempt to examine regulation of NGF protein expression in freshly isolated KOA osteocyte-like cells, they were treated with either rhTNF-α, PPS or a combination of these. NGF immunostaining was detected in all cases although cells exposed to rhTNF-α alone and PPS alone had qualitatively greater NGF expression than control, and cells treated with a combination of rhTNF-α and PPS showed qualitatively less staining (Fig 3).

Due to the unpredictable yields of osteocytes from individual patients' bone, it is technically difficult to achieve identical and sufficient numbers of resulting adherent viable cells between wells for quantitative assessment of treatments. Furthermore, since NGF is a secreted protein, it is difficult to interpret intracellular levels. We therefore studied the quantitative regulation of NGF secretion into the supernatants of differentiated cultures of osteocyte-like cells.

Effect of PPS on TNF induced proNGF secretion

To examine further the effects of PPS on NGF expression, osteocyte-like cultures derived from three KOA donors were treated after 3 days pre-treatment with differing concentrations of PPS, with rhTNFα in the absence or presence of the pre-treatment concentration of PPS. Supernatants were collected 48h following treatment and subjected to ELISA analysis, as described in Materials and Methods. A study by Malerba and colleagues [9] demonstrated that the presence of the immature pro-protein form of NGF, proNGF, together with mature NGF in an experimental sample, imparted false readings in many commercially-available ELISAs for NGF, and these effects were to an unpredictable magnitude and direction. Therefore, in this study proNGF levels were measured in the treated supernatants, as described in Materials and Methods. As was observed for mature NGF protein, basal proNGF was detectable in all donor cell culture supernatants (Fig 4). Recombinant human TNFα treatment significantly increased the levels of proNGF, consistent with the induction of NGF expression in response to this pro-inflammatory stimulus in an osteoarthritic setting [7, 31]. PPS strongly suppressed basal proNGF secretion in all donors' cells assayed at all of the PPS concentrations tested, down to 1 μg/ml. Important from a therapeutic viewpoint, PPS also strongly reversed the effect of rhTNF on proNGF secretion (Fig 4), again at all concentrations tested. The concentrations of PPS chosen were based on those reported previously [24]. A study by Dawes *et al.* [32] reported plasma concentrations of PPS of approximately 1–3 μg/ml in volunteers injected subcutaneously with PPS, supportive that the effective doses used here have clinical relevance. However, the lack of a dose response in our assays can be considered a study limitation. Strikingly similar findings were made for NOF cells (S2 Fig), suggesting that NGF expression and its regulation by PPS may be a common feature of osteocytes between skeletal sites and pathologies.

Effect of PPS on TNFα-induced *NGF* mRNA expression

To examine whether the effects of PPS on NGF/proNGF expression were at the transcriptional level, we also examined *NGF* mRNA expression using real-time RT-PCR (Fig 5). Exposure to

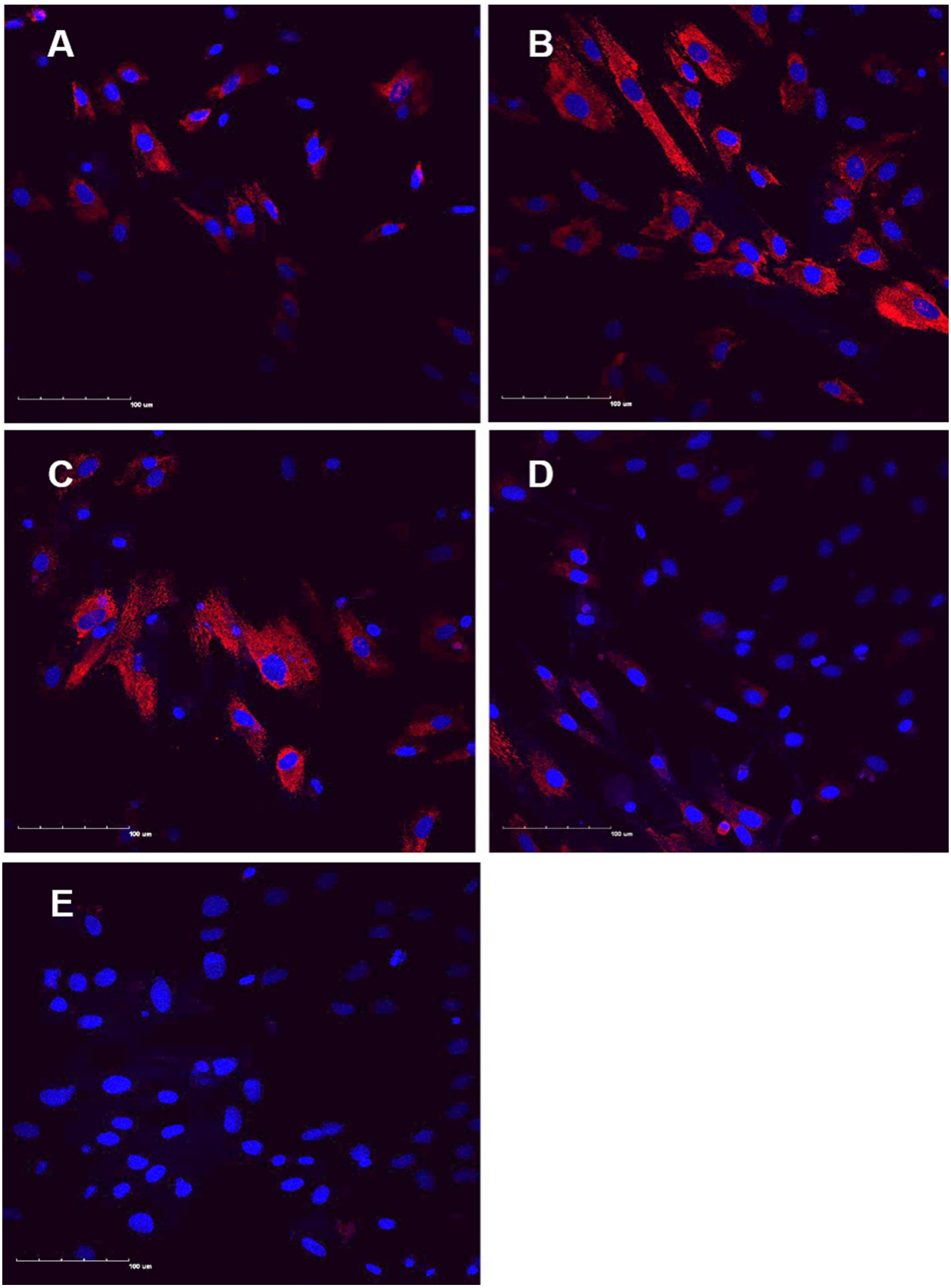
A
B
C
D
E

Fig 3. NGF expression in isolated human osteocytes. Osteocyte-enriched fractions of sequential human trabecular bone digests were cultured for 24h either untreated (A), treated with rhTNFα (B), PPS (0.5μg/ml) (C) or a combination of both (D), and then examined by confocal microscopy for NGF immunoreactivity. Control cells were also immunostained using an isotype-matched negative control primary antibody (E). Images are representative of data obtained for four individual donors cells. Scale bars in each image represent 100 μm.

https://doi.org/10.1371/journal.pone.0222602.g003

TNFα increased the relative expression of *NGF* mRNA. PPS at both 0.1 and 1 μg/ml had no apparent effect on basal *NGF* mRNA levels. However, PPS at 1 μg/ml significantly reduced NGF expression in the presence of TNFα, suggesting that at least some of the effect of PPS on osteocytes is at the transcriptional level. This is consistent with a previous report that PPS acts

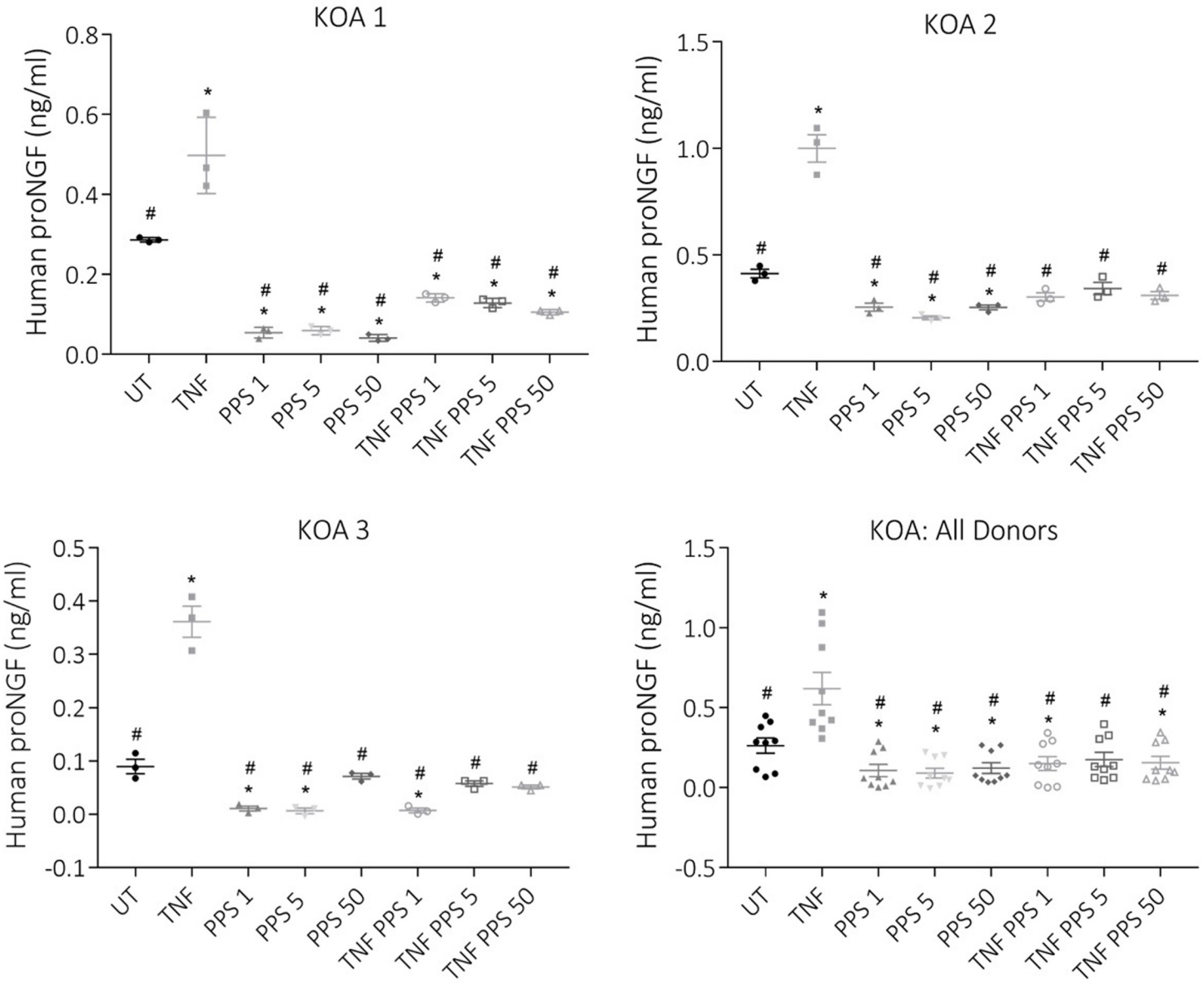

Fig 4. Human osteocyte-like cells secrete proNGF. Secretion of proNGF was tested from cultures of KOA osteocyte-like cells treated with combinations of rhTNF and PPS. Data are means + SD of supernatants harvested from triplicate wells. Significant difference to untreated control (UT) is indicated by *($p < 0.05$); significant difference to rhTNF treated cultures is indicated by #($p < 0.05$).

https://doi.org/10.1371/journal.pone.0222602.g004

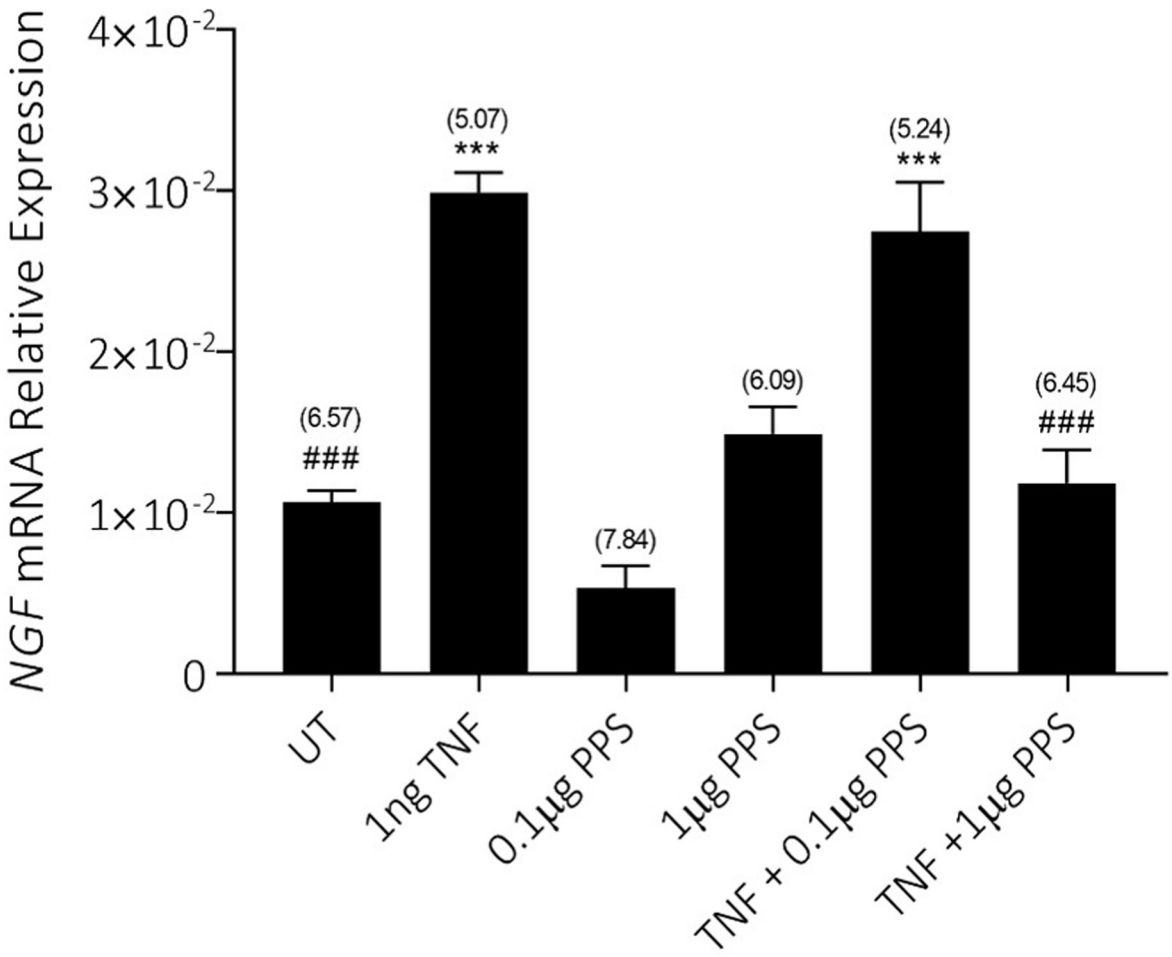

Fig 5. Effects of combinations of rhTNF and PPS on *NGF* gene expression in osteocyte-like cultures. Human differentiated osteocyte-like cultures were either untreated or pretreated with PPS (0.1 or 1.0 μg/ml) for 24h, then with or without rhTNFα (1 ng/ml) for a further 48h, and then real-time RT-PCR was performed for *NGF* mRNA. Data are mean + SD of triplicate real-time RT-PCR reactions normalised to the mRNA expression of the housekeeping gene *ACTB*.

https://doi.org/10.1371/journal.pone.0222602.g005

as a transcriptional inhibitor of intracellular signalling pathways elicited by TNFα/TNF receptor signalling [13].

This finding is consistent with the protein expression data and supports the hypothesis that PPS reverses the effects of proinflammatory mediators in KOA on the expression of mediators of pain. The expression by osteocytes of two of the known receptors for NGF was also examined by RT-PCR as well as immunohistochemistry. The expression of the high affinity receptor tropomyosin receptor kinase A (TrkA) was not detectable by RT-PCR in any donor's cells, consistent with a complete lack of signal by immunostaining/confocal microscopy (S3 Fig). The lack of expression of TrkA by human osteocytes is consistent with the findings of Castaneda-Corral *et al*., who reported that only neurons expressed detectable levels of this protein in mouse bone [33]. Very low levels of the NGF receptor *P75NTR* mRNA were however detected, although there was sporadic detection across the samples tested; as for TRKA, no detectable immunostaining for this molecule was observed (**S3 Fig**). These observations support the concept that NGF expression by osteocytes acts in a paracrine manner in the bone, with the most likely target cell being bone sensory neurons.

Conclusions

This study shows for the first time the effects of PPS on human primary osteocytes isolated from the subchondral bone in patients with osteoarthritis of the knee. It is also the first demonstration of the production and secretion of NGF/proNGF by this cell type. PPS inhibited basal and TNFα-induced levels of proNGF secretion and TNFα induced *NGF* mRNA expression. PPS also inhibited TNFα-induced levels of the collagenase MMP-13. Together, this provides evidence that PPS may act at multiple levels to suppress the release of NGF and potentially other pain mediators in the subchondral bone, to ameliorate pain associated with knee osteoarthritis.

Supporting information

S1 Fig. Mineralising properties of KOA and NOF osteoblast/osteocyte-like cultures. Cultures of KOA or NOF cells were cultured under osteogenic differentiating conditions and stained at 3d, 14d and 28d for mineral deposition using the Alizarin Red technique, as described in Materials and Methods. Calcium deposition is indicated by red staining. Representative wells are shown for each donors's cells at each time point.
(PPTX)

S2 Fig. Human NOF osteocyte-like cells secrete proNGF. Secretion of proNGF was tested from cultures of NOF osteocyte-like cells treated with combinations of rhTNF and PPS. Data are means + SD of supernatants harvested from triplicate wells. Significant difference to untreated control (UT) is indicated by $^{*}(p < 0.05)$; significant difference to rhTNF treated cultures is indicated by #($p < 0.05$).
(PPTX)

S3 Fig. Immunostaining of KOA-derived osteocytes for TrkA and P-75. Day 28 differentiated human primary osteocyte-like cultures were immunostained and examined by confocal microscopy, as described in Materials and methods, for (A) TrkA (B) P-75 or were stained with an isotype control monoclonal antibody (C). Scale bars in each case represent 50 μm.
(PPTX)

Acknowledgments

The authors thank the nursing and surgical staff of the Orthopaedic and Trauma Services of the Royal Adelaide Hospital and the Calvary Wakefield Hospital for the provision of patient samples. The authors also thank Dr. Sonja Klebe (Flinders University) for the kind provision of NCI-H266 cells.

This study was funded by a research grant from Paradigm Biopharmaceuticals Ltd (https://paradigmbiopharma.com/) and from a Project Grant awarded to GJA from the National Health and Medical Research Council of Australia (NHMRC) (Project ID1106029). CJMS was supported by an Australian Postgraduate Award scholarship. GJA is an NHMRC Senior Research Fellow. Paradigm Biopharmaceuticals Ltd provided additional funding in the form of salary to RK. The specific roles of these authors are articulated in the 'author contributions' section. The funders did not have any role in the study design, data collection and analysis, decision to publish, or preparation of the manuscript beyond those specified.

Author Contributions

Conceptualization: Ravi Krishnan, Gerald J. Atkins.

Data curation: Catherine J. M. Stapledon.

Formal analysis: Catherine J. M. Stapledon, Helen Tsangari, Gerald J. Atkins.

Funding acquisition: Gerald J. Atkins.

Investigation: Catherine J. M. Stapledon, Plinio Hurtado.

Methodology: Helen Tsangari, Plinio Hurtado, Gerald J. Atkins.

Resources: Lucian B. Solomon, David G. Campbell, Ravi Krishnan.

Supervision: Plinio Hurtado, Gerald J. Atkins.

Writing – original draft: Gerald J. Atkins.

Writing – review & editing: Catherine J. M. Stapledon, Lucian B. Solomon, David G. Campbell, Plinio Hurtado, Ravi Krishnan, Gerald J. Atkins.

References

1. Chevalier X, Eymard F, Richette P. Biologic agents in osteoarthritis: hopes and disappointments. Nat Rev Rheumatol. 2013; 9(7):400–10. Epub 2013/04/03. https://doi.org/10.1038/nrrheum.2013.44 PMID: 23545735.
2. Ayers DC, Li W, Harrold L, Allison J, Franklin PD. Preoperative pain and function profiles reflect consistent TKA patient selection among US surgeons. Clin Orthop Relat Res. 2015; 473(1):76–81. Epub 2014/06/25. https://doi.org/10.1007/s11999-014-3716-5 PMID: 24957788; PubMed Central PMCID: PMC4390921.
3. Tomlinson RE, Li Z, Li Z, Minichiello L, Riddle RC, Venkatesan A, et al. NGF-TrkA signaling in sensory nerves is required for skeletal adaptation to mechanical loads in mice. Proc Natl Acad Sci U S A. 2017; 114(18):E3632–E41. Epub 2017/04/19. https://doi.org/10.1073/pnas.1701054114 PMID: 28416686; PubMed Central PMCID: PMC5422802.
4. Lane NE, Schnitzer TJ, Birbara CA, Mokhtarani M, Shelton DL, Smith MD, et al. Tanezumab for the treatment of pain from osteoarthritis of the knee. N Engl J Med. 2010; 363(16):1521–31. Epub 2010/10/15. https://doi.org/10.1056/NEJMoa0901510 PMID: 20942668.
5. Schnitzer TJ, Ekman EF, Spierings EL, Greenberg HS, Smith MD, Brown MT, et al. Efficacy and safety of tanezumab monotherapy or combined with non-steroidal anti-inflammatory drugs in the treatment of knee or hip osteoarthritis pain. Ann Rheum Dis. 2015; 74(6):1202–11. Epub 2014/03/15. https://doi.org/10.1136/annrheumdis-2013-204905 PMID: 24625625.
6. Ekman EF, Gimbel JS, Bello AE, Smith MD, Keller DS, Annis KM, et al. Efficacy and safety of intravenous tanezumab for the symptomatic treatment of osteoarthritis: 2 randomized controlled trials versus naproxen. J Rheumatol. 2014; 41(11):2249–59. Epub 2014/10/03. https://doi.org/10.3899/jrheum.131294 PMID: 25274899.
7. Takano S, Uchida K, Miyagi M, Inoue G, Fujimaki H, Aikawa J, et al. Nerve Growth Factor Regulation by TNF-alpha and IL-1beta in Synovial Macrophages and Fibroblasts in Osteoarthritic Mice. J Immunol Res. 2016; 2016:5706359. Epub 2016/09/17. https://doi.org/10.1155/2016/5706359 PMID: 27635406; PubMed Central PMCID: PMC5007361.
8. Bradshaw RA, Pundavela J, Biarc J, Chalkley RJ, Burlingame AL, Hondermarck H. NGF and ProNGF: Regulation of neuronal and neoplastic responses through receptor signaling. Adv Biol Regul. 2015; 58:16–27. Epub 2014/12/11. https://doi.org/10.1016/j.jbior.2014.11.003 PMID: 25491371; PubMed Central PMCID: PMC4426037.
9. Malerba F, Paoletti F, Cattaneo A. NGF and proNGF Reciprocal Interference in Immunoassays: Open Questions, Criticalities, and Ways Forward. Front Mol Neurosci. 2016; 9:63. Epub 2016/08/19. https://doi.org/10.3389/fnmol.2016.00063 PMID: 27536217; PubMed Central PMCID: PMC4971159.
10. Giusto LL, Zahner PM, Shoskes DA. An evaluation of the pharmacotherapy for interstitial cystitis. Expert Opin Pharmacother. 2018; 19(10):1097–108. Epub 2018/07/05. https://doi.org/10.1080/14656566.2018.1491968 PMID: 29972328.
11. Sampson MJ, Kabbani M, Krishnan R, Nganga M, Theodoulou A, Krishnan J. Improved clinical outcome measures of knee pain and function with concurrent resolution of subchondral Bone Marrow Edema Lesion and joint effusion in an osteoarthritic patient following Pentosan Polysulphate Sodium treatment: a case report. BMC Musculoskelet Disord. 2017; 18(1):396. Epub 2017/09/14. https://doi.org/10.1186/s12891-017-1754-3 PMID: 28899386; PubMed Central PMCID: PMC5596862.

12. Kumagai K, Shirabe S, Miyata N, Murata M, Yamauchi A, Kataoka Y, et al. Sodium pentosan polysulfate resulted in cartilage improvement in knee osteoarthritis—an open clinical trial. (1472–6904 (Electronic)).
13. Sunaga T, Oh N, Hosoya K, Takagi S, Okumura M. Inhibitory effects of pentosan polysulfate sodium on MAP-kinase pathway and NF-kappaB nuclear translocation in canine chondrocytes in vitro. The Journal of veterinary medical science / the Japanese Society of Veterinary Science. 2012; 74(6):707–11. Epub 2012/01/05. https://doi.org/10.1292/jvms.11-0511 PMID: 22214865.
14. Bwalya EC, Kim S, Fang J, Wijekoon HMS, Hosoya K, Okumura M. Pentosan polysulfate inhibits IL-1beta-induced iNOS, c-Jun and HIF-1alpha upregulation in canine articular chondrocytes. PLoS One. 2017; 12(5):e0177144. Epub 2017/05/05. https://doi.org/10.1371/journal.pone.0177144 PMID: 28472120; PubMed Central PMCID: PMC5417682.
15. Atkins GJ, Findlay DM. Osteocyte regulation of bone mineral: a little give and take. Osteoporos Int. 2012; 23(8):2067–79. Epub 2012/02/04. https://doi.org/10.1007/s00198-012-1915-z PMID: 22302104.
16. Prideaux M, Findlay DM, Atkins GJ. Osteocytes: The master cells in bone remodelling. Curr Opin Pharmacol. 2016; 28:24–30. https://doi.org/10.1016/j.coph.2016.02.003 PMID: 26927500.
17. Ormsby RT, Cantley M, Kogawa M, Solomon LB, Haynes DR, Findlay DM, et al. Evidence that osteocyte perilacunar remodelling contributes to polyethylene wear particle induced osteolysis. Acta Biomater. 2016; 33:242–51. Epub 2016/01/23. https://doi.org/10.1016/j.actbio.2016.01.016 PMID: 26796208.
18. Yang D, Wijenayaka AR, Solomon LB, Pederson SM, Findlay DM, Kidd SP, et al. Novel Insights into Staphylococcus aureus Deep Bone Infections: the Involvement of Osteocytes. MBio. 2018; 9(2). Epub 2018/04/25. https://doi.org/10.1128/mBio.00415-18 PMID: 29691335; PubMed Central PMCID: PMC5915738.
19. Atkins GJ, Rowe PS, Lim HP, Welldon KJ, Ormsby R, Wijenayaka AR, et al. Sclerostin is a locally acting regulator of late-osteoblast/preosteocyte differentiation and regulates mineralization through a MEPE-ASARM-dependent mechanism. J Bone Miner Res. 2011; 26(7):1425–36. Epub 2011/02/12. https://doi.org/10.1002/jbmr.345 PMID: 21312267; PubMed Central PMCID: PMC3358926.
20. Atkins GJ, Welldon KJ, Wijenayaka AR, Bonewald LF, Findlay DM. Vitamin K promotes mineralization, osteoblast-to-osteocyte transition, and an anticatabolic phenotype by {gamma}-carboxylation-dependent and -independent mechanisms. Am J Physiol Cell Physiol. 2009; 297(6):C1358–67. Epub 2009/08/14. https://doi.org/10.1152/ajpcell.00216.2009 PMID: 19675304.
21. Kogawa M, Wijenayaka AR, Ormsby RT, Thomas GP, Anderson PH, Bonewald LF, et al. Sclerostin Regulates Release of Bone Mineral by Osteocytes by Induction of Carbonic Anhydrase 2. J Bone Miner Res. 2013; 28(12):2436–48. Epub 2013/06/06. https://doi.org/10.1002/jbmr.2003 PMID: 23737439.
22. Kumarasinghe DD, Sullivan T, Kuliwaba JS, Fazzalari NL, Atkins GJ. Evidence for the dysregulated expression of TWIST1, TGFβ1 and SMAD3 in differentiating osteoblasts from primary hip osteoarthritis patients. Osteoarthritis & Cartilage. 2012; 20:1357–66.
23. Wijenayaka AR, Kogawa M, Lim HP, Bonewald LF, Findlay DM, Atkins GJ. Sclerostin stimulates osteocyte support of osteoclast activity by a RANKL-dependent pathway. PLoS One. 2011; 6(10):e25900. https://doi.org/10.1371/journal.pone.0025900 PMID: 21991382; PubMed Central PMCID: PMC3186800.
24. Ghosh P, Wu J, Shimmon S, Zannettino AC, Gronthos S, Itescu S. Pentosan polysulfate promotes proliferation and chondrogenic differentiation of adult human bone marrow-derived mesenchymal precursor cells. Arthritis Res Ther. 2010; 12(1):R28. Epub 2010/02/20. https://doi.org/10.1186/ar2935 PMID: 20167057; PubMed Central PMCID: PMC2875662.
25. Prideaux M, Schutz C, Wijenayaka AR, Findlay DM, Campbell DG, Solomon LB, et al. Isolation of osteocytes from human trabecular bone. Bone. 2016; 88:64–72. Epub 2016/04/26. https://doi.org/10.1016/j.bone.2016.04.017 PMID: 27109824.
26. Iannone F, De Bari C, Dell'Accio F, Covelli M, Patella V, Lo Bianco G, et al. Increased expression of nerve growth factor (NGF) and high affinity NGF receptor (p140 TrkA) in human osteoarthritic chondrocytes. Rheumatology (Oxford). 2002; 41(12):1413–8. Epub 2002/12/07. https://doi.org/10.1093/rheumatology/41.12.1413 PMID: 12468822.
27. Zhang J, Wang LS, Ye SL, Luo P, Wang BL. Blockage of tropomyosin receptor kinase a (TrkA) enhances chemo-sensitivity in breast cancer cells and inhibits metastasis in vivo. Int J Clin Exp Med. 2015; 8(1):634–41. Epub 2015/03/19. doi: Not available. PMID: 25785038; PubMed Central PMCID: PMC4358493.
28. Rouillard AD, Gundersen GW, Fernandez NF, Wang Z, Monteiro CD, McDermott MG, et al. The harmonizome: a collection of processed datasets gathered to serve and mine knowledge about genes and proteins. LID—10.1093/database/baw100 [doi] LID—baw100 [pii]. (1758–0463 (Electronic)).
29. Atkins GJ, Welldon KJ, Halbout P, Findlay DM. Strontium ranelate treatment of human primary osteoblasts promotes an osteocyte-like phenotype while eliciting an osteoprotegerin response. Osteoporos Int. 2009; 20(4):653–64. https://doi.org/10.1007/s00198-008-0728-6 PMID: 18763010.

30. Bonewald LF. The amazing osteocyte. J Bone Miner Res. 2011; 26(2):229–38. Epub 2011/01/22. https://doi.org/10.1002/jbmr.320 PMID: 21254230.

31. Manni L, Aloe L. Role of IL-1 beta and TNF-alpha in the regulation of NGF in experimentally induced arthritis in mice. Rheumatol Int. 1998; 18(3):97–102. Epub 1998/12/02. PMID: 9833249.

32. Dawes J Fau—Prowse CV, Prowse Cv Fau—Pepper DS, Pepper DS. Absorption of heparin, LMW heparin and SP54 after subcutaneous injection, assessed by competitive binding assay. Thrombosis Research. 1986; 44(0049–3848 (Print)):683–93. https://doi.org/10.1016/0049-3848(86)90169-6 PMID: 2433788

33. Castaneda-Corral G, Jimenez-Andrade JM, Bloom AP, Taylor RN, Mantyh WG, Kaczmarska MJ, et al. The majority of myelinated and unmyelinated sensory nerve fibers that innervate bone express the tropomyosin receptor kinase A. Neuroscience. 2011; 178:196–207. Epub 2011/02/01. https://doi.org/10.1016/j.neuroscience.2011.01.039 PMID: 21277945; PubMed Central PMCID: PMC3078085.

Chapter 6

Concluding Remarks

The development of degenerative disorders concomitant with increasing life expectancy in the Western world has become an emerging issue in Australia over the past 30 years. There are currently no cures for diseases of ageing, such as Alzheimer's disease (AD) and osteoporosis (OP), only treatments that may variably halt the progression of the disease for an unknown length of time. It is imperative that further investigation into the effects of the amyloid beta peptide in the bone be undertaken to determine whether osteoporosis could be an indicator for the development of Alzheimer's disease or vice versa. Prior to the commencement of this PhD, expression of full-length APP in the bone or by bone cells was not well documented in the literature, nor were the effects of the neurotoxic amyloid beta peptide on human bone cells.

The overarching hypothesis investigated in this thesis was based on the idea that neurotrophic factors *APP, APLP2* and *NGF* were not only be expressed by the osteocyte and in the bone microenvironment, but that they could also be stimulated by known regulators of bone remodelling such as 1,25D, PTH and TNF-α. In Chapter 2, the conventional adjunct chapter, it was established that *APP* and *APLP2* were expressed at the mRNA level in models of osteoblastic differentiation (SaOS2, NHBC and NOF). The patterns of expression of *APP* and *APLP2* mRNA in each different bone cell culture model differed at different stages of the osteoblast to osteocyte differentiation process as well as under the stimulation of 50 nM PTH, 1 nM 1,25D and 10 nM 1,25D. As osteocytes have previously been shown to respond to TNF-α in vitro by increasing the pro-inflammatory cytokine, IL-6, in a dose-dependent manner, *APP* mRNA expression was

investigated in this context and displayed the same expression pattern as IL-6. The study whereby full-length APP protein expression was assessed in isolated osteocytes from bone biopsies showed that under normal conditions APP is produced by these cells and detectable by confocal microscopy, and that it is somewhat upregulated by stimulation with TNF-α. Further investigation into APP function in bone remodelling was examined through the study of the effects of App knockout in a murine model (APPKO). This model determined a function for *APP* in endocortical remodelling as there was a marked reduction in the endosteal perimeter of the femora in both male and female knockout mice. This finding gave rise to the idea that under physiological conditions there may be a role for APP in normal skeletal development, but under pathological conditions, like those seen in neurodegenerative disease, it can be detrimental.

Following the establishment of *APP* and *APLP2* in normal bone cell cultures and isolated osteocytes, it was then important to determine the levels of these genes in the context of bone pathology. In Chapter 3, a large-scale analysis was conducted to determine the gene expression profile of a cohort of neck of femur fracture patients. Comorbidities, blood markers (25(OH)vitamin D and creatinine) and genes involved in the CNS (*APP, APLP2, BACE1* and *NGF*) and in bone remodelling (*CYP27B1, DMP1, OCN, OPG, RANKL, RANKL:OPG, SOST* and *TRAP*), were analysed to determine relationships between the aforementioned markers and femoral structural parameters. The findings of this study indicated that there are a number of never before identified associations between neurotrophic factors and markers of bone remodelling, which may provide a new potential avenue for drug targets to reduce bone loss in the ageing population in the future. Further investigation into these findings at the protein level, as well as targeted drug studies, would need to be undertaken to establish further functional relationships between these markers.

The largest study presented in this thesis constitutes Chapter 4. This study tied together findings in Chapters 2 and 3, through the implementation of human samples, cell culture models and a murine model. The findings of this chapter revealed that synthetic amyloid beta peptides have the ability to induce osteocyte cell death in vitro, a phenomenon that has not been reported previously. It is well documented that damage to the osteocyte network can initiate apoptosis resulting in an increase in *RANKL*, which can stimulate resorption, another observation that was made in this study. The parallel increase in osteocytic osteolysis marker *MMP13* also supported this observation. This was supported by the use of the $App^{NL\text{-}G\text{-}F/NL\text{-}G\text{-}F}$ knock-in mouse model of familial AD, where we saw a significant age-related induction of an osteoporotic-like phenotype, indicated by a reduction in cancellous bone volume in knock-in mice when compared to WT littermate controls. Amyloid beta peptides were also discovered in the bone marrow of the knock-in mice, suggesting a potential for these neurotoxic peptides to act peripherally on bone cells, inducing cell damage and death. These findings further support the bone and brain link and also introduce a new player (Aβ) to the bone world as a potential therapeutic target for bone loss not only in AD but also in generalised ageing.

The final study presented in Chapter 5, was a novel investigation into the repurposing of pentosan polysulphate sodium (PPS) for the treatment of pain associated with knee osteoarthritis. The results of this study first revealed that NGF and its pro-protein form (pro-NGF) was not only expressed by osteocytes isolated from the bone of patients with knee OA, but also that when stimulated with TNF-α, expression could be suppressed by PPS. This was the first time demonstrating that neurotrophic mediators of pain (NGF and pro-NGF) were expressed by osteocytes and could be suppressed by this drug, providing hope for the treatment of pain associated with knee OA in the future. This work also has

implications for other sites of osteoarthritis and other bone pain related pathologies, such as rheumatoid arthritis and bone cancers.

In order to further build upon the work conducted in this thesis, a number of limitations need to be addressed. The work conducted in Chapter 2 requires repetition to ensure that the results can be replicated across each osteoblast to osteocyte differentiation model and to confirm patterns of expression across the differentiation process. The immunostaining of isolated human osteocytes could also be repeated using known markers of osteocytes such as Sclerostin or DMP1 to confirm that the isolated cells are mainly an osteocyte population. Furthermore, to account for possible extra-skeletal effects of the global *APP* knockout, which has been shown in other studies to produce unwanted effects on all tissue types due to its ubiquitous expression, a conditional osteocyte-specific knock-out of APP could be conducted, for example using the Cre/Lox approach and the osteocyte specific osteocalcin-Cre or Dmp1-Cre models. To further improve upon the NOF cohort study, increased participant numbers are required together with a more rigorous assessment and classification of cognition states at the time of recruitment, to allow examination of the relationships between fragility fractures of the hip with defined states of cognitive impairment (including AD). Inclusion of a non-fracture control cohort would also be informative and for this patients undergoing elective total hip replacement surgery for osteoarthritis could be recruited. This may not only better power the study but also assist in the clinical diagnosing of dementia within the NOF population. A co-culture system including osteocytes and osteoclasts would provide an interesting way to investigate the effects of amyloid beta peptides in a more bone-like environment in vitro. This would help to further understand the effects of osteocyte apoptosis induced by amyloid beta on osteoclast activity. As well as this, the use of BACE-1 inhibitors in this model would also

be of great interest, to determine if locally acting drugs could inhibit osteocyte cell death, like that seen in Chapter 5.

In conclusion, studies presented in this study support the idea that there is a link between the bone and the brain by virtue of the expression of neurotrophic factors APP, APLP2 and NGF. This idea has been explored through the implementation of cell culture models, murine models of gene knockout as well as conditional gene knock-in and primary human tissues, making for strong supporting evidence for this link existing. The combination of these studies provides a new insight into the regulation of CNS-related proteins in the bone as well as their ability to impact on normal bone cell function.

References

1. Florencio-Silva R, Sasso GR, Sasso-Cerri E, Simoes MJ, Cerri PS. Biology of Bone Tissue: Structure, Function, and Factors That Influence Bone Cells. Biomed Res Int. 2015;2015:421746.

2. Buckwalter JA, Glimcher MJ, Cooper RR, Recker R. Bone biology. I: Structure, blood supply, cells, matrix, and mineralization. Instr Course Lect. 1996;45:371-86.

3. Atkins GJ, Rowe PS, Lim HP, Welldon KJ, Ormsby R, Wijenayaka AR, et al. Sclerostin is a locally acting regulator of late-osteoblast/preosteocyte differentiation and regulates mineralization through a MEPE-ASARM-dependent mechanism. J Bone Miner Res. 2011;26(7):1425-36.

4. Bonewald LF. The amazing osteocyte. J Bone Miner Res. 2011;26(2):229-38.

5. Atkins GJ, Findlay DM. Osteocyte regulation of bone mineral: a little give and take. Osteoporos Int. 2012;23(8):2067-79.

6. Prideaux M, Findlay DM, Atkins GJ. Osteocytes: The master cells in bone remodelling. Curr Opin Pharmacol. 2016;28:24-30.

7. Gamsjaeger S, Masic A, Roschger P, Kazanci M, Dunlop JW, Klaushofer K, et al. Cortical bone composition and orientation as a function of animal and tissue age in mice by Raman spectroscopy. Bone. 2010;47(2):392-9.

8. Ito M, Koga A, Nishida A, Shiraishi A, Saito M, Hayashi K. Evaluation of mechanical properties of trabecular and cortical bone. Adv Exp Med Biol. 2001;496:47-56.

9. Li J, Bao Q, Chen S, Liu H, Feng J, Qin H, et al. Different bone remodeling levels of trabecular and cortical bone in response to changes in Wnt/beta-catenin signaling in mice. J Orthop Res. 2017;35(4):812-9.

10. Buckwalter JA, Glimcher MJ, Cooper RR, Recker R. Bone biology. II: Formation, form, modeling, remodeling, and regulation of cell function. Instr Course Lect. 1996;45:387-99.

11. Parfitt AM. The bone remodeling compartment: a circulatory function for bone lining cells. J Bone Miner Res. 2001;16(9):1583-5.

12. Mizoguchi T, Muto A, Udagawa N, Arai A, Yamashita T, Hosoya A, et al. Identification of cell cycle-arrested quiescent osteoclast precursors in vivo. J Cell Biol. 2009;184(4):541-54.

13. Teitelbaum SL. Bone resorption by osteoclasts. Science. 2000;289(5484):1504-8.

14. Teti A. Bone development: overview of bone cells and signaling. Curr Osteoporos Rep. 2011;9(4):264-73.

15. Ross FP, Teitelbaum SL. alphavbeta3 and macrophage colony-stimulating factor: partners in osteoclast biology. Immunol Rev. 2005;208:88-105.

16. Quinn JM, Elliott J, Gillespie MT, Martin TJ. A combination of osteoclast differentiation factor and macrophage-colony stimulating factor is sufficient for both human and mouse osteoclast formation in vitro. Endocrinology. 1998;139(10):4424-7.

17. Fan X, Biskobing DM, Fan D, Hofstetter W, Rubin J. Macrophage colony stimulating factor down-regulates MCSF-receptor expression and entry of progenitors into the osteoclast lineage. J Bone Miner Res. 1997;12(9):1387-95.

18. Silva I, Branco JC. Rank/Rankl/opg: literature review. Acta Reumatol Port. 2011;36(3):209-18.

19. Yasuda H, Shima N, Nakagawa N, Yamaguchi K, Kinosaki M, Mochizuki S, et al. Osteoclast differentiation factor is a ligand for osteoprotegerin/osteoclastogenesis-inhibitory factor and is identical to TRANCE/RANKL. Proc Natl Acad Sci U S A. 1998;95(7):3597-602.

20. Kong YY, Yoshida H, Sarosi I, Tan HL, Timms E, Capparelli C, et al. OPGL is a key regulator of osteoclastogenesis, lymphocyte development and lymph-node organogenesis. Nature. 1999;397(6717):315-23.

21. Simonet WS, Lacey DL, Dunstan CR, Kelley M, Chang MS, Luthy R, et al. Osteoprotegerin: a novel secreted protein involved in the regulation of bone density. Cell. 1997;89(2):309-19.

22. Wijenayaka AR, Kogawa M, Lim HP, Bonewald LF, Findlay DM, Atkins GJ. Sclerostin Stimulates Osteocyte Support of Osteoclast Activity by a RANKL-Dependent Pathway. PLoS One. 2011;6(10):e25900.

23. Takahashi N, Akatsu T, Udagawa N, Sasaki T, Yamaguchi A, Moseley JM, et al. Osteoblastic cells are involved in osteoclast formation. Endocrinology. 1988;123(5):2600-2.

24. Hecht M, von Metzler I, Sack K, Kaiser M, Sezer O. Interactions of myeloma cells with osteoclasts promote tumour expansion and bone degradation through activation of a complex signalling network and upregulation of cathepsin K, matrix metalloproteinases (MMPs) and urokinase plasminogen activator (uPA). Exp Cell Res. 2008;314(5):1082-93.

25. O'Brien CA, Nakashima T, Takayanagi H. Osteocyte control of osteoclastogenesis. Bone. 2013;54(2):258-63.

26. Kogawa M, Findlay DM, Anderson PH, Atkins GJ. Modulation of osteoclastic migration by metabolism of 25OH-vitamin D3. J Steroid Biochem Mol Biol. 2013;136:59-61.

27. Kogawa M, Anderson PH, Findlay DM, Morris HA, Atkins GJ. The metabolism of 25-(OH)vitamin D3 by osteoclasts and their precursors regulates the differentiation of osteoclasts. J Steroid Biochem Mol Biol. 2010;121(1-2):277-80.

28. Hauschka PV, Lian JB, Cole DE, Gundberg CM. Osteocalcin and matrix Gla protein: vitamin K-dependent proteins in bone. Physiol Rev. 1989;69(3):990-1047.

29. Abu-Amer Y, Erdmann J, Alexopoulou L, Kollias G, Ross FP, Teitelbaum SL. Tumor necrosis factor receptors types 1 and 2 differentially regulate osteoclastogenesis. J Biol Chem. 2000;275(35):27307-10.

30. Azuma Y, Kaji K, Katogi R, Takeshita S, Kudo A. Tumor necrosis factor-alpha induces differentiation of and bone resorption by osteoclasts. J Biol Chem. 2000;275(7):4858-64.

31. Teitelbaum SL. Osteoclasts, integrins, and osteoporosis. J Bone Miner Metab. 2000;18(6):344-9.

32. Muglia MA, Volpi G, Remaggi F, Cane V, Palazzini S, Zaffe D, et al. Activity of osteoclasts and osteocytes in compact human bone at various ages, both with and without osteoporosis. Ital J Orthop Traumatol. 1982;8(1):117-25.

33. Sambandam Y, Sundaram K, Saigusa T, Balasubramanian S, Reddy SV. NFAM1 signaling enhances osteoclast formation and bone resorption activity in Paget's disease of bone. Bone. 2017;101:236-44.

34. Coudert AE, de Vernejoul MC, Muraca M, Del Fattore A. Osteopetrosis and its relevance for the discovery of new functions associated with the skeleton. Int J Endocrinol. 2015;2015:372156.

35. Long F. Building strong bones: molecular regulation of the osteoblast lineage. Nat Rev Mol Cell Biol. 2011;13(1):27-38.

36. Atkins GJ, Bouralexis S, Haynes DR, Graves SE, Geary SM, Evdokiou A, et al. Osteoprotegerin inhibits osteoclast formation and bone resorbing activity in giant cell tumors of bone. Bone. 2001;28(4):370-7.

37. Xiong J, Onal M, Jilka RL, Weinstein RS, Manolagas SC, O'Brien CA. Matrix-embedded cells control osteoclast formation. Nat Med. 2011;17(10):1235-41.

38. Harada S, Rodan GA. Control of osteoblast function and regulation of bone mass. Nature. 2003;423(6937):349-55.

39. Han L, Zhang X, Tang G. [Indian Hedgehog signaling is involved in the stretch induced proliferation of osteoblast]. Hua Xi Kou Qiang Yi Xue Za Zhi. 2012;30(3):234-8.

40. Honjo T. The shortest path from the surface to the nucleus: RBP-J kappa/Su(H) transcription factor. Genes Cells. 1996;1(1):1-9.

41. Franz-Odendaal TA, Hall BK, Witten PE. Buried alive: how osteoblasts become osteocytes. Dev Dyn. 2006;235(1):176-90.

42. Alvarenga EC, Rodrigues R, Caricati-Neto A, Silva-Filho FC, Paredes-Gamero EJ, Ferreira AT. Low-intensity pulsed ultrasound-dependent osteoblast proliferation occurs by via activation of the P2Y receptor: role of the P2Y1 receptor. Bone. 2010;46(2):355-62.

43. Hock JM, Krishnan V, Onyia JE, Bidwell JP, Milas J, Stanislaus D. Osteoblast apoptosis and bone turnover. J Bone Miner Res. 2001;16(6):975-84.

44. Schaffler MB, Cheung WY, Majeska R, Kennedy O. Osteocytes: master orchestrators of bone. Calcified tissue international. 2014;94(1):5-24.

45. Barragan-Adjemian C, Nicolella D, Dusevich V, Dallas MR, Eick JD, Bonewald LF. Mechanism by which MLO-A5 late osteoblasts/early osteocytes mineralize in culture: similarities with mineralization of lamellar bone. Calcif Tissue Int. 2006;79(5):340-53.

46. Dallas SL, Bonewald LF. Dynamics of the transition from osteoblast to osteocyte. Ann N Y Acad Sci. 2010;1192:437-43.

47. Civitelli R. Cell-cell communication in the osteoblast/osteocyte lineage. Arch Biochem Biophys. 2008;473(2):188-92.

48. Atkins GJ, Prideaux M, Findlay DM. Osteocytes and bone regeneration. A Tissue Regeneration Approach to Bone Repair. 2015;H. Zreiqat, V. Rosen and C. Dunstan Eds. Springer-Verlag, Berlin, Germany.

49. Chen H, Senda T, Kubo K. The osteocyte plays multiple roles in bone remodelling and mineral homeostasis. J Medical Molecular Morpholohgy. 2015.

50. Bellido T. Osteocyte-driven bone remodeling. Calcified tissue international. 2014;94(1):25-34.

51. Chen H, Senda T, Kubo KY. The osteocyte plays multiple roles in bone remodeling and mineral homeostasis. Med Mol Morphol. 2015;48(2):61-8.

52. McArdle A, Marecic O, Tevlin R, Walmsley GG, Chan CK, Longaker MT, et al. The role and regulation of osteoclasts in normal bone homeostasis and in response to injury. Plast Reconstr Surg. 2015;135(3):808-16.

53. Nakashima T, Hayashi M, Fukunaga T, Kurata K, Oh-Hora M, Feng JQ, et al. Evidence for osteocyte regulation of bone homeostasis through RANKL expression. Nat Med. 2011;17(10):1231-4.

54. Xiong J, Onal M, Jilka RL, Weinstein RS, Manolagas SC, O'Brien CA. Matrix-embedded cells control osteoclast formation. Nature Medicine. 2011;17(10):1235-41.

55. Kennedy OD, Lendhey M, Mauer P, Philip A, Basta-Pljakic J, Schaffler MB. Microdamage induced by in vivo Reference Point Indentation in mice is repaired by osteocyte-apoptosis mediated remodeling. Bone. 2017;95:192-8.

56. Hemmatian H, Jalali R, Semeins CM, Hogervorst JMA, van Lenthe GH, Klein-Nulend J, et al. Mechanical Loading Differentially Affects Osteocytes in Fibulae from

Lactating Mice Compared to Osteocytes in Virgin Mice: Possible Role for Lacuna Size. Calcified tissue international. 2018;103(6):675-85.

57. Ito N, Wijenayaka AR, Prideaux M, Kogawa M, Ormsby RT, Evdokiou A, et al. Regulation of FGF23 expression in IDG-SW3 osteocytes and human bone by pro-inflammatory stimuli. Mol Cell Endocrinol. 2015;399:208-18.

58. Qing H, Ardeshirpour L, Pajevic PD, Dusevich V, Jahn K, Kato S, et al. Demonstration of osteocytic perilacunar/canalicular remodeling in mice during lactation. J Bone Miner Res. 2012;27(5):1018-29.

59. Zhao S, Zhang YK, Harris S, Ahuja SS, Bonewald LF. MLO-Y4 osteocyte-like cells support osteoclast formation and activation. J Bone Miner Res. 2002;17(11):2068-79.

60. Rachner TD, Khosla S, Hofbauer LC. Osteoporosis: now and the future. Lancet. 2011;377(9773):1276-87.

61. Kanis JA, Oden A, Johnell O, Johansson H, De Laet C, Brown J, et al. The use of clinical risk factors enhances the performance of BMD in the prediction of hip and osteoporotic fractures in men and women. Osteoporos Int. 2007;18(8):1033-46.

62. Health AIo, Welfare. Hip fracture incidence and hospitalisations in Australia 2015–16. Canberra: AIHW, 2018.

63. Center JR. Fracture Burden: What Two and a Half Decades of Dubbo Osteoporosis Epidemiology Study Data Reveal About Clinical Outcomes of Osteoporosis. Curr Osteoporos Rep. 2017;15(2):88-95.

64. Pasco JA, Mohebbi M, Holloway KL, Brennan-Olsen SL, Hyde NK, Kotowicz MA. Musculoskeletal decline and mortality: prospective data from the Geelong Osteoporosis Study. J Cachexia Sarcopenia Muscle. 2017;8(3):482-9.

65. Laine CM, Joeng KS, Campeau PM, Kiviranta R, Tarkkonen K, Grover M, et al. WNT1 mutations in early-onset osteoporosis and osteogenesis imperfecta. N Engl J Med. 2013;368(19):1809-16.

66. Riggs BL, Melton LJ, Robb RA, Camp JJ, Atkinson EJ, McDaniel L, et al. A population-based assessment of rates of bone loss at multiple skeletal sites: evidence for substantial trabecular bone loss in young adult women and men. J Bone Miner Res. 2008;23(2):205-14.

67. Eghbali-Fatourechi G, Khosla S, Sanyal A, Boyle WJ, Lacey DL, Riggs BL. Role of RANK ligand in mediating increased bone resorption in early postmenopausal women. J Clin Invest. 2003;111(8):1221-30.

68. Verdile G, Laws SM, Henley D, Ames D, Bush AI, Ellis KA, et al. Associations between gonadotropins, testosterone and beta amyloid in men at risk of Alzheimer's disease. Mol Psychiatry. 2014;19(1):69-75.

69. Ge YW, Lahiri DK. Regulation of promoter activity of the APP gene by cytokines and growth factors: implications in Alzheimer's disease. Ann N Y Acad Sci. 2002;973:463-7.

70. Sun L, Peng Y, Sharrow AC, Iqbal J, Zhang Z, Papachristou DJ, et al. FSH directly regulates bone mass. Cell. 2006;125(2):247-60.

71. Lystad RP, Cameron CM, Mitchell RJ. Mortality risk among older Australians hospitalised with hip fracture: a population-based matched cohort study. Arch Osteoporos. 2017;12(1):67.

72. Reynard LN. Analysis of genetics and DNA methylation in osteoarthritis: What have we learnt about the disease? Semin Cell Dev Biol. 2016.

73. Felson DT, Lawrence RC, Dieppe PA, Hirsch R, Helmick CG, Jordan JM, et al. Osteoarthritis: new insights. Part 1: the disease and its risk factors. Ann Intern Med. 2000;133(8):635-46.

74. Johnson VL, Hunter DJ. The epidemiology of osteoarthritis. Best Pract Res Clin Rheumatol. 2014;28(1):5-15.

75. Boyde A, Jones SJ, Aerssens J, Dequeker J. Mineral density quantitation of the human cortical iliac crest by backscattered electron image analysis: variations with age, sex, and degree of osteoarthritis. Bone. 1995;16(6):619-27.

76. ABS. Microdata: National Health Survey, 2017-18. Detailed microdata. Canberra: Australian Bureau of Statistics, 2019 2019. Report No.: Contract No.: 4324.0.55.001.

77. Felson DT. Obesity and osteoarthritis of the knee. Bull Rheum Dis. 1992;41(2):6-7.

78. MacGregor AJ, Antoniades L, Matson M, Andrew T, Spector TD. The genetic contribution to radiographic hip osteoarthritis in women: results of a classic twin study. Arthritis Rheum. 2000;43(11):2410-6.

79. Francisco V, Perez T, Pino J, Lopez V, Franco E, Alonso A, et al. Biomechanics, Obesity, and Osteoarthritis. The Role of Adipokines: When the Levee Breaks. J Orthop Res. 2017.

80. Ackerman IN, Pratt C, Gorelik A, Liew D. The projected burden of osteoarthritis and rheumatoid arthritis in Australia: A population-level analysis. Arthritis Care Res (Hoboken). 2017.

81. Adebajo A. Non-steroidal anti-inflammatory drugs for the treatment of pain and immobility-associated osteoarthritis: consensus guidance for primary care. BMC Fam Pract. 2012;13:23.

82. Hameed F, Ihm J. Injectable medications for osteoarthritis. PM R. 2012;4(5 Suppl):S75-81.

83. Cheng OT, Souzdalnitski D, Vrooman B, Cheng J. Evidence-based knee injections for the management of arthritis. Pain Med. 2012;13(6):740-53.

84. Lund H, Weile U, Christensen R, Rostock B, Downey A, Bartels EM, et al. A randomized controlled trial of aquatic and land-based exercise in patients with knee osteoarthritis. J Rehabil Med. 2008;40(2):137-44.

85. Alkatan M, Baker JR, Machin DR, Park W, Akkari AS, Pasha EP, et al. Improved Function and Reduced Pain after Swimming and Cycling Training in Patients with Osteoarthritis. J Rheumatol. 2016;43(3):666-72.

86. Ramirez AI, de Hoz R, Salobrar-Garcia E, Salazar JJ, Rojas B, Ajoy D, et al. The Role of Microglia in Retinal Neurodegeneration: Alzheimer's Disease, Parkinson, and Glaucoma. Front Aging Neurosci. 2017;9:214.

87. Park SB, Kiernan MC, Vucic S. Axonal Excitability in Amyotrophic Lateral Sclerosis : Axonal Excitability in ALS. Neurotherapeutics. 2017;14(1):78-90.

88. Nalivaeva NN, Turner AJ. The amyloid precursor protein: a biochemical enigma in brain development, function and disease. FEBS Lett. 2013;587(13):2046-54.

89. Dyrks T, Weidemann A, Multhaup G, Salbaum JM, Lemaire HG, Kang J, et al. Identification, transmembrane orientation and biogenesis of the amyloid A4 precursor of Alzheimer's disease. EMBO J. 1988;7(4):949-57.

90. Sandbrink R, Masters CL, Beyreuther K. APP gene family. Alternative splicing generates functionally related isoforms. Ann N Y Acad Sci. 1996;777:281-7.

91. Bayer TA, Cappai R, Masters CL, Beyreuther K, Multhaup G. It all sticks together--the APP-related family of proteins and Alzheimer's disease. Mol Psychiatry. 1999;4(6):524-8.

92. Klevanski M, Saar M, Baumkotter F, Weyer SW, Kins S, Muller UC. Differential role of APP and APLPs for neuromuscular synaptic morphology and function. Mol Cell Neurosci. 2014;61:201-10.

93. Lenkkeri U, Kestila M, Lamerdin J, McCready P, Adamson A, Olsen A, et al. Structure of the human amyloid-precursor-like protein gene APLP1 at 19q13.1. Hum Genet. 1998;102(2):192-6.

94. Weyer SW, Klevanski M, Delekate A, Voikar V, Aydin D, Hick M, et al. APP and APLP2 are essential at PNS and CNS synapses for transmission, spatial learning and LTP. EMBO J. 2011;30(11):2266-80.

95. Izumi R, Yamada T, Yoshikai S, Sasaki H, Hattori M, Sakaki Y. Positive and negative regulatory elements for the expression of the Alzheimer's disease amyloid precursor-encoding gene in mouse. Gene. 1992;112(2):189-95.

96. Zheng H, Jiang M, Trumbauer ME, Sirinathsinghji DJ, Hopkins R, Smith DW, et al. beta-Amyloid precursor protein-deficient mice show reactive gliosis and decreased locomotor activity. Cell. 1995;81(4):525-31.

97. d'Uscio LV, Katusic ZS. Vascular phenotype of amyloid precursor protein-deficient mice. Am J Physiol Heart Circ Physiol. 2019;316(6):H1297-H308.

98. Xu TH, Yan Y, Kang Y, Jiang Y, Melcher K, Xu HE. Alzheimer's disease-associated mutations increase amyloid precursor protein resistance to gamma-secretase cleavage and the Abeta42/Abeta40 ratio. Cell Discov. 2016;2:16026.

99. Hartl D, Klatt S, Roch M, Konthur Z, Klose J, Willnow TE, et al. Soluble alpha-APP (sAPPalpha) regulates CDK5 expression and activity in neurons. PLoS One. 2013;8(6):e65920.

100. Klevanski M, Herrmann U, Weyer SW, Fol R, Cartier N, Wolfer DP, et al. The APP Intracellular Domain Is Required for Normal Synaptic Morphology, Synaptic Plasticity, and Hippocampus-Dependent Behavior. J Neurosci. 2015;35(49):16018-33.

101. De Strooper B, Annaert W. Proteolytic processing and cell biological functions of the amyloid precursor protein. J Cell Sci. 2000;113 (Pt 11):1857-70.

102. Coronel R, Lachgar M, Bernabeu-Zornoza A, Palmer C, Dominguez-Alvaro M, Revilla A, et al. Neuronal and Glial Differentiation of Human Neural Stem Cells Is Regulated by Amyloid Precursor Protein (APP) Levels. Mol Neurobiol. 2019;56(2):1248-61.

103. Caille I, Allinquant B, Dupont E, Bouillot C, Langer A, Muller U, et al. Soluble form of amyloid precursor protein regulates proliferation of progenitors in the adult subventricular zone. Development. 2004;131(9):2173-81.

104. Pandey P, Rachagani S, Das S, Seshacharyulu P, Sheinin Y, Naslavsky N, et al. Amyloid precursor-like protein 2 (APLP2) affects the actin cytoskeleton and increases pancreatic cancer growth and metastasis. Oncotarget. 2015;6(4):2064-75.

105. Tyan SH, Shih AY, Walsh JJ, Maruyama H, Sarsoza F, Ku L, et al. Amyloid precursor protein (APP) regulates synaptic structure and function. Mol Cell Neurosci. 2012;51(1-2):43-52.

106. Milward EA, Papadopoulos R, Fuller SJ, Moir RD, Small D, Beyreuther K, et al. The amyloid protein precursor of Alzheimer's disease is a mediator of the effects of nerve growth factor on neurite outgrowth. Neuron. 1992;9(1):129-37.

107. Ewald CY, Li C. Caenorhabditis elegans as a model organism to study APP function. Exp Brain Res. 2012;217(3-4):397-411.

108. Luo LQ, Martin-Morris LE, White K. Identification, secretion, and neural expression of APPL, a Drosophila protein similar to human amyloid protein precursor. J Neurosci. 1990;10(12):3849-61.

109. Torroja L, Chu H, Kotovsky I, White K. Neuronal overexpression of APPL, the Drosophila homologue of the amyloid precursor protein (APP), disrupts axonal transport. Curr Biol. 1999;9(9):489-92.

110. Musa A, Lehrach H, Russo VA. Distinct expression patterns of two zebrafish homologues of the human APP gene during embryonic development. Dev Genes Evol. 2001;211(11):563-7.

111. Joachim CL, Mori H, Selkoe DJ. Amyloid beta-protein deposition in tissues other than brain in Alzheimer's disease. Nature. 1989;341(6239):226-30.

112. Pandey P, Sliker B, Peters HL, Tuli A, Herskovitz J, Smits K, et al. Amyloid precursor protein and amyloid precursor-like protein 2 in cancer. Oncotarget. 2016;7(15):19430-44.

113. Takagi K, Ito S, Miyazaki T, Miki Y, Shibahara Y, Ishida T, et al. Amyloid precursor protein in human breast cancer: an androgen-induced gene associated with cell proliferation. Cancer Sci. 2013;104(11):1532-8.

114. von Koch CS, Zheng H, Chen H, Trumbauer M, Thinakaran G, van der Ploeg LH, et al. Generation of APLP2 KO mice and early postnatal lethality in APLP2/APP double KO mice. Neurobiol Aging. 1997;18(6):661-9.

115. Heber S, Herms J, Gajic V, Hainfellner J, Aguzzi A, Rulicke T, et al. Mice with combined gene knock-outs reveal essential and partially redundant functions of amyloid precursor protein family members. J Neurosci. 2000;20(21):7951-63.

116. Needham BE, Wlodek ME, Ciccotosto GD, Fam BC, Masters CL, Proietto J, et al. Identification of the Alzheimer's disease amyloid precursor protein (APP) and its

homologue APLP2 as essential modulators of glucose and insulin homeostasis and growth. The Journal of pathology. 2008;215(2):155-63.

117. Miller DL, Papayannopoulos IA, Styles J, Bobin SA, Lin YY, Biemann K, et al. Peptide compositions of the cerebrovascular and senile plaque core amyloid deposits of Alzheimer's disease. Arch Biochem Biophys. 1993;301(1):41-52.

118. Glenner GG, Wong CW. Alzheimer's disease: initial report of the purification and characterization of a novel cerebrovascular amyloid protein. Biochem Biophys Res Commun. 1984;120(3):885-90.

119. Masters CL, Simms G, Weinman NA, Multhaup G, McDonald BL, Beyreuther K. Amyloid plaque core protein in Alzheimer disease and Down syndrome. Proc Natl Acad Sci U S A. 1985;82(12):4245-9.

120. Hardy JA, Higgins GA. Alzheimer's disease: the amyloid cascade hypothesis. Science. 1992;256(5054):184-5.

121. Ballatore C, Lee VM, Trojanowski JQ. Tau-mediated neurodegeneration in Alzheimer's disease and related disorders. Nat Rev Neurosci. 2007;8(9):663-72.

122. Doecke JD, Perez-Grijalba V, Fandos N, Fowler C, Villemagne VL, Masters CL, et al. Total Abeta42/Abeta40 ratio in plasma predicts amyloid-PET status, independent of clinical AD diagnosis. Neurology. 2020;94(15):e1580-e91.

123. Cui S, Xiong F, Hong Y, Jung JU, Li XS, Liu JZ, et al. APPswe/Abeta regulation of osteoclast activation and RAGE expression in an age-dependent manner. J Bone Miner Res. 2011;26(5):1084-98.

124. Li S, Liu B, Zhang L, Rong L. Amyloid beta peptide is elevated in osteoporotic bone tissues and enhances osteoclast function. Bone. 2014;61:164-75.

125. Franceschi C, Bonafe M, Valensin S, Olivieri F, De Luca M, Ottaviani E, et al. Inflamm-aging. An evolutionary perspective on immunosenescence. Ann N Y Acad Sci. 2000;908:244-54.

126. Sanguineti R, Puddu A, Mach F, Montecucco F, Viviani GL. Advanced glycation end products play adverse proinflammatory activities in osteoporosis. Mediators Inflamm. 2014;2014:975872.

127. Licastro F, Candore G, Lio D, Porcellini E, Colonna-Romano G, Franceschi C, et al. Innate immunity and inflammation in ageing: a key for understanding age-related diseases. Immun Ageing. 2005;2:8.

128. Prince M, Bryce R, Albanese E, Wimo A, Ribeiro W, Ferri CP. The global prevalence of dementia: a systematic review and metaanalysis. Alzheimers Dement. 2013;9(1):63-75 e2.

129. Wolters FJ, Ikram MA. Erratum to: Epidemiology of Dementia: The Burden on Society, the Challenges for Research. Methods Mol Biol. 2018;1750:E3.

130. Health AIo, Welfare. Deaths in Australia. Canberra: AIHW, 2019.

131. Beyreuther K, Masters CL. Amyloid precursor protein (APP) and beta A4 amyloid in the etiology of Alzheimer's disease: precursor-product relationships in the derangement of neuronal function. Brain Pathol. 1991;1(4):241-51.

132. Hardy J, Allsop D. Amyloid deposition as the central event in the aetiology of Alzheimer's disease. Trends Pharmacol Sci. 1991;12(10):383-8.

133. Selkoe DJ. The molecular pathology of Alzheimer's disease. Neuron. 1991;6(4):487-98.

134. Desikan RS, Fan CC, Wang Y, Schork AJ, Cabral HJ, Cupples LA, et al. Genetic assessment of age-associated Alzheimer disease risk: Development and validation of a polygenic hazard score. PLoS Med. 2017;14(3):e1002258.

135. Strittmatter WJ, Saunders AM, Schmechel D, Pericak-Vance M, Enghild J, Salvesen GS, et al. Apolipoprotein E: high-avidity binding to beta-amyloid and increased frequency of type 4 allele in late-onset familial Alzheimer disease. Proc Natl Acad Sci U S A. 1993;90(5):1977-81.

136. Mahley RW. Apolipoprotein E: cholesterol transport protein with expanding role in cell biology. Science. 1988;240(4852):622-30.

137. Mahley RW, Rall SC, Jr. Apolipoprotein E: far more than a lipid transport protein. Annu Rev Genomics Hum Genet. 2000;1:507-37.

138. Sanan DA, Weisgraber KH, Russell SJ, Mahley RW, Huang D, Saunders A, et al. Apolipoprotein E associates with beta amyloid peptide of Alzheimer's disease to form novel monofibrils. Isoform apoE4 associates more efficiently than apoE3. J Clin Invest. 1994;94(2):860-9.

139. Wolk DA, Dickerson BC, Alzheimer's Disease Neuroimaging I. Fractionating verbal episodic memory in Alzheimer's disease. Neuroimage. 2011;54(2):1530-9.

140. Morales I, Guzman-Martinez L, Cerda-Troncoso C, Farias GA, Maccioni RB. Neuroinflammation in the pathogenesis of Alzheimer's disease. A rational framework for the search of novel therapeutic approaches. Front Cell Neurosci. 2014;8:112.

141. Joe E, Ringman JM. Cognitive symptoms of Alzheimer's disease: clinical management and prevention. BMJ. 2019;367:l6217.

142. Norton S, Matthews FE, Barnes DE, Yaffe K, Brayne C. Potential for primary prevention of Alzheimer's disease: an analysis of population-based data. Lancet Neurol. 2014;13(8):788-94.

143. Norton MC, Clark CJ, Tschanz JT, Hartin P, Fauth EB, Gast JA, et al. The design and progress of a multidomain lifestyle intervention to improve brain health in middle-

aged persons to reduce later Alzheimer's disease risk: The Gray Matters randomized trial. Alzheimers Dement (N Y). 2015;1(1):53-62.

144. Rogers SL, Friedhoff LT. The efficacy and safety of donepezil in patients with Alzheimer's disease: results of a US Multicentre, Randomized, Double-Blind, Placebo-Controlled Trial. The Donepezil Study Group. Dementia. 1996;7(6):293-303.

145. Tariot PN, Cummings JL, Katz IR, Mintzer J, Perdomo CA, Schwam EM, et al. A randomized, double-blind, placebo-controlled study of the efficacy and safety of donepezil in patients with Alzheimer's disease in the nursing home setting. J Am Geriatr Soc. 2001;49(12):1590-9.

146. Rosler M, Anand R, Cicin-Sain A, Gauthier S, Agid Y, Dal-Bianco P, et al. Efficacy and safety of rivastigmine in patients with Alzheimer's disease: international randomised controlled trial. BMJ. 1999;318(7184):633-8.

147. Wilcock GK, Lilienfeld S, Gaens E. Efficacy and safety of galantamine in patients with mild to moderate Alzheimer's disease: multicentre randomised controlled trial. Galantamine International-1 Study Group. BMJ. 2000;321(7274):1445-9.

148. Farlow MR. The SERAD study of the safety and efficacy of galantamine in severe Alzheimer's disease. Lancet Neurol. 2009;8(1):22-3.

149. Apelt J, Kumar A, Schliebs R. Impairment of cholinergic neurotransmission in adult and aged transgenic Tg2576 mouse brain expressing the Swedish mutation of human beta-amyloid precursor protein. Brain Res. 2002;953(1-2):17-30.

150. Craig LA, Hong NS, McDonald RJ. Revisiting the cholinergic hypothesis in the development of Alzheimer's disease. Neurosci Biobehav Rev. 2011;35(6):1397-409.

151. Bell KF, Ducatenzeiler A, Ribeiro-da-Silva A, Duff K, Bennett DA, Cuello AC. The amyloid pathology progresses in a neurotransmitter-specific manner. Neurobiol Aging. 2006;27(11):1644-57.

152. Gutierres JM, Carvalho FB, Schetinger MR, Marisco P, Agostinho P, Rodrigues M, et al. Anthocyanins restore behavioral and biochemical changes caused by streptozotocin-induced sporadic dementia of Alzheimer's type. Life Sci. 2014;96(1-2):7-17.

153. Bartus RT, Dean RL, 3rd, Beer B, Lippa AS. The cholinergic hypothesis of geriatric memory dysfunction. Science. 1982;217(4558):408-14.

154. Gordon BA, Blazey TM, Su Y, Hari-Raj A, Dincer A, Flores S, et al. Spatial patterns of neuroimaging biomarker change in individuals from families with autosomal dominant Alzheimer's disease: a longitudinal study. Lancet Neurol. 2018;17(3):241-50.

155. Rogaev EI, Sherrington R, Rogaeva EA, Levesque G, Ikeda M, Liang Y, et al. Familial Alzheimer's disease in kindreds with missense mutations in a gene on chromosome 1 related to the Alzheimer's disease type 3 gene. Nature. 1995;376(6543):775-8.

156. Sherrington R, Rogaev EI, Liang Y, Rogaeva EA, Levesque G, Ikeda M, et al. Cloning of a gene bearing missense mutations in early-onset familial Alzheimer's disease. Nature. 1995;375(6534):754-60.

157. Nakano Y, Kondoh G, Kudo T, Imaizumi K, Kato M, Miyazaki JI, et al. Accumulation of murine amyloidbeta42 in a gene-dosage-dependent manner in PS1 'knock-in' mice. Eur J Neurosci. 1999;11(7):2577-81.

158. Tysiewicz-Dudek M, Pietraszkiewicz F, Drozdzowska B. Alzheimer's disease and osteoporosis: common risk factors or one condition predisposing to the other? Ortop Traumatol Rehabil. 2008;10(4):315-23.

159. Hussain A, Barer D. Fracture risk in Alzheimer's disease patients. J Am Geriatr Soc. 1995;43(4):454.

160. Melton LJ, 3rd, Beard CM, Kokmen E, Atkinson EJ, O'Fallon WM. Fracture risk in patients with Alzheimer's disease. J Am Geriatr Soc. 1994;42(6):614-9.

161. Chang KH, Chung CJ, Lin CL, Sung FC, Wu TN, Kao CH. Increased risk of dementia in patients with osteoporosis: a population-based retrospective cohort analysis. Age (Dordr). 2014;36(2):967-75.

162. Liu D, Zhou H, Tao Y, Tan J, Chen L, Huang H, et al. Alzheimer's Disease is Associated with Increased Risk of Osteoporosis: The Chongqing Aging Study. Curr Alzheimer Res. 2016;13(10):1165-72.

163. Zhou R, Zhou H, Rui L, Xu J. Bone loss and osteoporosis are associated with conversion from mild cognitive impairment to Alzheimer's disease. Curr Alzheimer Res. 2014;11(7):706-13.

164. May H, Murphy S, Khaw KT. Age-associated bone loss in men and women and its relationship to weight. Age Ageing. 1994;23(3):235-40.

165. Kano K. Relationship between exercise and bone mineral density among over 5,000 women aged 40 years and above. J Epidemiol. 1998;8(1):28-32.

166. Unni J, Garg R, Pawar R. Bone mineral density in women above 40 years. J Midlife Health. 2010;1(1):19-22.

167. Yaffe K, Browner W, Cauley J, Launer L, Harris T. Association between bone mineral density and cognitive decline in older women. J Am Geriatr Soc. 1999;47(10):1176-82.

168. Jeon JH, Park JH, Oh C, Chung JK, Song JY, Kim S, et al. Dementia is Associated with an Increased Risk of Hip Fractures: A Nationwide Analysis in Korea. J Clin Neurol. 2019;15(2):243-9.

169. Tolppanen AM, Taipale H, Tanskanen A, Tiihonen J, Hartikainen S. Comparison of predictors of hip fracture and mortality after hip fracture in community-dwellers with

and without Alzheimer's disease - exposure-matched cohort study. BMC Geriatr. 2016;16(1):204.

170. Wei YJ, Simoni-Wastila L, Lucas JA, Brandt N. Fall and Fracture Risk in Nursing Home Residents With Moderate-to-Severe Behavioral Symptoms of Alzheimer's Disease and Related Dementias Initiating Antidepressants or Antipsychotics. J Gerontol A Biol Sci Med Sci. 2017;72(5):695-702.

171. Lv X-L, Zhang J, Gao W-Y, Xing W-M, Yang Z-X, Yue Y-X, et al. Association between Osteoporosis, Bone Mineral Density Levels and Alzheimer's Disease: A Systematic Review and Meta-analysis. International Journal of Gerontology. 2018;12(2):76-83.

172. Hsu B, Bleicher K, Waite LM, Naganathan V, Blyth FM, Handelsman DJ, et al. Community-dwelling older men with dementia are at high risk of hip fracture, but not any other fracture: The Concord Health and Aging in Men Project. Geriatr Gerontol Int. 2018;18(10):1479-84.

173. Baker NL, Cook MN, Arrighi HM, Bullock R. Hip fracture risk and subsequent mortality among Alzheimer's disease patients in the United Kingdom, 1988-2007. Age Ageing. 2011;40(1):49-54.

174. Li S, Yang B, Teguh D, Zhou L, Xu J, Rong L. Amyloid beta Peptide Enhances RANKL-Induced Osteoclast Activation through NF-kappaB, ERK, and Calcium Oscillation Signaling. Int J Mol Sci. 2016;17(10).

175. Xia WF, Jung JU, Shun C, Xiong S, Xiong L, Shi XM, et al. Swedish mutant APP suppresses osteoblast differentiation and causes osteoporotic deficit, which are ameliorated by N-acetyl-L-cysteine. J Bone Miner Res. 2013;28(10):2122-35.

176. Brod SA. Unregulated inflammation shortens human functional longevity. Inflamm Res. 2000;49(11):561-70.

177. McGrattan AM, McGuinness B, McKinley MC, Kee F, Passmore P, Woodside JV, et al. Diet and Inflammation in Cognitive Ageing and Alzheimer's Disease. Curr Nutr Rep. 2019;8(2):53-65.

178. McGeer PL, McGeer EG. Inflammatory processes in amyotrophic lateral sclerosis. Muscle Nerve. 2002;26(4):459-70.

179. Alzamil H. Elevated Serum TNF-alpha Is Related to Obesity in Type 2 Diabetes Mellitus and Is Associated with Glycemic Control and Insulin Resistance. J Obes. 2020;2020:5076858.

180. Corrado E, Rizzo M, Muratori I, Coppola G, Novo S. Older age and markers of inflammation are strong predictors of clinical events in women with asymptomatic carotid lesions. Menopause. 2008;15(2):240-7.

181. Krstic D, Madhusudan A, Doehner J, Vogel P, Notter T, Imhof C, et al. Systemic immune challenges trigger and drive Alzheimer-like neuropathology in mice. J Neuroinflammation. 2012;9:151.

182. Sudduth TL, Schmitt FA, Nelson PT, Wilcock DM. Neuroinflammatory phenotype in early Alzheimer's disease. Neurobiol Aging. 2013;34(4):1051-9.

183. Heneka MT, Kummer MP, Latz E. Innate immune activation in neurodegenerative disease. Nat Rev Immunol. 2014;14(7):463-77.

184. Holmes C, Cunningham C, Zotova E, Woolford J, Dean C, Kerr S, et al. Systemic inflammation and disease progression in Alzheimer disease. Neurology. 2009;73(10):768-74.

185. Chakrabarty P, Herring A, Ceballos-Diaz C, Das P, Golde TE. Hippocampal expression of murine TNFalpha results in attenuation of amyloid deposition in vivo. Mol Neurodegener. 2011;6:16.

186. Griffin WS, Stanley LC, Ling C, White L, MacLeod V, Perrot LJ, et al. Brain interleukin 1 and S-100 immunoreactivity are elevated in Down syndrome and Alzheimer disease. Proc Natl Acad Sci U S A. 1989;86(19):7611-5.

187. Patel NS, Paris D, Mathura V, Quadros AN, Crawford FC, Mullan MJ. Inflammatory cytokine levels correlate with amyloid load in transgenic mouse models of Alzheimer's disease. J Neuroinflammation. 2005;2(1):9.

188. Banks WA, Farr SA, Morley JE. Permeability of the blood-brain barrier to albumin and insulin in the young and aged SAMP8 mouse. J Gerontol A Biol Sci Med Sci. 2000;55(12):B601-6.

189. Harrison NA, Doeller CF, Voon V, Burgess N, Critchley HD. Peripheral inflammation acutely impairs human spatial memory via actions on medial temporal lobe glucose metabolism. Biol Psychiatry. 2014;76(7):585-93.

190. Bu XL, Xiang Y, Jin WS, Wang J, Shen LL, Huang ZL, et al. Blood-derived amyloid-beta protein induces Alzheimer's disease pathologies. Mol Psychiatry. 2017.

191. Kyrkanides S, Tallents RH, Miller JN, Olschowka ME, Johnson R, Yang M, et al. Osteoarthritis accelerates and exacerbates Alzheimer's disease pathology in mice. J Neuroinflammation. 2011;8:112.

192. Lin PC, Li CH, Chou PL, Chen YM, Lin LC. Prevalence of pain-related diagnoses in patients with dementia: a nationwide study. J Pain Res. 2018;11:1589-98.

193. Jamsen E, Peltola M, Puolakka T, Eskelinen A, Lehto MU. Surgical outcomes of hip and knee arthroplasties for primary osteoarthritis in patients with Alzheimer's disease: a nationwide registry-based case-controlled study. Bone Joint J. 2015;97-B(5):654-61.

194. Alvarenga JC, Fuller H, Pasoto SG, Pereira RM. Age-related reference curves of volumetric bone density, structure, and biomechanical parameters adjusted for weight and height in a population of healthy women: an HR-pQCT study. Osteoporos Int. 2016.

195. Blain H, Chavassieux P, Portero-Muzy N, Bonnel F, Canovas F, Chammas M, et al. Cortical and trabecular bone distribution in the femoral neck in osteoporosis and osteoarthritis. Bone. 2008;43(5):862-8.

196. Rubinacci A, Tresoldi D, Scalco E, Villa I, Adorni F, Moro GL, et al. Comparative high-resolution pQCT analysis of femoral neck indicates different bone mass distribution in osteoporosis and osteoarthritis. Osteoporos Int. 2012;23(7):1967-75.

197. Logan CY, Nusse R. The Wnt signaling pathway in development and disease. Annu Rev Cell Dev Biol. 2004;20:781-810.

198. Dong Y, Lathrop W, Weaver D, Qiu Q, Cini J, Bertolini D, et al. Molecular cloning and characterization of LR3, a novel LDL receptor family protein with mitogenic activity. Biochem Biophys Res Commun. 1998;251(3):784-90.

199. Ikeya M, Lee SM, Johnson JE, McMahon AP, Takada S. Wnt signalling required for expansion of neural crest and CNS progenitors. Nature. 1997;389(6654):966-70.

200. Braune EB, Seshire A, Lendahl U. Notch and Wnt Dysregulation and Its Relevance for Breast Cancer and Tumor Initiation. Biomedicines. 2018;6(4).

201. Zardawi SJ, O'Toole SA, Sutherland RL, Musgrove EA. Dysregulation of Hedgehog, Wnt and Notch signalling pathways in breast cancer. Histol Histopathol. 2009;24(3):385-98.

202. Tamai K, Semenov M, Kato Y, Spokony R, Liu C, Katsuyama Y, et al. LDL-receptor-related proteins in Wnt signal transduction. Nature. 2000;407(6803):530-5.

203. Lewis SL, Khoo PL, De Young RA, Steiner K, Wilcock C, Mukhopadhyay M, et al. Dkk1 and Wnt3 interact to control head morphogenesis in the mouse. Development. 2008;135(10):1791-801.

204. Semenov MV, Tamai K, Brott BK, Kuhl M, Sokol S, He X. Head inducer Dickkopf-1 is a ligand for Wnt coreceptor LRP6. Curr Biol. 2001;11(12):951-61.

205. Li J, Sarosi I, Cattley RC, Pretorius J, Asuncion F, Grisanti M, et al. Dkk1-mediated inhibition of Wnt signaling in bone results in osteopenia. Bone. 2006;39(4):754-66.

206. Morvan F, Boulukos K, Clement-Lacroix P, Roman Roman S, Suc-Royer I, Vayssiere B, et al. Deletion of a single allele of the Dkk1 gene leads to an increase in bone formation and bone mass. J Bone Miner Res. 2006;21(6):934-45.

207. Parr C, Mirzaei N, Christian M, Sastre M. Activation of the Wnt/beta-catenin pathway represses the transcription of the beta-amyloid precursor protein cleaving enzyme (BACE1) via binding of T-cell factor-4 to BACE1 promoter. FASEB J. 2015;29(2):623-35.

208. Guo X, Tang P, Liu P, Liu Y, Chong L, Li R. Dkk1: A promising molecule to connect Alzheimer's disease and osteoporosis. Med Hypotheses. 2016;88:30-2.

209. Yang B, Li S, Chen Z, Feng F, He L, Liu B, et al. Amyloid beta peptide promotes bone formation by regulating Wnt/beta-catenin signaling and the OPG/RANKL/RANK system. FASEB J. 2020.

210. Angeletti PU, Levi-Montalcini R, Calissano P. The nerve growth factor (NGF): chemical properties and metabolic effects. Adv Enzymol Relat Areas Mol Biol. 1968;31:51-75.

211. Grills BL, Schuijers JA. Immunohistochemical localization of nerve growth factor in fractured and unfractured rat bone. Acta Orthop Scand. 1998;69(4):415-9.

212. Culmsee C, Gerling N, Lehmann M, Nikolova-Karakashian M, Prehn JH, Mattson MP, et al. Nerve growth factor survival signaling in cultured hippocampal neurons is mediated through TrkA and requires the common neurotrophin receptor P75. Neuroscience. 2002;115(4):1089-108.

213. Aragona M, Panetta S, Silipigni AM, Romeo DL, Pastura G, Mesiti M, et al. Nerve growth factor receptor immunoreactivity in breast cancer patients. Cancer Invest. 2001;19(7):692-7.

214. Descamps S, Pawlowski V, Revillion F, Hornez L, Hebbar M, Boilly B, et al. Expression of nerve growth factor receptors and their prognostic value in human breast cancer. Cancer Res. 2001;61(11):4337-40.

215. Descamps S, Toillon RA, Adriaenssens E, Pawlowski V, Cool SM, Nurcombe V, et al. Nerve growth factor stimulates proliferation and survival of human breast cancer cells through two distinct signaling pathways. J Biol Chem. 2001;276(21):17864-70.

216. Krygier S, Djakiew D. Neurotrophin receptor p75(NTR) suppresses growth and nerve growth factor-mediated metastasis of human prostate cancer cells. Int J Cancer. 2002;98(1):1-7.

217. Melck D, De Petrocellis L, Orlando P, Bisogno T, Laezza C, Bifulco M, et al. Suppression of nerve growth factor Trk receptors and prolactin receptors by endocannabinoids leads to inhibition of human breast and prostate cancer cell proliferation. Endocrinology. 2000;141(1):118-26.

218. Indo Y. [Nerve growth factor and the physiology of pain: the relationships among interoception, sympathetic neurons and the emotional response indicated by the molecular pathophysiology of congenital insensitivity to pain with anhidrosis]. No To Hattatsu. 2015;47(3):173-80.

219. Iannone F, De Bari C, Dell'Accio F, Covelli M, Patella V, Lo Bianco G, et al. Increased expression of nerve growth factor (NGF) and high affinity NGF receptor (p140 TrkA) in human osteoarthritic chondrocytes. Rheumatology (Oxford). 2002;41(12):1413-8.

220. Zhuang YF, Li J. Serum EGF and NGF levels of patients with brain injury and limb fracture. Asian Pac J Trop Med. 2013;6(5):383-6.

221. Zhang R, Liang Y, Wei S. The expressions of NGF and VEGF in the fracture tissues are closely associated with accelerated clavicle fracture healing in patients with traumatic brain injury. Ther Clin Risk Manag. 2018;14:2315-22.

222. Bittles AH, Glasson EJ. Clinical, social, and ethical implications of changing life expectancy in Down syndrome. Dev Med Child Neurol. 2004;46(4):282-6.

223. Baird PA, Sadovnick AD. Life expectancy in Down syndrome adults. Lancet. 1988;2(8624):1354-6.

224. Day RJ, McCarty KL, Ockerse KE, Head E, Rohn TT. Proteolytic Cleavage of Apolipoprotein E in the Down Syndrome Brain. Aging Dis. 2016;7(3):267-77.

225. Angelopoulou N, Souftas V, Sakadamis A, Mandroukas K. Bone mineral density in adults with Down's syndrome. Eur Radiol. 1999;9(4):648-51.

226. McKelvey KD, Fowler TW, Akel NS, Kelsay JA, Gaddy D, Wenger GR, et al. Low bone turnover and low bone density in a cohort of adults with Down syndrome. Osteoporos Int. 2013;24(4):1333-8.

227. Fowler TW, McKelvey KD, Akel NS, Vander Schilden J, Bacon AW, Bracey JW, et al. Low bone turnover and low BMD in Down syndrome: effect of intermittent PTH treatment. PLoS One. 2012;7(8):e42967.

228. Pan JX, Tang F, Xiong F, Xiong L, Zeng P, Wang B, et al. APP promotes osteoblast survival and bone formation by regulating mitochondrial function and preventing oxidative stress. Cell Death Dis. 2018;9(11):1077.

229. Mulcahy LE, Taylor D, Lee TC, Duffy GP. RANKL and OPG activity is regulated by injury size in networks of osteocyte-like cells. Bone. 2011;48(2):182-8.

230. Cabahug-Zuckerman P, Frikha-Benayed D, Majeska RJ, Tuthill A, Yakar S, Judex S, et al. Osteocyte Apoptosis Caused by Hindlimb Unloading is Required to Trigger Osteocyte RANKL Production and Subsequent Resorption of Cortical and Trabecular Bone in Mice Femurs. J Bone Miner Res. 2016;31(7):1356-65.

231. Wiren KM, Toombs AR, Semirale AA, Zhang X. Osteoblast and osteocyte apoptosis associated with androgen action in bone: requirement of increased Bax/Bcl-2 ratio. Bone. 2006;38(5):637-51.

232. Zhang C, Wei W, Chi M, Wan Y, Li X, Qi M, et al. FOXO1 Mediates Advanced Glycation End Products Induced Mouse Osteocyte-Like MLO-Y4 Cell Apoptosis and Dysfunctions. J Diabetes Res. 2019;2019:6757428.

233. Kennedy OD, Herman BC, Laudier DM, Majeska RJ, Sun HB, Schaffler MB. Activation of resorption in fatigue-loaded bone involves both apoptosis and active pro-osteoclastogenic signaling by distinct osteocyte populations. Bone. 2012;50(5):1115-22.

234. Annweiler C, Dursun E, Feron F, Gezen-Ak D, Kalueff AV, Littlejohns T, et al. 'Vitamin D and cognition in older adults': updated international recommendations. J Intern Med. 2015;277(1):45-57.

235. Yesil Y, Kuyumcu ME, Kara O, Halacli B, Etgul S, Kizilarslanoglu MC, et al. Vitamin D status and its association with gradual decline in cognitive function. Turk J Med Sci. 2015;45(5):1051-7.

236. Yu J, Gattoni-Celli M, Zhu H, Bhat NR, Sambamurti K, Gattoni-Celli S, et al. Vitamin D3-enriched diet correlates with a decrease of amyloid plaques in the brain of AbetaPP transgenic mice. J Alzheimers Dis. 2011;25(2):295-307.

237. Ormsby RT, Solomon LB, Yang D, Crotti TN, Haynes DR, Findlay DM, et al. Osteocytes respond to particles of clinically-relevant conventional and cross-linked

polyethylene and metal alloys by up-regulation of resorptive and inflammatory pathways. Acta Biomater. 2019;87:296-306.

238. Prideaux M, Schutz C, Wijenayaka AR, Findlay DM, Campbell DG, Solomon LB, et al. Isolation of osteocytes from human trabecular bone. Bone. 2016;88:64-72.

239. Yang D, Wijenayaka AR, Solomon LB, Pederson SM, Findlay DM, Kidd SP, et al. Novel Insights into Staphylococcus aureus Deep Bone Infections: the Involvement of Osteocytes. MBio. 2018;9(2).

240. Kogawa M, Wijenayaka AR, Ormsby RT, Thomas GP, Anderson PH, Bonewald LF, et al. Sclerostin Regulates Release of Bone Mineral by Osteocytes by Induction of Carbonic Anhydrase 2. J Bone Miner Res. 2013;28(12):2436-48.

241. da Rocha JF, da Cruz e Silva OA, Vieira SI. Analysis of the amyloid precursor protein role in neuritogenesis reveals a biphasic SH-SY5Y neuronal cell differentiation model. J Neurochem. 2015;134(2):288-301.

242. Stapledon CJM, Tsangari H, Solomon LB, Campbell DG, Hurtado P, Krishnan R, et al. Human osteocyte expression of Nerve Growth Factor: The effect of Pentosan Polysulphate Sodium (PPS) and implications for pain associated with knee osteoarthritis. PLoS One. 2019;14(9):e0222602.

243. Prideaux M, Wijenayaka AR, Kumarasinghe DD, Ormsby RT, Evdokiou A, Findlay DM, et al. SaOS2 Osteosarcoma Cells as an In Vitro Model for Studying the Transition of Human Osteoblasts to Osteocytes. Calcif Tissue Int. 2014;95(2):183-93.

244. Atkins GJ, Kostakis P, Pan B, Farrugia A, Gronthos S, Evdokiou A, et al. RANKL expression is related to the differentiation state of human osteoblasts. J Bone Miner Res. 2003;18(6):1088-98.

245. Atkins GJ, Welldon KJ, Halbout P, Findlay DM. Strontium ranelate treatment of human primary osteoblasts promotes an osteocyte-like phenotype while eliciting an osteoprotegerin response. Osteoporos Int. 2009;20(4):653-64.

246. Vincent C, Findlay DM, Welldon KJ, Wijenayaka AR, Zheng TS, Haynes DR, et al. Pro-inflammatory cytokines TNF-related weak inducer of apoptosis (TWEAK) and TNFalpha induce the mitogen-activated protein kinase (MAPK)-dependent expression of sclerostin in human osteoblasts. J Bone Miner Res. 2009;24(8):1434-49.

247. Welldon KJ, Findlay DM, Evdokiou A, Ormsby RT, Atkins GJ. Calcium induces pro-anabolic effects on human primary osteoblasts associated with acquisition of mature osteocyte markers. Mol Cell Endocrinol. 2013;376(1-2):85-92.

248. Sommer G, Kralisch S, Lipfert J, Weise S, Krause K, Jessnitzer B, et al. Amyloid precursor protein expression is induced by tumor necrosis factor α in 3T3-L1 adipocytes. Journal of Cellular Biochemistry. 2009;108(6):1418-22.

249. Cappai R, Mok SS, Galatis D, Tucker DF, Henry A, Beyreuther K, et al. Recombinant human amyloid precursor-like protein 2 (APLP2) expressed in the yeast Pichia pastoris can stimulate neurite outgrowth. FEBS Lett. 1999;442(1):95-8.

250. Takahashi N, Yamana H, Yoshiki S, Roodman GD, Mundy GR, Jones SJ, et al. Osteoclast-like cell formation and its regulation by osteotropic hormones in mouse bone marrow cultures. Endocrinology. 1988;122(4):1373-82.

251. Woeckel VJ, Alves RD, Swagemakers SM, Eijken M, Chiba H, van der Eerden BC, et al. 1Alpha,25-(OH)2D3 acts in the early phase of osteoblast differentiation to enhance mineralization via accelerated production of mature matrix vesicles. J Cell Physiol. 2010;225(2):593-600.

252. De Benedetti F, Rucci N, Del Fattore A, Peruzzi B, Paro R, Longo M, et al. Impaired skeletal development in interleukin-6-transgenic mice: a model for the impact

of chronic inflammation on the growing skeletal system. Arthritis Rheum. 2006;54(11):3551-63.

253. Axmann R, Bohm C, Kronke G, Zwerina J, Smolen J, Schett G. Inhibition of interleukin-6 receptor directly blocks osteoclast formation in vitro and in vivo. Arthritis Rheum. 2009;60(9):2747-56.

254. Cummings SR, Melton LJ. Epidemiology and outcomes of osteoporotic fractures. Lancet. 2002;359(9319):1761-7.

255. Zupan J, Mencej-Bedrac S, Jurkovic-Mlakar S, Prezelj J, Marc J. Gene-gene interactions in RANK/RANKL/OPG system influence bone mineral density in postmenopausal women. J Steroid Biochem Mol Biol. 2010;118(1-2):102-6.

256. Watts JJ, Abimanyi-Ochom J, Sanders KM, editors. Osteoporosis costing all Australians: a new burden of disease analysis - 2012 to 20222013.

257. Kanis JA, Johnell O, De Laet C, Johansson H, Oden A, Delmas P, et al. A meta-analysis of previous fracture and subsequent fracture risk. Bone. 2004;35(2):375-82.

258. AIHW. Dementia in Australia. 2012(Cat. no. AGE 70).

259. Alzheimer's A. 2015 Alzheimer's disease facts and figures. Alzheimers Dement. 2015;11(3):332-84.

260. Downey CL, Young A, Burton EF, Graham SM, Macfarlane RJ, Tsapakis EM, et al. Dementia and osteoporosis in a geriatric population: Is there a common link? World J Orthop. 2017;8(5):412-23.

261. Friedman SM, Menzies IB, Bukata SV, Mendelson DA, Kates SL. Dementia and hip fractures: development of a pathogenic framework for understanding and studying risk. Geriatr Orthop Surg Rehabil. 2010;1(2):52-62.

262. Guo P, Wang S, Zhu Y, Shen X, Jin X, Qian M, et al. Prevalence of osteopenia and osteoporosis and factors associated with decreased bone mineral density in elderly

inpatients with psychiatric disorders in Huzhou, China. Shanghai Arch Psychiatry. 2012;24(5):262-70.

263. Wang HK, Hung CM, Lin SH, Tai YC, Lu K, Liliang PC, et al. Increased risk of hip fractures in patients with dementia: a nationwide population-based study. BMC Neurol. 2014;14:175.

264. Liu Y, Wang Z, Xiao W. Risk factors for mortality in elderly patients with hip fractures: a meta-analysis of 18 studies. Aging Clin Exp Res. 2018;30(4):323-30.

265. Maravic M, Ostertag A, Urena P, Cohen-Solal M. Dementia is a major risk factor for hip fractures in patients with chronic kidney disease. Osteoporos Int. 2016;27(4):1665-9.

266. ANZHFR. ANZHFR Bi-National Annual Report of Hip Fracture Care 2018. Australian and New Zealand Hip Fracture Registry 2018.

267. Amouzougan A, Lafaie L, Marotte H, Dẻnariẻ D, Collet P, Pallot-Prades B, et al. High prevalence of dementia in women with osteoporosis. Joint bone spine. 2017;84(5):611-4.

268. Frame G, Bretland KA, Dengler-Crish CM. Mechanistic complexities of bone loss in Alzheimer's disease: a review. Connective tissue research. 2020;61(1):4-18.

269. Kang HG, Park HY, Ryu HU, Suk SH. Bone mineral loss and cognitive impairment: The PRESENT project. Medicine. 2018;97(41):e12755.

270. Zhou R, Deng J, Zhang M, Zhou HD, Wang YJ. Association between bone mineral density and the risk of Alzheimer's disease. Journal of Alzheimer's disease : JAD. 2011;24(1):101-8.

271. Walsh MC, Choi Y. Biology of the RANKL-RANK-OPG System in Immunity, Bone, and Beyond. Frontiers in immunology. 2014;5:511.

272. Dallas SL, Prideaux M, Bonewald LF. The osteocyte: an endocrine cell ... and more. Endocr Rev. 2013;34(5):658-90.

273. Zarrinkalam MR, Mulaibrahimovic A, Atkins GJ, Moore RJ. Changes in osteocyte density correspond with changes in osteoblast and osteoclast activity in an osteoporotic sheep model. Osteoporosis international : a journal established as result of cooperation between the European Foundation for Osteoporosis and the National Osteoporosis Foundation of the USA. 2012;23(4):1329-36.

274. Milovanovic P, Zimmermann EA, Riedel C, vom Scheidt A, Herzog L, Krause M, et al. Multi-level characterization of human femoral cortices and their underlying osteocyte network reveal trends in quality of young, aged, osteoporotic and antiresorptive-treated bone. Biomaterials. 2015;45:46-55.

275. Tiede-Lewis LM, Dallas SL. Changes in the osteocyte lacunocanalicular network with aging. Bone. 2019;122:101-13.

276. Hemmatian H, Bakker AD, Klein-Nulend J, van Lenthe GH. Aging, Osteocytes, and Mechanotransduction. Current Osteoporosis Reports. 2017;15(5):401-11.

277. Qin L, Liu W, Cao H, Xiao G. Molecular mechanosensors in osteocytes. Bone research. 2020;8:23.

278. Ben-awadh AN, Delgado-Calle J, Tu X, Kuhlenschmidt K, Allen MR, Plotkin LI, et al. Parathyroid hormone receptor signaling induces bone resorption in the adult skeleton by directly regulating the RANKL gene in osteocytes. Endocrinology. 2014;155(8):2797-809.

279. Xiong J, Piemontese M, Thostenson JD, Weinstein RS, Manolagas SC, O'Brien CA. Osteocyte-derived RANKL is a critical mediator of the increased bone resorption caused by dietary calcium deficiency. Bone. 2014;66:146-54.

280. Mueller RJ, Richards RG. Immunohistological identification of receptor activator of NF-kappaB ligand (RANKL) in human, ovine and bovine bone tissues. J Mater Sci Mater Med. 2004;15(4):367-72.

281. Li S, Liu B, Zhang L, Rong L. Amyloid beta peptide is elevated in osteoporotic bone tissues and enhances osteoclast function. Bone. 2014;61:164-75.

282. Hodkinson HM. Evaluation of a mental test score for assessment of mental impairment in the elderly. Age and ageing. 1972;1(4):233-8.

283. Creavin ST, Wisniewski S, Noel-Storr AH, Trevelyan CM, Hampton T, Rayment D, et al. Mini-Mental State Examination (MMSE) for the detection of dementia in clinically unevaluated people aged 65 and over in community and primary care populations. The Cochrane database of systematic reviews. 2016(1):Cd011145.

284. Hummon AB, Lim SR, Difilippantonio MJ, Ried T. Isolation and solubilization of proteins after TRIzol extraction of RNA and DNA from patient material following prolonged storage. Biotechniques. 2007;42(4):467-70, 72.

285. Livak KJ, Schmittgen TD. Analysis of relative gene expression data using real-time quantitative PCR and the 2(-Delta Delta C(T)) Method. Methods. 2001;25(4):402-8.

286. Myers GL, Miller WG, Coresh J, Fleming J, Greenberg N, Greene T, et al. Recommendations for improving serum creatinine measurement: a report from the Laboratory Working Group of the National Kidney Disease Education Program. Clin Chem. 2006;52(1):5-18.

287. Ceriotti F, Boyd JC, Klein G, Henny J, Queralto J, Kairisto V, et al. Reference intervals for serum creatinine concentrations: assessment of available data for global application. Clin Chem. 2008;54(3):559-66.

288. Krzanowski M, Krzanowska K, Dumnicka P, Gajda M, Woziwodzka K, Fedak D, et al. Elevated Circulating Osteoprotegerin Levels in the Plasma of Hemodialyzed Patients With Severe Artery Calcification. Ther Apher Dial. 2018;22(5):519-29.

289. Baumgartner R, Heeren N, Quast D, Babst R, Brunner A. Is the cortical thickness index a valid parameter to assess bone mineral density in geriatric patients with hip fractures? Arch Orthop Trauma Surg. 2015;135(6):805-10.

290. Dorr LD, Faugere MC, Mackel AM, Gruen TA, Bognar B, Malluche HH. Structural and cellular assessment of bone quality of proximal femur. Bone. 1993;14(3):231-42.

291. Sah AP, Thornhill TS, LeBoff MS, Glowacki J. Correlation of plain radiographic indices of the hip with quantitative bone mineral density. Osteoporos Int. 2007;18(8):1119-26.

292. Buenzli PR, Thomas CD, Clement JG, Pivonka P. Endocortical bone loss in osteoporosis: the role of bone surface availability. Int J Numer Method Biomed Eng. 2013;29(12):1307-22.